CRANFIELD UNIVERSITY

DEFENCE COLLEGE OF MANAGEMENT AND TECHNOLOGY
DEPARTMENT OF INFORMATION SYSTEMS

PhD THESIS

Academic Year 2004-2007

Shahid Ali

Indoor Geolocation for Wireless Networks

Supervisor: Dr Philip Nobles

July 2007

ABSTRACT

An ever growing demand for 'location based services' and the unprecedented growth of wireless local area networks (WLAN) has, in the past few years, attracted the focus of the research community to investigate and develop accurate indoor geolocation systems. Performance of any geolocation system is based upon the reported distance error . The accuracy required varies from application to application. For example an accurate geolocation system is required to apprehend a rogue client (illegitimate connection) inside a building in a dense wireless environment. At present this is possible only through wireless radio frequency (RF) interception of signals. The received signal strength (RSS) of a signal can be used to report the position of a client by triangulation. The hostile indoor environment presents many challenges including multipath and wall attenuation that needs to be considered for determining accurate indoor location. In this thesis a novel method to reduce the variation in RSS values is demonstrated by exploiting the frequency diversity existing across multiple channels of devices equipped with the IEEE 802.11 a/b/g wifi (wireless fidelity) standards. Absorption of the RF signal due to walls is observed and identified as one of the major factors that influence location estimation. RSS from different directions and within different environments is also studied. The processed RSS values are then applied to location estimation using a novel RSS threshold algorithm based upon a RF propagation model. The algorithm is designed based on the room dimensions where location sensors are placed. The algorithm's main feature is to correctly identify the walls existing between the sensors and client. Correct determination of walls together with a data fusion process produces accurate location results. For a set of example locations, the algorithm gives an accuracy of 3m for 75% of the locations and in terms of mean location error, is shown to be 2.16m for 100% of the locations. The reported accuracy is superior to the most accurate existing systems. The research trend for indoor geolocation has recently focused upon a 'finger-printing' technique, which is environment dependant and time consuming. The results achieved and presented in this thesis revive the use of simple propagation modelling for indoor geolocation applications.

ACKNOWLEDGEMENT

'ALL THANKS TO ALLAH, THE MOST GRACIOUS THE MOST GIVING'

I am truly grateful to Dr P Nobles not only as a supervisor but also as a mentor. His enthusiasm and devotion to work has made a profound impression on me. This thesis would not have been completed without his constant encouragement and guidance. He has taught me the art of independent research and critical thinking.

I owe special thanks to my thesis committee (Mr Ian Whitworth and Prof P C J Hills) for their able guidance at each step of PhD process. I am full of praise for my colleagues, Mr Chris Hargreaves, Alexies Garcia, Azfar Ali Syed for their insightful comments in completing the thesis. I am thankful to the department and academic registry for all their admin support that I required during my stay at DCMT (Cranfield University).

I dedicate this success to my late father who always wanted me to pursue higher education. His commitment to give me best education is a strong motivation factor in completion of my PhD. I recognise prayers from my mother for my success and well being throughout my stay in UK. This acknowledgement is not complete without mention of my brother Zahid Ali, for his constant encouragement and help in times of distress and need. And of course, I am grateful to my wife and children who have been so cooperative and patient during my long absences from home while busy doing my PhD in late hours on week days and weekends.

At the end, I am thankful to Higher Education Commission (HEC), National University of Sciences and technology (NUST) and Pakistan Navy for sponsoring my expenses for studies and living.

LIST OF CONTENTS

LIST OF FIGURES

LIST OF TABLES

GLOSSARY

λ	Wavelength
c	Client
d	Distance
dB	Decibel
dBm	Decibel Milliwatts
m/s	Metres per Second
n	Path Loss Component
ns	Nano-Second
r	Radius of Circle
AoA	Angle of Arrival
ADSL	Asymmetric Digital Subscriber Line
Ae	effective aperture
A_{eb}	Effective Aperture of antenna 'b'
AP	Access point
B	Breadth
BSS	Basic Service Set
C	Velocity of Light
CCA	Clear Channel Assessment
CTS	Clear to Send
D	Delay Spread
EIRP	Effective Isotropic Radiated Power
EP	Estimated Position
ESS	Extended Service Set
EuCAP	European Conference on Antennas and Propagation
EW	Electronic Warfare
G_a	Gain of Antenna 'a'
G_b	Gain of Antenna 'b'
G_R	Gain of the Receiver
G_T	Gain of the Transmitter
GBP	Great Britain Pound
GHz	Giga Hertz

GPS	Global Positioning System
GRNN	General Regression Neural Network
HEC	Header Error Check
IAPP	Inter Access Point Protocol
IBSS	Independent Basic Service Set
ID	Identity
IEEE	Institute of Electrical and Electronics Engineers
IR	Infrared
KNN	K – Nearest Neighbours
L	Length
L_{FSL}	Free Space Loss
LoS	Line of Sight
L_R	Feeder Loss at Receiver
L_T	Feeder Loss at Transmitter
L_X	Loss (RSS) equal to the longest side of a room with adjacent room considered
L_{Xd}	Loss (RSS) equal to the diagonal length of a room
L_{Xs}	Loss (RSS) equal to the shortest side of a room
MAC	Medium Access Control
MHz	Mega Hertz
MLP	Multilayer Perceptron
MPDU	MAC Protocol Data Unit
NIC	Network Interface Card
NLoS	Non Line of Sight
NN	Nearest Neighbour
OSI	Open System Interconnection
P_r	Received Power
P_t	Transmitted Power
PLCP	Physical Layer Convergence Procedure
PMD	Physical Medium Dependant
PPDU	PLCP Protocol Data Unit
PR1	Effective Received Power

PT1	Effective Transmitted Power
RF	Radio Frequency
ROCRSSI	Ring Overlapping based on Comparison of RSSI
RSN	Robust Security Network
RSS	Received Signal Strength in dBm
RSSI	Received Signal Strength Indicator
RTS	Ready to Send
S	Power Density
SFD	Start Frame Delimiter
SSID	Sensor Set Identifier
ToA	Time of Arrival
TDoA	Time Difference of Arrival
UTD	Uniform theory of diffraction
Wc	Coherence Bandwidth
WEP	Wired Equivalent Privacy
WiFi	Wireless Fidelity
WLAN	Wireless Local Area Network
WPA	WiFi Protected Access
WPNC	Workshop on Positioning Navigation and Communication
X	Longest Length of a Room when the Adjacent Room is considered
X_d	Length of the diagonal of a room
X_s	Length of Shortest side of a room

CHAPTER 1

INTRODUCTION

1.1 Background and motivation

Location based services have recently emerged as an important area of wireless research. The United States Federal Communications Commission's (FCC) E911 tele communication initiatives require that wireless phone providers develop a way to locate any phone that makes a 911 emergency call (Hightower, 2001). Since then companies have been more active in undertaking research for location aware services. There can be many location based applications both outdoor and indoor ranging from finding the nearest taxi, making an emergency 911 call or locating a rogue network client (illegitimate wireless connection), printer or medical tools inside a building. The accuracy required for such services varies from application to application. A number of applications for the indoor environment require an accuracy ranging from 1 to 10 m (Sayed et al. 2005). For instance, a 'child tracking' service might require accuracies within a few metres. Locating a printer inside a building may require room level accuracy. A rogue client on a wireless local area network (WLAN) poses a threat and provides a security hole within a network that needs to be located.

Today we are living in a security conscious world which is encountering a technological boom in the wireless industry and related applications. An unprecedented growth in wireless LAN technology has been witnessed over the last few years. According to a recent market report *Network news* (2007):

"WLAN revenue is forecast to grow by at least 51% by 2010, giving it overall revenue of more than $ 4 billion"

'Infonetics Research'

Nearly all the latest laptops, personal digital assistants (PDAs) and mobile phones now come equipped with a wireless network interface card. This demonstrates that there is a growing demand for WLAN, which is not only restricted to businesses but equally in demand at universities, offices and homes.

Wireless technology brings with it security concerns, one of which is the rogue wireless intruder. Rogue wireless clients in sensitive places such as military establishments must be accurately located. "There is no method available to know exactly where a rogue client is other than to intercept the wireless signal and to locate the client using a technique such as triangulation. In dense wireless environments within a small area or room as is the case with densely populated cities (Tokyo, Mumbai, New York, London), locating a rogue clients warrants accurate indoor location reporting. Accuracy as good as below 3m is desirable for such applications.

Wirelessly locating a mobile or client inside a building can be achieved using various sensing technologies, such as infra-red (IR), ultrasound and radio frequency (RF) signal. IR and ultrasound technologies are limited due to constraints discussed later in this thesis. RF offers the advantage of a larger coverage area and is deployed by most appliances including WLAN. RF radio signal technology, therefore, has received the most attention from the research community, and is the most used technology for indoor location estimation (Bahl et al. 2000). A recent market forecast for wireless location technology is provided in figure 1-1, *Location based services* (2003), with a predicted revenue of US$ in billion.

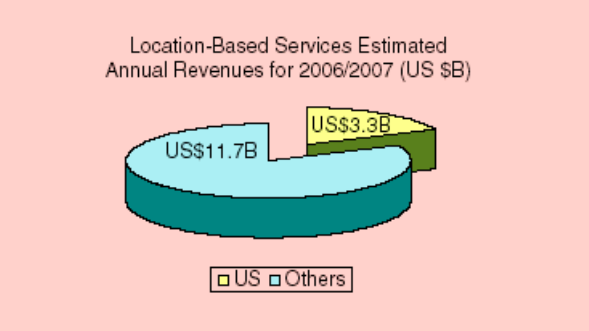

Figure 1-1 Forecast revenue for location based services (*Location based services*, 2003)

Location estimation inside a building is a challenging task, especially for applications which require accurate location reporting. The Global Positioning System (GPS) performs very well in outdoor environments. GPS receives signals from multiple satellites and employs a triangulation process to calculate position within approximately 10m accuracy (Enge et al. 1999). GPS is, however, rendered ineffective inside a building due to the walls, other obstructions and the multipath phenomenon (Bellusci et al. 2007; Pandya 2003). RF propagation inside a building encounters reflection, diffraction, scattering and multipath. All of these factors deteriorate the received signal and adversely affect the measurement of various parametres of a signal required for location estimation. Under these circumstances algorithms need to be very complex to give reasonable accuracy in reported location estimation. Despite complexity, existing algorithms still report large errors and therefore are not reliable for many applications.

There are many metrics which can be deployed to find location of an emitter inside a building; namely, angle of arrival (AoA), received signal strength (RSS), time of arrival (ToA) and time difference of arrival (TDoA). The techniques of ToA and TDoA require a degree of time synchronisation that is difficult to achieve using off-the-shelf WLAN hardware. RSS methods require a reliable propagation model or detailed calibration. Recent published research has concentrated upon the time consuming 'finger-printing' method of obtaining RSS maps of the particular deployment environment.

The research reported in this thesis concentrates; however, on obtaining an understanding of the propagation environment to develop a more sophisticated but straightforward approach to indoor geolocation. A Path loss model is difficult to

construct for the indoor environment and therefore it is difficult to attain accuracy in reported geolocation using triangulation. According to (Hightower, 2001 and SearchNetworking), Triangulation is a process according to which location of a transmitter can be determined by measuring either the radial distance or the direction of the received signal from two or three different points. Lateration is the term used to measure distance. Angulation is used to measure angles. Both these terms are subsets of the triangulation technique to report location. In this thesis, however, the term triangulation will be used to mention location determined by measuring radial distances. More detailed explanation on triangulation is covered in chapter 3. The measuring metric, RSS, varies drastically due to multipath and other obstructions such as walls. Variation of RSS can be as much as 10 decibels (dB) (Jonge, 2005). What is missing in current research, to date, is effective mitigation of multipath so that the accuracy of RSS can be improved and the positional accuracy reported by the algorithms increased. Moreover, most path loss models require accurate values for the losses of walls and other obstructions. There is a need to develop an algorithm that does not require detailed inputs such as material of walls, number of walls etc. Existing non trainable (triangulation) algorithms do not fare very well when compared against trainable (finger-printing) algorithms (Kaemarasungi, 2005). In previous research Nobles (1999) suggests that if the effect of multipath on RSS is minimised then walls are the primary factor in deviation of measured received signal from theoretical values. This is investigated further in the context of WLANs to provide improved location estimation results based on a simple and easy to implement propagation model. A mean accuracy of 2.16m is achieved which to the author's knowledge is superior to any existing systems. The reliability of reporting accurate results less than 3m was as high as 75%.

This dissertation presents a novel algorithm that does not require any inputs from users other than the dimensions of the room where sensors are placed. Instead it determines the position of walls with respect to sensors in the WLAN infrastructure and then geolocates wireless clients with respect to the access point (sensor) locations. In Chapter 6 it is shown that correctly determining the position of walls improves the overall accuracy reported by the geolocation system. The algorithm (triangulation) makes use of RSS measurements, which are processed to minimise multipath and thus ensures

accurate signal strengths for location estimation. To achieve accurate RSS values averaging across the channels of all RSS values available on IEEE 802.11 is applied.

1.2 Research aim

The aim of the research presented in this thesis is to improve geolocation accuracy inside a building using a propagation model by considering the indoor propagation environment and correctly determining the presence of walls between a sensor and a client.

1.3 Research hypotheses

- **Hypothesis 1**: By applying frequency diversity to (WLAN) RF signals inside a building the spread of RSS values due to multipath can be minimised.

- **Hypothesis 2**: By determining the presence of walls between a location sensor (AP) in a room of known dimensions and a client, the accuracy of the location estimate may be improved.

1.4 Contributions to knowledge

In summary, the research contribution of this work falls in three categories:

- A novel method of using multiple WLAN channels to provide frequency diversity demonstrates that the effect of multipath on received signal strengths may be mitigated.

- A novel geolocation algorithm, which determines the presence of walls between sensors and clients inside a building.

- A data fusion method which improves the accuracy and reliability of reported location results.

Contribution 1: At present the use of received signal strength method for triangulation by three or more sensors is considered an inaccurate method. The Major reason for reporting inaccurate results is the multipath phenomenon inside a building. It has been demonstrated that by averaging across the WLAN channels, the resulting signal strength value remains consistent over time with very little spread as compared to the spread over individual channels. This promises to revive the use of triangulation using the signal strength method for applications such as positioning. As demonstrated, the accuracy achieved using this method is comparable to any other existing technique. Moreover the equipment used is inexpensive and available off the shelf at a current cost no more than 40 GBP.

Contribution 2: The algorithm takes as input the dimensions of the rooms which contain the sensors. The location of walls is accurately determined between a sensor and the client using signal strength threshold values. Signal strength readings processed using the method of contribution 1 is translated into distances to triangulate the position of clients. Many experiments are conducted to gain confidence on the validity of results.

Contribution 3: As discussed in Chapter 4 (4.10) and shown in results (appendix A), the final result after averaging from all sets of triangulation results for a common client always remain within the desired accuracy or expected limit. In some cases one set of triangulation results (3 sensors) gives an error of over 5m, but when combined with other sets of results, that error reduces to less than 3m. On average, the net result is close to the expected value. This method of improving accuracy and reliability is a contribution to knowledge. Many experiments are conducted to gain confidence regarding the validity of the results. A mean accuracy of 2.16m is achieved which is superior to any existing system as per the authors knowledge. The reliability of reporting accurate results less than 3m is as high as 75%.

1.5 Thesis structure

Chapter 2 reviews the literature on indoor positioning systems and forms the basis for the research presented in this thesis. The review identifies a lack of research in effectively mitigating the RF propagation inside a building.

Chapter 3 describes theoretical aspects that are required for the reported experiments. The 'Open System Interconnection (OSI)' network architecture layers, wireless communication, wireless architecture and brief security issues about wireless connections are discussed. RF propagation and diversity techniques followed by an explanation of various metrics used in determining location estimation are presented.
Chapter 4 presents the theory and the design of the proposed location algorithm. The algorithm design and logic is explained in detail. Different design features of the algorithm are explained. The impact of different features in achieving accurate results was observed by conducting experiments. Reference to a continued discussion in Chapter 6 is made where analyses of particular features is discussed in light of empirical results.

The environment, equipment and experiment setup is discussed in Chapter 5. The experiments are designed for off the shelf, low cost, easily available equipment that could be independently deployed. Chapter 5 also presents the description of the experimental method.

Discussion and analysis of results is given in Chapter 6. It is demonstrated that useful signal strength values can be attained by applying frequency diversity. Location estimation results achieved from the algorithm show that the knowledge of the position of walls in an indoor environment greatly improves location estimation. A Performance evaluation of algorithm is also covered to show achieved accuracy and reliability of reported location estimates.

Chapter 7 identifies major conclusions from the research that leads to the contribution to knowledge. Suggestions for further work are also explored.

1.6 Publications

- 'A Novel Indoor Location Sensing mechanism for IEEE 802.11 b/g Wireless LAN'. Published in IEEE proceedings for workshop on Positioning, Navigation and Communication (WPNC'04) at Leibniz University Hannover, Germany. March 22, 2007.Pages: 9-16. IEEE Catalogue Number: 07EX1645.ISBN:1-4244-0870-9: Library of Congress: 2006939401.

- Indoor Geolocation for Wireless Intrusion Detection and Device tracking. Accepted for publication in the Conference proceedings on 'The Second European Conference on Antennas and Propagation (EuCAP 2007) at Edinburgh, 11-16 November 2007.

CHAPTER 2
LITERATURE REVIEW

2.1 Introduction

This chapter reviews the literature on indoor positioning systems forming the basis of the research initiative. The structure is as follows:

Section 2.2 gives an overview of geolocation system and describes the three main components of a generic geolocation system.

Section 2.3 gives a brief review of the literature on categorisation of the geolocation systems according to the sensor technology and the method of measurement.

Section 2.4 reviews the literature regarding path loss models as applied for geolocation using RSS metrics. The existing research on the indoor environment (effects of multipath and walls) on accuracy achieved when deploying path loss models is also discussed. In the second part of the section, indoor location algorithms that deploy RSS metrics as raw data to calculate distances and location are researched. The current research trends of are investigated and less focused areas of research are explored.

Section 2.5 highlights the performance metrics in use by the research community to determine how well a geolocation system is performing. The accuracy and precision

metrics are explored in the light of the latest research and the granularity of available accuracies based on various available algorithms is presented.

Section 2.6 brings out the missing important research areas and sets the tone to formulate the hypotheses and experiments for this thesis.

2.2 Overview of a location system

A basic block diagram showing different components of a location system has been proposed by (Pahalvan, 2002) and is reproduced in figure 2-1.

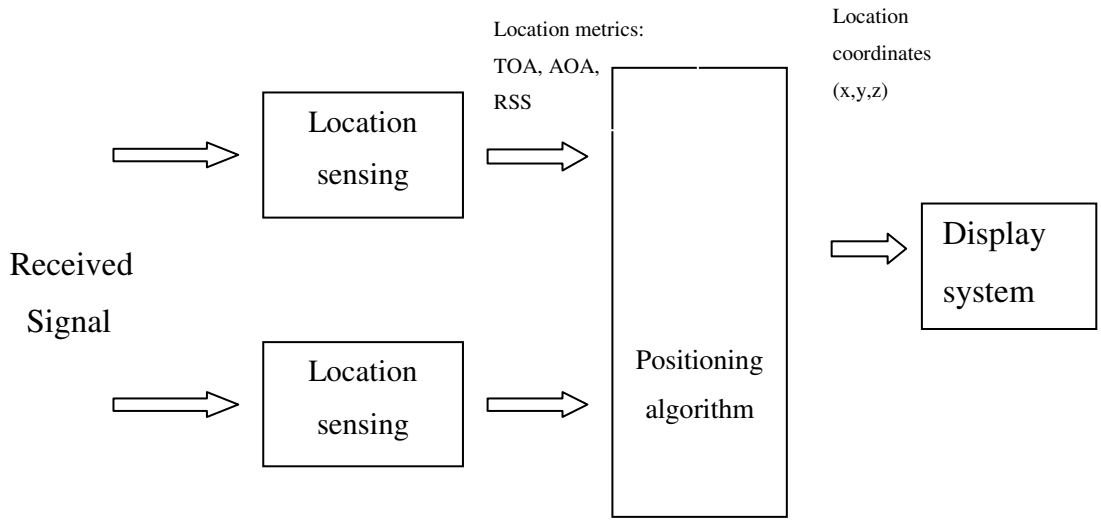

Figure 2-1 A functional block diagram of wireless geolocation system (Pahalvan, 2002)

Sensors constitute the first part of the positioning system, which can be RF, ultrasound or infrared based. These three kinds of sensors have their advantages and disadvantages discussed in section 2.3.1. The sensed signal provides information on angle of arrival (AoA), time of arrival (ToA) or received signal strength (RSS). The last two metrics are used for estimation of distance. The estimated distance is then deployed for triangulation (location algorithm), which forms the second major part of a location estimate system. The display system is the final component of wireless indoor position reporting system. It may display the x, y coordinates for a two dimensional room/area or display position in a three dimension space.

2.3 Categorisation of indoor wireless positioning system

Indoor wireless positioning system can be categorized on the basis of sensing technology (IR, RF, Ultrasound sensors) or measurement method (distance, angle) (Kaemarungsi, 2005). Hightower et al. (2001) in his work categorized location systems in another class on the basis of system properties and is not discussed here.

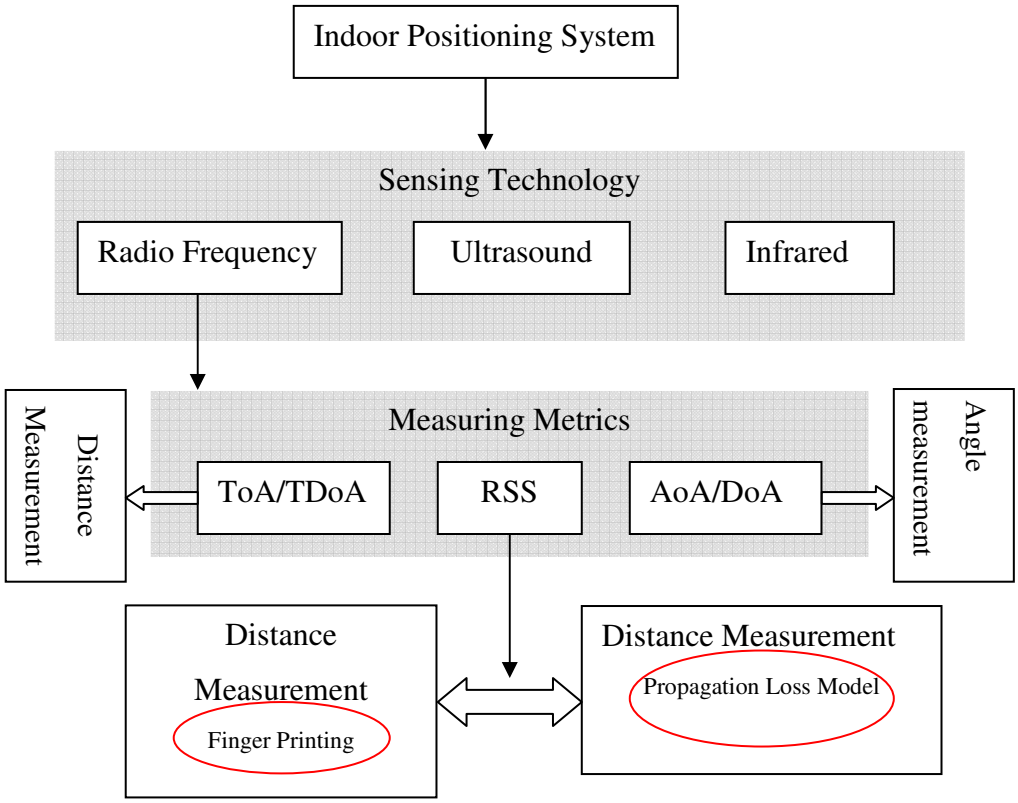

Figure 2-2 A taxonomy of indoor positioning system

2.3.1 Classification of positioning systems according to sensors

Different wireless sensors can be deployed to produce the raw data for indoor positioning system. Each has its own merits and demerits. Sensors (IR, RF and ultrasound) are limited in their performance based on the signal characteristics. All these signals are subject to reflection, diffraction, absorption and multipath and the

effect is different at different frequencies (Tauber, 2002). Moreover, propagation speed, available bandwidth, cost, safety, power constraints and regulatory constraints also play their role to influence the selection of sensors for the design of positioning systems. Depending on the requirement and application, different sensors or a combination can be used to achieve the best accuracy. In addition there are other technologies such as laser ranging, scene analysis and inertial based systems, (Kaemarungsi, 2005), but these are beyond the scope of this study. Three major sensing technologies, according to Ni et al. (2003) and Tauber (2002) are as follows:

- **Infrared (Tauber, 2002)**: Infrared technology limits the design of indoor positioning system to line of sight and short-range applications. IR propagation is fast but the effective bandwidth is limited by interference from ambient light and from other IR devices in the range. The Typical range is limited to 5m. The Indoor environment is packed with obstructions, walls and furniture of different material which also limit the range. The technology is therefore not suitable to be applied indoors.

- **Ultrasound (Ni et al. 2003)**: Ultrasound signals propagate at speed of sound $(343m/s)$. Due to this slow propagation speed, signal metrics such as TOA can exploit slow clock rates to produce accurate positioning. Systems are reported to have produced accurate results within 9 cm of the actual position for 95% of locations. Ultrasound is however, substantially effected by the indoor environment. It does not penetrate into walls and walls reflect the entire signal. Ultrasound has a short but accurate range of 3 to 10m. Changes in humidity and temperature also influence ultrasound propagation.

- **Radio frequency (Ni et al. 2003)**: RF technology fares better over its contemporaries in many aspects. RF can penetrate through walls and therefore provide a means to calculate positioning estimates over a longer range, typically 10 to 30m. The accuracy reported by this technology is not as good as reported by the technologies discussed above. Unlicensed frequencies are available freely for use by the research community and other applications.

2.3.2 Classification of indoor wireless system based on measurement methods

Indoor wireless systems may also be categorised according to the method of measurement used. The measured parameter is distance, angle of arrival or power. Different metrics used to retrieve distance and angle information are: AoA, RSS and ToA. Any of these metrics can be deployed to arrive at positioning information derived from the arriving signal. In a WLAN environment the signal characteristics in the form of the metrics can be measured at any end; access point (AP) or client (mobile station). Figure 2-2 shows the classification of indoor positioning systems according to sensing technology and method of measurement.

According to (Hightower and Borriello, 2001), lateration is the term used to measure distance. Angulation is used to measure angles. Both these terms are subsets of the triangulation technique to report location. The metrics deployed to arrive at a distance or angle measurement to report position are briefly discussed below (Caffery and Stuber, 1998; Krishnakumar and Krishnan, 2005; Pahalvan et al. 2000)

- **Angle of Arrival (AoA)**: At least two base stations (sensors) are required, which make use of antenna arrays to measure the angle of the arriving signal from a mobile or stationary unit. The accuracy of the measured angle depends upon distance. A line of sight (LoS) signal is likely to produce a correct angle. However as distance increases and obstructions between the receiver (base stations) and the transmitter increases, scattering and multipath effects cause the measurement system to report erroneous AoA, which results in wrong positioning information (Niculescu and Badrinath, 2003).

- **Time of arrival (ToA)**: RF signals travel at the speed of light in free space. The propagation delay between the transmitter and receiver can be measured to determine distance. GPS is an excellent example that uses the ToA technique to report the location of an object carrying a GPS receiver. The distance reported

by three or more sensors then triangulates to report location of the object that in the GPS case (outdoors) is 1-5m for 95% of the time (Krishnakumar and Krishnan, 2005). The line of sight (LoS) inside a building is severely affected due to materials and wall obstruction that restricts GPS performance inside buildings (Getting, 1993; Pandya et al. 2003; Jonge, 2005). This also results in multipath, which again makes the technique susceptible to reporting an accurate location. Moreover, the available equipment, off the shelf, does not provide an accurate time reference, which induces errors in measured time of flight. For example in a 802.11 wireless LAN system, according to Krishnakumar and Krishnan (2005), the typical time reference available is of the order of 100ns (30m error), which is insufficient for accurate location based on ToA. Gunther and Hoene (2005) have provided a method to increase the resolution by using multiple delay measurements and applying statistical techniques to improve accuracy. Izquierdo et al. (2006) also measures round trip time of transmitted and received frame and uses special hardware to overcome the synchronisation error of a software system.

- **Received Signal Strength (RSS)**: RSS is another metric used to measure distance from a given transmitter for use in triangulation to estimate location of an object under consideration. As shown in figure 2-3, it is used in two different techniques, 'Finger printing' and 'Propagation Loss Model', to measure distance between a transmitter and receiver.

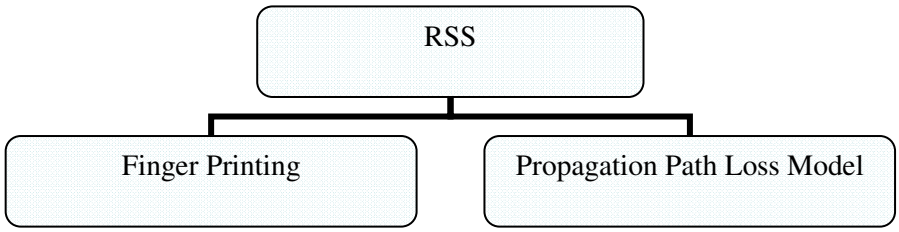

Figure 2-3 Techniques that deploys RSS for measuring distance between transmitter and receiver

Finger printing technique is based on the fact that characteristics of the propagation signal are different at each location. This means each location has a

unique ‘signature’. Hence, signal strength signatures of a wireless device are collected at different locations away from access points. This is carried out in an off line phase and a database of location finger prints is stored (figure 2-4). In an on line phase the measured RSS value is compared, using a pattern-matching algorithm, with the database having stored fingerprints and their corresponding locations to report position as illustrated in figure 2-4. The off line phase entails the tedious work of dividing the test area into grids and then hours and hours of time is spent in developing the database of collected signal strength signatures (Kaemarungsi, 2005). However, finger printing methods are often combined with a ray tracing approach in an attempt to speed up the offline process.

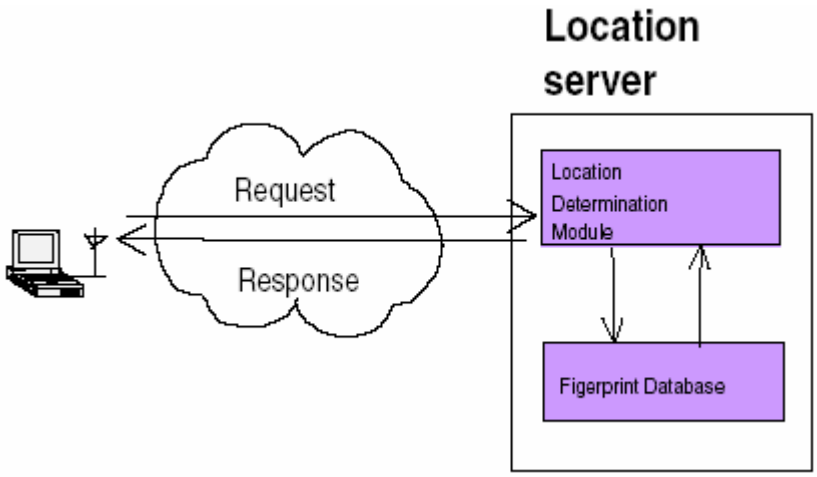

Figure 2-4 Basic setup describing location fingerprinting components (Jan and Lee, 2003)

The use of RSS in the finger printing technique is considered to be a more accurate method for reporting location (Wassi et al, 2005).

The biggest disadvantage attached to this method is the redo of the entire off line phase when any change occurs to the environment. Early research in this area has been reported by Bhal and Padmanabhan (2000). They used NN (nearest neighbour) as pattern matching algorithm to report position. The accuracies reported are 1.92m and 2.94m for 25^{th} and 50^{th} percentile. When 50 percent results are considered, the accuracy reported was 2.94m, which may be barely sufficient for many applications, especially when room sizes are small. Many

wireless clients operating in a small area could be confused. After this initial work in finger printing technique, this line of research was adopted and several different algorithms were applied to improve upon the results. Wassi et al. (2005), reports that the NN (nearest Neighbour) algorithm is the best choice to report accurate location for finger printing techniques when training data considered is not large. Results produced by Wassi et al. (2005) to compare different algorithms used in location finger printing technique are reproduced below in table 2-1

Table 2-1 25th and 50th percentile values of the distance error on the testing data (Wassi et al, 2005)

Algorithm	25th (metre)	50th (metre)
KNN (K-Nearest Neigbours) **(Wassi et al. 2005)**	1.26	2.4
MLP (Multilayer Perceptron) **(Wassi et al. 2005, Demuth, HB. 2004)**	1.39	3.09
GRNN (General Regression Neural Network) **(Demuth, HB. 2004)**	1.37	2.94
RADAR (It is only a name given to a building wide tracking and not to be confused with Radio Detection and Ranging system) **(Bahl et al. 2000)**	1.92	2.94

The above table when analyzed shows that at the 50th percentile the best results obtained are 2.94 m. More research in this area is conducted by Ganu et al. (2004) and Brunato and Kallo (2002). A good pictorial description of fingerprinting technique is proposed by Jan and Lee (2003) and reproduced as figure 2-4.

Propagation based technique is other method of measuring distance between a transmitter and receiver using reported signal strength (RSS). According to

Wassi et al. (2005), propagation techniques are less accurate when compared to the finger printing techniques. The argument is discussed in detail in the next section.

2.4 Path loss model and indoor positioning systems using wireless LANs

This section surveys the literature regarding RF based wireless indoor positioning systems. RSS is explored as a metric for measuring distances using a propagation path loss model. The popularity of wireless LANs around the world has generated significant interest amongst the research community in accurate indoor geolocation. Indoor wireless geolocation forms a vital component of wireless network hierarchy as shown in figure 2-5.

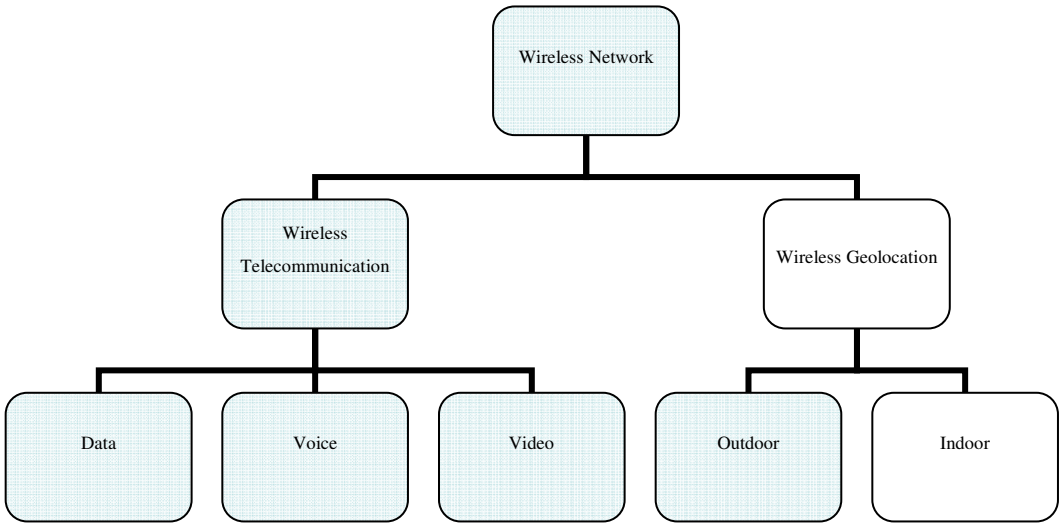

Figure 2-5 Wireless applications

Wireless LANs are based on the 802.11 a/b/g standard that operates at 2.4 and 5 GHz frequency bands. The components of wireless LANs are available off the shelf at very moderate prices. Signal strength readings can be extracted from the RF signal as it arrives at the receiver.

Different techniques of geolocation based on different method of measurement have been discussed in the previous section. According to many researchers including Wassi et al. (2005), the propagation model method using RSS is not a very accurate method to design an indoor geolocation system. According to Pahlavan et al. (2006) and Pahlavan and Li (2002), an indoor RF propagation model to determine distance between a transmitter and receiver is grossly affected by multipath and walls inside the building. That is why, more recently, the focus of research into geolocation indoors has been mainly devoted to fingerprinting technique using RSS metrics. Very little literature is available on efforts to improve algorithms using propagation models for determining accurate geolocation.

In the following sections, the discussion continues. Initially, the effect of indoor environment on RF propagation like multipath, presence of walls and their effects on received signal strength are discussed. It is followed by the remedies adopted by research community to built better indoor propagation models. At the end the algorithms deployed to report the position using propagation model are discussed.

2.4.1 The Indoor environment – Multipath and walls

The propagation parameters of indoor environment vary from the outdoor environment. Line of sight (LoS) is not usually available over any long distance. Walls exist that are made of different materials. Furniture (wood and steel) is common in offices. The density and movement of people inside a building changes rapidly. Humidity and temperature are more controllable inside a building. All of these factors cause the RF signal to reflect, diffract, scatter and absorb differently in different indoor environments. The factors discussed above produce a phenomenon called multipath (Wassi et al. 2005; Pahlavan et al. 2006; Pahlavan and Li, 2002). The signal arrives at the receiver following different paths and then combines constructively or destructively depending upon the received phases of the different signal components. The research community, including Wallbaum and Spaniol (2006) and Gustafson et al. (2006), believes that multipath is the most influential factor causing large variations in reported signal strength readings. An example of the multipath effect on RF signal inside a building is shown in figure 2-6. The error shown in figure describes delay in nano seconds for the

arriving strongest component of the signal. In figure it is shown to be delayed by ~ 38 nsec.

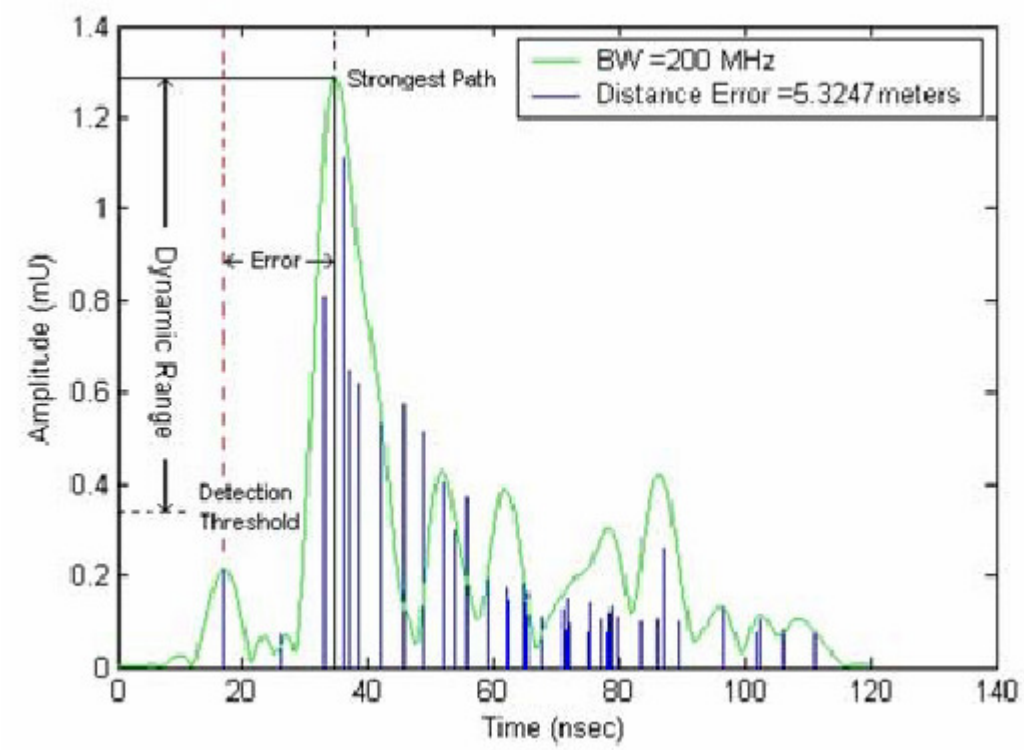

Figure 2-6 Typical indoor multipath RF signature (Gustafson et al. 2006).

In figure 2-6 above, received signal amplitude is plotted against time delay. The direct path amplitude is illustrated as being below the detection threshold of a geolocation system while the amplitude of several indirect paths is higher than the receiver threshold. These components when added together at a receiver in a WLAN, report RSS values which are distorted (Chiu and Lin, 1996). Hashemi (1993) carried out an in-depth analysis of indoor radio propagation channels. According to his findings, the multipath affect on RF signals inside a building is more severe than within the outdoor environment. In ever-present multipath conditions and temporal variations associated with the indoor propagation channel, it has been a challenging task to propose a general indoor propagation model.

The Research community has attempted to develop an indoor path loss model in the presence of walls and a multipath environment since the introduction of wireless indoor gadgets. There have been two different approaches adopted by the research community

to predict indoor propagation. In the first approach, propagation models related to those for describing free space propagation are empirically or statistically fitted to measurement data (Seidel, et al. 1989, 1991, 1992; Rappaport, 1989; Devasirvatham, 1991). In another approach electromagnetic theory is applied using ray tracing techniques such as uniform theory of diffraction (UTD) and requires detailed site specific information about the particular building (Cheung et al,1998). Ray tracing is beyond the scope of this study and will not be discussed further.

After 1997 with the inception of the *IEEE Std 802.11* (1997) and widespread adoption of indoor WLANs, it became incumbent on the research community to find more accurate ways of solving the indoor geolocation problem as there now existed a huge market for indoor applications. As mentioned by Pahlavan et al. (2006), there are tens of millions of IEEE 802.11 WLAN network cards and several billion cellular phones that are connected in various ways to the internet and can be used for RF localization. Other applications include locating instrumentation and other equipment in hospitals, surgical equipment in operation room, specific items in warehouses. However, since then, there have been few attempts to improve upon an indoor path loss model. Greater efforts have been concentrated on the finger printing technique as it alleged better accuracy as mentioned in section 2.3.2.

All path loss models are based on the principle that received signal power follows an inverse exponent law with the distance between antennas.

$$P(d) = P_o d^{-n} \qquad (2\text{-}1)$$

P(d) = Power received at distance d.

P_o = Power at 1m.

Path loss is therefore proportional to d^{-n}, where n (path loss exponent) depends upon the environment. On a logarithmic distance scale with P(d) in dB, this corresponds to a straight line path loss with a slope of $10n\log(d)$. As research progressed models begin to include losses and absorption effects due to walls, floors and other materials in a

building. The generic evolution of the path loss model is briefly discussed below (Hashemi, 1993).

Model 1: A simple model as given in equation 2-1. According to this model the reported values of n in equation 2-1 are 1.5-1.8 for LOS and 2.4-2.8 for obstructed factory channels (Rappaport and McGillem 1989; Rappaport, 1989). Remember that path loss in free space follows a d^{-2} law where n is 2. The higher values of n are due to large attenuations encountered when transmitted signals have to penetrate walls, ceilings, floors etc.

Model 2. This model also follows a d^{-n} law as in model 1. The exponent n, however changes with increasing distance. The value of n estimated from data was 2 for 1-10m, 3 for 10-20m, 6 for 20 – 40m and 12 for greater than 40m. The large values of n are due to an increasing number of walls and absorbing materials encountered at longer distances.

Model 3: This model associates logarithmic attenuations with various types of structure between the transmitter and receiver antennas. Adding these individual attenuations the total path loss can be calculated (Hashemi, 1993). Model 3 is the most adopted model in recent years as given in work by Cheung et al. (1998) and Lloret et al. (2004). In this model, effects due to walls, floors and ceiling are considered. A recent report on wall absorption at 2.4 GHz for different materials is given in Stein (n.d). The information is reproduced below in table 2-2.

Table 2-2 Signal attenuation at 2.4 GHz (Stein, n.d)

Window Brick Wall	2 dB
Metal Frame Glass Wall into Building	6 dB
Office Wall	6 dB
Metal Door in Office Wall	6 dB
Cinder Block Wall	4 dB
Metal Door in Brick Wall	12.4 dB
Brick Wall next to Metal Door	3 dB

Different materials exhibit a wall attenuation factor ranging between 2 and 12 dB. As an extension to this model Cheung et al. (1998) studies the effects of diffraction, angle dependence of attenuation factor and distance dependence of the path loss exponent. Cheung et al. (1998) compares actual path loss (straight line in figure 2-7) with the predicted path loss (crosses in fig 2-7). In Figure 2-7(a), the comparisons are for the new model while in Figure 2-7(b) they are for the conventional model (Molkdar, 1991). It is shown in 2-7(b) that conventional model does not perform well when it encounters walls and it overestimate the actual path loss by almost 40 dB as evident by the downward curving scatter plot in Figure 2-7(b). An increase in accuracy is demonstrated in new model 2-7(a).

To develop new model by (Cheung et al. 1998) consideration was given to collect site specific information like wall attenuation factor (WAF), floor attenuation factor (FAF), distance of break point (dbp) governing the value of n (path loss exponent) and effect of diffraction. One limitation of this model is that the effect of reflection is not considered and in more reflective environment it may not work very well. Moreover the break point concept is not effective when considering small rooms'. In this thesis the site specific information has been minimised and algorithm determines position of walls when only

diagonal length of each room with access point (sensor) is given as input. This also overcomes the requirement of dependency on changing path loss exponent as done by Cheung et al. (1998).

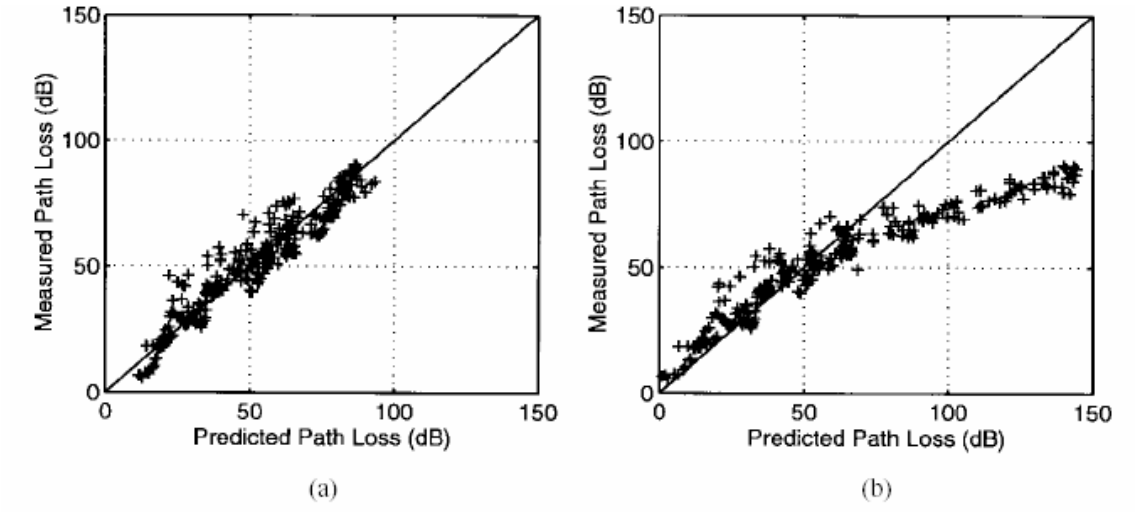

Figure 2-7 **Results in figure (a) are from new propagation model and figure (b) shows results with basic propagation model (Wang et al. 2004, Cheung et al. 1998)**

Surveying the published research suggests that multipath and walls are the main constituents that would effect the propagation inside a building. As is mentioned by Stein (n.d); Wallbaum. and Spaniol (2006); Gustafson et al.(2006); Yufei et al. (2004), multipath introduces rapid fluctuation or variations in the received signal envelop and phase. Signal components arriving from indirect and direct paths combine to produce a distorted version of the transmitted signal. Hence, a method to mitigate multipath needs to be researched. A multipath mitigated environment can provide more consistent geolocation results using path loss propagation models. A novel method of mitigating the indoor RF multipath phenomenon is presented in Chapter 6 with results and analysis.

2.4.2 Indoor location algorithms

Location estimation algorithms can be divided into two main groups; trainable and non-trainable algorithms. Trainable algorithms are applied in finger printing techniques for reporting location and such algorithms are also referred to as scene analysis algorithms.

The non trainable algorithms do not apply any kind of training to locate a position inside the building. They are usually applied to path loss models to report location. Figure 2.8 groups various algorithms which are briefly described below.

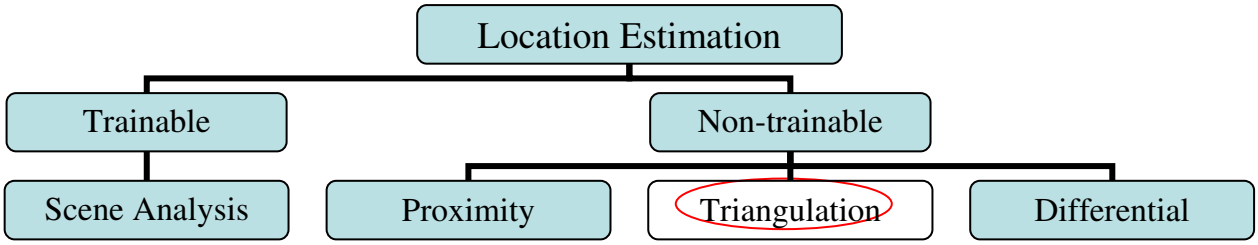

Figure 2-8 Location estimation methods

- Scene analysis method (Marias et al. 2006) deploys comparison of signatures (off line data) stored in a database with online data.

- The proximity method identifies the mobile device by the AP (access point) to which it binds. Then the location is determined by sensors when the mobile device / object are near the known location (Marias et al. 2006).

- Triangulation works on the relationship between distance and RSS (Raman et al. 2006).A Minimum of three APs is required. This method is further explained in Chapter 3.

- Differential triangulation works on the proportion between two distances as reported by two APs for a client or mobile (Jonge, 2006).

A great deal of work is seen in recent years on trainable algorithms. The focus of this thesis is on non-trainable algorithms; so no further discussion will take place on trainable algorithms. There are many algorithms already published for finger printing (trainable algorithms), and a few non-trainable algorithms. These are proximity; triangulation and differential triangulation. The Proximity algorithm is briefly defined above. As the name suggests, the mobile estimates its location with respect to the

nearest AP to which it is connected. The signal strength is measured and translated into distance using a path loss model. Non trainable algorithms including triangulation are not considered by many researchers to be a good method for location estimation inside buildings (Ni et al. 2006). All such algorithms depend on accuracy of measured signal strength. The measured RSS seriously suffers from multipath effect (Ni et al. 2006). Therefore, every indoor location system deploying non trainable algorithms reports position in two steps. In the first step some kind of filter is applied to reduce variation within the RSS values. In the next step this data (filtered RSS values) is applied to algorithms that estimate the location of a mobile. Processed RSS values, free of environmental effects such as multipath will give more accurate location estimate when applied within the algorithms. Method of reducing noise variation of RSS values and consequently position location algorithm are discussed together in the ensuing paragraphs.

- **Triangulation - Signal strength minimal value**: True values of RSS will give accurate geolocation. But we know that true values of RSS are difficult to obtain due to the hostile indoor environment. Wang et al. (2004) in his method reads a number of strength values and then takes the minimal value (actually the maximum value, because the values are negative) of that number of values and therefore taking the strongest RSS and calculate the location from there. Based on this reasoning Wang et al. (2004) proposed the minimal value algorithm. A group of signal strength values at different points are collected and then the strongest signal at each point from a group of readings is given as the true value. The authors have not detailed experiments to discuss the validity of the proposed minimal value algorithm. Moreover results on accuracy of RSS values obtained by applying this filter are also not covered in any research paper. Jonge (2005) used this method with a triangulation algorithm and reported an average error distance in metres to be 7.28m, which is not very encouraging when compared to accuracies, achieved using trained algorithms.

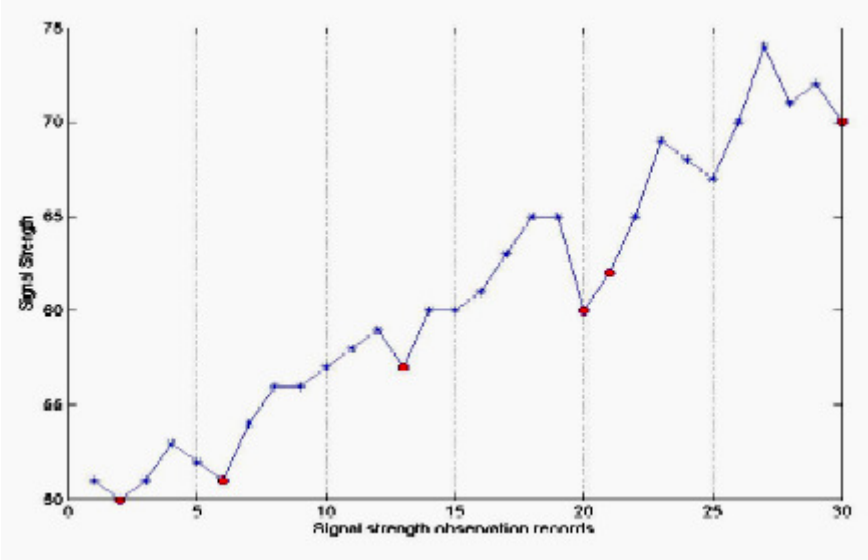

Figure 2-9 **Strongest signal from group of readings is picked as true RSS value (Wang et al. 2004)**

- **Differential method for non trainable algorithms**: In this method Wang et al. (2004) propose a differential filter to mitigate the errors that are common to all receivers, It relies on the assumption that certain types of error are common to all components of the system and if they are quantified then they can be eliminated or removed by differencing (Grant et al. 1990). According to Jonge (2005), this method makes use of the signal strength from a nearby desktop computer to calculate the difference in the RSS on specific times. Because the desktop is located at a fixed spot, it can use the RSS from the desktop to minimise the environment effects on the RSS. When close to this desktop the RSS's should fluctuate about the same rate and this way it can minimise those effects.

  The authors show experiments at 5, 10, and 15m ranges and demonstrate an algorithm that helps in reducing the standard deviation when differential methods are applied. However, it fails to produce good results as the range increases beyond 15m. Probably the environment did not remain the same over longer distances.

- **Weighted centre of mass based trilateration algorithm**: This approach again aims to improve upon the reporting of accurate geolocation inside a building. In this algorithm Sharma (2006), has deployed more than three sensors which

reports RSS values of a mobile device. Distance is calculated from a path loss model (Guvenc et al, 2003). Circles around the sensor centres are drawn based on distances converted from RSS values. The author makes use of a Kalman filter to obtain accurate RSS values. In a second phase the location is determined. All intersection points of the circles are joined by straight lines which form a polygon as shown in figure 2-10. The weighted centre of the polygon is calculated. The weights assigned to each vertex of the polygon are the sum of RSS values of the access points (sensors) which create that point through intersection of the three circles. Different polygons for all combinations of two circles are considered. Finally the weighted centroid of all polygons is calculated which is the estimated location of the mobile client (**G1**).

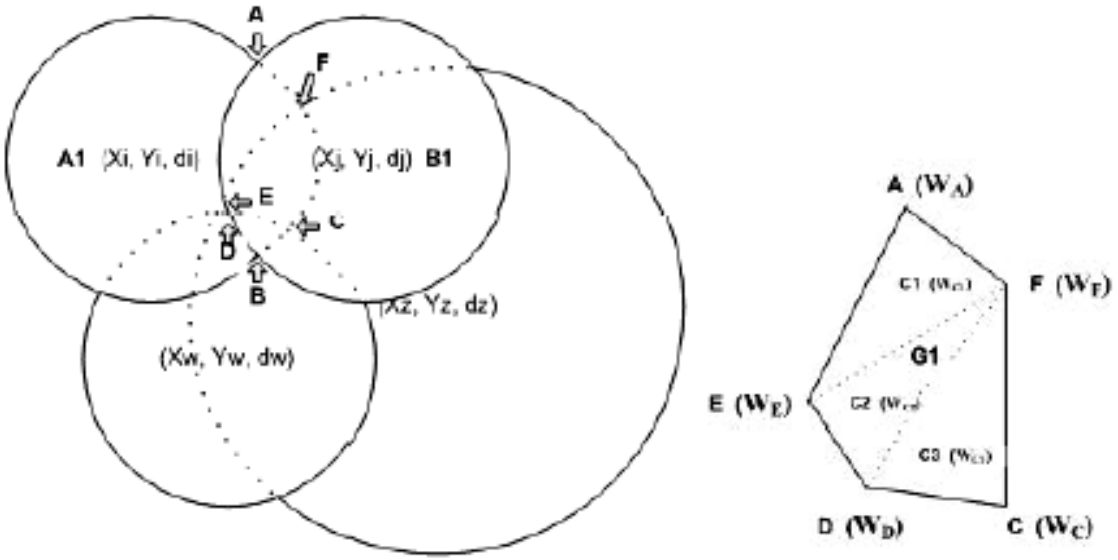

Figure 2-10 Intersection of circles and derived polygon (Sharma, 2006)

Sharma (2006) shows that accuracy increases with more sensors. Effect of human population density within the building on reported accuracy is studied. With standard strength of people inside building, reported accuracy is approximately 3.4m, 3m and 2.2m when measured by 4, 6 and 8 sensors.

- **Differential triangulation algorithm**: This algorithm is proposed by Jonge (2005). All non trainable algorithms apply calculations of distance for given RSS value from a path loss model. Direct distance is then used to draw circle for

equal radius. In the differential algorithm approach the author calculates the distance as a proportion between distances between two access points. The proof of algorithm is covered in (Jonge, 2005). This algorithm being non-trainable also depends for reporting positional accuracy on initial RSS values.

- **Ring overlapping based on comparison of RSSI (ROCRSSI):** This is a range free localization algorithm that uses ring overlapping to estimate the location of a mobile. This algorithm is claimed to be robust in hostile indoor environments. As per the explanation by Liu et al. (2004), it compares the relative signal strength of RSS and does not depend on absolute RSS values. A mobile or client knows its signal strength with respect to an AP1. Other APs (AP2, AP3) in the coverage range also know their signal strength with respect to AP1. Now the mobile compares its signal strength with AP2 and AP3. Consequently rings are formed which adjust to report final location as shown in figure 2-11

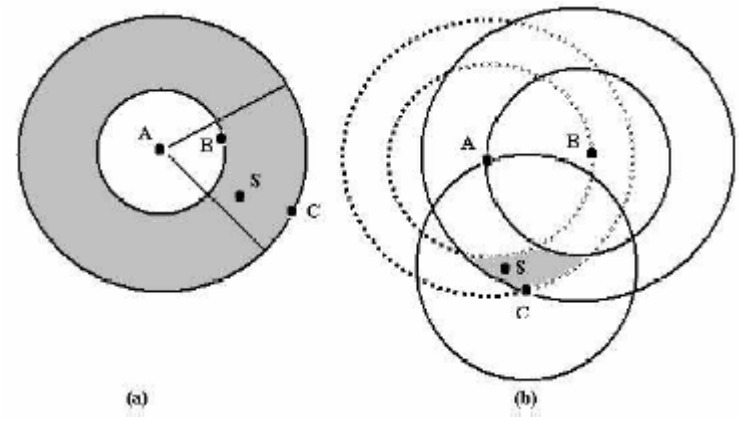

Figure 2-11 Example of ROCRSSI (Liu et al. 2004)

According to Liu et al. (2004), rings are formed around APs and mobile clients, based on a Path loss model. Again the initial correct RSS value is very important for the mobile client to compute correct rings. The algorithm has not been tried empirically to prove its validity and accuracy. Moreover, insufficient research by other peers from the research community has gone in to exploring this algorithm. Nothing can be speculated about this method with certainty.

2.5 Indoor geolocation accuracy and precision

The third and final component of a geolocation system as shown in figure 2-1 is the display system. The coordinates of the located client are displayed in XY plane. The metrics used to define accuracy of reported position are the error distance between the estimated location and the actual position of a mobile client (Kaemarungsi, 2005), measured in metres or feet. The performance of geolocation systems is defined as the error in reported metric (Alavi et al. 2003). Apart from error distance, there could be more performance metrics that may be applied to compare different existing location systems. These are delay, capacity, coverage and scalability (Krishnamurthy, 2002). Delay refers to the time taken for a system to report location. Capacity gives number of location estimates a system is capable of reporting in a unit time. Coverage tells you the total area the system can cover for reporting location. Scalability is the measure of the system performance for an extended coverage area and a greater number of devices. There is a need for further research to explore these performance metrics. As research to date has mostly given results of location systems in the form of distance error, the same metrics can be compared for different algorithms. The accuracy in positioning system has mostly been linked to precision. For instance 10m (accuracy) for 99% of measurements (precision) or accuracies of 1-5m for 93% of the time (Siebert et al. 2004). Thus accuracy refers to the range of error distance from the actual position and precision refers to the reliability that the reported position is actually the estimated position. Hence it can be deduced that as accuracy increases, the precision decreases.

Jonge (2005), in his research paper has carried out benchmarking of various existing indoor location systems based on path loss models. A table from Jonge (2005) is reproduced as figure 2-3. Jonge (2005) has included several non trainable algorithms and one trainable algorithm (RADAR – Manhattan and Euclidean). RADAR, a building wide tracking system has been developed by a a Microsoft Research group based on IEEE 802.11 WLAN technology (Bahl, 2000). Microsoft developed two RADAR implementations based on scene analysis and lateration. The accuracy offered by scene analysis is within 3m for 50% of the times and it is 4.3m for 50% of the time using lateration. Different techniques are applied in the form of Kalman filter, minimal filter

and no filter to remove noise attached to signal strength readings. Reported accuracies are given in the form of average error distance in metres. For non trainable algorithms 3 APs and many APs are considered in turn. For indoor environment distance of upto 20m is considered and algorithms are tested for accuracy as given in table 2-3. Detailed indoor environment is not defined by Jonge (2005). For RADAR Bahl (2000) has reported an accuracy of 3m for 50% of the time using scene analysis, however Jonge (2005) in another environment reports accuracy of 4.49m for RADAR but using Kalman filter. Similarly for 'Triangulation' Jonge (2005) uses Minimal and Kalman filter to remove noises attached to RSS values. In proposed algorithm (this thesis) RSS variation is controlled by a new method (frequency diversity) using existing 802.11 frequency channels. It was concluded by Jonge (2005) that the trainable algorithm produced superior accuracy compared to all the non-trainable algorithms including triangulation, proximity and differential triangulation. However, the author has omitted a triangulation algorithm proposed by (Sharma 2006) and, as explained in figure 2-6 above, this algorithm performs better as number of APs is increased. With 4 APs, Sharma (2006) has claimed an average accuracy of approximately 3.4 metres as deduced from graphs presented in his work. This is the only existing system which claims to give such an accuracy using a propagation path loss model.

Table 2-3 'Average error distance in meters' and 'delay' for different algorithms (Jonge, 2005)

	No Filter	Minimal	Kalman	Time(ms)
Proximity	6.81	5.99	5.96	60
Triangulation (3 AP's)	6.61	5.86	5.77	80
Triangulation (Many AP's)	7.59	7.28	6.96	90
RADAR (Manhattan Distance)	5.80	4.77	4.49	3100
RADAR (Euclidean Distance)	5.32	4.22	4.21	3100
Differential Triang. (3 AP's)	7.48	6.64	6.50	70
Differential Triang. (Many AP's)	6.79	6.28	6.36	130

Kaemarasungi (2005), also compares the accuracy and precision reported by trainable algorithms normally used for the finger printing technique. Accuracies reported by different algorithms range from 6 ft to 40 ft for 90% of the time. The same is reproduced in Table 2-4.

Table 2-4 Performance comparison of indoor positioning system (Kaemarasungi 2005)

System	Algorithm Type	Accuracy and Precision
RADAR (Bahl, 2000)	Nearest Neighbour	Within 2.1336m
Saha et al.(2003)	Nearest Neighbour & Neural Network	No specified accuracy, 90%
Roos et al.(2002)	Bayesian	Best within 2.52m, 90%
Battiti et al.(2002)	Bayesian, Neural Networks and weighted K nearest neighbours	All within 4.87-5.18m, 90%
Ladd et al. (2002)	Bayesian	1.52m, 77%
Prasithsangaree et al.(2002)	Weighted K-nearest neighbours	7.62m at 75%& 12.19m at 95%
Youssef et al. (2003)	Bayesian	Within 2.133m, more than 90%
Xiang et al. (2004)	Baysian with RSS distribution model	Within 1.82m, 90% (static device.

The accuracy achieved in table 2-4 can be analysed more realistically, if the parameters and environment is described for each case. Same can be seen in Table 2-5 which give parameter comparison for indoor positioning systems taken from Kaemarungsi (2005) and reproduced.

Table 2-5 Parametric comparison of indoor positioning systems (Kaemarungsi 2005)

System	Spacing	Positions	Samples/Pos.	APs	Orient.	Env.
RADAR (Bahl, 2000)	Nonuniform	70	80	3	4	Hallway
Saha et al.(2003)	Min. 3.12m	19	1200	3	N/A	1-floor
Roos et al.(2002)	Uniform, 2m	155	40	10	N/A	1-floor
Battiti et al.(2002)	N/A	257	N/A	6	N/A	1-floor
Ladd et al. (2002)	3m,	11	1307 packets	5	2	Hallway
Prasithsangaree et al.(2002)	1.5m,3m	60	40	2-7	4	1-floor
Youssef et al. (2003)	1.5m	110	300	4	N/A	Hallway
Xiang et al. (2004)	N/A	100	300 (2sec/sample)	5	4	1-floor

2.6 Conclusion

The unprecedented growth of wireless LANs in the last decade or so has attracted the research community to explore the hidden advantages linked with the technology. One area where researchers have focused is indoor geolocation. After the standardisation of 802.11 b/g (IEEE standard, 1997), research for indoor geolocation commenced at full pace. Indoor geolocation may be classified according to either measurement technique and/or sensor technology as used in its design. Two types of algorithm are found in existing research that use RSS metrics to report location of a mobile client inside a building; trainable and non trainable. Trainable algorithms are those which are used in scene analysis methods such as finger printing and they involve an off line phase when a database of RSS signatures is stored for later comparison in an online phase. The second group of algorithms are non trainable such as triangulation. The indoor propagation environment has a very serious effect on such algorithms when attempting to report accurate location, which otherwise might work very fine in outdoor environment e.g. GPS (Small et al. 2000).

A generally applicable path loss model is difficult to construct for the indoor environment and therefore it is difficult to attain good accuracy in reported geolocation using triangulation. The measurement metric, RSS, varies drastically due to multipath and obstructions such as walls. The Variation of RSS can be as much as ±10 dB (Jonge, 2005). What is missing in current research to date is effective mitigation of multipath for WLANs so that the accuracy of RSS can be improved leading to an improved positional accuracy. Moreover, most path loss models require the calibration of the losses of walls and other obstructions. There is a need to develop an algorithm that does not require detailed plan of the layout of the building such as the material of walls, number of walls etc to account for in reporting positions. We have seen in table 2-3 that existing triangulation algorithms do not fare very well when compared in accuracy with trainable algorithms (Kaemarasungi, 2005).

This dissertation provides a novel algorithm that does not require any inputs from users for calibration other than the basic dimensions of the room. The detail of algorithm

design is covered in Chapter 4 and performance with results is mentioned in Chapter 6.

CHAPTER 3

WIRELESS LANS, INDOOR PROPAGATION AND GEOLOCATION

3.1 Introduction

This chapter provides the necessary theoretical concepts for understanding the results discussed and analysed in Chapter 6. Three fields, wireless LANs, indoor propagation and geolocation are covered in some detail. The chapter is structured as follows:

Section 3.2 (IEEE 802.11 Wireless LAN) provides basic theoretical concepts regarding wireless network components, types of wireless networks and an overview of the OSI layers with an emphasis on the medium access control (MAC) and Physical layers. The MAC layer is discussed with the scanning, authentication and association processes explained. The Physical layer description includes PLCP and PMD sub layer, followed by an explanation of received signal strength indicator (RSSI) and 802.11 frequency channels.

Section 3.3 (Indoor RF Propagation) describes the Friis transmission formula, and the concepts of path loss and free space loss. This is followed by a discussion of the sensitivity of measured distance with change in RSS. At the end of the section the phenomenon of multipath propagation inside buildings is presented.

In section 3.4 (Indoor Geolocation), diversity techniques are described followed by an explanation of triangulation techniques and error estimation. Triangulation algorithms were also explained at some length in Chapter 2.

3.2 IEEE 802.11 Wireless networks

The use of wireless networks has grown exponentially in recent years. Prior to 1997, when the IEEE 802.11 standards (referred to henceforth as 802.11) were published, the use of wireless networks was minimal and users had to rely upon single vendor solutions to set up networks. Since the standardization of 802.11, the ease of utilization, flexibility and properties such as mobility, cost effectiveness and ease of deployment has fostered tremendous interest amongst consumers to deploy more and more wireless networks. The acceptance of wireless 802.11 in offices, buildings, homes and industry is highlighted by the fact that all new laptops come already equipped with 802.11 b/g wireless adapter cards. On top of this, easy and simple network set up procedures allow every one to connect to any network with stroke of a key. This feature of mobility has relegated the traditional wired network as did the mobile telephone to its contemporary the landline phone.

802.11 wireless networks operate in the frequency range of 2.4 GHz ISM-band. The ISM (industrial scientific medical) bands are generally license free provided that devices are low powered.

3.2.1 Wireless network components

There are three basic components of a wireless LAN. These are access points (APs), a wireless medium and a station or client (laptop). These are defined below (Gast, 2002).

- Access point: The AP bridges the gap between a client and the wired network or internet.

- Wireless Medium: Air acts as a medium between a client and an AP or another client. The RF physical layer provides the wireless medium to transfer data between stations or a station and an AP. The 802.11 architecture allows multiple physical layers to be developed to support a single 802.11 MAC (Medium access control).

- Client/Station: Networks are built to transfer data between clients or between clients and an AP. Clients are computing devices with wireless network interfaces. Typically clients are laptops.

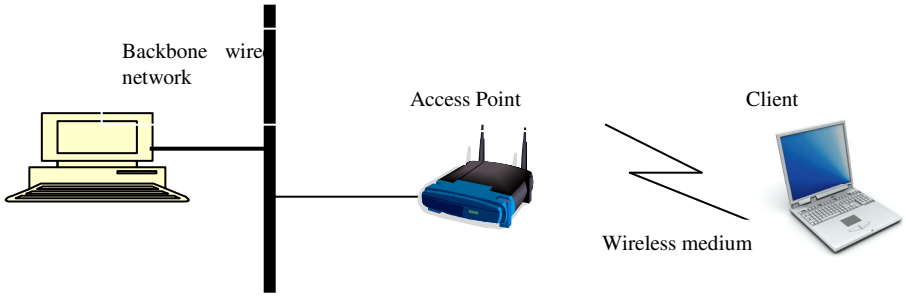

Figure 3.1 Components of an 802.11 LAN

3.2.2 Types of networks

The 802.11 standard divides wireless networks into two main categories; Basic service set (BSS) and extended service set (ESS). The basic service set is further sub divided into two components, which are; Independent basic service set (IBSS) and Infrastructure basic service set (BSS). These are briefly explained below:

Independent basic service set (IBSS): The smallest possible 802.11 wireless network is an IBSS between two clients/stations. An IBSS does not require an access point. All clients/stations on IBSS communicate directly with each other. An IBSS is also referred to as an ad hoc network. This type of network is usually set up temporarily to cover a meeting or conferences where people connect on an ad hoc basis to communicate with each other. The network connections terminate at the end of the meeting or conference.

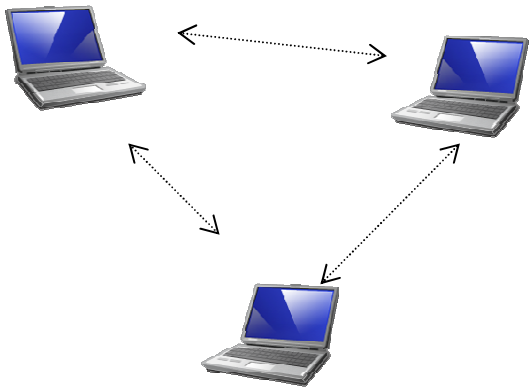

Figure 3.2 Independent basic service set

Infrastructure basic service set: The BSS can be modified to include an AP to form a infrastructure basic service set. All communication between the clients/stations now take place through the AP. Stations cannot communicate directly. This approach offers several advantages over an IBSS:

The coverage area between two clients/stations is increased, since this is determined by the AP.

The AP can assist stations in preserving power. A station may enter a power saving mode. The AP can then buffer all data frames directed to that station. Hence, battery operated stations can turn off their wireless transceiver and power up only to transmit and retrieve the buffered frames from the AP (Gast, 2002).

A wireless connection to the internet may be provided via typically an ADSL modem at home or on office LAN.

A mobile station can associate with only one AP at a time. However, there is no restriction on the number of mobile stations that can connect to a single AP (Gast 2002).

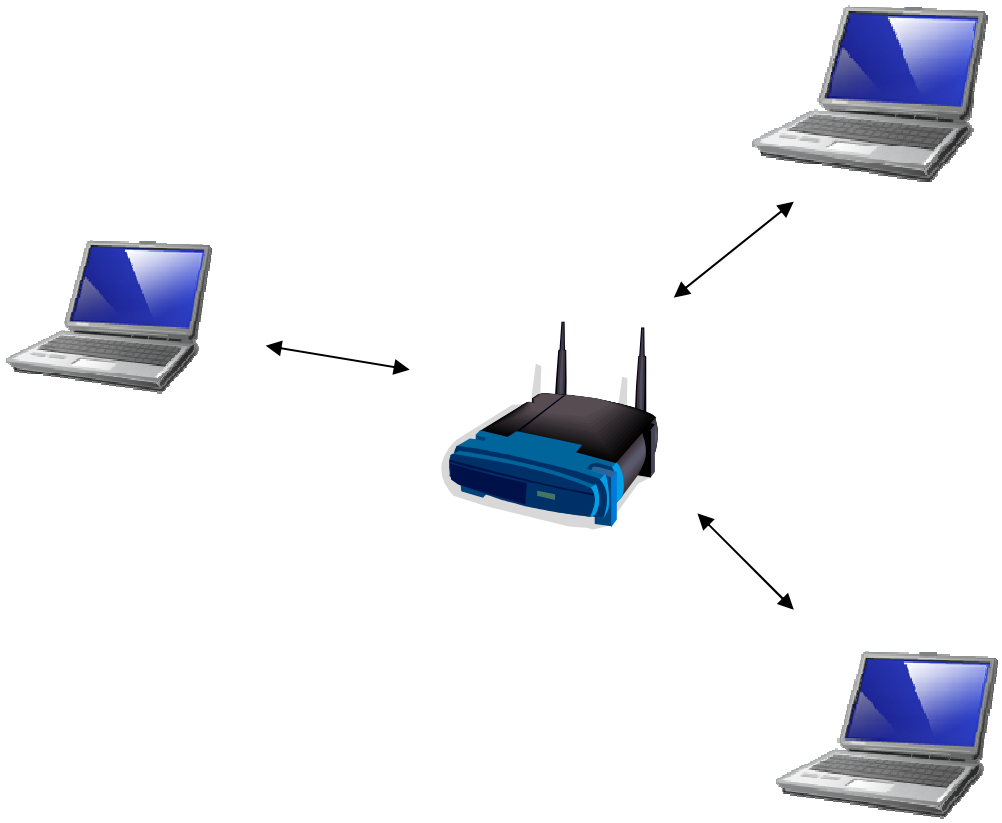

Figure 3-3 Infrastructure Basic Service Set

Extended service set (ESS): combining a number of BSSs to cover a larger area wireless area as shown in figure 3-4, creates an ESS.

In this example, four BSSs are connected to form an ESS. Any mobile station can move to any BSS and address any mobile client/station in any BSS. All frames are routed through the AP to which a client is associated. Any request from the outside world is addressed to the single MAC address of the router, which distributes it on the backbone Ethernet. The AP to which addresses the mobile is associated gathers the frames and forwards to the mobile station.

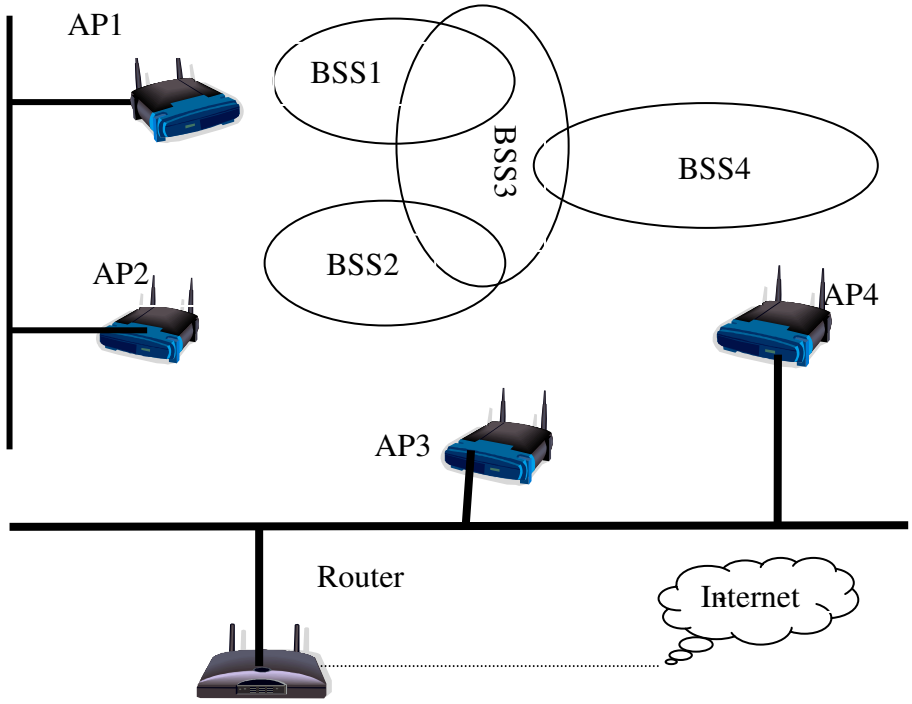

Figure 3-4 Extended Service Set (Gast,2002)

The management of association between clients and the APs within an ESS is an important consideration. All APs need to know details of the clients / mobile stations connected to different APs within the ESS. In figure 3-4, AP4 must be aware of stations associated to AP1. If a station on AP4 sends a frame to a station on AP1, the bridging engine inside AP4 must then forward this frame to AP1, where it is sent to the intended station. This is ensured by the inter access point protocol (IAPP).

3.2.3 OSI model - Overview

The OSI model (Open system interconnection reference model) is a layered, abstract description of communication and computer network protocol design (Wikipedia, 2006). The OSI model consists of following 7 layers starting from top:

Table 3-1 Overview of OSI model (Wikipedia, 2006)

Layer		Data Unit	Functions
Application	Host Layers	Data	Network process to application
Presentation			Data representation and encryption
Session			Inter-host communication
Transport		Segment	End to end connections (TCP
Network	Media Layers	Packet	Path Determination and Logical Addressing (IP)
Data Link		Frames	Physical addressing (MAC and LLC)
Physical		Bits	Media, signal and binary transmission

These layers are referred to at length in *ISO* (1982) and will not be discussed here except for the MAC and Physical layers, which are briefly discussed in the following sections.

3.2.4 802.11 MAC layer:

The Medium access control layer (MAC) is a common platform provided by 802.11 to ensure communication between access points and wireless clients/stations. The physical layer of 802.11 families such as 802.11a/b/g is used for transmission or reception of 802.11 frames. Some of the important functions performed by the MAC layer are explained below; especially those that relate to the infrastructure BSS architecture of wireless networks:

- **Scanning (Geier, 2002)**: According to the standard, *IEEE standard 802.11* (1997) both passive and active scanning is possible. Passive scanning, receive mode only, is compulsory. The network interface card (client's NIC) scans the wireless medium for any beacon frames transmitted from APs in the surrounding coverage area. The beacon frames contain basic information about the BSS

including SSID (name of AP) and available data rate. APs transmit beacon frames at typically 100 ms intervals by default which can be changed or switched off. The client/station also measures the received signal strength from beacon frames. Based on this information it decides to connect with one of the AP in the vicinity.

In active scanning, the radio network interface card (NIC) initiates the process by sending a probe frame. All APs in range immediately respond by returning a probe response.

- **Authentication (Geier, 2002)**: Another service provided by the MAC layer. Before the client or station can connect to the network through an AP, its identity must be verified. 802.11 provide two authentication methods; mandatory Open system authentication or Shared key authentication. The mandatory open system authentication is a two-step process as shown in Figure 3-5.

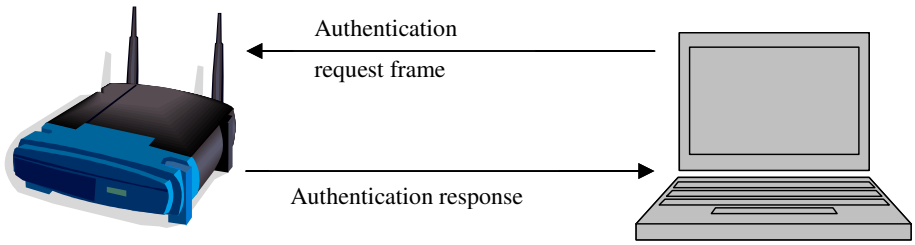

Figure 3-5 Open system authentication – two step process

The station or client initiates an authentication request frame. If the AP is configured for open system authentication then an authentication response is sent to the client for permission to associate. Where an AP is configured for shared key authentication then permission to associate the AP is denied through an authentication response frame.

The shared key authentication process (optional) involves four steps as specified by 802.11 standard. These are shown in Figure 3-6.

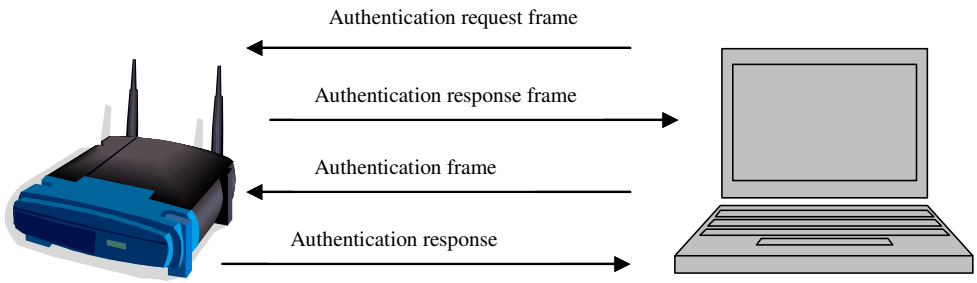

Figure 3-6 Shared key authentications – 4 steps process

An identity check is performed on the station/client with NIC, which asks for permission to associate. It first sends an authentication request frame. The AP sends response frame by adding a challenge text for client to apply encryption key. The encrypted challenge text is sent back to AP via another authentication frame (third step). The AP decrypts it using the encryption WEP (wired equivalent privacy) key. If the text is the same, then the authentication is valid and the client with the NIC is authenticated in a final authentication response. The client can now associate.

WEP is not very secure (Borisov et al., 2001; Walker, 2000). There are more preventive security standards now available which are considered to be more secure than WEP. The WPA (WiFi Protected Access) standard was introduced to account for the security vulnerabilities of WEP. However, recently some weaknesses in WPA have been highlighted (Moen et al. 2004). In 2006, IEEE 802.11i (WPA2) was ratified which is an extension of WPA. A wireless network that implements a complete set of the 802.11i standard is called a Robust Security Network (RSN).

Association (Geier, 2002): Once authenticated, the radio NIC must associate with the access point prior to sending data frames. Association is necessary to synchronize the radio NIC and access point with important information, such as supported data rates. The radio NIC initiates the association by sending an association request frame containing elements such as SSID and supported data rates. The access point responds by sending an association response frame

containing an association ID along with other information regarding the access point. Once the radio NIC and access point complete the association process, they can then send data frames to each other. Vice versa, a station has to disassociate itself from an AP to get off the network. The MAC (Medium access control) is, however, designed to accommodate stations which leave networks without formally disassociating (Gast, 2002).

There are more services such as clear to send/ ready to send (CTS/RTS), station power consumption, etc which are elaborated in Gast (2002) and are not discussed here since they are not directly relevant to the work involved in this thesis.

3.2.5 802.11 Physical layer

The lowest Physical layer in the case of wireless communication and networking changes from wired to wireless (RF). The physical layer logical architecture is given in figure 3-7. Remaining layers are referred at length in *ISO* (1982) and will not be discussed here.

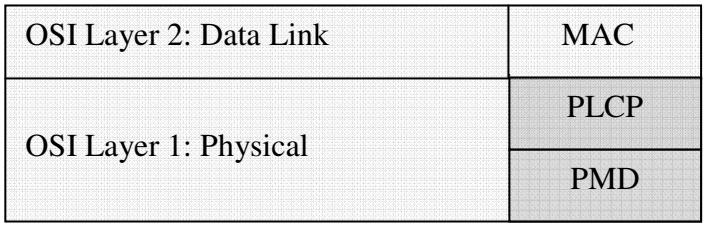

Figure 3-7 802.11 Physical layer logical architecture (Gast, 2002)

The items mentioned in figure 3-7 are specified by the 802.11 standards for the physical layer. The two components of the Physical layer are the Physical layer convergence procedure (PLCP) and Physical medium dependant (PMD) sublayers. The interaction between MAC and the Physical layer is governed by the PLCP sublayer, which directs the PMD to transmit and receive data frames as instructed by the MAC layer. The interaction between MAC and physical layer is further explained using Figure 3-8.

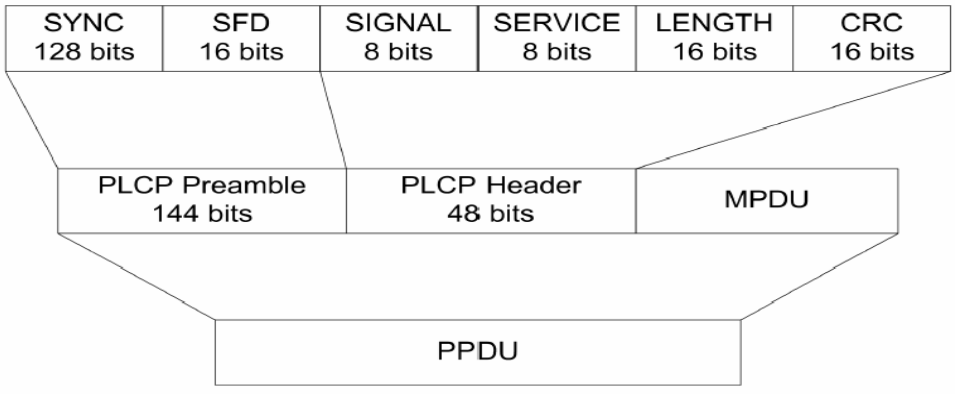

Figure 3-8 PLCP protocol data unit frame (Mobile computing, 2007)

- **PLCP Sub Layer** : The PLCP sub layer acts as a coordinator between the frames of MAC and the radio transmissions. When the MAC layer requests the PLCP to do so, the PLCP prepares MAC protocol data units (MPDUs) for transmission. The PLCP takes each 802.11 frame that a station wants to transmit and forms a PLCP protocol data unit (PPDU) (Geier,2002). The PPDU is in a format suitable for transmission by the PMD sublayer. In the process, PLCP adds its own header and preamble to MPDU in forming a PPDU (Gast, 2002). Further description of the PPDU frame fields can be found in Geier (2002).

- **PMD Sub layer**: The second sub layer of physical layer is the Physical medium dependant sub layer (PMD) that works under the instructions of the PLCP (figure 3-7). This sublayer facilitates transmission and reception of physical layer data units between two stations via the wireless medium. To provide this service PMD interfaces with the wireless medium (RF) and provides modulation and demodulation of the frame. Transmit power, data rate and RSSI values are provided by this layer to the PLCP and MAC layer. The process of modulation/demodulation and other functions are not considered in this dissertation. These are covered in detail by Gast (2002) and *IEEE Std 802.11b* (1999).

3.2.6 Received signal strength indicator (RSSI)

802.11 Std 802.11b (1999) defines RSSI as follows:

"Received signal strength indicator (RSSI) is an optional parametre that has a value of 0 through RSSI Max. This parametre is measured by the PHY sublayer of the energy observed at the antenna used to receive the current PPDU. RSSI shall be measured between the beginning of the start frame delimiter (SFD) and the end of the PLCP header error check (HEC). RSSI is intended to be used in a relative manner. Absolute accuracy of the RSSI reading is not specified".

In above definition the statement 'Absolute accuracy of RSSI reading is not specified' raises few questions. Is RSSI useable as a metric? As highlighted in the above definition and additional research (Bradwell, 2002), all vendors have their own RF measurement accuracy, range of RSSI values (0 to RSSI Max) and granularity. So, different cards will give different RSSI values, which in order to standardise must be mapped to dBm using a conversion map provided by each vendor. There are however, some vendors who provide RSSI reported directly as dBm values (Microsoft developer network, 2005; Kaemarungsi, 2006; Pearn, 2004). All 802.11 equipment utilising the Broadcom chip or Broadcom wireless utility measures and report RSSI in dBm (Pearn, 2004).

Signal strength (RSSI) is measured at the receiver antenna by the PMD sub layer. It passes the channel status to the MAC layer by reporting the energy detected. This process as given in *802.11 Std 802.11b* (1999) is called the clear channel assessment (CCA). Mobile stations use the RSSI value to support the roaming features of 802.11 in which the radio card periodically scans all access points and re-associates with the access point having the strongest signal (if the current AP signal is below the specific threshold) as given by Geier (2002).

The AP used for measuring RSSI in the experiments reported in this thesis is the Linksys WRT54G, which contains the Broadcom chip to provide WIFI connectivity and has a Broadcom utility that provides RSS values in dBm (Wikipedia, 2007). RSS

(received signal strength) values in all results presented in this thesis are therefore in dBm.

3.2.7 Channel basics

In infrastructure mode, an AP and the radio card communicate directly with each other on a common channel. The channel (frequency) is set by the AP and the radio interface cards in range of this AP will tune themselves to this frequency. The radio cards then continue with the process of scanning, authentication and association as described above in sub section 3.2.4. 802.11 provides 14 channels (transmit frequencies) that an AP may set for communication with the clients. In Europe channels 1 -13 are used. Japan uses channel 14 only and USA is allocated channels 1 -11 (Geier, 2002). The following list provides centre frequencies for each channel. A spacing of 5 MHz separates each centre frequency. Note that 802.11a uses frequencies in the 5GHz band.

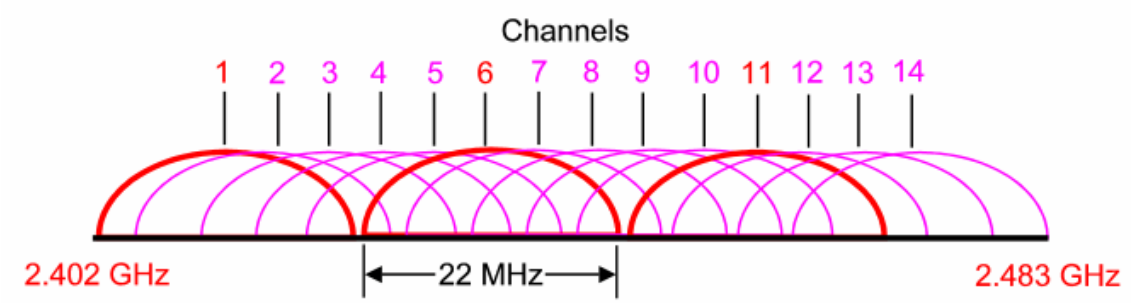

Figure 3-9 Frequency channels for 802.11 b/g overlapping (Wireless Networks [online])

However it can be seen in figure 3-9 that channels overlap and there are only 3 channels 1, 6 and 11 which do not overlap at all. For the purpose of communication these three channels can be used to set up wireless network to avoid interference if network is deployed in same coverage area. Single channel bandwidth is 22 MHz and each channel interferes with other channel. However this interference between channels becomes less as the separation of channels increases. For instance channel 1 and channel 2 have major portion of their bandwidth that overlaps and if channel 1 is compared to channel 5 there is only a very small portion of their bandwidths that overlaps.

3.3 Indoor RF Propagation

RF propagation indoors encounters many objects, bends, walls and other obstruction materials that cause reflection, diffraction, scattering and multipath of the received signal. These effects are very difficult to quantify inside a building. Propagation models are typically presented for indoor propagation based on a free space path loss model. In free space the received signal strength is a function of distance between transmitter and receiver and frequency. The received power is inversely proportional to the square of the distance between transmitter and receiver as explained below.

3.3.1 Friis Formula: Antennas in free space (Saunders, 1999)

Consider an isotropic antenna that transmits power in all directions of a sphere. If the total power transmitted is P, then the power density (S) is given by:

$$S = \frac{P}{4\pi r^2} \tag{3-1}$$

Where r is the radius of the sphere or the distance at which power density is measured. If received power is Pr, then a constant of proportionality between Pr and power density (S) is called the effective aperture (Ae) of the antenna in square metres. The P_r is then given by

$$P_r = A_e S \tag{3-2}$$

The gain (G) of an antenna is related to the effective aperture by the following equation:

$$G = \frac{4\pi}{\lambda^2} A_e \tag{3-3}$$

Where λ is wavelength.

Consider two antennas A and B separated by distance r. If the power input to antenna A is Pt (transmitter power) then the power density on antenna B from equation 3.1 is:

$$S = \frac{P_t G_a}{4\pi r^2} \tag{3-4}$$

Where G_a is the maximum gain of antenna A in direction of the path . To calculate received power on antenna B, equation 3-2 is applied to obtain:

$$P_r = \frac{P_t G_a A_{eb}}{4\pi r^2} \tag{3-5}$$

Where A_{eb} is the effective aperture of antenna B. If the value of effective aperture is replaced from equation 3-3, then the received and transmitted powers are related as follows:

$$\frac{\mathrm{Pr}}{Pt} = GaGb\left(\frac{\lambda}{4\pi r}\right)^2 \tag{3-6}$$

This is the Friss transmission formula.

3.3.2 Path loss

Now, consider two antennas, a transmitter and a receiver. Transmitted power and received power will encounter losses and gains, which are specified as shown in the figure 3-10.

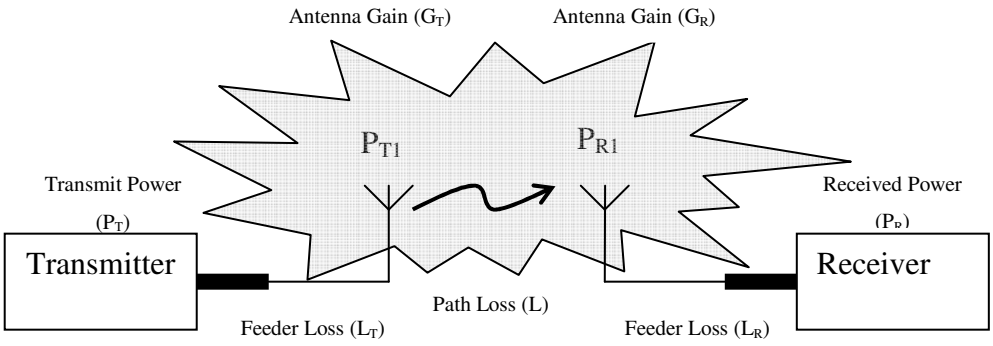

Figure 3-10 Elements involved in a wireless communication system (Saunders, 1999)

The received power is then given by equation

$$P_R = \frac{P_T G_T G_R}{L_T L L_R} \tag{3-7}$$

All gains and losses are given as power ratio and power in Watts. Effective isotropic radiated power (EIRP) can be calculated and is given as:

$$EIRP = \frac{P_T G_T}{L_T} = P_{T1} \tag{3-8}$$

where P_{T1} is effective isotropic radiated power. Similarly, effective isotropic received power is calculated as P_{R1}:

$$P_{R1} = \frac{P_R L_R}{G_R} \tag{3-9}$$

Two equations 3-8 and 3-9 together give the ratio of transmitted power to the received power which is the path loss. We can also say that the loss between in an idealized system where feeder losses are zero and antenna gains are unity then loss is the ratio between effective transmitted power and effective received power. It is given by equation:

$$L = \frac{P_{T1}}{P_{R1}} \tag{3-10}$$

Hence, from equation 3-10, path loss can be given independently of system gains and losses. The path loss expressed in decibels is:

$$L = 10\log\left(\frac{P_{T1}}{P_{R1}}\right) \tag{3-11}$$

3.3.3 Free space loss

From equation 3-6, (Friis transmission formula) and equation 3-10 , free space loss can be defined as

$$L_{FSL} = \frac{PtGaGb}{\Pr} = \left(\frac{4\pi r}{\lambda}\right)^2 = \left(\frac{4\pi rf}{c}\right)^2 \tag{3-12}$$

Where c is the velocity of electromagnetic propagation (velocity of light).

Free space loss is dependant on frequency and distance. In dB, the equation is modified, when distance 'd' is in metres, and for an assumed 802.11 channel centre frequency of 2.4 GHz is given by taking the log of the above equation and simplifying:

$$L_{FSL} = 40.23 + 20\log(d) \tag{3-13}$$

At 2.4 GHz, the free space loss is given by equation 3-13. If loss is known, distance can be calculated and vice versa.

3.3.4 Received signal strength (RSS)

Equation 3-7 can also be presented in dB as follows:

$$\Pr(dB) = Pt(dBm) + Gt(dB) + Gr(dB) - Lt(dB) - Lr(dB) - L(dB) \qquad (3\text{-}14)$$

Where
Pr = Received power
Pt = Transmitted power
Gt and Gr = transmitter and receiver gains
Lt and Lr = transmitter and receiver feeder gains
L = path loss

If we assume unity gain and losses for antennas and feeders, which is 0 dB, then equation (3-14) is reduced to:

$$\Pr(dB) = Pt(dBm) - L \qquad (3\text{-}15)$$

As explained in section 3.2.5, the PMD layer provides transmit power information to the associated sensor. It is assumed therefore that the receiver (WRT54G) normalizes the transmitted power. The above equation is thus modified as follows to give received signal strength (RSS) as:

$$RSS(dBm) \equiv -L \qquad (3\text{-}16)$$

3.3.5 Sensitivity in the path loss model

The logarithmic change in free space path loss with distance creates sensitivity to the distance-loss relationship described in equation 3-13. As distance increases, a slight change in the reported signal strength results in a larger change in distance and vice versa. This suggests that at longer distances the positioning information will also

become more sensitive. Small errors in reported signal strengths will accrue larger errors at longer distances as compare to shorter distances. Same can be seen from the graph of equation 3-13 in Figure 3-11.

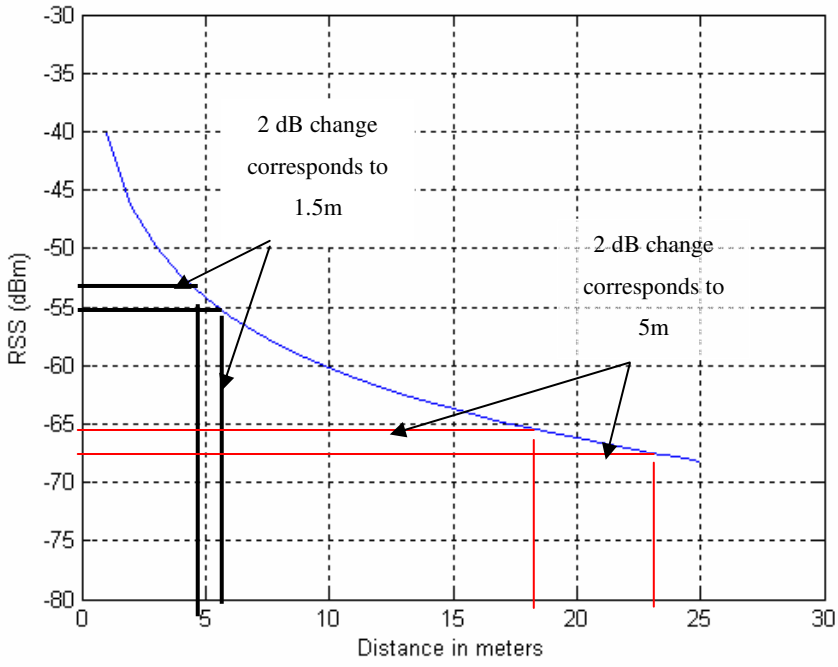

Figure 3-11 Small change in dB level causes larger change in reported distance at longer distances.

As can be seen in Figure 3-10, a ~2dBm change (~53dBm – ~55dBm) corresponds to ~1.5m change in distance (~4.5m – ~6m). Contrary to this, at relatively longer distances (~18 – ~23m), a ~5m change takes place with a change of ~2dB (~65dB – ~67dB).

3.3.6 Multipath

There are three processes of physics that govern propagation inside a building. These are reflection, diffraction and scattering (Rappaport, 1996). At 2.4 GHz, the wavelength is ~12.49 cm calculated by the formula

$$\lambda = \frac{c}{f} \qquad (3\text{-}17)$$

where c is the speed of light (3×10^8 m/s) and f is frequency in GHz. High frequencies, small wavelengths, will encounter many flat surfaces inside a room which will result in *reflection* and *absorption* of the signal depending on the signal and physical properties of the surfaces. Mostly reflection and absorption will take place due to walls, windows, ceilings and floors. The signal also experiences *diffraction* inside a room or building that occurs when obstacles have sharp edges. The amount of diffraction is subject to the signal properties (amplitude, phase) and geometry of the edge. The third phenomenon is *scattering* and takes place when the signal impinges upon an obstruction which is small as compared to the wavelength. The propagated wavefront scatters in many directions adding to the constructive and destructive interference of a signal. The multipath phenomenon takes place due to reflection, diffraction and scattering behaviour of a signal inside a building.

It has been discussed at length in Chapter 2 (sub section 2.4.1) that indoor propagation is severely affected by multipath (Saunders, 1999; Pahlavan, 2000; Stein, n.d; Parsons, 2000). Multipath occurs when a transmitted signal arrives at a receiver following multiple paths as shown in figure 3-12.

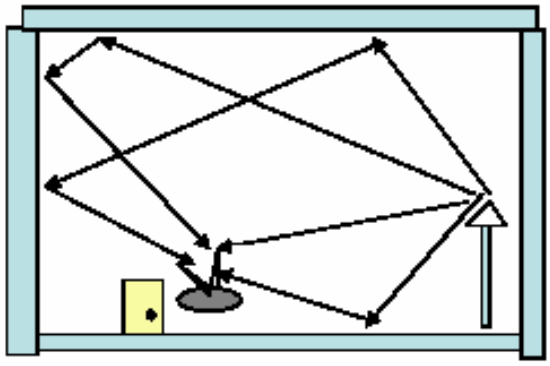

Figure 3-12 Signal arrives at receiver following multiple paths

The different components of the signal, when arriving at the receiver, superimpose. These signals, depending upon their phase at the time of arrival on the antenna, either sum constructively to the signal amplitude or destructively to produce signal strength values that vary with frequency and location. This results in rapid signal strength variation (Ni et al. 2006; Wallbaum et al. 2006; Gustafson et al. 2006). A 10 dB average

signal strength variation is common as reported by many researchers including (Youssef, 2003; Stein, n.d).

3.3.7 Small scale fading and Rician distribution

Small scale fading is described as rapid fluctuations of the amplitude, phases or multipath delays of a signal over a short period of time or travel distance. Fading is caused by interference between two or more components of same signal arriving at receiver at slightly different times. Theses waves combine at the receiver to give resultant signal which can vary widely in amplitude and phase, depending on the distribution of the intensity and relative propagation time of the waves. Results presented and discussed in research (Walker et al. 1998, Cuinas, 2001) demonstrate that Rician distribution is a suitable approximation that can be assumed for indoor propagation in LoS environment.

In indoor environment there is a dominant stationary (non-fading) component of a signal present, such as a line of sight propagation path, and then the small scale fading envelope distribution is Rician. In such a situation, random multipath components arriving at different angles are superimposed on a stationary dominant signal. As the dominant signal becomes weaker, the composite signal resembles a noise signal which has an envelope that is Rayleigh. Thus, the Rician distribution degenerates to a Rayleigh distribution when dominant component fades away (Rappaport, 1996). Let A denote the direct wave peak amplitude, and σ the standard deviation of the overall received signal envelop R (Carroll, 2003), then the Rician K-factor is given as

$$K = \frac{A^2}{2\sigma^2}$$

The Rician cumulative distribution function (CDF) is dependent on the value of K, and for k=0 it degenerates into that of a Rayleigh distribution. The Rician CDF is calculated as follows:

$$C_{rice}(R) = 1 - C_{rice}(R)$$

Where

$$C_{rice}(R) = \exp[-(k + \frac{R^2}{2\sigma^2})]\sum_{m=0}^{\infty}(\frac{\sigma\sqrt{2k}}{R})^m I_m(\frac{R\sqrt{2k}}{\sigma})$$

And $I_m(\ )$ is the modified mth order Bessel function of the first kind. Although the computation of Rician CDF appears difficult because of the summation of an infinite number of terms, in practice the summation of m=50 terms is sufficient to reduce the remaining terms contribution to a negligible level (Rappaport ,1996).

3.3.8 Frequency selective fading

From above description it is clear that both the Rician and Rayleigh fading is expected in an indoor environment depending upon the LoS and NLoS conditions. However, considering the effects of multipath propagation on these signals, let us consider the case of two frequency components within the message bandwidth. If these frequencies are close together then the different propagation paths within the multipath medium have approximately the same electrical length for both components and their amplitude and phase variations will be very similar. So, in other words, although there will be fading due to multipath, the two frequency components will behave in a very similar way. As the frequency separation increases, however, the behaviour at one frequency tends to become uncorrelated with that at the other, because the phase shifts along the various paths are different at the two frequencies. The extent of decorrelation depends on the time of spread delay since the phase shift arises from the excess path lengths (Parsons, 2000). Hence, signals which occupy a bandwidth greater than the bandwidth over which spectral components are effected in a similar way will become distorted since the amplitudes and phases of the various spectral components in the received version of the signal are not the same as they were in the transmitted version (Parsons, 2000). This phenomenon is known as frequency selective fading and appears as a variation in received signal strength (RSS) as a function of frequency.

3.4 Indoor geolocation

Indoor geolocation has been touched upon in Chapter 2. Various algorithms were discussed. Triangulation will be explained here and is subsequently used as an algorithm to produce location estimations, as explained in Chapters 5 and 6. The algorithm will be based on two steps:

- reducing variation in received signal strength (RSS) due to multipath
- A reliable path loss model

3.4.1 Diversity techniques

Applying diversity techniques can mitigate fading of the signal due to multipath. A fundamental requirement of any diversity technique is that the independent fading in received signals is uncorrelated. This means that the fading characteristics of the same signal at two different timings or two different frequencies is different. Different types of diversity techniques are briefly explained below (Parsons, 2000; Smart antenna, 2000):

- **Space Diversity (Parsons, 2000):** For multiple antennas, sufficient separation is provided such that the received signal from two antennas is uncorrelated. A half wavelength separation is typically assumed to have uncorrelated signal characteristics.

- **Polarization Diversity**: An antenna can transmit a horizontally or a vertically polarized wave. If both vertical and horizontal polarized waves are transmitted simultaneously, then the two signals arriving at the receiver will exhibit uncorrelated characteristics.

- **Angle Diversity**: Due to multipath, the signal arrives at the antenna following different paths. Hence, different signal components will arrive at different angles. Directional antennas can isolate the angle of arrival by receiving all components of the signal at different angles. These received signal components at the same frequency are uncorrelated.

- **Time Diversity**: The signal may be transmitted at intervals large enough to cause uncorrelated characteristics at the receiver. The time separation is at least as great as the reciprocal of the fading bandwidth, which is defined as twice the speed of the mobile station divided by the wavelength. The time separation is, therefore, inversely proportional to the speed of the mobile. Time diversity therefore, although not typically useful, could be useful in certain circumstances.

- **Frequency Diversity**: signals transmitted at different frequencies which sufficiently far apart exhibit different fading characteristics in a multipath environment, so that fading associated with different frequencies is uncorrelated. According to Saunders (1999), two frequency components spaced wider than the coherence bandwidth experience uncorrelated fading, providing another means of obtaining diversity.

  Different channels in 802.11 operate at different frequencies. As is explained in section 3.2.5 (Table 3-1), the separation between two adjacent channel centre frequencies is 5 MHz. Frequency diversity can be assumed between these channels. According to *Coherence – Bandwidth, Wikipedia* (2007), the coherence bandwidth Wc is given by:

$$Wc = \frac{1}{2\pi D} \qquad (3\text{-}18)$$

  where, D is the delay spread in seconds and Wc is the coherence bandwidth in Hertz. If 100 ns is the standard delay spread experienced indoors (*wireless channels*, n.d; Krishnakumar et al. 2005), then Wc (coherence bandwidth) is

calculated to be 1.59 MHz. This shows that the 5 MHz separations between channels can be assumed to be uncorrelated. The fading characteristics attached to each frequency can therefore be assumed to be uncorrelated (Parsons, 2000). Hence, we can assume that the adjacent WLAN channels are uncorrelated and there exists frequency diversity between them. This assumption forms the basis of the averaging process described later in this thesis. It may be noted that for the purpose of research in this thesis the channels considered are 1 to 13.

3.4.2 RSS triangulation and geometric dilution of precision (GDOP)

RSS triangulation is a method to locate the position of a wireless station when its distance from at least three APs (sensors) is known. The distance of the mobile station from each AP is determined from the RF signal strength (RSS) of the station at each AP. The RSS may be translated to distance using the path loss equation given in 3-13.

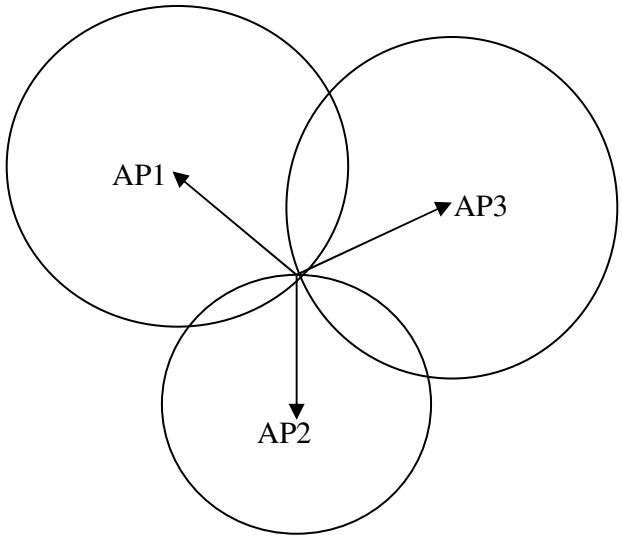

Figure 3-13 Common intersection point which gives location of the client/ station

Triangulation may take place if data (signal strength values) of a client are reported by at least three APs (Zhou, 2005). The distance translated from the reported signal strength (AP1) forms the radius of a circle drawn about that AP1. The client/station is thus somewhere on the circle of AP1 in any direction. The distance measurement and

the corresponding circle drawn about AP2 bring the possibility of position within the overlap area of AP1 and AP2. Likewise, the third AP then translates distance from the RSS of AP3. The circle drawn about AP3 now provides an intersection point through which all three circles pass. This is the exact theoretical position of the client/station as shown in figure 3-13. However, it is not usually possible to achieve an exact intersection point and instead an overlapping area is determined and the client/station is estimated to be some where (a number of possibilities) within that overlap area. Figure 3-14 shows such an area created from three sensors. Current location can be anywhere within the shaded overlap area. The precision is said to be diluted as the area grows larger (Codepedia 2007). This occurs due to the inaccuracies of RSS readings as explained in section 3.3.6. Consequently the translated distance is also erroneous as shown in figure 3-14.

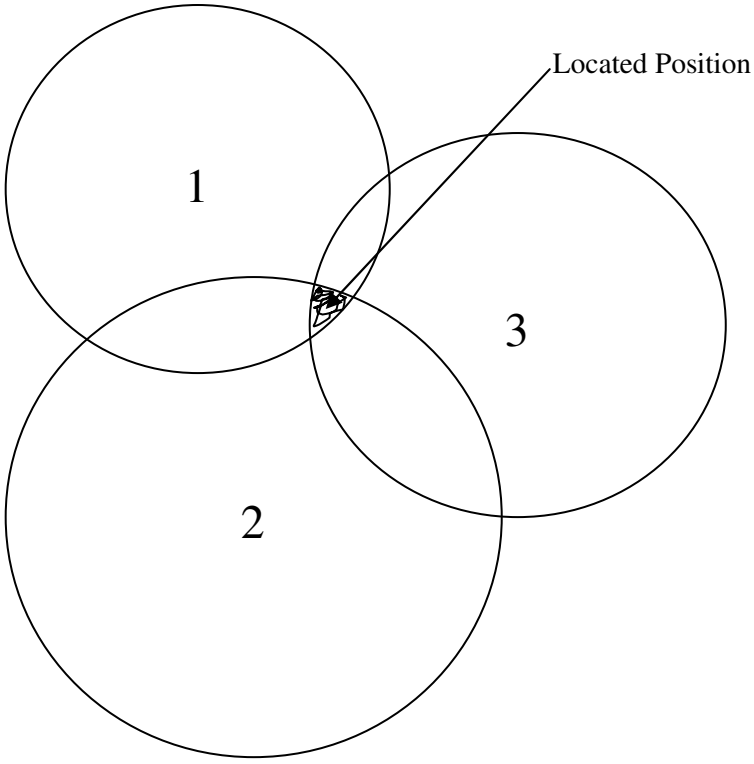

Figure 3-14 Triangulation showing overlap area in which the client is assumed to be located.

The common overlap area is considered to be the most likely area to contain the location of the client approximated as a triangle and the centre of this triangle is calculated and is referred to as the triangulation point (Wolfram Mathworld, 2007).

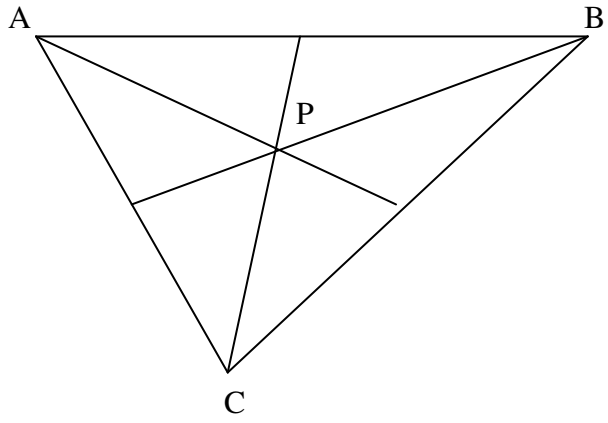

Figure 3-15 Triangulation point (Wolfram Mathworld, 2007)

Position P in figure 3-15 is the triangulation point (reported position) for sensors A,B and C, and is compared to the known position so that the actual error reported by the client may be quantified as illustrated in Figure 3-15. The error triangle (overlap area) is the area considered to be nearest to the actual position. The actual position may or may not lie within this overlap area. Stansfield (1947) refers to the triangle formed from three bearings of a target reported by three DF stations as a 'cocked hat', analogous to the problem of triangulation under discussion in this dissertation. The overlap area can be compared to the cocked hat formed from three bearings of a target reported by DF stations. According to (Stansfield, 1947), if the cocked hat formed is small then the true position will very probably be outside it; whereas if a very large cocked hat (triangle of reported position) is formed then the actual or true position is very likely to be inside it.

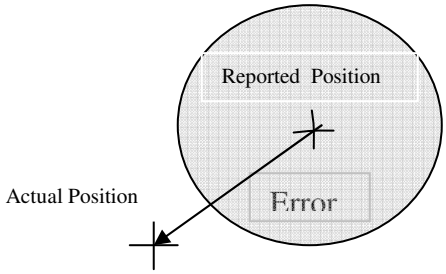

Figure 3-16 Location error between actual and reported position

The error (E) between actual position and the reported position may be calculated using the Euclidean distance formula, which is given by equation 3-19. If x1, y1 is the actual position and x2, y2 is the reported position then according to the Euclidean formula (PlanetMath, 2007).

$$E = \sqrt{(x_2 - x_1)^2 + (y_2 - y_1)^2} \qquad (3\text{-}19)$$

Due to the errors in RSS values, the overlap area, which may or may not contains the actual position, moves around this actual position (Ciurana et al. 2007) as can be interpreted from given figure 3-17.

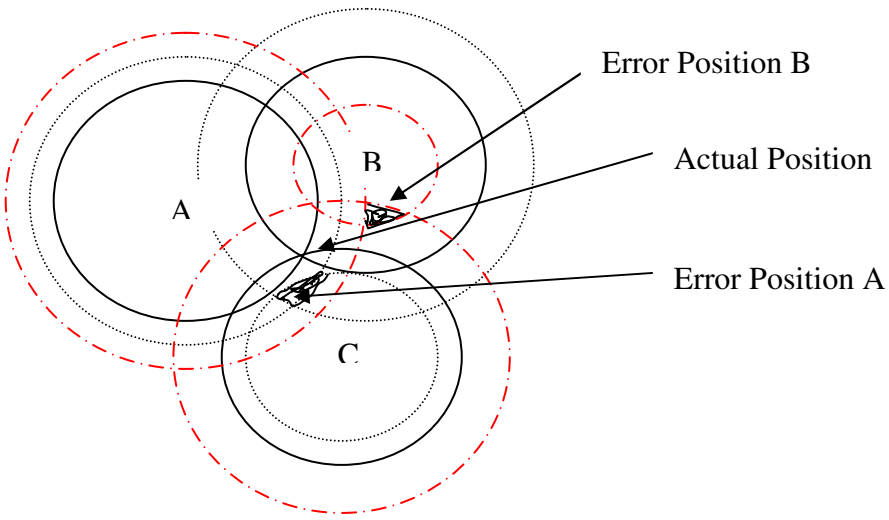

Figure 3-17 Why error estimate is away from the actual position

Three positions are shown as reported by a triangulation algorithm. The first set of three circles (solid line) intersects at a common point to give the exact location of the client. Consider the manner in which the reported position deviates from this actual position. Due to errors in RSS values, the set of circles in red (dotted) moves the position or likely overlap area away from the actual original position (Ciurana et al. 2007). Similarly another combination of circles (dotted lines), depending on the RSS values, produces a possible position of the client at another location.

A question arises here; how to predict which point in the reported triangle is closest to the actual position or in other terms how dilution of precision can be controlled. (Sharma, 2006) has proposed minimizing the error reported from more than 3 AP by using a polygon weighted method as explained in Chapter 2, figure 2-10. The philosophy is to find the centre of the polygon. For three APs, then the centre of the triangle is considered to be the reported position. With more APs the accuracy of the reported position or dilution of precision is likely to improve because more sets of data are available and by the law of averages the reliability or precision of the reported position accuracy increases. Another cause of increased dilution of precision in reported location is the wrong selection of the sensors reporting position estimation of a client. It is explained in section 6.9.2 under analysis of 'Experiment location 19'. (Stansfield (1947) on this issue discusses the most probable point within the triangle (Cocked hat) for the outdoor environment using DF stations to triangulate reported bearing of a target. Large triangles are formed. In the inside environment where the overlap area represents no more than 3 m^2, it is immaterial to find the probable point inside the triangle and instead efforts are concentrated to bring this overlap area closest to the true or actual position, as attempted by (Sharma, 2006). For indoor geolocation there is very little previously published literature on reducing errors by bringing the overlap area closer to the actual position. This issue needs further research.

CHAPTER 4
GEOLOCATION ALGORITHM

4.1 Introduction

This chapter proposes an algorithm for indoor geolocation and explains its design and features in detail. Discussion and analysis on results produced by the algorithm are covered in Chapter 6. The algorithm has been developed for reporting location coordinates of a mobile client in the x-y axis inside a building. A set of coordinates within the predefined space is used to present location of an entity by a GPS in an outdoor environment. The latitude, longitude and altitude are the set of coordinates that gives positional information of an entity in three dimensions on earth's surface. However, inside a building there are different floors and a dedicated geolocation network of wireless sensors can be set up to report location estimation on each floor independently. So, it can have set of coordinates with positional information in xy plane and floor number and may be the room number as well. Therefore, most of the research work (Kaemarungsi, 2005; Wassi et al. 2005; Wang et al. 2003, Bahl, 2000) for indoor geolocation entails study and investigation based on xy planes only. A major cause for inconsistent signal strength readings inside a building is identified as absorption due to walls and also multipath phenomenon as discussed previously in Chapters 2 and 3.

Previous algorithms have been developed to report position inside a building using triangulation (Chapter 2). However, in the presence of multipath these algorithms need to be complex to cater for variations in signal strengths. Moreover, such algorithms

require detailed inputs from the user such as the material of walls, other obstructions, orientation, detailed floor plans etc. Information on all these aspects makes an algorithm specific to particular site. Moreover, it will depend a lot on the user to give inputs which may be erroneous thus resulting erroneous location estimation. If a general algorithm with minimum of inputs is designed, it will be more desirable. None of the algorithms developed so far attempt to locate the position of walls, despite walls being the major factor determining RSS.

An algorithm with a novel design based on room dimensions only is developed to identify walls between a client and an access point (sensor). Absorptions due to walls, orientation, steel cupboards or any other structure is correctly identified and correction is applied to calculate revised estimates for received signal strengths, which are further processed with a fine adjustment through a forced overlap method to arrive at optimum RSS estimates.

The algorithm design and logic is explained at depth in this chapter. Different features relevant to the design of the algorithm are explored. The impact of these different features in achieving accurate results is observed by conducting experiments. Sections of this chapter refers, as the need arise, to the respective sections of Chapter 6 for discussion and analysis of particular features, which are discussed in light of empirical results.

Section 4.2 using a functional block diagram, elaborates the working of the algorithm. A progressive understanding of the algorithm is provided as it achieves a final location estimate for an unknown client inside a building.

Section 4.3 describes the main factors which are critical for implementing the threshold aspect of the algorithm.

The threshold aspect of the algorithm is explained in sections 4.4 to 4.6. firstly the theory of how square and rectangular rooms can be used to identify the walls between a client and the sensor is given. Wall absorption and the longest distance within a room

from centre are key factors in the design. After generalising the design, it is applied to an example test area of 450m^2 where rooms for placing sensors are chosen. The performance of an algorithm is evaluated in Section 6.9. Section 4.7 describes the design of an absolute threshold for the test area, which explains how extra absorption encountered by the sensors is detected and accounted for.

The method of applying fine corrections to the RSS values to arrive at as accurate an estimated location as possible through intelligent forced overlapping is presented in section 4.8.

Section 4.9 presents the geometric design that determines the intersecting points of the circles that corresponds to the overlap area that is likely to contain the position of the rogue client. Section 4.10 describes and proposes a data fusion process for four sets of triangulation results from combinations of three sensors. Finally, section 4.11 summarises the chapter.

4.2 Algorithm design – Functional block diagram

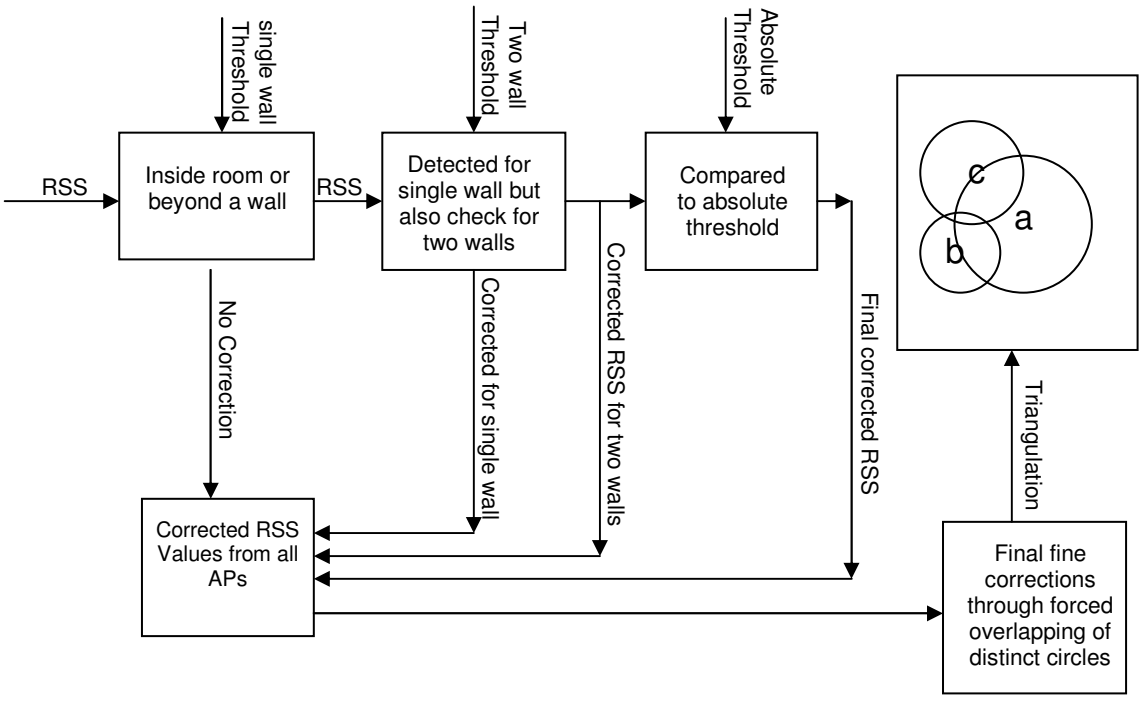

Figure 4-1 Algorithm functional block diagram

A functional diagram for the algorithm is shown in figure 4-1. The received signal strengths (RSS) of a client for each access point (sensor) is compared to a threshold value to determine the presence of one or more walls in the following sequence:

- In step 1 the collected RSS value from the first sensor is compared against a calculated threshold to ascertain if the location of client is within the room or outside the room which houses the AP. If the RSS is greater than the threshold then it is assumed to be inside the room and the RSS value is stored in 'Corrected RSS Matrix' without applying any correction.

- If RSS is found less than the one-wall threshold for the AP under consideration then it is assumed to lie beyond the wall. This RSS value is now compared to a second threshold value to ascertain whether the client is located beyond the two walls. If the RSS is greater than the two wall threshold value then a correction of 5 dB is applied with the assumptions that the client is beyond one wall and the value is stored in the 'Corrected RSS Matrix'. 5dB is assumed as average wall absorption factor based on previous research and experiments conducted in test area as explained in section 6.4. This is illustrated as the second block in the block diagram.

- If during comparison in the second block shown in the block diagram (figure 4-1), RSS is still less than the two wall threshold, then accordingly the original RSS value is corrected by 10 dB.

- In the next step, the third block, RSS values which are corrected are again compared to an absolute threshold value. If the RSS is less than the absolute threshold value of individual sensors then the RSS is decreased to assume the absolute threshold set for that sensor as explained in section 4.7. The value so achieved is then stored in the 'Corrected RSS Matrix'.

- The above steps are followed for data collected from all access points (APs). Once data from three access points is stored in the Corrected RSS matrix, three circles are generated corresponding to the distances given by the corrected RSS

values. If the circles are not overlapping then they are expanded or contracted to overlap. The resulting triangulation is shown in the block diagram.

For the purpose of error estimation, the algorithm is fed with the actual position of the client. The centre of smallest overlap area is taken as the location reported by the algorithm. The distance error is calculated using the Euclidean formula to determine the deviation between the actual position and the position reported by the algorithm.

The above paragraphs represented a brief overview of the operation of the algorithm. The next few sections will present the rational and thinking in the design of the algorithm. A general equation is derived to determine a simple criteria for determining the presence of a client in a room from the length of the room side and RSS, design of room thresholds; how overlapping is enforced and finally how the likely location is determined from available overlaps. Each section as required will refer to Chapter 6 where the corresponding results will be analyzed and discussed to validate the algorithm. Analysis and discussion will be based on empirical data collected from 4 different access points placed in a test area of 450 m^2 as explained in section 4.10.

4.3 Factors critical in implementing the threshold algorithm

There are two major factors that affect the implementation of the algorithm. These are the effects of multipath on RSS and the relationship between RSS, room size and the client location..

4.3.1 Multipath environment

The nature of the environment inside a building is such that RF propagation is severely affected by multipath distortion. This will affect the received signal strength readings reported by sensors. It is important that deviation in received signal strengths recorded at same point be minimised. This is determined by averaging across the channel as described in section 6.3.2. By applying this technique, the received signal strengths are accurate and with a residual spread of readings within a 3dB range. Any error in the RSS leads to an error in range calculations and thus an error in locating the client.

4.3.2 Selecting room for placing access points

The second factor that influenced the design of the algorithm is the dimensions (shape) of the room. It is assumed that the rooms where access points (sensor) are placed are square or rectangular in shape. The relationship between room dimensions, RSS and client location is investigated firstly for a square room.

4.4 Design threshold for a square room

The following assumptions are made for the threshold design to work for a square room.

- Each sensors is placed in the centre of the room
- The wall loss is considered to be 5 dB.
- The room dimensions are known
- The room is square
- The received signal strength follows free space path loss.
- AP (sensors) and client antennas are omni-directional

Requirement To determine that the client is beyond the wall.

Solution: Consider the conditions where the client is assumed to be at the shortest distance from the AP that is just beyond the wall as shown in figure 4-2. Using equation 3-13 (free space loss equation), the received signal strength of a client (RSS) can be calculated. Client placed just beyond the wall will have a loss (RSS), given by

$$RSS = -[40.23 + 20\log(Xs) + 5] \quad \text{(dBm)} \quad \text{(4-2)}$$

Where

RSS = received signal strength of client just beyond the wall in dBm

Xs= small side half length

5 is the assumed wall absorption in dB

Consider figure 4-2, where client's position, Xs (half side length) and diagonal length (X_d) are shown. From the figure it can be explicitly deduced that the signal strength (RSS) of a client must be less than the signal strength of Xd (diagonal length) which is represented by L_{Xd}, in order to guarantee that the client is beyond the wall. So, the condition becomes:

If $RSS < -L_{Xd}$ then client is outside the room (4-3)

If this condition is true then the probability of having client inside the room is zero, which means that client is outside the room. The 5 dB wall loss added in equation 4-2 ensures that the clients (RSS) circle will be greater than the threshold circle L_{Xd} as shown in figure 4-2. This condition allows algorithm to detect wall between client and the access point with certainty.

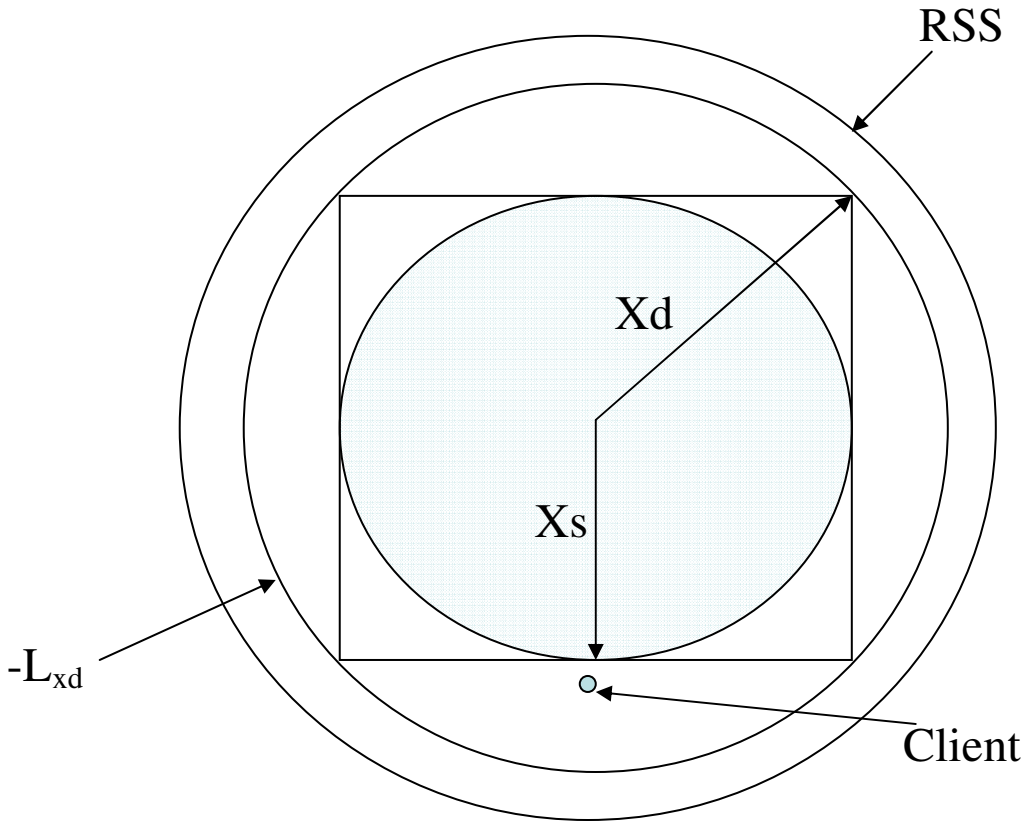

Figure 4-2 Square room threshold design

From free space loss equation 3-13, now we can calculate L_{Xd} which is

$$L_{Xd} = 40.23 + 20\log(Xd) \qquad (4\text{-}4)$$

Assuming infinitely thin wall with a wall loss of 5 dB and a client just on the other side of a wall at Xs. Using the two equations 4-2 and 4-4 we can plot a graph to analyse the condition of equation 4-3. From figure (4-3), it is clear that for any side length of a square room the RSS (loss reported by a client) is always less than the loss of diagonal length L_{Xd}. The difference between RSS just beyond the wall, at the nearest point Xs, and L_{xd} is a constant 2 dB, as plotted in figure 4-4.This shows confidence about selecting square rooms. The threshold algorithm will pick a wall between a client and an access point with certainty.

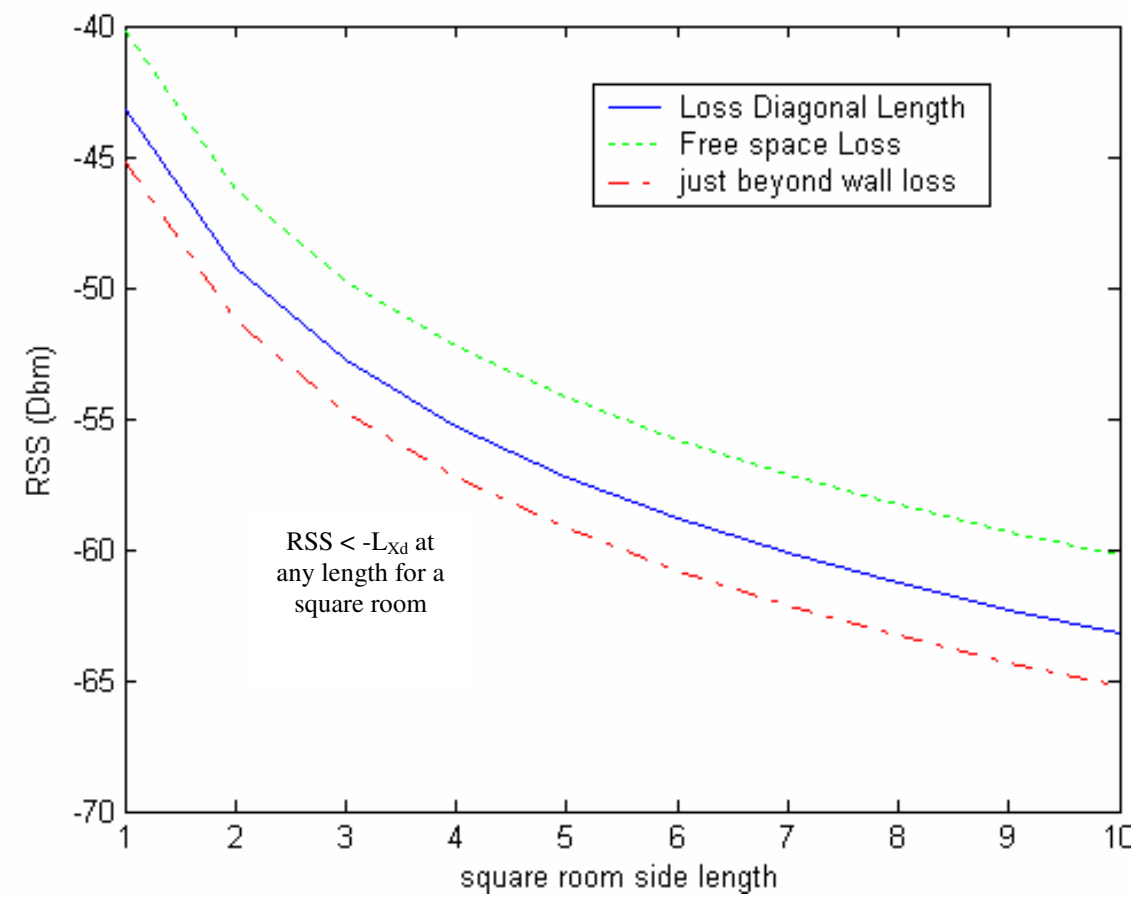

Figure 4-3 Illustration for RSS always less than L_{Xd} for a square room provided wall loss is assumed as 5 dB

This proves that for a square room, a minimum of 3dB wall loss is sufficient to fulfil the condition of equation 4-3 i.e.

$$RSS < -L_{Xd}$$

Or $$-(L_{Xs} + 3) < -L_{Xd}$$

Therefore, the client is always definitely outside the room. Only if the wall loss is < 3 dB there is an ambiguity as to whether a client is inside or outside the room. There is still a 2 dB margin to ensure that this threshold works for rectangular rooms as well.

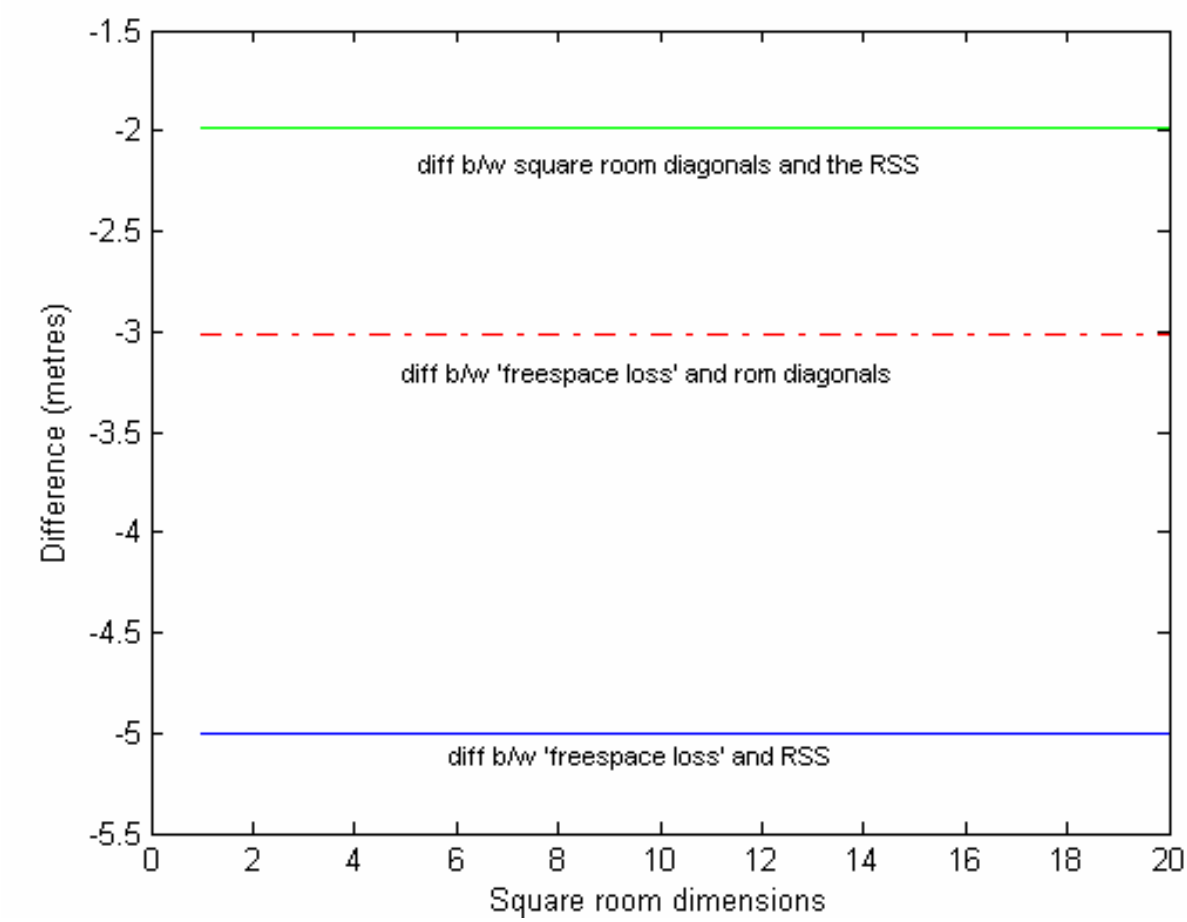

Figure 4-4 Differences between graphs in figure 4-3

From figure 4-4, it can be deduced that the absorption by walls play a very vital role. The research (Li et al, 2005) gives a wall absorption figure as 5.5 dB.

The condition is satisfied that any client outside the square room will theoretically exhibit received signal strength (loss) which will always be less than the set threshold

for square room, thus meeting the condition set in 4-3. However, not all the rooms are square. In a rectangular room the shorter side needs to qualify a minimum length for this condition to be true.

If the wall loss is greater than 3dB then certain rectangular rooms will also meet the criteria identified above. The loss exhibited by the shorter side length ($-L_{Xs}$) of the rectangular room and 5dB loss added to it together should always be less than the ($-L_{Xd}$), when client is placed just beyond the shortest possible distance beyond the wall of a rectangular room. Again, the condition in equation 4-3 is required to be satisfied.

4.5 Design threshold for a rectangular room – single wall

Before discussing the rectangular room threshold design, following assumptions are made.

- The received signal strength values are accurate readings.
- The rooms considered for placing APs (sensors) are rectangular in shape.
- Sensors are placed in the centre of the room.
- Wall loss is 5 dB.
- The received signal follows free space path loss theory.
- The sensor and client antennas are all omni-directional.

Requirement: Determine if a wall occurs between a sensor and a client when rooms are rectangular in shape.

Solution: Given the criteria, minimum length of the shortest side of a rectangular room needs to be determined. It can then be decided if the algorithm will correctly identify the walls with respect to the client's position.

Consider figure 4-5, which represents a rectangular room with shorter side, diagonal length and client shown just outside wall on shortest side.

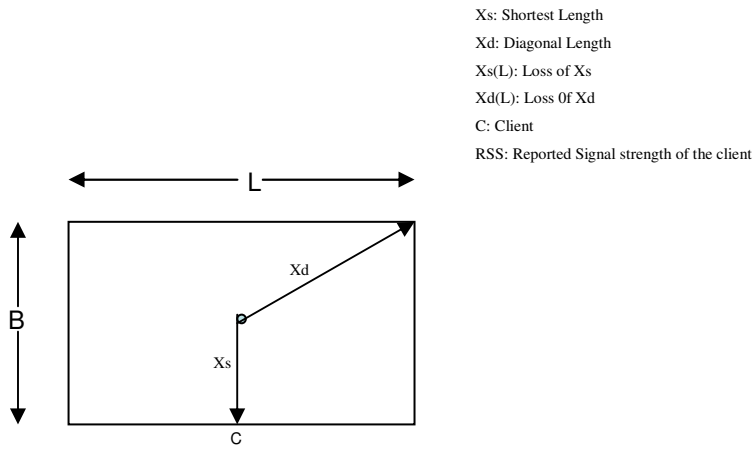

Figure 4-5 Threshold design

If

Xs = Half length of short side
Xd = Half diagonal Length
L_{Xs} is the free space path loss for distance Xs
L_{Xd} is the free space path loss for distance Xd

Then it is implied that:

The threshold loss is the loss of the diagonal length of the room where the sensor is placed. Ideally, any reported signal strength (loss) of client (RSS) beyond wall should be less than loss of diagonal length as given by condition in equation 4-3, which is reproduced below.

If $RSS < -L_{Xd}$ then client is outside the room.

This means RSS less than -L_{Xd} suggests that client is beyond the wall. However, as the room becomes more rectangular, the above condition will not hold true. Since the shorter side has reduced to a level where 5 dB loss, together with the loss of the shorter side is not sufficient to guarantee that the RSS is less than the threshold L_{Xd}. This means that despite RSS being greater than -L_{Xd}, the position of client may theoretically fall outside the wall on shorter side but inside the threshold set by longer side as it is depicted in figure 4-6.

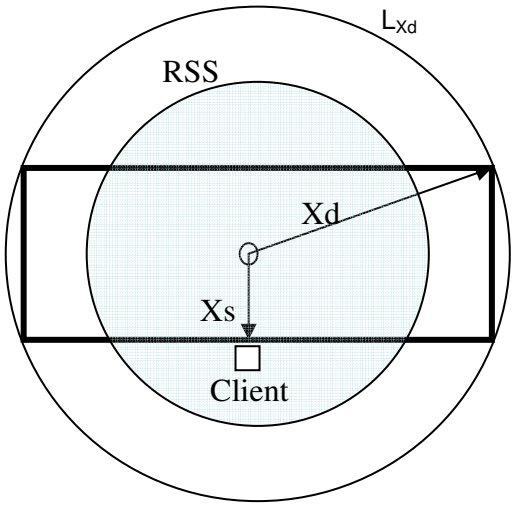

Figure 4-6 Depicting the case where equation 4-3 is not true

This concludes that the room cannot be rectangular beyond a certain limit which is determined by the length of the shorter side for a given diagonal length. Hence a general equation needs to be derived to determine the minimum shorter side length for any given diagonal length of a rectangular room. If X_d is the diagonal length, X_s is shorter side and L_s is the longer side of a triangle, then diagonal length is calculated using Pythagorean Theorem

$$X_d = \sqrt{X_s^{\,2} + X_L^{\,2}} \qquad (4\text{-}5)$$

A general equation is designed in the next section that will determine the minimum shorter side length for any given diagonal length for the condition in equation 4-3 to be true.

4.5.1 Design of general equation to ascertain presence of wall between sensor and client

Let us consider figure 4-5, where

Xd = half diagonal length
Xs = Half shorter side length
X_L= Half Longer side length
B = Breadth of rectangular room
L = Length of a rectangular room
c = Client location

The client is placed just outside the room and for all calculations it is assumed to be beyond the wall which is assumed infinitesimally thin. The reported signal strength of a client is denoted by RSS. As mentioned above a general equation needs to be derived to meet the requirement set in the condition given in equation 4-3.

Equation 3-13, determines the loss for a given distance in free space. It is reproduced below.

$$\text{Loss} = 40.23 + 20\text{Log}(d)$$

If the loss for half length of the diagonal is represented by L_{Xd}, and the loss for the half length of shorter side by L_{Xs}, then free space loss equation becomes:

$$L_{Xd} = 40.23 + 20\text{Log}(X_d) \quad (4\text{-}6)$$

$$\text{RSS} = -\left[40.23 + 20\text{Log}(X_s) + 5\right] \quad (4\text{-}7)$$

An extra 5 dB is added to equation 4-7 which represents wall loss as a client is placed beyond the wall on shortest possible direction from the sensor. We know from the condition given in equation 4-3 that RSS < $-L_{Xd.}$, so equations 4-6 and 4-7 become:

$$20\text{Log}(X_s) + 5 < 20\text{Log}(X_d)$$

$$\text{Log}(X_s) < \text{Log}(X_d) - 0.25$$

$$X_s < \text{Log}^{-1}(\text{Log}(X_d) - 0.25) \qquad (4\text{-}8)$$

Equation 4-8 gives the lower limit for the shortest length in a rectangular room for a given diagonal length. The equation is worked out with the assumption that both RSS and L_{Xd} are negative values. However, length of room cannot be negative so the above equation (4-8) will become:

$$X_s > Log^{-1}(Log(X_d) - 0.25)$$

If room's shorter side length is greater than the length calculated by equation 4-8, then the algorithm will correctly determine a wall between a client and the AP as illustrated in table 4-1.

The above criteria may be applied to see if the rooms selected in the test area (4-1) qualify so that the algorithm can identify a wall between a sensor and client with certainty. The same test area is later used to conduct experiments which are attached as appendix A.

Table 4-1 Minimum smaller side determined with respect to diagonal length to meet algorithm threshold criteria

1	2	3	4	5	6	7	8
AP	**X_L (m)**	**X_s (m)**	**X_d (m)**	**$X_s < [Log^{-1}(Log(X_d)-0.25)$ Minimum shorter length (m)**	**RSS(L_{Xs}+5) dBm**	**L_{Xd} (dBm)**	**RSS<L_{Xd}**
1	6.25	4.25	7.56	4.24	-57.79	-57.78	yes
2	3.75	3.25	4.96	2.789	-55.46	-54.13	yes
3	5	3.25	5.96	3.351	-55.46	-55.73	No
4	4.25	2.35	4.86	2.73	-52.65	-53.94	No

Hence the equation designed in 4-8 can be applied to any size room, square to rectangular, to determine the minimum shorter side length with respect to the diagonal length. If the shorter side of a room under consideration is greater than the calculated Xs, as the case demonstrated in table 4-1, then the wall is correctly detected by the algorithm without ambiguity.

The table 4-1 has been further interpreted in figures 4-7 to 4-9.

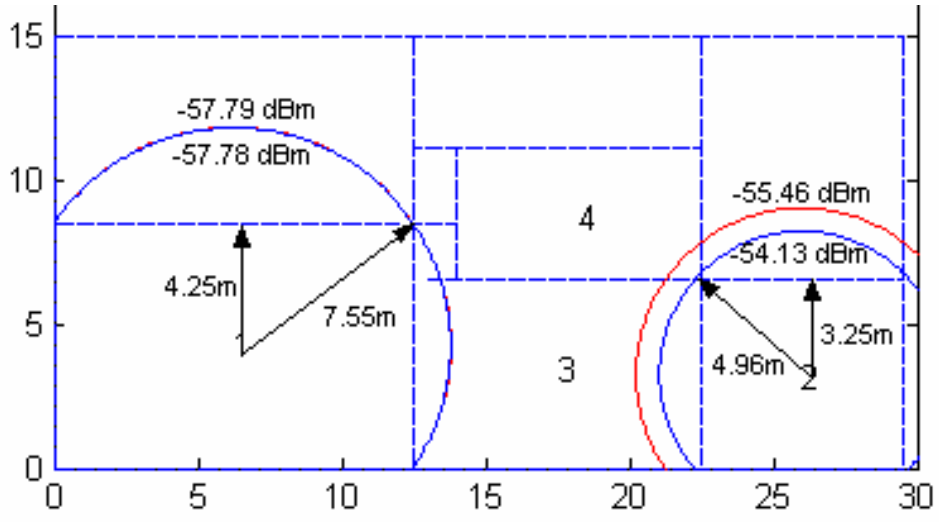

Figure 4-7 Single wall thresholds for sensor 1 and 2

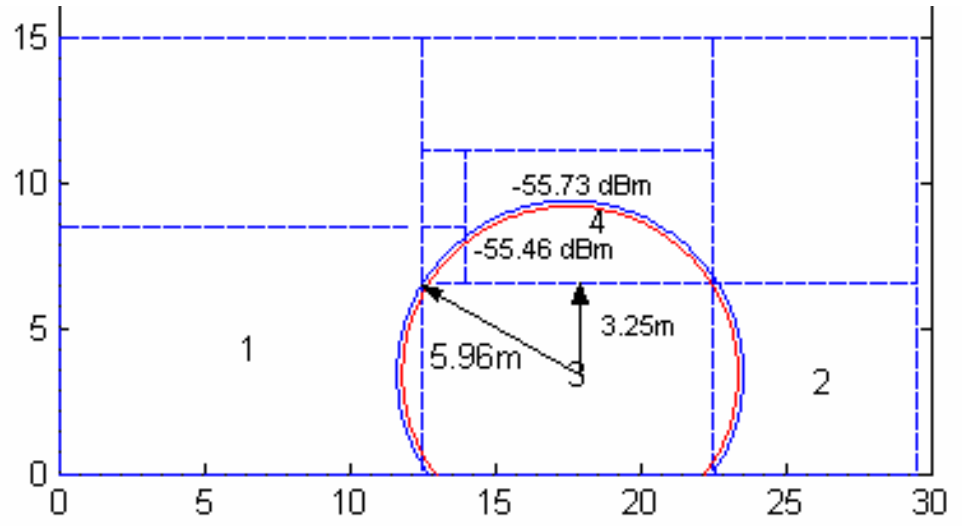

Figure 4-8 Single wall threshold sensor 3

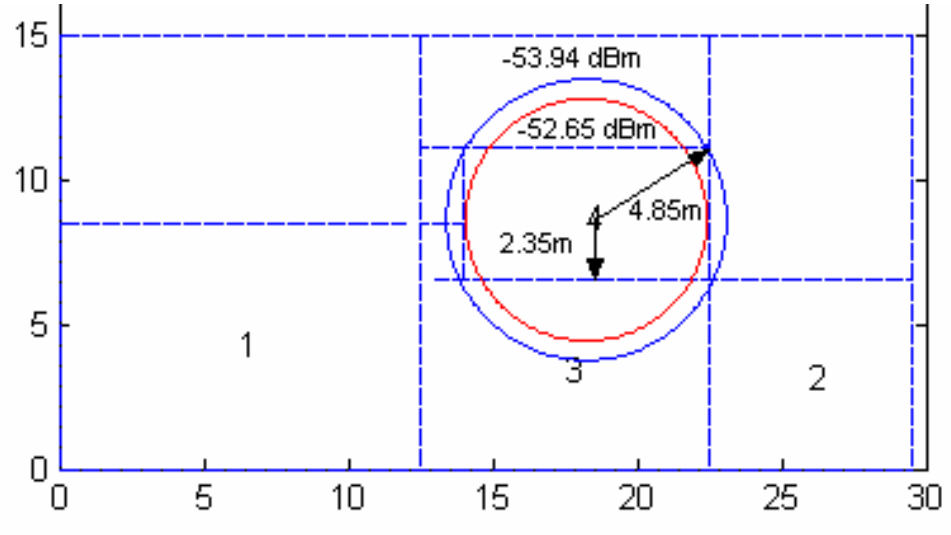

Figure 4-9 Single wall threshold sensor 4

It can be seen in table 4-1 that sensor 1 and sensor 2 are placed in rooms which theoretically will not cause any ambiguity in determining the walls as the smaller sides qualify when tested in equation 4-8. It is however, not the case with sensor 3 and 4. In case of these sensors the shorter sides of the respective rooms are slightly less (0.1m and 0.38m) than the minimum threshold calculated as shown in table 4-1. This corresponds to 0.28 and 1.39 dB values which is not a very significant margin. The RSS values are in any case likely to deviate in the range of 3 to 4 dBm. Let us consider a scenario where sensor 1 has not been able to pick up the wall correctly. The remaining three sensors are correct in reporting the walls between them and the client. The wrong sensor predicts wrong distance. The circle from sensor1 in the triangulation result will obviously be out of place with respect to the other correctly reported circles. In such a scenario, the algorithm has two provisions to minimise the effect from sensor1. Firstly it will apply correction on circle 1 by forcing it to overlap in the correct direction (section 4.8). Secondly, the averaging (section 4.10) will reduce the overall location error.

The design to determine if a client is located beyond two walls will be discussed in the next section.

4.6 Two wall threshold design

Requirement: To determine that a client is beyond two walls from the AP.

Solution: Assumptions remain the same for this design as illustrated for single wall design in section 4.5, except that 10 dB loss is assumed on account of two walls between a client and an AP (sensor). Condition in equation 4-3 needs to be true for algorithm to determine that walls exist between the client and AP(sensor). Same concept applies here as discussed in section 4.5. However, the longest side may not be the diagonal length as adjacent room also comes into consideration. Adjacent rooms are only those which have their walls common with each other as shown in figure 4-10. The shaded rooms are not the adjacent rooms. They will be referred as diagonal rooms. For the purpose to detect walls for clients placed in diagonal rooms, these rooms may present losses which could be taken as single or two walls (a random function) depending on the environment and location of client. Any errors caused due to this will be neutralized through averaging (4.10) and forced overlap (data fusion).

As explained in section 4.5, the general equation is desired to determine shortest length of a rectangular room for a given longest distance for combined AP room with the two adjacent rooms.

Consider figure 4-10. For simplicity we denote the loss in signal strength for longest length X_2 as L_{X2} and L_{Xs2} for shorter side X_{s2}. If client is just outside the wall on shortest side then the length of shorter side is extended just beyond the second wall. This means an added loss of 10 dB to the shorter side. The total loss is L_{xs2} + 5dB +5dB.The longest length loss is given by L_{X2} (loss of the longest length + 5dB).

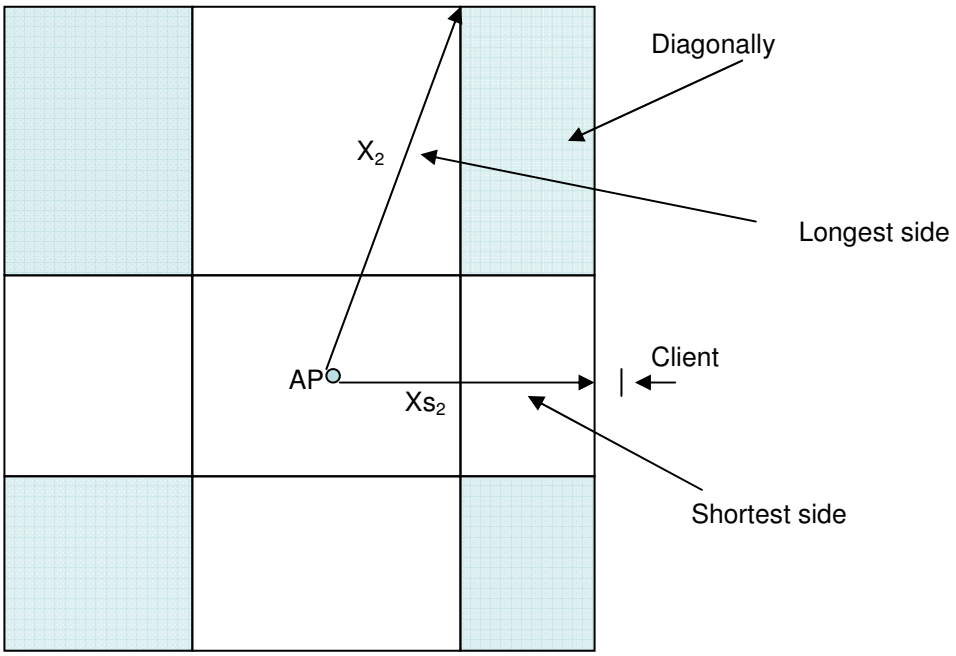

Figure 4-10 Shortest and adjacent room lengths

The longest length for adjacent rooms from sensor is determined and its calculated loss is taken as the threshold value for the two wall model. Also the shortest side from the AP (sensor) for adjacent rooms is considered as the point for comparison, with the client positioned just beyond the shortest distance second wall from the sensor under consideration.

If

X_{s2} = shortest second wall distance

X_2 = Longest second wall distance from AP under consideration

L_{Xs2} = Loss in dBm of length X_{s2}

L_{X2} = Loss in dBm of length X_2

Then

$$X_2 - Xs_2 > 0 \qquad (4\text{-}9)$$

$$L_{X2} > L_{Xs2} \qquad (4\text{-}10)$$

The condition for ascertaining that the client is beyond the second wall on the shortest side from sensor under consideration is:

If $RSS < -L_{X2}$ then the client is located beyond the second wall.

If the client is assumed to be just beyond the second wall on the shortest side then equation 3-13 (free space loss equation) for RSS can be modified as:

$$RSS_{2walls} = -[40.23 + 20\text{Log}(Xs) + 10] \quad (4\text{-}11)$$

Similarly equation 3-13 is modified for calculating the loss on the longest adjacent side as:

$$L_{X2} = 40.23 + 20Log(X) + 5 \quad (4\text{-}12)$$

Equating these for the condition of equation (4-3), we obtain

$$20\text{Log}(Xs_2) + 10 < 20\text{Log}(X_2) + 5$$
$$\text{Log}(Xs_2) < \text{Log}(X_2) - 0.25$$
$$Xs_2 < \text{Log}^{-1}(\text{Log}(X_2) - 0.25) \quad (4\text{-}13)$$

This is a general equation that determines the minimum length required on the shortest adjacent side in order for RSS to be less than the threshold. Theoretically, this will eliminate the chances of the client falling inside the second wall towards shortest adjacent side. The thickness of wall is not taken into consideration. Walls are assumed to be infinitesimally thin.

If the shorter length arrived at after including the adjacent room falls short of the length determined by equation 4-13 then the condition mentioned in equation 4-3 is not always true and for RSS_{2walls} greater than $L_{X2,}$ theoretically the client is inside the second wall on longest side but it may be beyond second wall on shorter side.

The equation 4-13 is applied to the example test area as shown in figure 4-11. All four rooms where the sensors are placed will be considered in turn.

4.6.1 Sensor 1 – design of 2 wall threshold

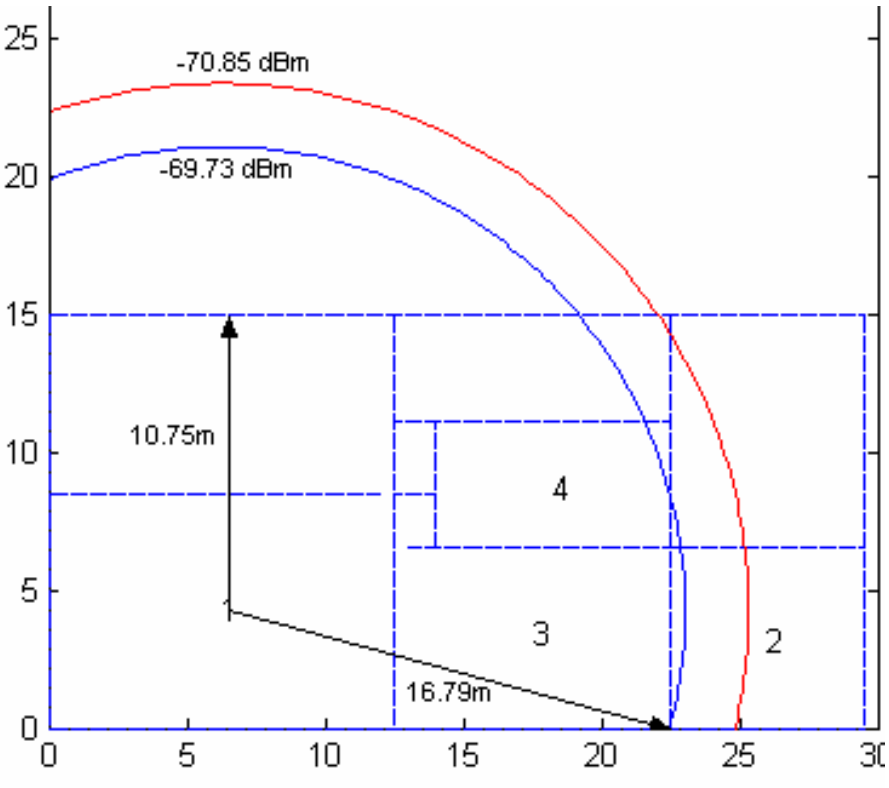

Figure 4-11 Two wall threshold design for sensor 1

Applying equation 4-13 to sensor 1 the longest length from sensor 1 for adjacent sides is 16.79m. When equated in equation 4-13 this gives:

$$Xs_2 < 9.44m$$

Any value greater than 9.44 is then used in equation 4-11 to determine if RSS_{2walls} is less than the threshold for this distance (-69.73 dBm). The value arrived at from equation 4-13 with X_{s2} being 9.46 is -69.74 dBm, which is less than the threshold (-69.73).

For the chosen test area the shortest adjacent side length is 10.75m. Any client just outside the shortest possible length beyond two walls will theoretically give signal strength which will always be less than the 2 wall threshold. It can be seen in figure 4-11 that the RSS in this case is -70.85 dBm and is plotted as a circle, which is always less

than the threshold circle (-69.73 dBm). Similarly, any value greater than the threshold is considered to be beyond a single wall for sensor 1.

4.6.2 Sensor 2 – Design of 2 wall threshold

Calculating the minimum adjacent shortest side using equation 4-13 gives 7.80m. The test area shown below in figure 4-12 gives X_{s2} as 11.75m for sensor 2. This suggests that a client beyond the shortest adjacent side will give an RSS which will always be greater than the threshold for the longest length, calculated as 68.07 dBm. The minimum loss reported in any direction falling on the circle shown in figure 4-12 will be greater than the threshold.

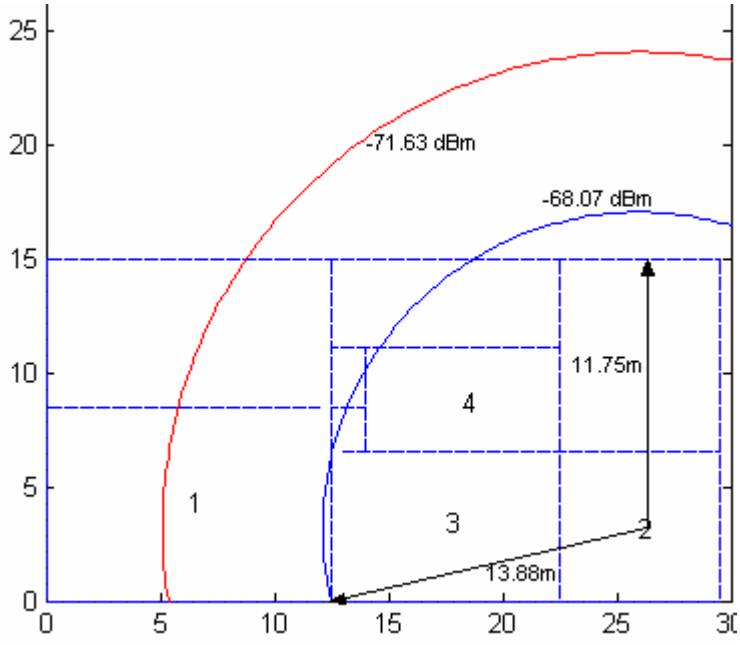

Figure 4-12 Two wall threshold design for sensor 2

4.6.3 Sensor 3 – Design of 2 wall Threshold

For sensor 3, the shortest qualifying adjacent length is calculated, using equation 4-13, to be 10.19m. The smallest side of the room with sensor 3 measures 8.05m, shorter by 2.14m. The RSS_{2walls} at 8.05m, though outside two walls is calculated as -68.34 dBm which is greater than the threshold -70.39dBm. This is a margin of about 2.05 dB. The reasoning given in section 4.5 to explain the same scenario in the case of sensor 3 and 4

for single wall also holds true here. The forced overlapping and averaging processes will minimise errors such as this where walls can possibly be reported incorrectly.

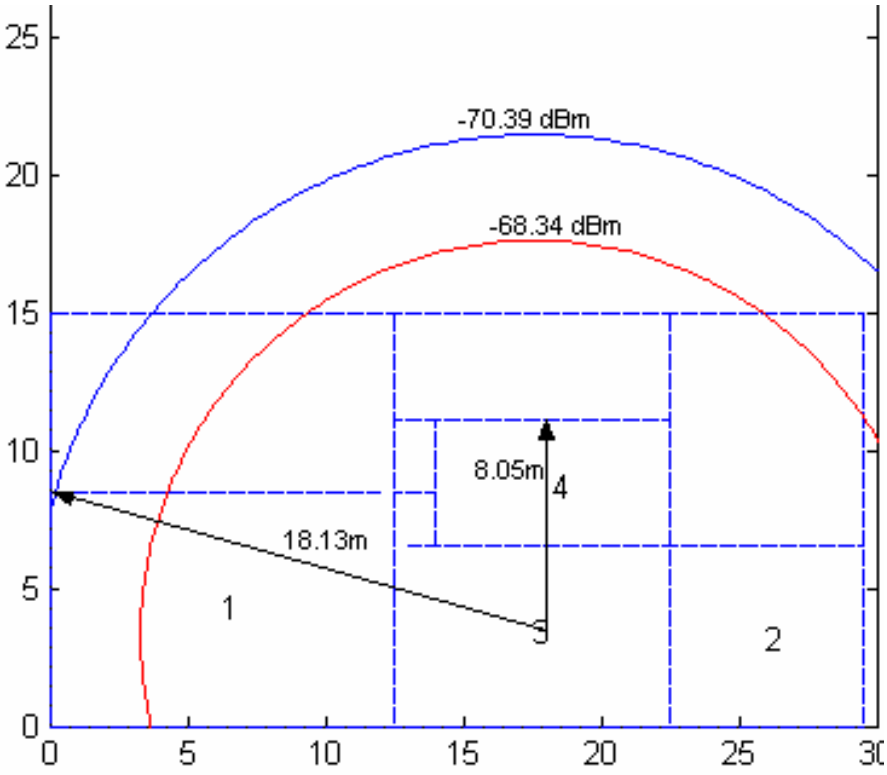

Figure 4-13 Two wall threshold design for sensor 3

4.6.4 Sensor 4 – Two wall threshold design

The above procedure is repeated to determine the shortest qualifying length of adjacent rooms. See figure 4-14.

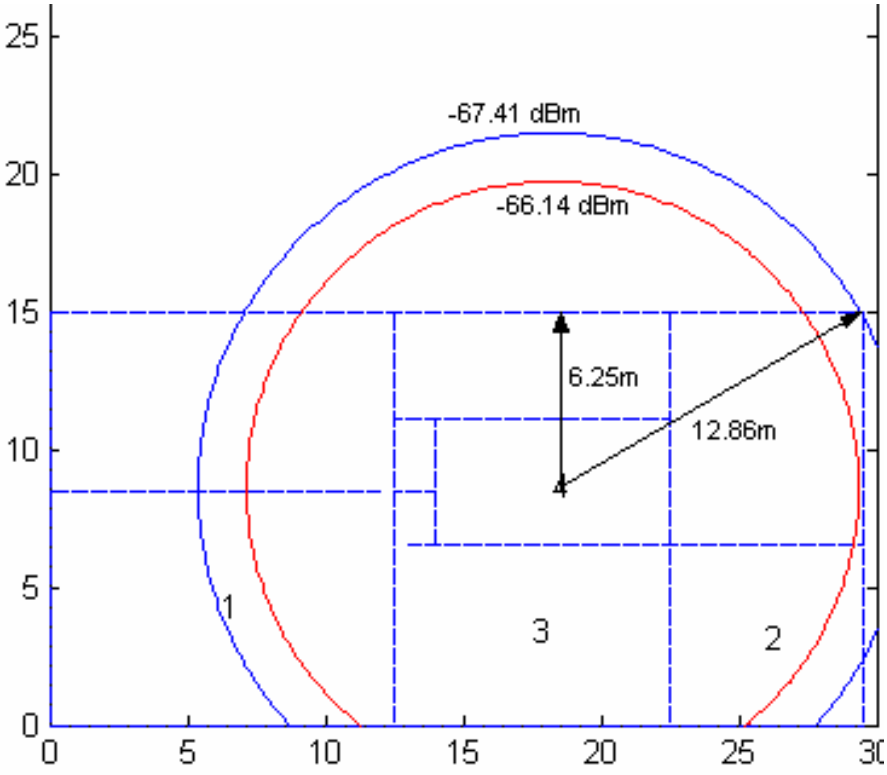

Figure 4-14 Two wall threshold design for sensor 4

According to equation 4-13, X_{s2} should be a minimum 7.23m. Theoretically RSS of a client beyond the wall on shortest side can have a situation where it is greater than the threshold thus creating doubt in locating the position within or beyond the second wall. The same procedure will be adopted here as explained in previous section for sensor 3.

Having discussed the thresholds, it may be noted that the RSS at certain points may not be exactly or near to what is expected. The design discussed above is theoretical based on the free space path loss equation (3-13). However, there can be instances when the reported value could be less than or more than the expected theoretical value as a result of multipath, reflections, refractions and absorptions and may cause incorrect detection of walls.

As explained in figure 4-1, the corrected RSS value is checked against an individual sensor threshold. The design of this absolute threshold is given in the next section.

4.7 Absolute threshold design

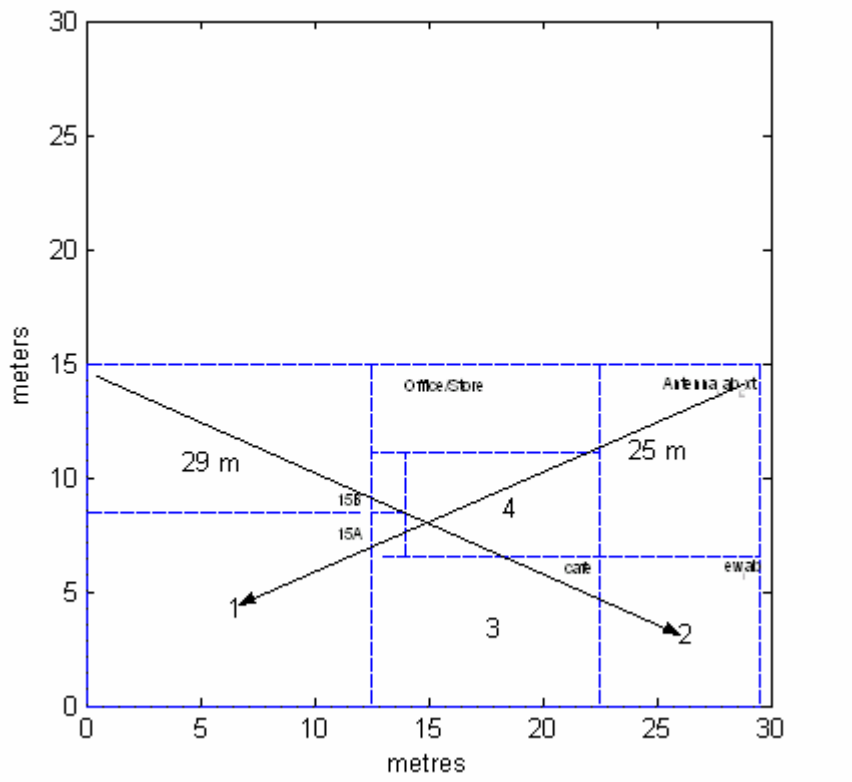

Figure 4-15 Maximum distance that an AP can encounter on a given test area

Figure 4-15 shows the test area example. The maximum distance where a client can be placed from individual sensors is different. For instance, farthest distance from sensor 1 is 25m. Similarly, from sensor 2 the farthest position of client is 29m as shown in the figure 4-15. Individual absolute thresholds for each sensor are therefore calculated.

Hence in all practical situations, given these test area boundaries, the reported signal strength (RSS) will not exceed individual absolute threshold when calculated using free path loss equation 3-13. For sensor 1 to sensor 4, the absolute thresholds are set at -67, -68, -66 and -65.5 dBm respectively. The algorithm applies correction to the original RSS reported by each sensor for the client. The final corrected value (RSS) is then compared to the individual threshold set for each sensor.

If the final corrected RSS value (correction for 2 walls) is less than individual absolute threshold of the sensor then RSS is assumed equal to the absolute threshold set for that sensor. See Table 6-5 and its explanation to describe the implementation of absolute

threshold in light of experiment at location 8 shown in test area. Also see figure 6-29 on improvement of results due forced overlap process. Table 6-5 also shows that for this experiment sensor 1 and 3 did not require absolute threshold to be applied for assigning final distance value. From the fixed positions of sensors (AP) circles are drawn representing the distance corresponding to each corrected RSS value. However, it is still possible that the corrected RSS values are not accurate, resulting in circles which are not producing an overlap area from three circles as required for the triangulation process explained in Chapter 3 (section 3.4.2). Hence there is a need for a further fine tuning of RSS values.

4.8 Further correction to minimise the error in RSS values

The corrected RSS values may result in circles which do not overlap. Two possible cases are circles which are separate from each other or within each other as shown in figure 4-16.

The circles reported by the algorithm must overlap to produce a likely area for location of the client. Ideally three circles should intersect on a common point, and provided the received signal strength readings are accurate, the common intersection point will be the exact location of the client.

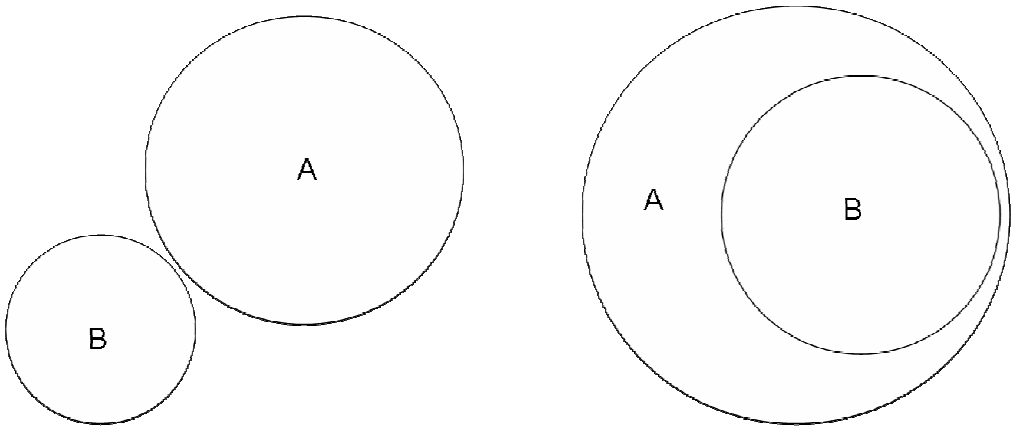

Figure 4-16 The two cases of non-overlapping circles

However, owing to the multipath environment, the received signal strength is unlikely to be accurate for a client from all available sensors at the same time (Ciurana et al,

2007). In this scenario when translated distances for received signal strengths from all sensors are error prone, there exists a possibility for all sensors to produce overlapping circle intersecting at a common point that is not the correct position (Stansfield, 1947). This is the case illustrated in figure 4-17 where the error is 4.3m despite the circles overlapping at a common point.

Residual errors due to the multipath, variation in wall losses and unknown obstacles will produce an error in corrected RSS values and hence give circles that do not overlap at a common point. The next process described will detect this condition to bring the circles to overlap.

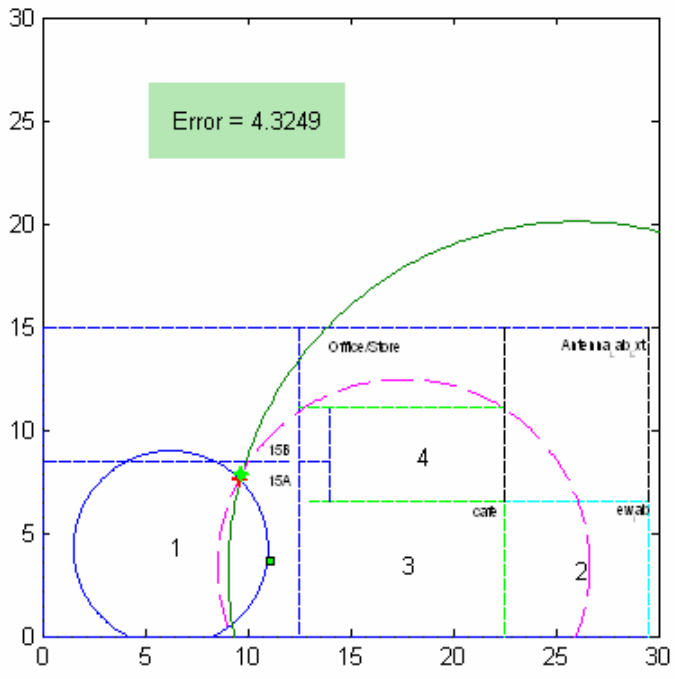

Figure 4-17 Common intersect point is not always the correct reported location

If the difference is greater than 3m between any two circles then the larger circle, which is assumed to be for the farthest sensor from the client is contracted to within a 3m difference. Since farthest sensor from the client is likely to have more errors due RF environmental constraints, it is contracted and in process is likely to be corrected as it approaches near the smaller circle which is expected to represent correct distance from the client. This small circle should not be disturbed for more than 1.5m which is a maximum it does if need be, according to this logic. Once circle from farthest sensor comes at 3m distance from expected correct circle; both circles contract and expand an

equal distance to overlap. In this process the presumed correct circle only incurs small error, if at all. Circles are considered for contraction and expansion on above logic in sequence 1,2,3 and 4. Any one circle cannot alter more than one time to avoid inducing an undue error. Section 6.8.3 shows results on forced overlap with figure 6-30 and 6-31 showing the improvement achieved due forced overlap. The following geometric principles are followed to achieve this correction.

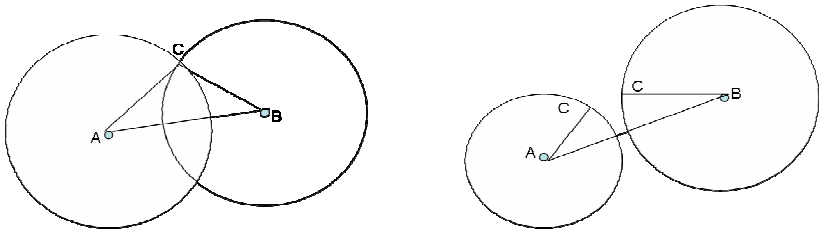

Figure 4-18 Geometry for overlap circles

Considering the layout of two circles A and B as illustrated in figure 4-18, two equations can be formed as follows:

$$AC + BC > AB \quad (4\text{-}14)$$

$$AC + BC < AB \quad (4\text{-}15)$$

Where

AB = Distance between the centres of two overlapping or distinct circles.
AC = Radius of circle A
BC = Radius of circle B

Equation 4-14 implies that the circles overlap and equation 4-15 implies that circles do not overlap. Based on these principles the algorithm detects that the circles are overlapping or distinct and accordingly applies a correction to bring them closer by forced overlap. There could be another case of distinct circles where the circles are within each other as shown in figure 4-19.

In figure 4-19, C1 and C2 are centres of two circles. P1 and P2 are points on the circumference of the circles. The distance between the two centres C1C2 is known. C2P1 is the radius of the circle 2 which is known and C1P2 is the radius of circle 1 which is also known. The minimum distance required to overlap the two circles is P1P2 which can be calculated as follows:

$$P1P2 = P2C1 - (C1C2 + C2P1) \qquad (4\text{-}16)$$

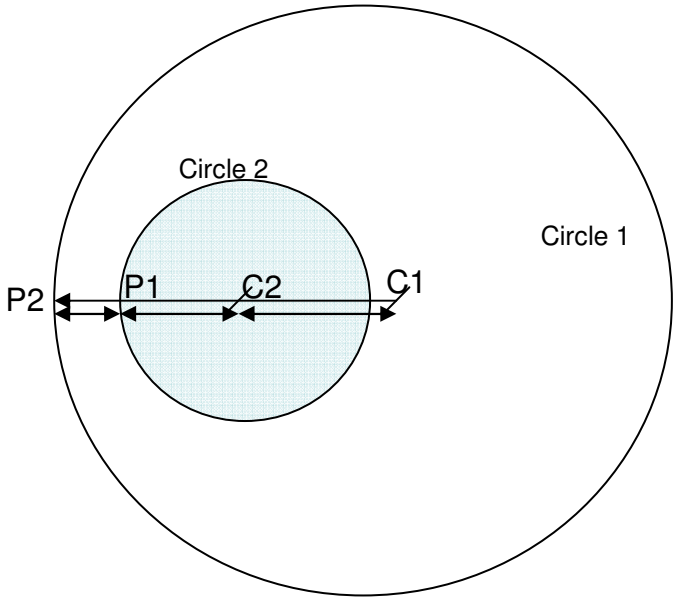

Figure 4-19 Geometry for distinct circles within each other

4.9 Identifying Intersection points (Bourke, 1997)

Bourke (1997) has given procedure to find intersection points of two circles when overlapping. The same procedure has been reproduced in para below.

The following note describes how to find the intersection point(s) between two circles on a plane, the following notation is used. The aim is to find the two points $P_3 = (x_3, y_3)$ if they exist.

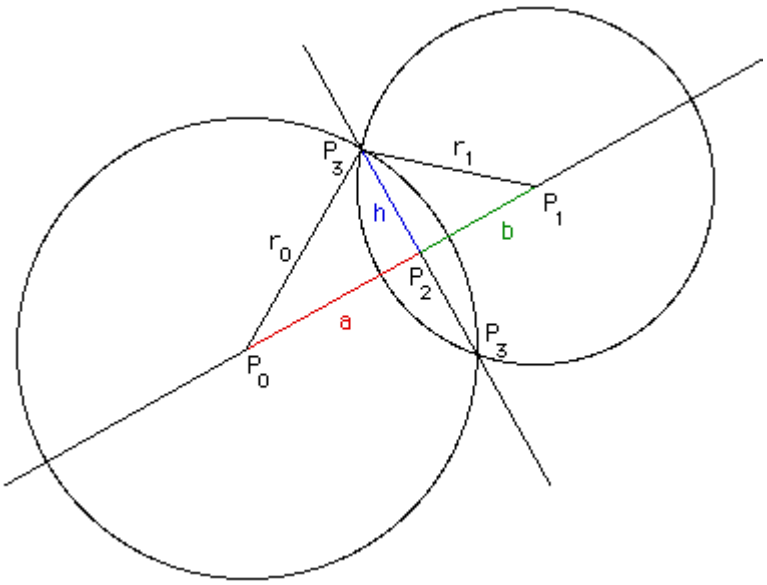

Figure 4-20 Geometry to find intersection points (Bourke, 1997)

First calculate the distance'd' between the centre of the circles. $d = \| P_1 - P_0 \|$.
If $d > r_0 + r_1$ then there are no solutions, the circles are separate. Also, if $d < \| r_0 - r_1 \|$ then there are no solutions because one circle is contained within the other.

Considering the two triangles $P_0P_2P_3$ and $P_1P_2P_3$ we can write

$$a^2 + h^2 = r_0^2 \text{ and } b^2 + h^2 = r_1^2 \qquad (4\text{-}17)$$

Using $d = a + b$ we can solve for a,

$$a = (r_0^2 - r_1^2 + d^2) / (2\,d) \qquad (4\text{-}18$$

It can be readily shown that this reduces to r_0 when the two circles touch at one point,

$$d = r_0 + r_1 \qquad (4\text{-}19)$$

Solve for h by substituting a into the first equation, $h^2 = r_0^2 - a^2$
So

$$P_2 = P_0 + a (P_1 - P_0) / d \qquad (4\text{-}20)$$

And finally, $P_3 = (x_3,y_3)$ in terms of $P_0 = (x_0,y_0)$, $P_1 = (x_1,y_1)$ and $P_2 = (x_2,y_2)$, is

$$x_3 = x_2 +- h (y_1 - y_0) / d \qquad (4\text{-}21)$$

$$y_3 = y_2 -+ h (x_1 - x_0) / d \qquad (4\text{-}22)$$

The algorithm adopts the above explained procedure to determine intersection points of two overlapping circles. Likewise, intersection points of three circles (six in number) are determined. Once the six intersection points are known, the closely overlapped area is again selected. The Euclidean distance formula is then used and closest distances between common points are identified and are marked with a cross or asterisk as shown in the figure below.

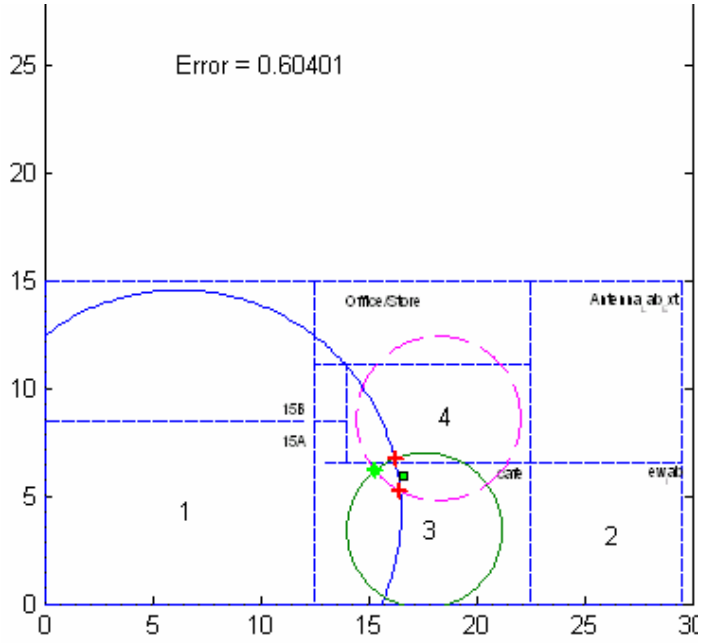

Figure 4-21 Overlap area with intersection points

4.10 Triangulation with four sensors (Data Fusion)

As described in section 4.2, the algorithm triangulates the position of a client inside a building based on RSS data reported by 4 different sensors for a common client. The algorithm is based on the room's threshold values, which are the free space signal strength values calculated from the lengths and breadths of the room in which the sensors are deployed. It is assumed that sensors are placed in the centre of the room. Data (RSS values) for a common client are stored in a matrix. A minimum of 4 sensors are selected to give redundancy against faulty data from one of the sensors. Based upon this philosophy it is assumed that the more sensors there are in the test bed area the chances calculating an accurate location increases. Three sensors are sufficient to give a triangulation result. How data from four sensors may be combined in groups of three is described to illustrate a single data fusion process. For sensors 1 2 3 and 4 the possible combination of sensors is:

- 1 2 3
- 1 2 4
- 1 3 4
- 2 3 4

The triangulation result from each set of sensors provides the position which is centre of the overlap area. This gives four set of results from four triangulations for estimating the position of a common client. If these sets of points are (x1, y1), (x2, y2), (x3, y3) and (x4, y4), the final estimated position (EP) of these reported positions is the average of these points given by:

$$EP = \frac{X1 + X2 + X3 + X4, Y1 + Y2 + Y3 + Y4}{4}$$

4.11 Summary

This chapter proposed and described a novel location algorithm. The design was based on room dimensions. The algorithm produces accurate results provided all assumptions made in the chapter are met. The algorithm does not require many input parameters from the user. The only input that is provided is the dimensions of the rooms but not their relationship. If the signal strength readings picked up by the access point (sensor) are accurate and the error of received signal strength is small, then accurate results are produced.

CHAPTER 5
EXPERIMENTAL METHOD

5.1 Introduction

The environment, equipment and experiment design is discussed in this chapter. The experiments are designed using off the shelf, low cost, easily available equipment, so that could be deployed as an independent system. Experiment results are analysed and discussed in Chapter 6. This chapter is structured as follows:

Sections 5.2 describes the environment in which the experiments are conducted at Heaviside Labs of Cranfield University. The rooms where experiments were conducted are discussed.

In section 5.3, the test equipment used to collect and record data is discussed. The firmware used and set up is also mentioned.

This is followed by section 5.4 covering the experimental set up and design. In this section the experimental method is explained. These experiments are required to analyse the effects of RF propagation at 2.4GHz inside a building and to see the variation in RSS (received signal strength) values with and without walls between transmitter and receiver. The effect of walls is also studied. A novel way of collecting RSS values is

designed and the experiment method to reduce inconsistency in RSS values is described.

There is a separate section 5.5, which describes the test area used and location of the fixed sensors for conducting experiments to test the threshold location algorithm. A summary of the chapter is presented in section 5.6

5.2 Test area environment

The location selected for experiments was Heaviside laboratory at Cranfield University, Shrivenham, which houses many laboratories and offices. Human traffic within the laboratory area where experiments were conducted was not very dense. Normally few persons were present at any one time during experiments. Laboratories house different equipment ranging from computers to test equipment and simulators. The furniture contained in the laboratories included tables, chairs, white-boards, stools and steel/wood cupboards. The walls were mostly concrete built. Labs had windows on most walls. The particular rooms where sensors were placed were named 15A, store, café, and EW-lab. Other than these, experiments were also conducted in a large electrical lab. The test area is shown in figure 5-1. It is drawn to scale.

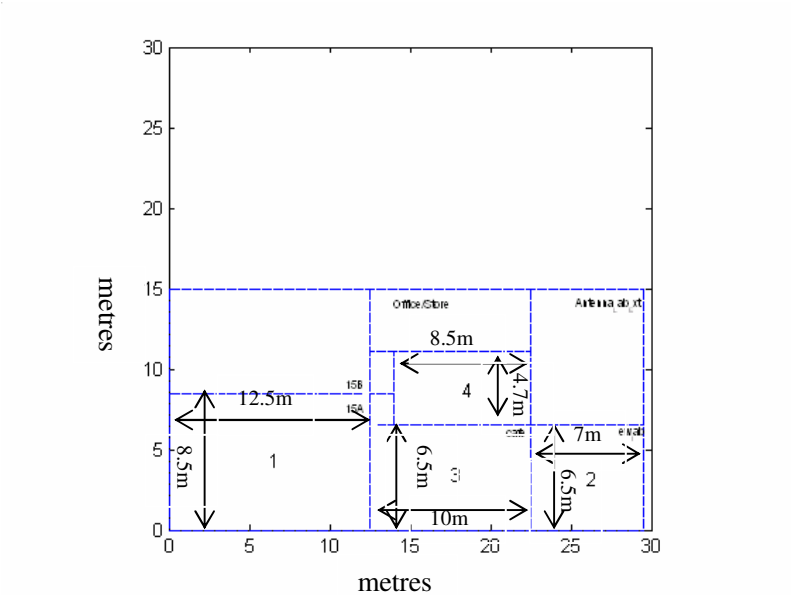

Figure 5-1 Rooms for sensors with dimensions in Experiment test area

The dimensions of Lab 15A with sensor 1 are 12.5m x 8.5m. Lab 15A is a computer Lab that houses approximately 24 computers (desktops) each with a 17" monitor. Two walls are common with other labs. One exterior wall faces an open parking area and the fourth boundary is formed by a wall common with a corridor. The lab also contained metallic cupboards of a standard size. Figure 5-2 shows a photograph of this lab, which gives the layout of the laboratory. The position of the access point (sensor 1) is indicated by a circle.

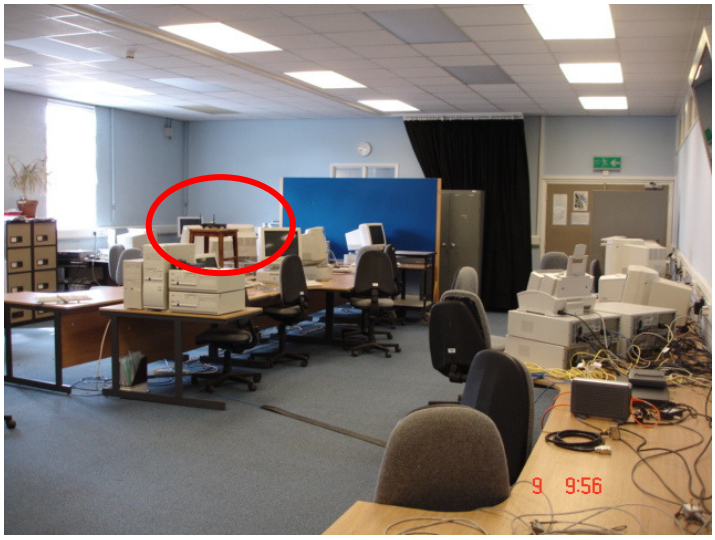

Figure 5-2 Room 15A with sensor1 in centre

The EW lab with AP 2 was situated towards the far end of the test area. The dimensions of the Lab are 7m by 6.5m and the Lab contains a few computers and a area for two research students. A picture of the EW laboratory is shown in figure 5-3 which also shows the location of sensor 2 circled.

Figure 5-3 EW Lab with sensor 2 placed at centre

Sensor 3 was placed in an old café, with dimensions of 10m by 6.5m. The café has furniture and area for three research students. A steel pole separates an area (a cubicle) for another student. The cafe has many reflecting surfaces in the form of mountings and windows glasses. The AP was placed in the centre of the room.

Figure 5-4 Old Café with sensor 3 in centre

The fourth and final AP was placed in a store room with dimensions of 8.5m by 4.7m. The store room contains wood and steel cabinets, about 2.2m tall, which houses

electronic test equipment. This a very unfavourable environment for RF propagation. Figure 5-5, also showing the position of AP4 placed in centre of the room.

Figure 5-5 Sensor 4 placed in centre of store

Another area of Heaviside Lab is an Electrical lab with the dimensions of 15m x 30m. The electrical Lab houses many steel pillars and simulators (1.5m tall) throughout the room. This laboratory also offered a challenging environment for RF propagation. The environment is termed obstructed line of sight (OLoS)

5.3 Equipment and tools

The equipment selected for recording and measuring results is shown in figure 5-6. One of the major considerations was to use equipment which was available off the shelf and affordable to deploy as an independent system for the specific purpose of geolocation. The equipment used is listed below:

- 3COM Office Connect Wireless 11g PC Card
- Acer TravelMate 240 Laptop
- Compaq notebook EvoN1005v
- WRT54G Access Points

Figure 5-6 Equipment used for experiments

5.3.1 WRT54G ver.2 – Access Point

The WRT54G is a wireless router from Linksys, and is famous for being the first consumer based network device that had its firmware source code released for the research community. This allowed programmers and researchers to modify the firmware to change or add functionality.

The existing default firmware on the WRT54G was updated with a modified firmware DD-WRT v.23 (DD-WRT Wikipedia, 2007; DD-WRT, 2006). This firmware was selected to avail the feature of extracting signal strength values from the received RF signal and provides signal strengths for all attached clients. One of the windows is shown in figure 5-7, which shows the signal strength value of one of the detected clients, in dBm.

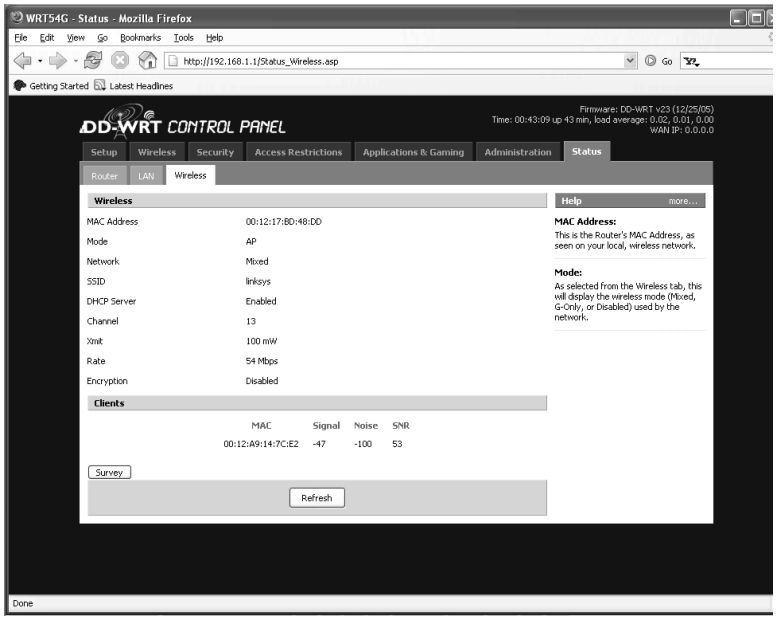

Figure 5-7 Web based utility of WRT54G displaying wireless data including RSS under the 'Status Window'

Other important information available was the MAC address of clients, access point and the channel on which the network is established. These were the minimum information required for the conduct of experiments. Experiments involved the collection of RSS values on different channels. For this a private wireless network was set up to control channels switching through the web interface utility (figure 5-8) of the AP.

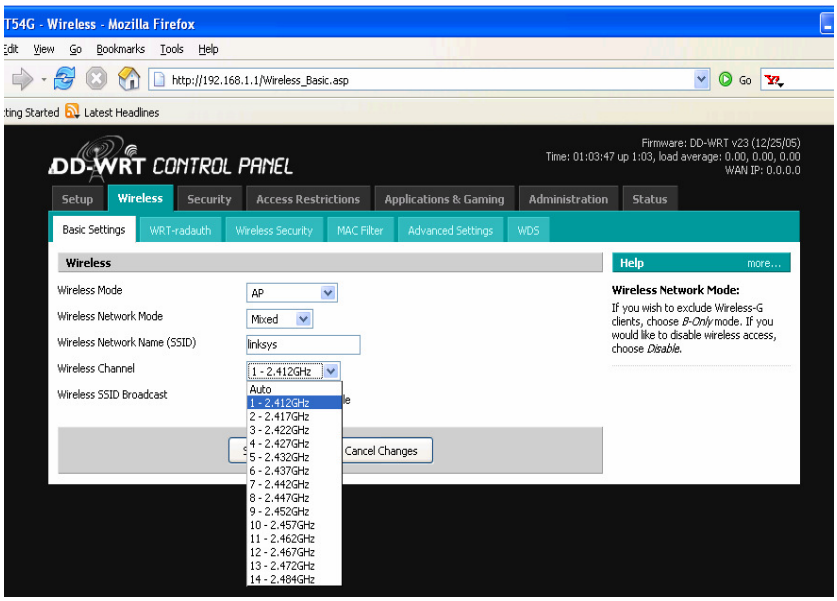

Figure 5-8 Web interface utility showing window to change channels

If required, the IP address of the router could be changed from the network set up window. The wireless network mode was set to mix to use networks operating on IEEE 802.11 b (11Mbps) or IEEE 802.11g (54Mbps).However, all RSS readings reported in this thesis are measured at 54 Mbps (802.11g) by using Office-connect wireless network card (3CRWE1**54G**72) which supports 802.11g (Fig. 5-7).

5.3.2 Acer Laptop / Compaq note book

The laptop, or notebook, was used as a wireless client with an Office Connect wireless network adaptor card (3CRWE154G72) from 3COM attached to it.

5.3.3 Office connect Wireless 11 b/g PC Card ver 2.0 3CRWE154G72 from 3COM

The Office Connect is a wireless adapter card that conforms to the IEEE 802.11b/g standard and has a maximum transmit power output of +17 dBm. The card was configured through the TCP/IP properties setup to the desired IP address so that it could access and talk to the WRT54G router. This card tuned to the available AP (sensor) on the selected channel. Each time the channel was changed on the AP (sensor), the wireless adapter also tuned to the new frequency channel. Once a private network was setup, all changes to channels and extraction of signal strength data was done through the web interface, as explained in section 5.3.1.

5.3.4 Data collection

In all experiments, it was required to collect the RSS (reported signal strength) value of the associate client. The laptop with the NIC card (client) was wirelessly associated to one of the wrt54g sensor. The AP (sensor) was upgraded with a new firmware, DD WRT 23.1, which offered the web interface utility. Using this utility, the received signal strength (RSS) of the associated client was extracted as given in 5.3.1. The RSS readings were collected for the client across the channels 1 to 13 in turns. These were recorded in tabular form for each sensor on 13 channels. Channels are changed from web interface utility manually and RSS readings are noted. For each channel approximately 35 sec are needed. However, if the system is automated it may reduce to

~ 20 seconds. Since dedicated system is used to get geolocation estimation by setting private network, the network overhead was not important ant therefore not considered. The WRT54G presents the RSS values in dBm. The WRT54G provides WIFI connectivity using the BroadCom chipset (Wikipedia, 2007) that according to Pearn (2004) gives the reading of RSS values in dBm.

5.4 Experimental Set Up

The results of these experiments are discussed in Chapter 6. Experiments were designed to show the variation in the received signal strength on a single channel, multiple channels and to investigate the effect of walls. Initially the effect of the environment was investigated by using a laptop (client) and a single access point (sensor). The effect of the environment and different directions on RSS was also demonstrated by deploying multiple sensors. The location experiments were conducted using a minimum of 4 sensors.

5.4.1 Single channel - RSS variation against distance

An experiment was designed to observe the effect of indoors multipath on received signal strength. The TravelMate 240 Laptop was placed on a stool (0.6m high) or a trolley (0.7m high) in one of the laboratories of the test area (figure 5-1), with a wireless adaptor card (3COM Office Connect). The AP (WRT54G) was fixed at a common point on another stool 0.8m in height. The Laptop was placed at 1m distance from AP (access point). RSS reading was recorded on a single frequency - channel 1, before it was moved to 2m distance from the sensor for next RSS reading on the same channel. Same process was repeated to record RSS values up to 10m. Readings were plotted using Matlab and are shown in figure 6-1. The set up is shown in figure 5-9

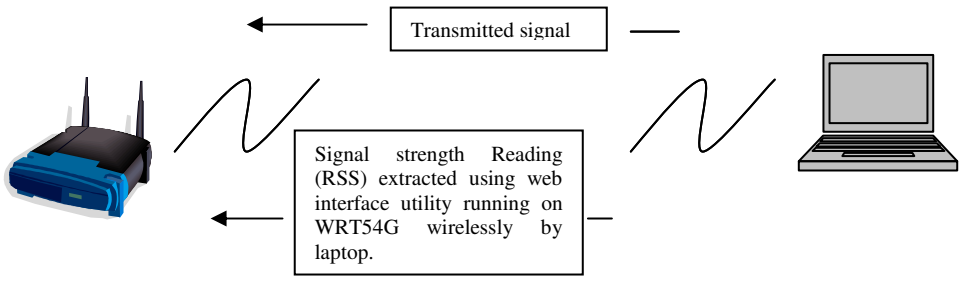

Figure 5-9 **RSS of transmitted signal measured by sensor and passed back to the client for recording**

5.4.2 Multi-channel RSS measurements

- **Four different channels-RSS variation vs distance**: The above experiment (figure 5-9) was extended to see the multipath propagation effect by taking readings on four different channels. It was intended to observe the variation level of signals spread over different channels, which were randomly chosen as 1, 4, 6 and 9. The experiment was conducted in the same room HL 15A. The environment of this room was discussed in section 5.2. The method of performing the experiment was the same as explained in section 5.4.1 repeated for 4 different channels (including channel 6) at each distance. The results are discussed in section 6.3.1.

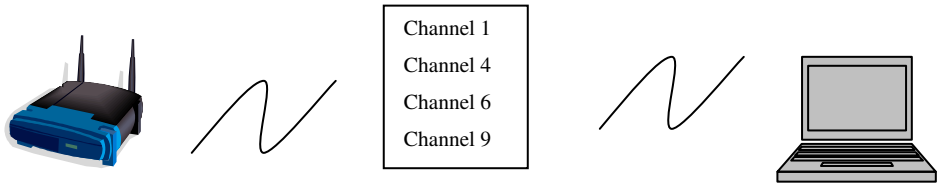

Figure 5-10 Signal strength readings recorded for 4 different channels

- **Effect of frequency selective readings on RSS measurements**: The same experiment layout of figure 5-10 was used to extract RSS values at distances of 2m, 4m and 7m. At each distance, RSS values were recorded on all channels (1-13). Channels were changed on the AP using the web interface utility as explained in section 5.3.1. The results are discussed in Chapter 6 (6.3.2)

- **Effect of averaging across the channels**: The experiment layout in figure 5-10 was used to collect RSS values across the channels at multiple distances. The 3COM Office connect wireless card was associated to WRT54G. At fixed distances the signal strength of the associated client was extracted using the web-based utility on WRT54G. The collected RSS readings were averaged and plotted against distance. The effect on variation in RSS values is shown and plotted in figure 6-5

5.4.3 Effect of walls on propagation

In order to develop the geolocation algorithm, it was considered an important factor to study the amount of absorption by the walls in the test area (figure 5-1). Walls pose one of the major concerns in design of indoor location algorithms. Correct identification of walls in an indoor environment can drastically improve the chances of reporting accurate location estimation.

An experiment was designed so that RSS readings collected beyond a single wall were recorded. For this a common wall between two rooms in the test area was chosen between an AP and the client as shown in figure 5-11.

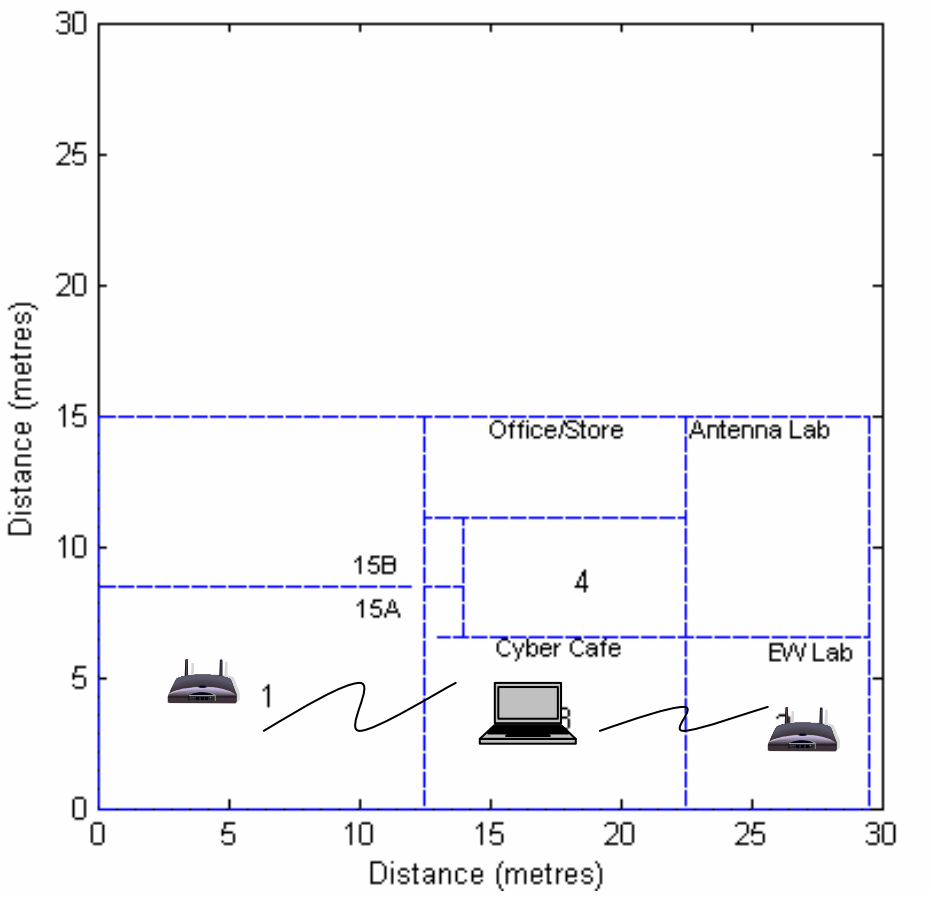

Figure 5-11 Test bed area showing equipment layout for measuring wall loss

The client was placed in the old café and the sensors were placed in 15A and the EW lab. The sensor in 15A reports RSS value for the client at randomly selected distances and then the sensor in EW lab reports RSS value for the client at randomly selected

distances. At each distance RSS readings were collected for all channels and averaged. The results are discussed in section 6.4

5.4.4 Experiments with multiple Sensors

All experiments so far were conducted with a single sensor. This section presents the experiments extended to multiple sensors.

- **Variation in RSS from different locations**: An experiment was designed to compare the effect in change of reported signal strength values from three different positions around the sensor. An experiment was set up in HL 15A (figure 5-1). Three WRT54Gs (sensors) were placed at fixed points inside the lab as shown in figure 5-12. The client was associated to each sensor (AP) one by one after setting up a small private network so that the client could communicate to each of the access points placed in the room. While the client was associated to each AP (sensors), in it from the signal strength of the associated client was collected using web interface utility of WRT54G as explained in section 5.3. Signal strengths (RSS) were collected across the channel 1 to 13 for every distance and averaged.

  Only one AP is 'ON' (powered up) at a time to collect readings. This is necessary since by default clients will always associate to the AP with the highest received signal strength. For every change of channel, the client disassociates and will connect to the next available AP with strongest signal. Results from this experiment are explained and discussed in section 6.5.

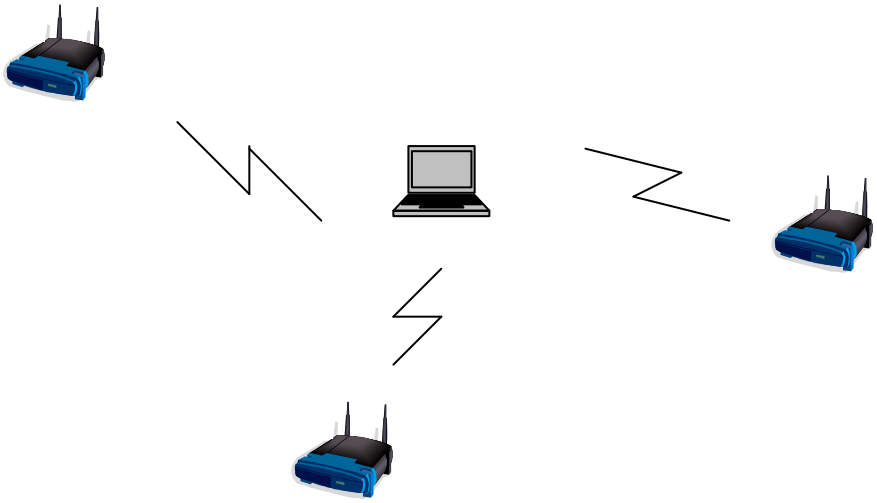

Figure 5-12 Equipment set-up to measure the effect of multipath on signal strength as received from three different directions

- **Effect on RSS values collected in an alternate indoor environment**: To continue towards development of a model for any indoor environment, an experiment was designed to investigate RF propagation in different environments. For this experiment the electrical laboratory was selected (electrical lab) which had a different environment as mentioned in section 5.2. The sensors were placed at fixed positions within the room (Electrical lab) as shown in the layout of figure 5-12. A small private wireless network was established and each sensor was associated in turn to obtain signal strength readings spread over randomly selected distances. Section 6.5.2 presents the results.

- **RSS values with single/double walls between multiple sensors/client:** The client in a practical indoor environment faced the challenge of multiple walls separating it and different sensors. The sensors were placed in different directions/ locations as shown in figure 5-13.

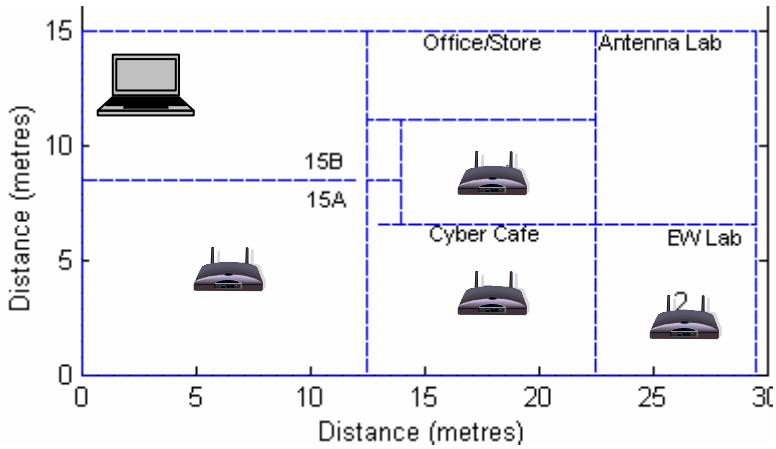

Figure 5-13 Layout of multiple walls between client and multiple sensors

Each sensor collected RSS value on all 13 channels which were then averaged. The results showing the absorption affect on RSS readings with single and double walls are presented in figure 6-11.

5.5 Threshold algorithm location experiments for use indoors

Having ascertained that a free space loss model was suitable for use inside a building in line of sight, an algorithm was developed which has already been explained in Chapter 4. The algorithm reports the location coordinates of a mobile client in the x-y axis. Matlab software was used as the source language for developing the algorithm. Experiments were conducted with four APs (sensors) placed in a test area as shown in figure 5-13.The test area was explained in section 5.2 (figure 5-1). Each sensor was placed in the centre of the room, which was a requirement of the algorithm design (Chapter 4). Sensors, WRT54G, were running modified firmware capable of reporting signal strengths of the associated client.

To demonstrate the correct working of the algorithm, the client was moved to 24 different locations inside the test area, as shown in figure 5-14. Efforts were made to cover an area all around the test bed.

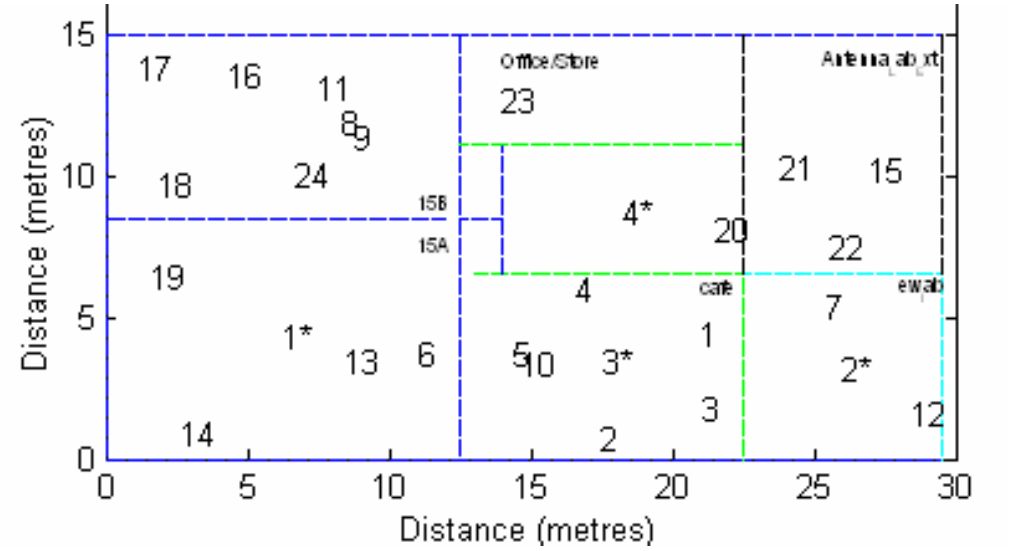

Figure 5-14 Locations are numbered 1 to 24 for client positions to test algorithm

For each location, the following procedure was adopted:

- The client was associated to all four sensors one by one at each position.
- Each sensor reported the signal strength (RSS) of the client under consideration.
- RSS for each client was collected across the channels and then averaged.
- The averaged RSS values from four different sensors for a common client position were used to produce triangulated positional information by the novel threshold algorithm.

5.6 Summary

Experiments were designed with an aim and demonstrating that the variation in received signal strengths could be reduced through frequency diversity. A novel method of applying frequency diversity in a WLAN was explored. The same wireless adapter card was used throughout the experiments. Experiments were designed to see effects such as change in the environment, orientation of the client and the wall absorption. The test

area, individual rooms where sensors are placed, has been discussed to give an idea about the adverse conditions that exist for RF propagation. Experiments were designed so as to produce triangulation from four sensors to obtain location estimates.

CHAPTER 6
RESULTS AND DISCUSSIONS

6.1 Introduction

Chapter 5 described the equipment used and the method adopted in obtaining the results while Chapter 4 described the algorithm developed in Matlab to report positional accuracy of a client inside a building. This chapter presents the experimental results.

The chapter is structured as follows: Section 6.2 to 6.3 presents the results for the set of experiments investigating the effect of multipath propagation on received signal strength (RSS) of an RF signal on single and multiple channels. It also illustrates the results for variation of RSS values inside a building when the frequency diversity technique is exercised. Section 6.4 provides results for the effect of absorption due to walls. Results obtained from the experiment to observe the effect of a client placed at different directions at an equal distance from an AP (sensor) is covered in section 6.5. Section 6.5 also presents the effect on RSS values when experiments were conducted in different environment and is followed by results that show the effect of walls between APs (sensor) and the client.

The algorithm results are discussed at length in sections 6.6 to 6.9. In section 6.7 error estimates in reported location are analysed under the following conditions:

- RSS on single channel – No walls, No forced overlapping
- Averaged RSS on multiple channels – No walls, No overlapping
- Averaged RSS multiple channels – No walls, but forced overlap
- Averaged RSS multiple channel – Walls, No overlap
- Averaged RSS multiple Channel – Walls with Overlap

Location 11 (figure 5-14) is chosen to analyse in detail the results on the basis mentioned above. Section 6.8 carries out detailed analysis to progressively explain the functioning of the algorithm. This analysis includes an explanation of corrections applied due to detection of walls and extra absorption beyond threshold limit of the test area. The forced overlap of circles is also discussed. The logic of the evolution of the forced overlap is also explained. All these steps are elaborated with the help of location estimation results obtained for location 8 (figure 5-14). In section 6.9, the algorithm performance in terms of reported errors is evaluated and the reasons for the errors in the location results presented in appendix A are analysed. The chapter is summarised in section 6-10.

6.2 RSS vs distance for a single WLAN channel

The experimented method is described in section 5.4.1. The multipath effect was observed on a single channel at increasing distances in a line of sight (LoS) location. The effect of multipath shown in figure 6-1 was further analysed. Two plots, a theoretical free space path loss curve and RSS values as reported by the sensor (WRT54G) over a distance of 1m to 10m for a single channel are shown in figure 6-1.

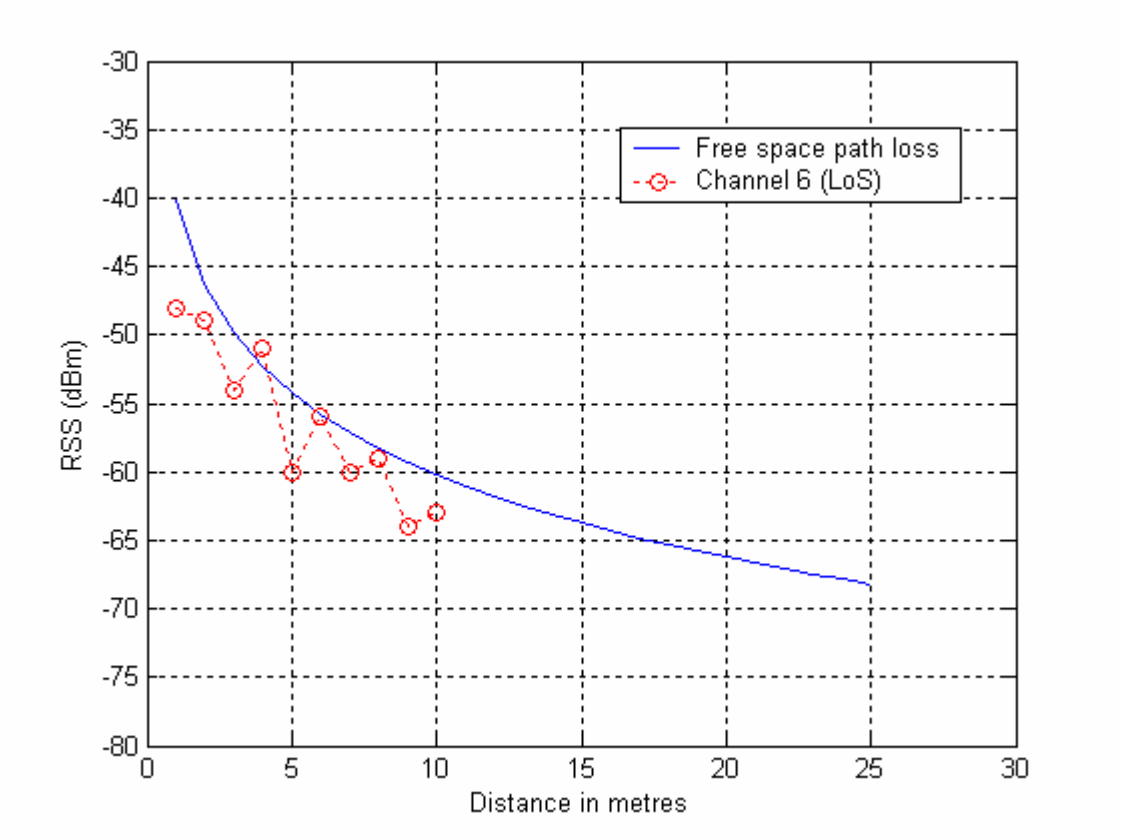

Figure 6-1 **RSS values as reported on a single channel plotted against distance and compared to the theoretical free space path loss curve.**

Discussion: RSS values were measured on a single channel (channel 6) for 1 to 10m. The Figure 6-1 shows the RSS values varying when compared to the theoretical free path loss curve. Note that at 4m, the reported loss is -51 dBm and it is –60 dBm at 5m, having a difference of 9 dB. While, at the same distances the theoretical curve depicts 52.3 and 54.2 dBs respectively, a difference of only 1.5 dB. Again the RSS observed at 6m was only 56 dBm which was far less than that reported and observed at 5m. This inconsistency in RSS values could be observed, over the range from 1 to10m. The impact of inconsistency in RSS values on converted distances is explained in Figure 6-2.

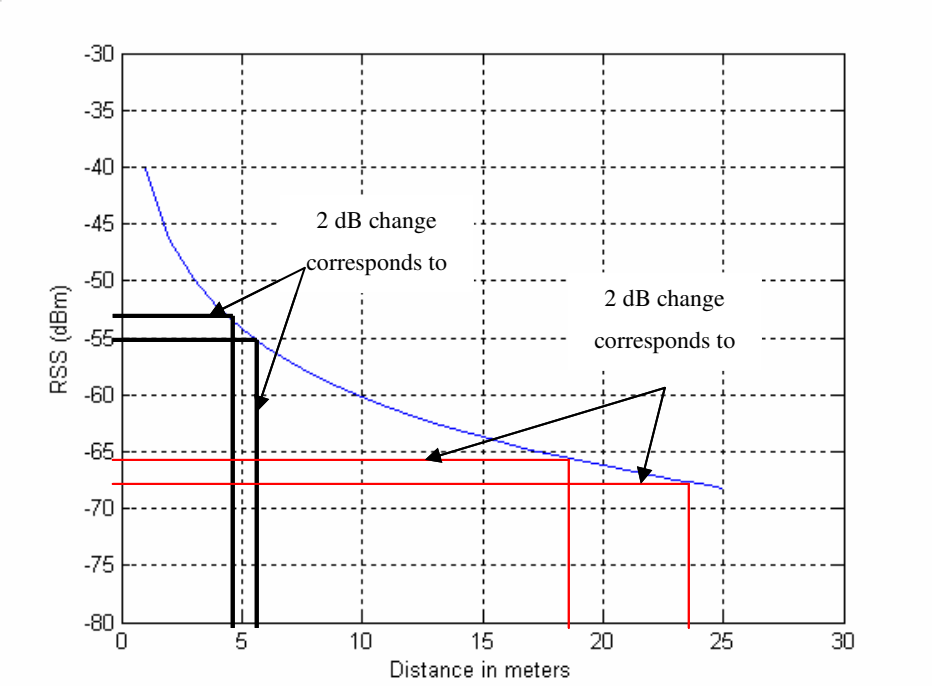

Figure 6-2 Distance sensitivity to change in RSS values

The figure 6-2 gives a measure of the sensitivity attached to reported distances viz a viz variation in RSS values. As distance increases so does the sensitivity to errors in RSS measurement. A ~2dB variation in RSS correcponds to a ~±1m distance error, whereas a ~2 dB variation at longer distances over 17m corresponds to ~±5m error. At longer distances a small RSS error could lead to drastically incorrect results if used for location estimation.

6.3 RSS vs distance for multiple WLAN channels

6.3.1 4 Channels

In the previous experiment the effect of multipath on propagation over a single channel was observed. The results suggest that RSS was severely affected by the multipath phenomenon inside the building. To have a more precise analysis experiment was repeated to see the effect of multipath on different channels (LoS) over a range of 10m. The method of conducting experiment has been described in section 5.4.2. The results obtained are displayed in figure 6-3.

Discussion: Part of data from figure 6-3 is given in table 6-1, showing the variation in spread of RSS values at distances 1m apart, the maximum noted for each channel across a range of 10m. The readings in the last column 'Variation' show big spreads for each channel. It could result in an error distance of more than double the actual distance. The variation as observed in figure 6-3 was seen in all results. All channels were reporting signal strength variation over a wide range (up to 10 dB). With this diverse range of variation in reported RSS values between channels on a common distance, the reported RSS values if translated on these four different channels on common distance could result in a wide range of varying distance. This suggested that such model, subject to severe multipath distortion inside a building would give erroneous result if applied for location estimation unless a method is devised to minimise the effect due to multipath phenomenon.

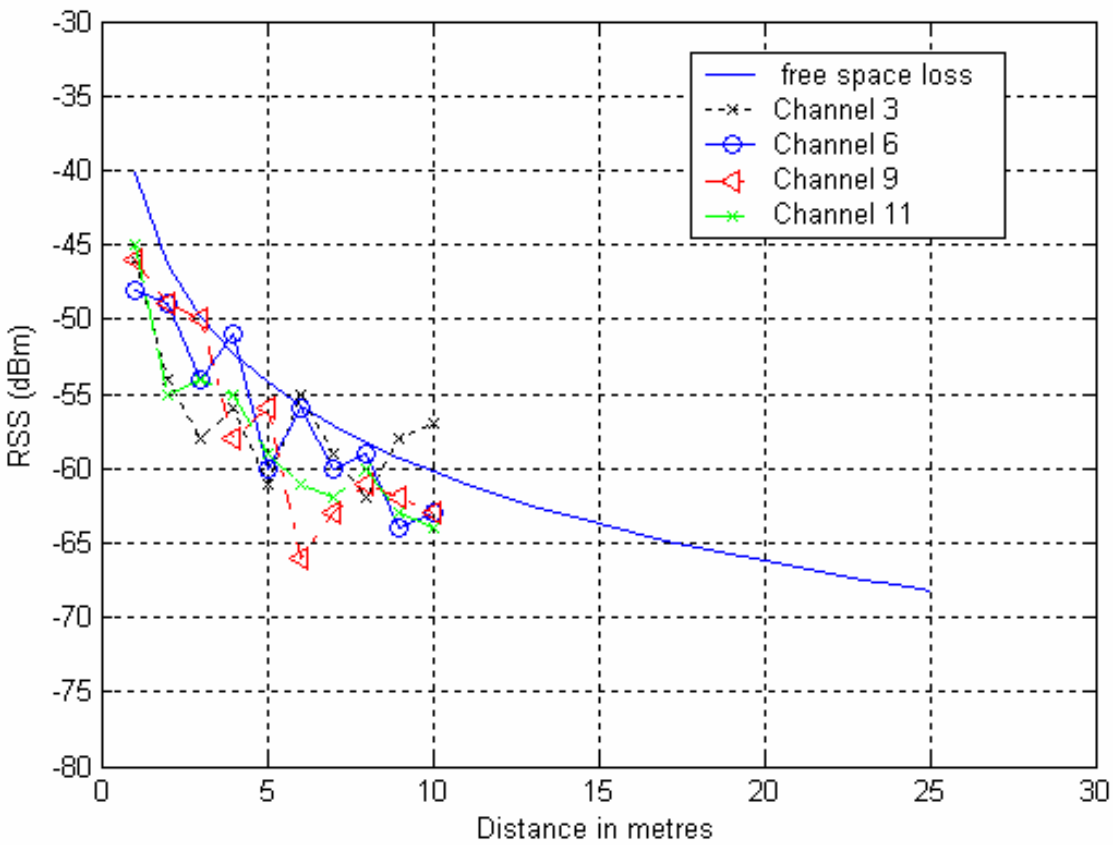

Figure 6-3 **Variation in RSSI values as reported on four different channels**

Table 6-1 Range of fluctuation observed for different channels on adjacent distance points

channel	Distance 1m apart	RSS dBm	Variation RSS dBm
9	5m	-56	10
	6m	-66	
3	1m	-46	8
	2m	-54	
6	4m	-51	9
	5m	-60	
11	1m	-45	10
	2m	-55	

The table 6-2 gives us the varying RSS readings on common distance for each channel and their effect on the translated distance.

Table 6-2 Error resulting from varying RSSI values for four channels when translated into distance at 3m and 6m distance points (data extracted from figure 6-3)

True Distance (m)	RSS Values (dBm)				Theoretical Translated Distance (m)				Max error (m)
	CH 3	*CH 6*	*CH 9*	*CH 11*	*CH 3*	*CH 6*	*CH 9*	*CH 11*	
6	-55	-56	-66	-61	6	6.2	18	11	12
3	-58	-54	-50	-55	8	5	3	6	5

At expected distance of ~6m, an error of ~12m was beyond acceptance limit. Similarly an error of ~5m at 3m distance was unacceptable. Hence, in order to utilize the distance and loss relationship of RF signal for developing location reporting systems (equation 3-13), a dire need was felt to find out ways for mitigating multipath inside a building.

6.3.2 Effect of frequency selective fading on RSS readings - Result

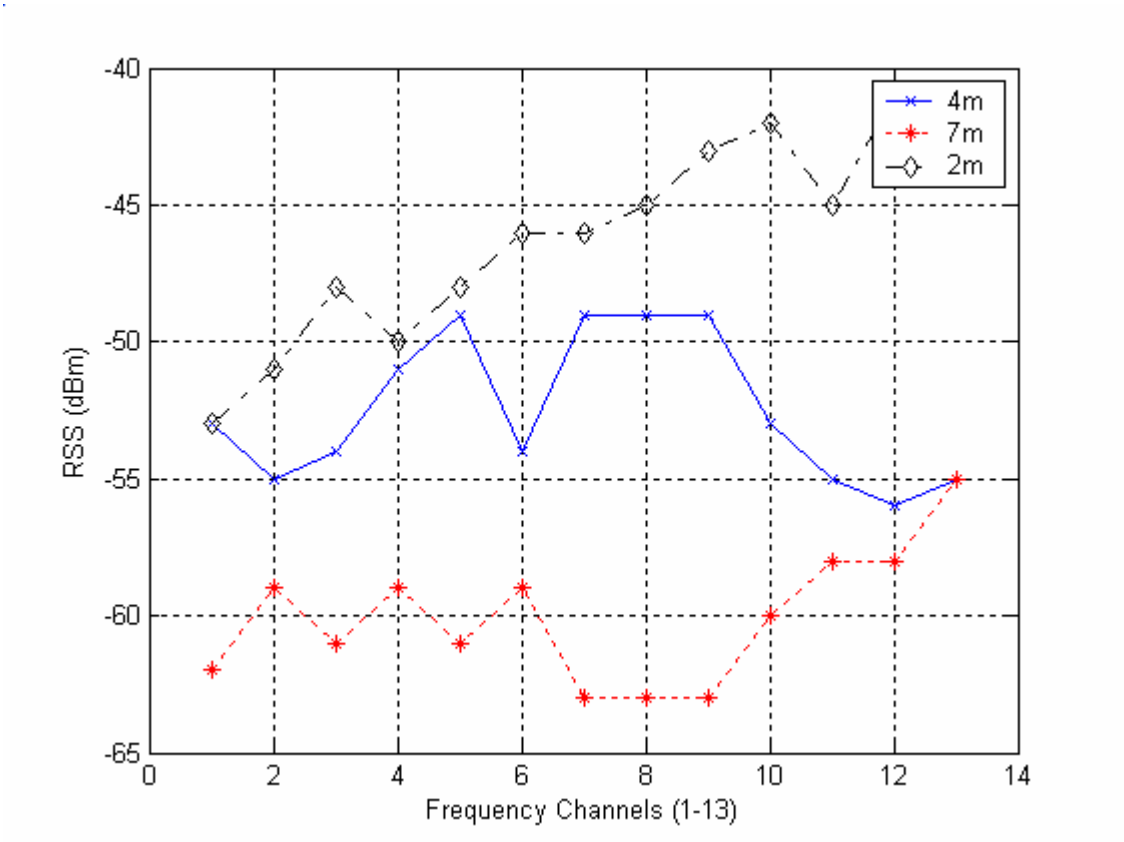

Figure 6-4 Variation in reported RSS on different frequencies CH 1-13

Figure 6-4 shows variation in signal strength readings reported by a sensor for a client at three different distances; 2, 4 and 7m. The RSS variation on the different channels from 1 to 13 is obvious. These three readings were taken at very small intervals in one sitting. Same experiment was repeated next evening after about 36 hours with equipment fixed on original position and following results were observed which are demonstrated in Figure 6-4 (a). For 2m , variation is observed between -43 to -53 dBm and -45 to -48 dBm for figures 6-4 and 6-4a. Similarly at 7m, variation observed in RSS for the two figures is between -55 to -63. The two figures shows that trends are different on two occasions that could be because of difference in environment that can happen with passing time. Even the change in posture of the person collecting readings effects changes in variation of RSS values. These results demonstrate that RSS readings taken on a single channel only will produce large distance errors if used for geolocation. The trend for 2m in figure 6-4(a) has changed as for other distances.The particular trend of increasing dBm could be a random occurance.

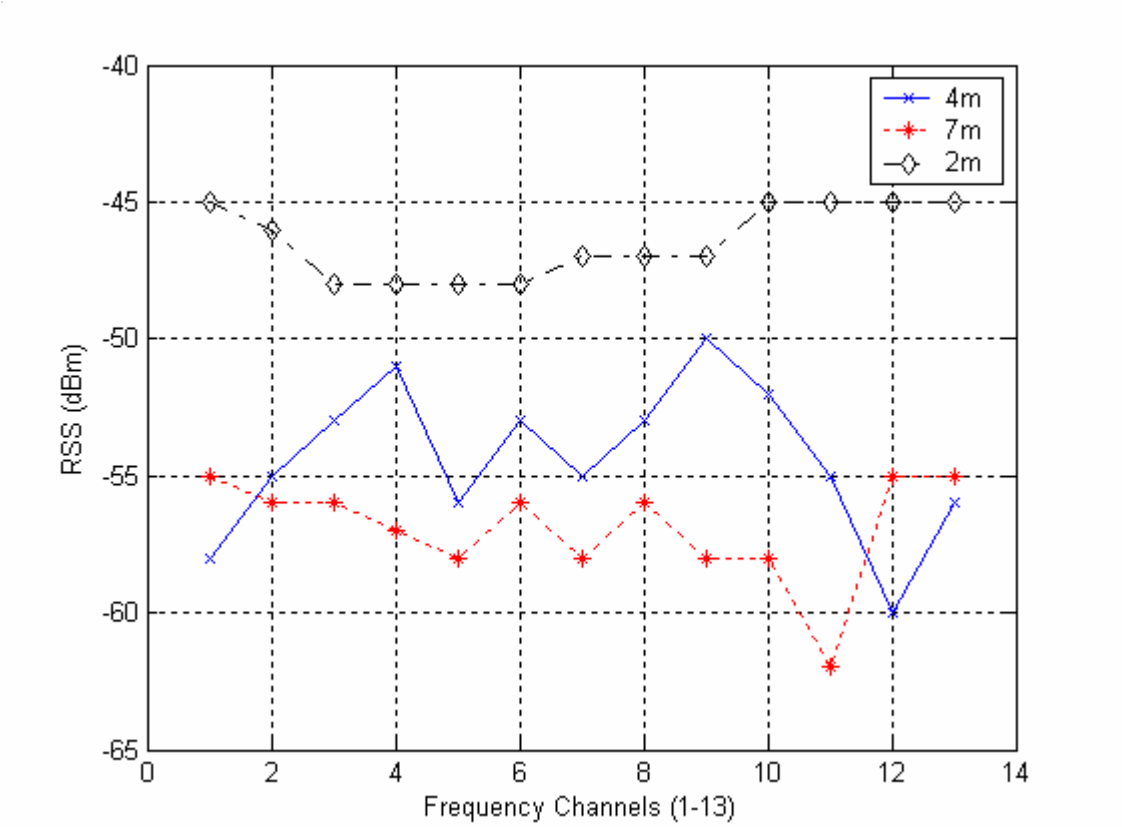

Figure 6-4(a) Variation in RSS on different frequncies (CH 1- 13)

6.3.2 Averaged results

Section 5.4.2 explains the method used to gather these results. The plot in figure 6-5 presents three curves; a theoretical path loss curve, the spread of RSS values reported on a single channel (channel 6) and the RSS averaged across all 13 channels.

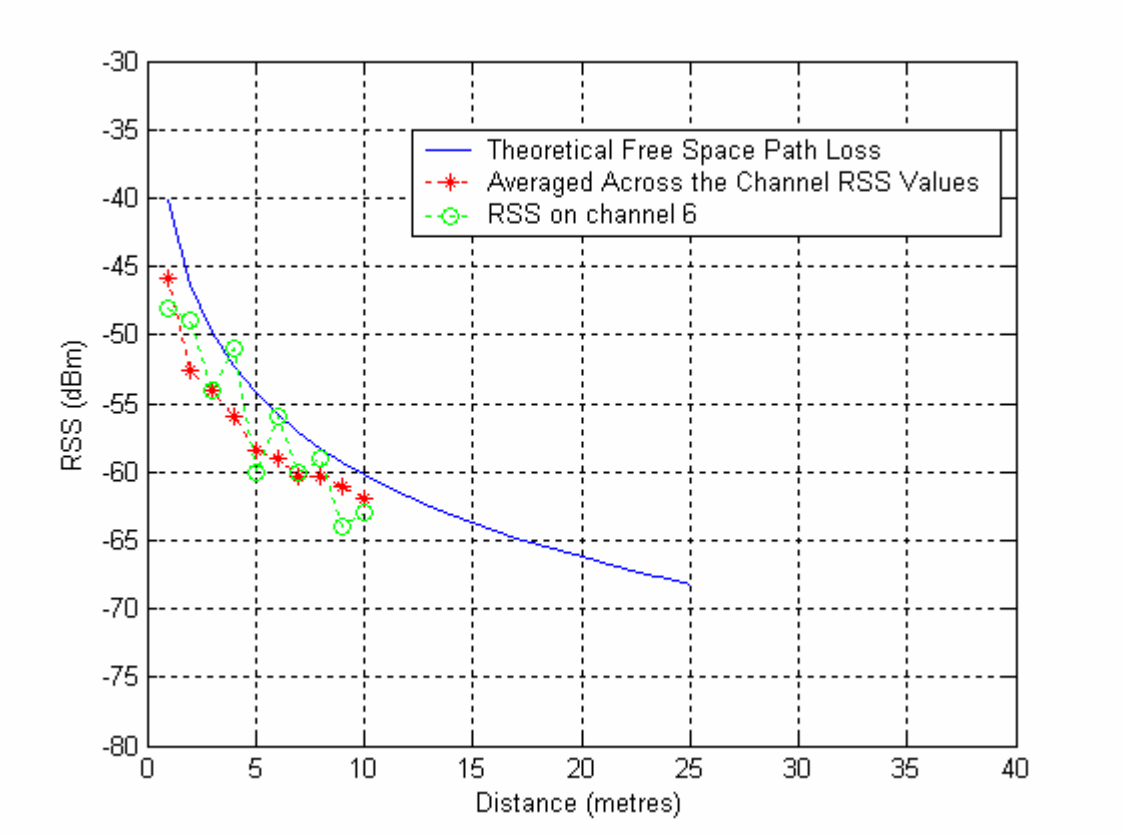

Figure 6-5 **Averaged (across the channel) received signal strength readings**

Discussion: Averaging across the channels, a method of frequency diversity produces averaged RSS values that have less variation and are more consistent with free space path loss. Further results that validate this finding will be discussed in subsequent experiments. These findings prove that frequency diversity as explained in section 3.4.1 existed across the 13 channels and could be exploited to mitigate multipath environment inside a building. The demonstrated method was not found in published material so far, therefore it can be regarded as a novel method of mitigating multipath environment inside a building using affordable off-the-shelf (802.11) equipment. The concept of frequency diversity is not new but the manner it is applied to achieve frequency diversity indoors using 802.11 is novel.

The 'averaged across the channel' curve in figure 6-5 approximately follows the theoretical free space path loss curve. A constant offset can be observed in measured and theoretical path loss curves. It could be because all measured readings were taken in same environment with access point fixed at one point and in LoS environment. We can

see that the trend of measured averaged RSS values follows more closely to the theoretical curve as readings are taken from different directions and then averaged as demonstrated in Figure 6-12.

It was worthwhile to analyse the data (signal strength readings) in statistical terms. The variance was calculated to determine the spread of RSS readings against distance, randomly picked, and comparison was drawn between the variance reported for 'across the channel averaged RSS readings' and 'individual channel RSS readings' and is given in figure 6-6.

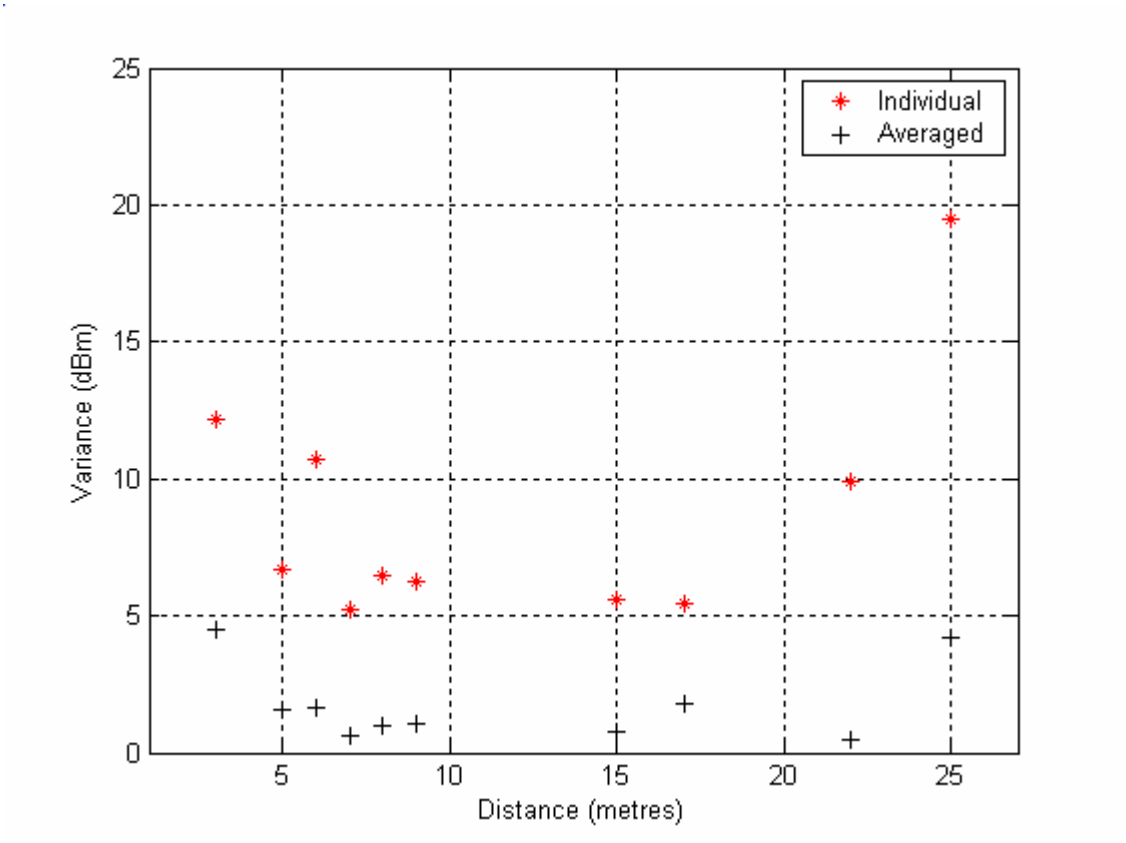

Figure 6-6 Variance in reported signal strength

The '+' signs show the variance in reported signal strength readings when frequency diversity is applied (averaged across the channel readings). Similarly the data collected for distances at individual channels were reported for variance with '*'. It is evident that applying frequency diversity has reduced the variance in RSS readings caused by multipath. It does appear that the effect of multipath on RSS is independent of distance.

Exploiting the frequency diversity of the 13 frequency channels through averaging should also improve the accuracy of geolocation.

6.4 Wall absorption - Results

Walls pose one of the major concerns in the design of indoor location algorithms. Correct identification of the location of walls in an indoor environment may drastically improve the chance of reporting accurate location estimation. The attenuation of walls is a key parameter, such as reported by Li et al, (2005) to be 5.5 dB for concrete walls.

The results of an experiment conducted in the test area with a wall between the client and sensor is given in figure 6-7. For sensors reported at increasing distance from the wall and client in the figure it is shown that the absorption by the wall varied between 3.5 to 8 dB for the distances given in figure 6-7. The mean was taken of all readings to give an average absorption loss of 5 dB.

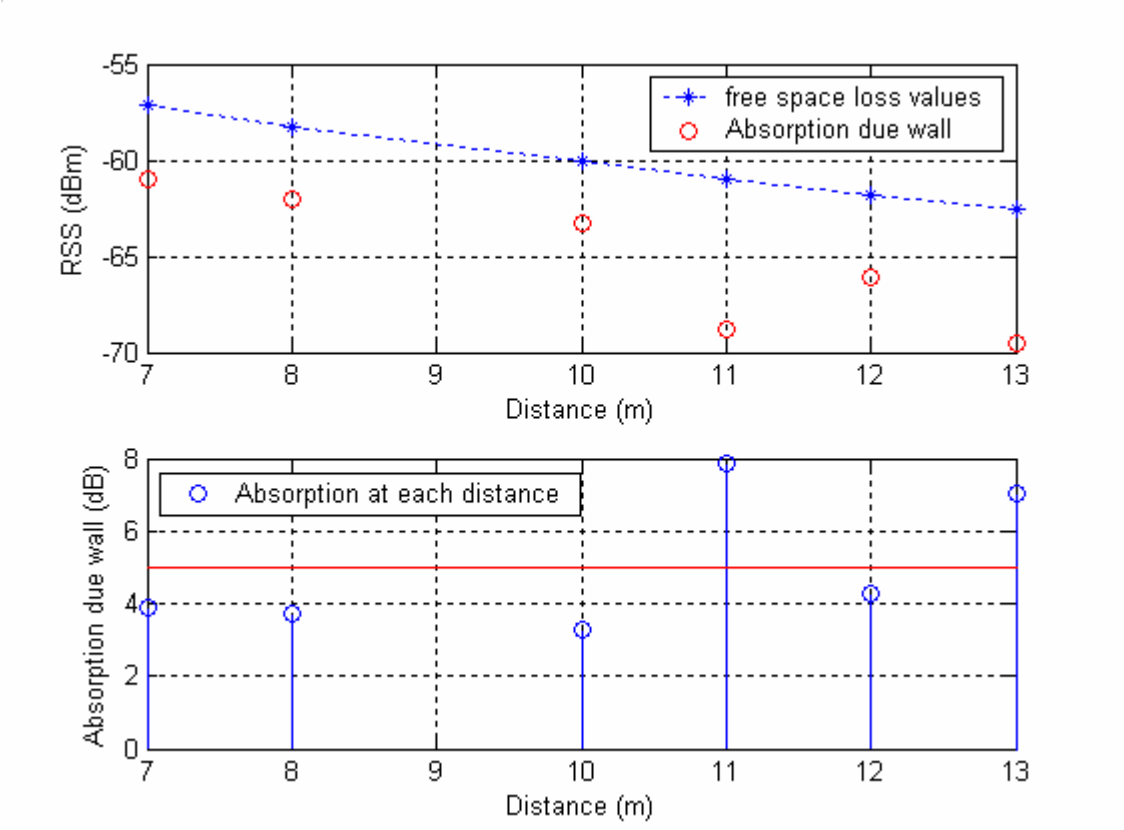

Figure 6-7 Average wall absorption

6.5 Multiple access points - Results

6.5.1 RSS values reported from different locations

The effect on RSS from three different directions is shown in figure 6-8 plotted on a log scale. The method of data collection has been explained in section 5.4.4. RSS values averaged across the channel were plotted at each distance (1m to 11m) as reported by three different APs (sensors), thus offering different orientation/direction.

Discussion: The figure 6-8 depicts RSS readings collected by different sensors (WRT54G) from three different directions as shown in figure 5-12. For each sensor the data was obtained after averaging the RSS values collected across the channels, repeated for all distances.

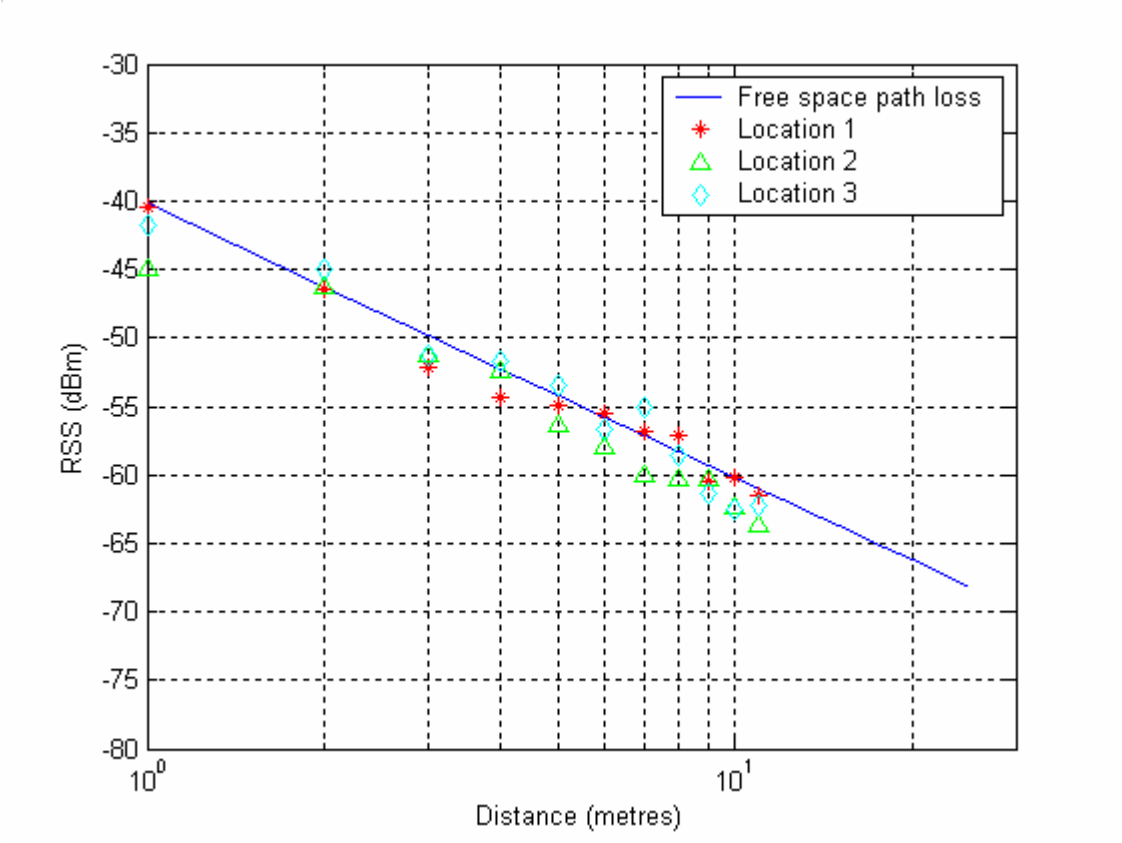

Figure 6-8 RSS as reported by three sensors from different locations

The three plots of collected signal strength readings served two purposes:

- The plots validate the initial finding (sec 6.3.2) that averaged signal strengths collected across the channels minimise the effects of severe multipath environment on RSS inside a building. The variation of RSS readings from each AP (sensor) was reduced compared to the situation for a single channel (sect 6.2; 6.3.1).

- The effect of orientation (different directions with respect to the sensor) was also reduced to some extent by averaging across the channel for the received RSS values. It was noted that the spread at common distances (Figure 6-8) was not as severe as compared to the readings obtained over for a single channel (Figure 6-5).

Having observed that the frequency diversity gives some control over the variation in RSS it was thought to see the effect in variation of RSS if fewer channel are considered.

6.5.2 Effect of frequency diversity on RSS - channels 1,2,3,4 and 1,5,9,13 considered

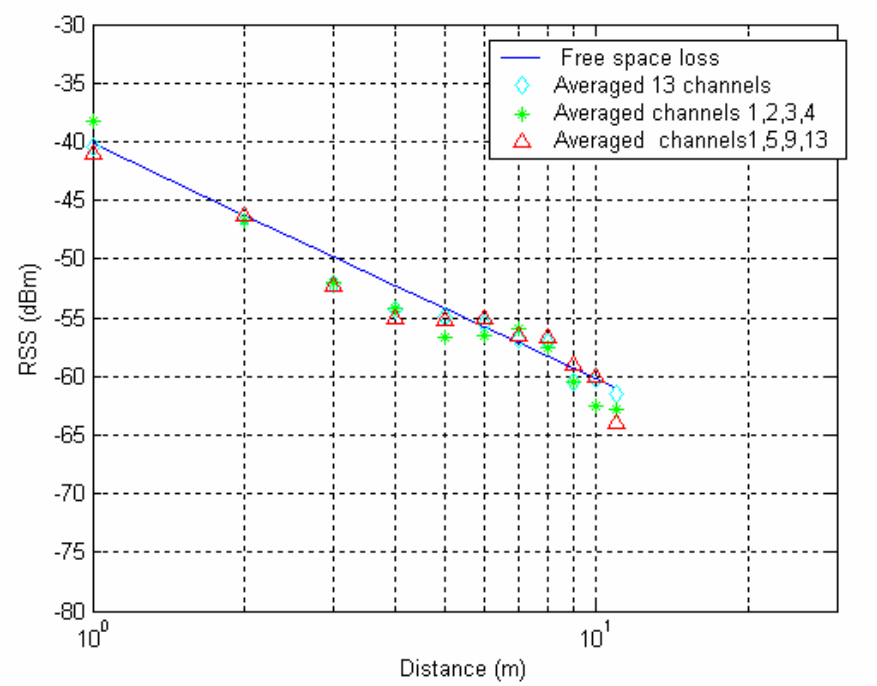

Figure 6-9 Effect of frequency diversity with different number of channels at location 1

In figure 6-9 and 6-10, comparison is drawn between effect of frequency diversity when channels 1,2,3,4 and channels 1,5,9,13 are selected in turn and also compared to the spread of RSS achieved when all 13 channels are considered. Channels (1, 2, 3, 4) have frequency coverage which overlaps as explained in section 3.2.7. Channels (1, 5, 9, 13) have overlap frequency coverage which is either very less or nothing at all as explained in section 3.2.7. Hence closer the channels, more is the frequency overlap. The experiment result given in figure 6-9 and 6-10 investigates as to how it effects the variation spread as compare to channels closer and apart from each other. Finally it also compares to spreads of RSS achieved from 13 channels. It can be observed that some effect of frequency diversity is taking place in all combinations of channels. The above result in figure 6-9 is based from one location of sensor. Let's observe the effect from another location with same distances. Results are given in figure 6-10 to 6-10(b).

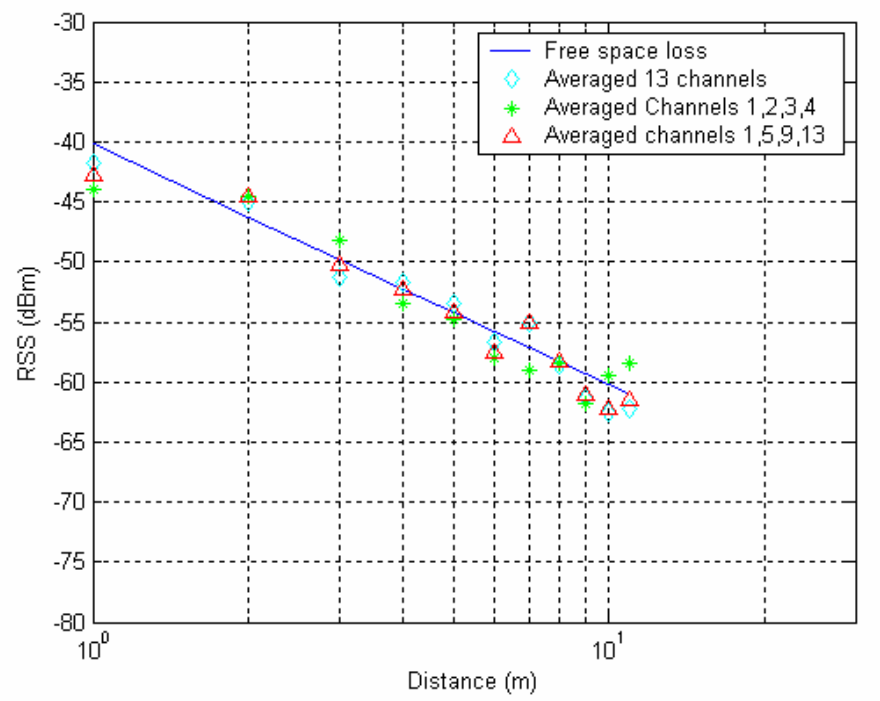

Figure 6-10 Effect of frequency diversity over different number of channels at location 2

The effect of correlation between channels is demonstrated in figures 6-10 (a) and 6-10(b) where variance of data for channels 1,2,3,4 is compared to data for channels 1,5,9,13 and it is shown that data is uncorrelated for channels selected apart as compare to channels which are adjacent as the variance between data sets at most distances is less for channels 1,2,3,4 than Channels 1, 5, 9, 13.

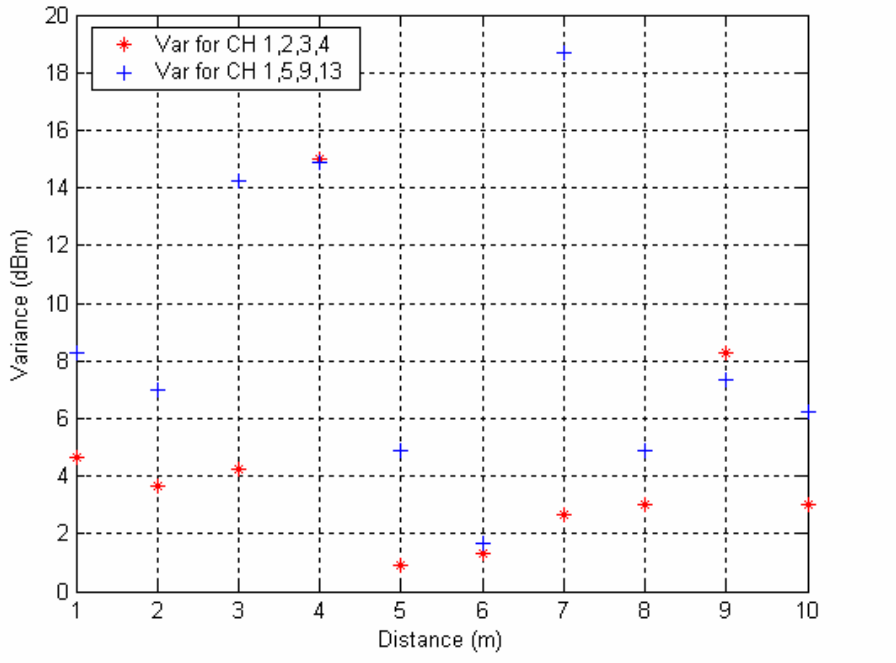

Figure 6-10(a) Variance comparison for data set (CH 1,2,3,4 and CfH 1,5,9,13) – location 1

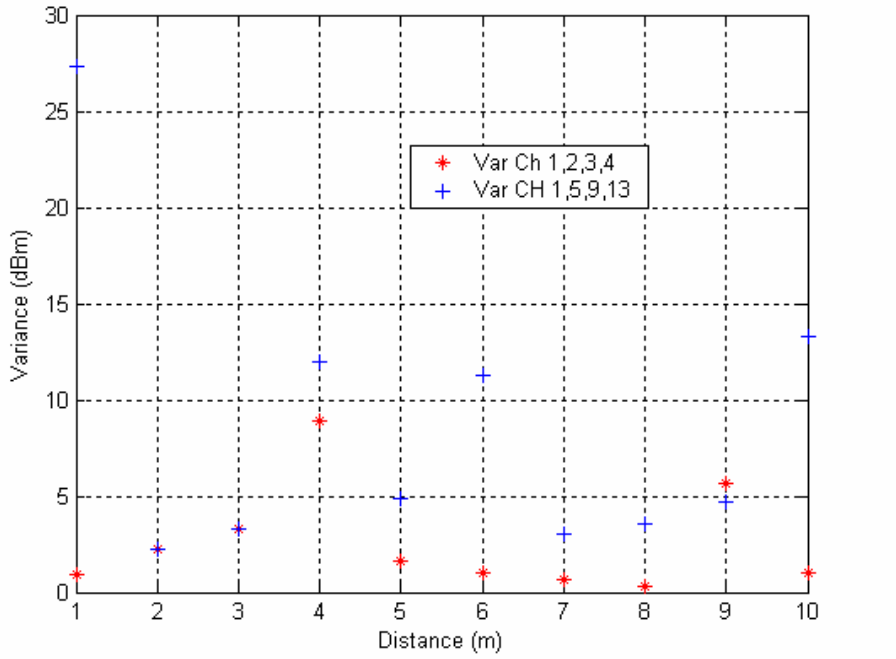

Figure 6-10(b) Variance comparison for data set (Ch 1,2,3,4 and Ch 1, 5, 9 , 13) – location 2

Results discussed above shows that fewer channels can be assumed to achieve frequency diversity to some degree thus giving some control over RSS spread. This can also reduce the overall time required to carry out location estimation when 4 to 6 channels are considered to apply frequency diversity as compare to 13 channels.

6.5.3 Effect on RSS values of a changed environment

Figure 6-11 shows the collected signal strength values after averaging across the channel for each distance. Locations were chosen randomly to cover a 25m range starting from 5m. This was still a LoS environment with a number of obstructions as the distance increased. The method for conducting experiment has already been explained in section 5.4.4.

Discussion: We can see that the data obtained after averaging across the channel showed good results as the variation of RSS at common distances from the three different APs (sensors) was small. Again, as was the case in the previous experiment, the spread was within 3 dB.

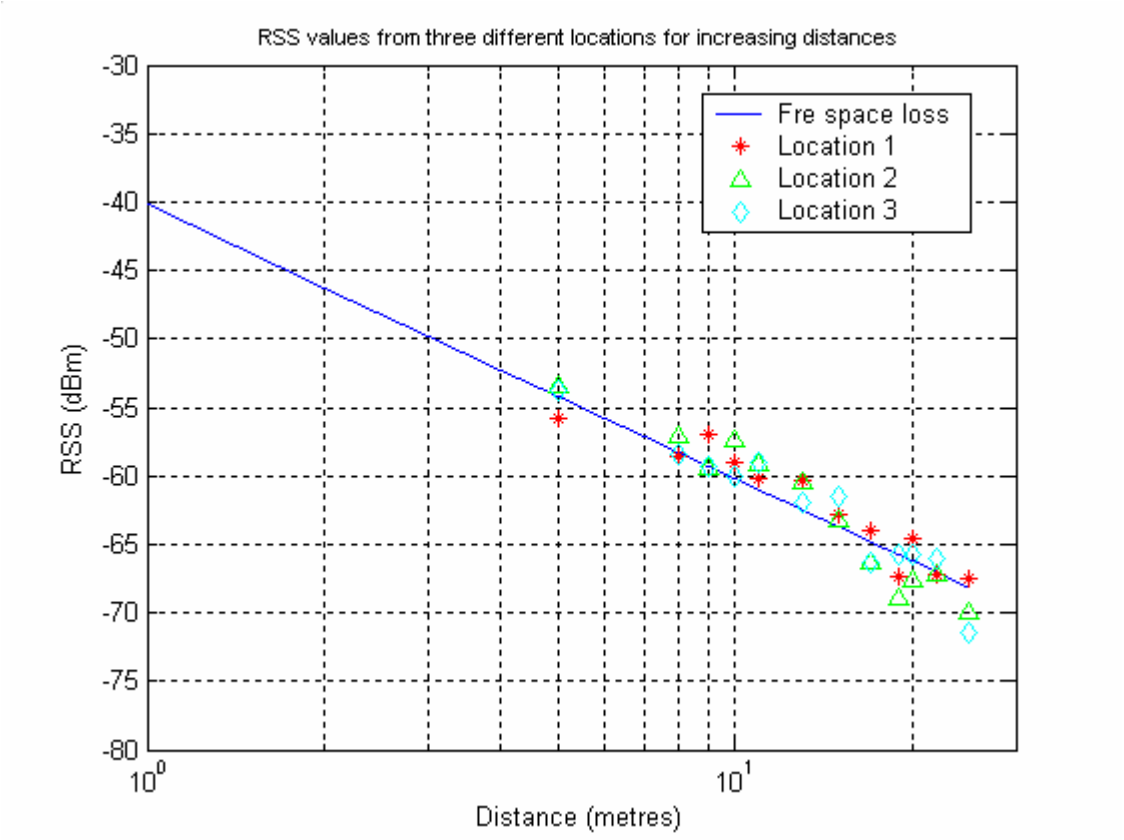

Figure 6-11 Effect of change in environment of RSS from three different locations (averaged across channels)

The results prove that:

- The novel method of applying frequency diversity to collect RSS values was consistently reporting accurate readings with little variation. Therefore, the method applied to mitigate multipath could be regarded as effective.

- Although the environment had changed on moving from one laboratory to a different laboratory, which varied in dimensions, equipment and structure, the RSS values with frequency diversity applied followed theoretical free space loss.

- Moreover, the common measurement points for this figure and the previous one (6-8) produced results which were close to each other. These are shown in table 6-3.

Table 6-3 Correlation between two figures 6-8 and 6-11 about reporting RSSI values on common distances.

Common Distance	**5m**			**8m**			**9m**			**10m**			**11m**		
RSS (dBm) Fig (6-8)	56	55	54	60	57	56	61	60	60	60	62	62	61	62	63
RSS (dBm) Fig (6-11)	56	54	54	58	58	56	59.5	59.5	56	59	59	57	59	60	60
Difference RSS (dBm)	0	1	0	2	1	0	1.5	0.5	4	1	3	5	2	2	3

Based on results in figure 6-8 and 6-11, a propagation model was devised by merging the data into one figure. The readings of RSS values at each distance point from all positions were averaged and the result so produced is displayed in figure 6-12.

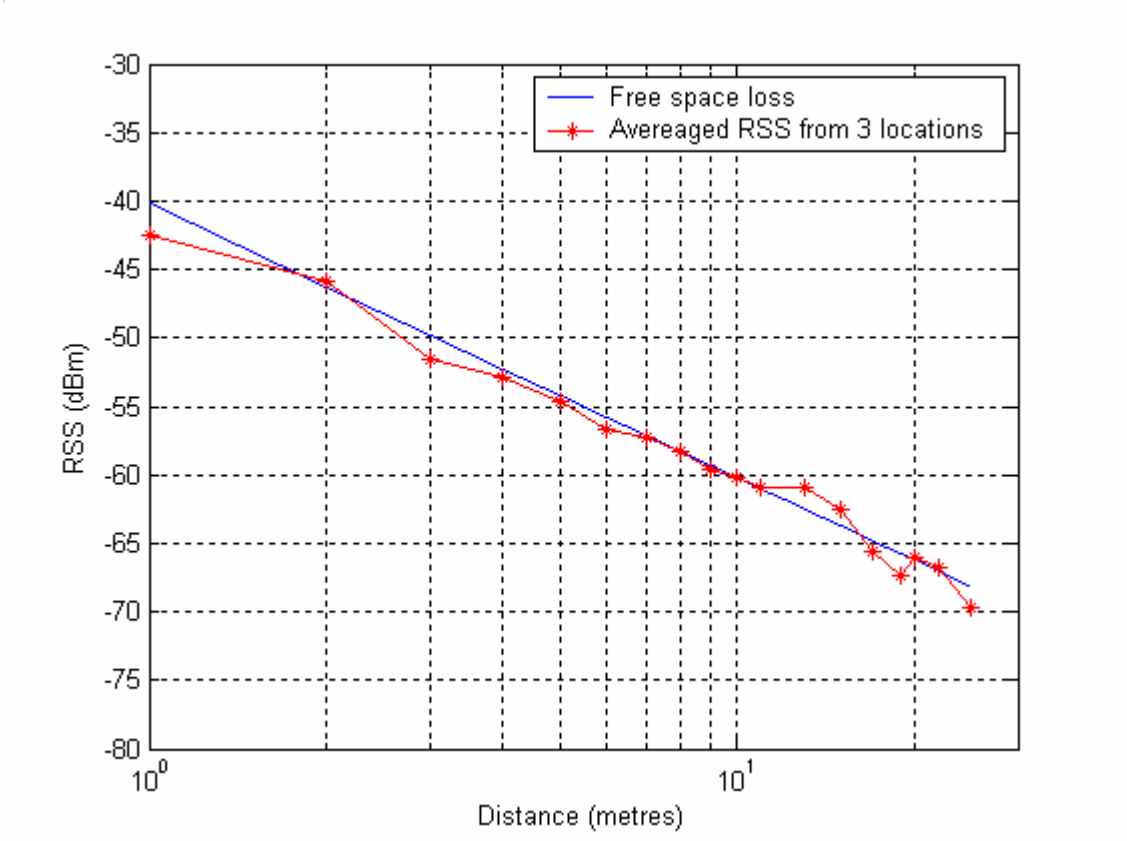

Figure 6-12 Comparison of averaged sensor readings from two environments (rooms)

The figure clearly shows that there was a strong correlation between the theoretical and empirical readings. Hence the theoretical path loss model could be adopted inside a building (LoS environment) provided variation in RSS values was minimised. A Free space path loss model could therefore be applied to location estimation of a client inside a building through triangulation. Before proceeding with explanation of results produced by the location algorithm, it was important to take into account the effect of walls across the test area.

6.5.4 RSS values across the test area with walls

The results in figure 6-13 present four different datasets. The blue solid line is the free space path loss curve, green and red solid lines are the free space loss curve offset by 5 and 10 Db respectively. The black crosses represent LoS (line of sight) location, green '+' signs are RSS values at varying distances from different sensors with one wall between the sensor and the client and the red '*' show the dataset (RSS values) for a

client with two walls between the sensor and the client. These RSS values were obtained from four sensors placed at different locations as shown in figure 5-13.

Note the difference in RSS values in three different scenarios; LoS, one wall and two walls. The RSS values measured beyond single wall and 2 walls can be seen spread across the two offset curves. The 5 dB offset curve has spread of RSS values cluttered slightly on top and few under the curve suggesting the average measured RSS values beyond single wall assumes an approximate value of ~ 4.5 dB loss. But overall spread for 5 dB offset curve is within 5 dBm. Similarly spread can be seen around the 10 dB offset curve for the RSS values of a client collected beyond 2 walls. Again mostly spread at common distance is seen within 5 dBm. This shows that the assumption of 5dB and 10 dB wall absorption was a fair estimate.The absorption by walls (Helen et al, 2001; Li et al, 2005) is clearly observed as a major hindrance in locating clients with accuracy. The position of walls, if known, could be used to aid accurate geolocation.

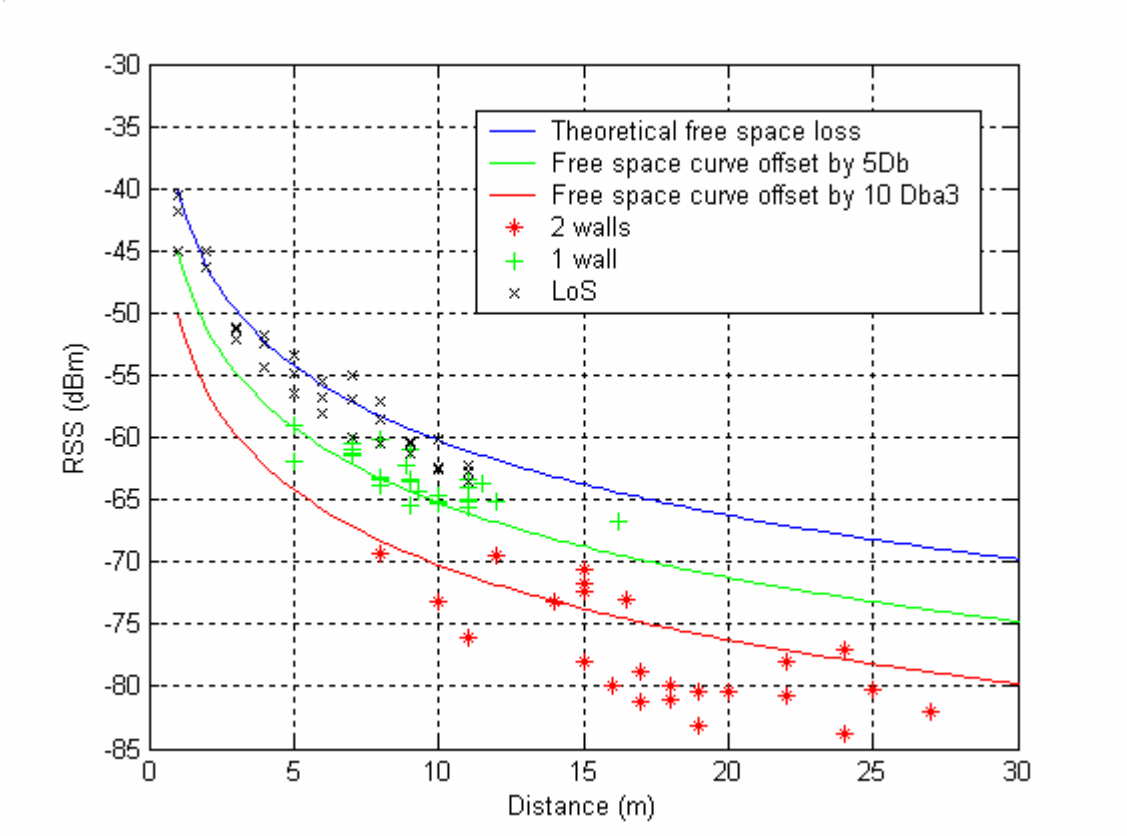

Figure 6-13 Effect of walls on RSS values

6.6 Novel algorithm design using triangulation to produce a location estimate

The free space propagation model has been shown in figure 6-12 as suitable for use in a threshold algorithm for location estimation using triangulation

The algorithm results are discussed at length in the following two sections followed by a summary of the couplet set of location results presented in appendix A. In section 6.7 error estimates for the reported location are analysed under the following conditions:

- RSS on single channel – No walls, No forced overlapping
- Averaged RSS on multiple channels – No walls, No overlapping
- Averaged RSS multiple channels – No walls, but forced overlap
- Averaged RSS multiple channel – Walls, No overlap
- Averaged RSS multiple channels – Walls with Overlap

Location 11 (figure 5-14) was chosen to analyse the operation of the algorithm in detail.

Section 6.8 carries out detailed analysis to progressively explain functioning of the algorithm in arriving at location estimate. This analysis includes explanation on applied corrections due to detection of walls and extra absorption beyond threshold limit of the test area. The forced overlap of circles to arrive at correct results is also discussed. The evolution of forced overlap logic is also explained. All these steps are elaborated with help of location estimation results obtained for location 8 in figure 5-14.

6.7 Location accuracy analysis

6.7.1 Geolocation using RSS on single channel – No walls, No forced overlap

Two channels, 2 and 7 were chosen to investigate the triangulation result when walls were not considered and forced overlapping (section 4.8) was also neglected. The results are shown in figure 6-14.

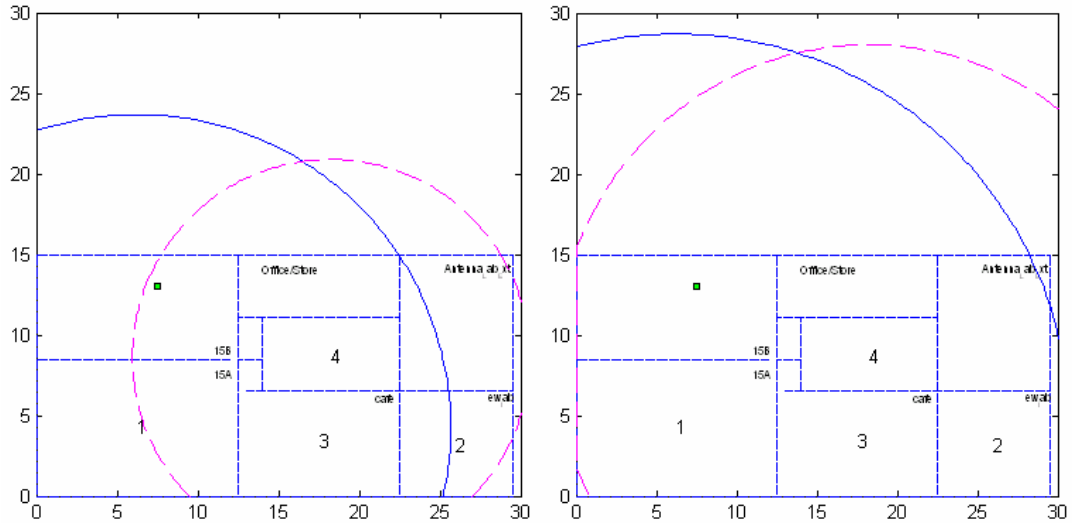

Figure 6-14 Channel 2 and 7 location data – no walls and no overlapping

The two figures (test area with x and y axis in metres) show the variation in RSS values on channel 2 and 7. At channel 2 the circle for 4 AP reported an RSS which was translated into a distance passing close to the correct location. On channel 7, the RSS value translated into a distance far away from the location. Circles 2 and 3 were not visible due to the low RSS values from these sensors suggesting that there were walls between the client and the sensor. Hence without information about the presence of walls, the accurate location could not be determined. With only two circles overlapping, the intersections give ambiguous locations at approximately 11m and 20m from the true location.

6.7.2 Geolocation using averaged RSS across channels (1-13) – no walls, no overlap

Averaged RSS value from all 13 channels was used as metric to draw circles for location estimation. The algorithm (without walls and forced overlap) gave a location as shown in figure 6-15.

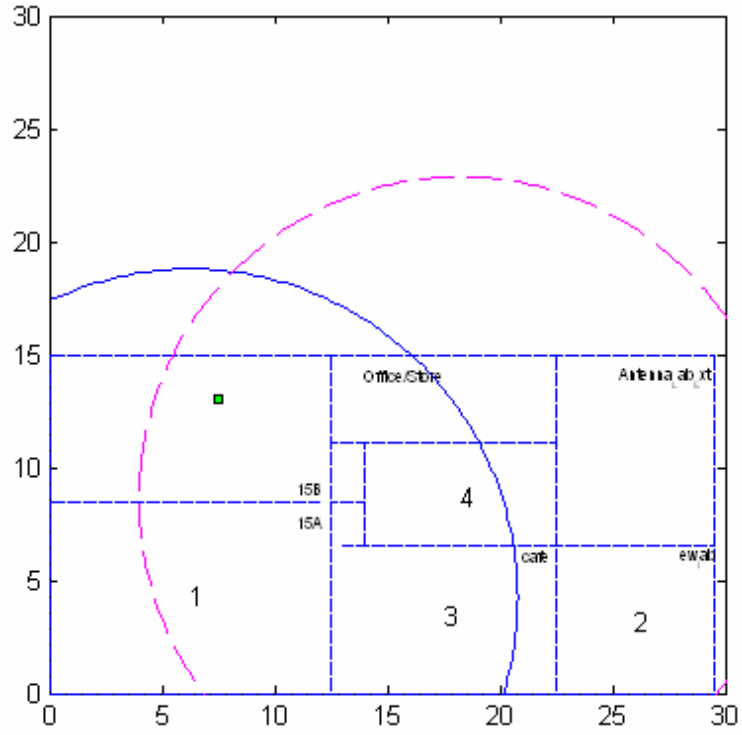

Figure 6-15 Averaged RSS – No walls and no forced overlap

With averaged RSS across the channel (1-13), the exact location could not be determined. Although the intersection point was closer to the location (square) as compared to figure 6-14, the two circles from sensors 2 and 3 were not visible in the scale of the figure. This suggested that the position of walls with respect to sensor 2 and 3 were required and a correction was needed to be applied to bring the other two invisible circles within the test area.

6.7.3 Geolocation using averaged RSS across channels (1-13) – no walls but forced to overlap

Figure 6-16 illustrate the effect of using the forced overlap algorithm for all circles from all four sensors. The wall position was still not known but the circles, which were not overlapping, were forced to overlap. The error reported was 11m and as can be seen in the figure the estimated location fell outside the test area.

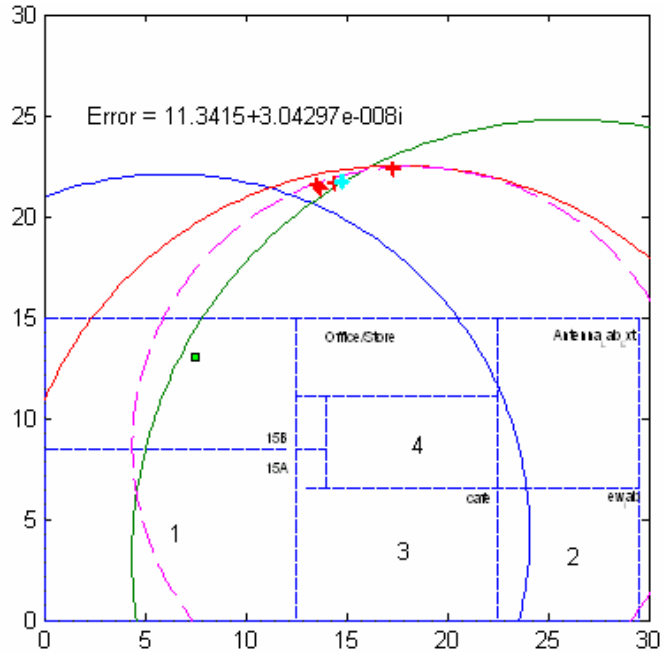

Figure 6-16 Averaged RSS – Forced overlapping but no walls

6.7.4 Geolocation using averaged RSS with known walls position, non-forced overlapping

With the presence of walls estimated, all four circles pass close to the client position shown in figure 6-17. As correction due to the known position of walls is applied, two circles (sensor 1 and sensor 3) are almost exactly through passing from client's position. The remaining two circles from sensors 2 and sensor 4 are also near.

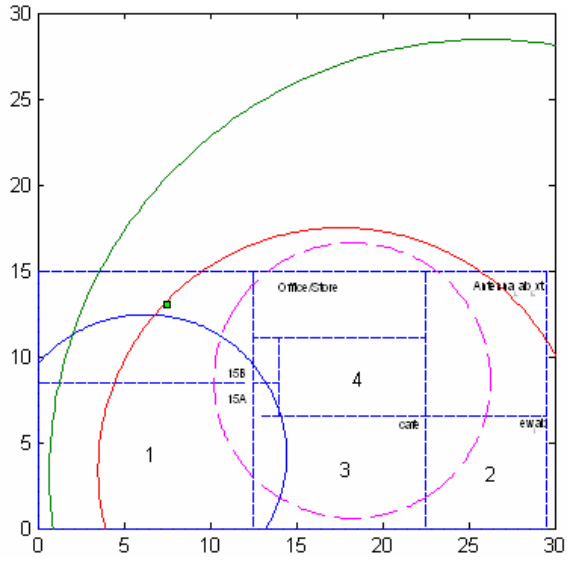

Figure 6-17 Averaged RSS – Known walls position

6.7.5 Geolocation using averaged RSS with known walls and forced overlap

From figure 6-18 it can be seen that together with the known position of walls and fine-tuning through forced overlapping, the results are significantly improved. These are shown in figure 6-18.

These results lead to the following conclusion

- The position of walls inside a building must be known to obtain an accurate location estimation

- Forced overlap is applied, if required, for circles not overlapping after the correction for walls is applied to improve the location estimation.

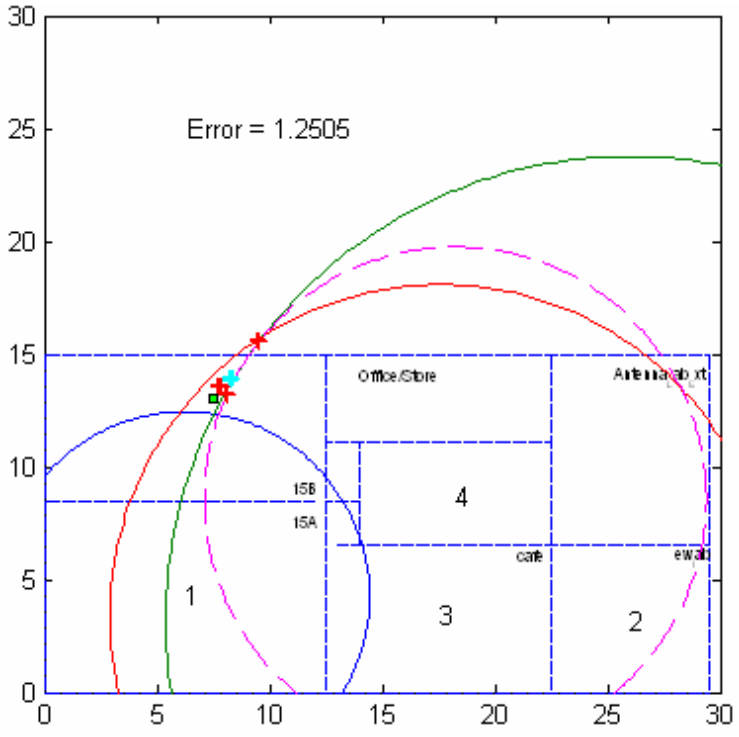

Figure 6-18 Averaged RSS with known walls position and forced overlap

6.8 Algorithm results – Detailed analysis and discussion

The functional block diagram in section 4.2 has been previously discussed. Here, each step explained in the block diagram will be demonstrated with the aid of results achieved when the algorithm is applied on raw data (RSS) collected from the sensors for a client under consideration.

6.8.1 Scenario 1 – Example with accurate results achieved

In step 1, the algorithm compares the received signal strength values from all four sensors for a client against a threshold for each sensor as explained in section 4.5 to 4.7. One of the experiments conducted for location 8 (figure 5-14) will be discussed in the ensuing paragraphs. Table 6-4 provides the initial data as given by the sensors for a client. The algorithm checks these RSS values against the threshold for each room where a sensor is placed and decides weather the client is inside the room or beyond a wall (row 4 table 6-4). The threshold calculated for the rooms are given in row three of the table. From this data it is quiet clear that the client is beyond the wall with respect to each sensor. The same can be verified by looking at figure 6-19. The solid square dot represents the client and is not in any of the rooms which contain sensors. The next row of the table shows the translated distances of the signal strengths reported by the sensors, using equation 3-13. The reported distances are large figures. Sensor 2 and sensor 3 are reporting the client placed at 103 and 61 m distance respectively. Section 4.7 demonstrates that the maximum distance reported by any sensor for a client cannot exceed 29m for the example test area.

Table 6-4 Received signal strength values for a client and translated distance without applied correction

	Sensor 1	Sensor 2	Sensor 3	Sensor 4
RSS (dBm)	60.90	83.15	76.07	63.30
Threshold (dBm)	57.814	53.749	55.739	53.913
Beyond single wall	yes	yes	yes	yes
Translated Distance without correction (m)	10.82	139.95	61.94	14.27

In step 2, the raw RSS values in row 1 of table 6-4 are checked for the client's position beyond 2 walls. Again the RSS values are compared with calculated thresholds for two walls determined by the algorithm. Same are shown in table 6-5.

Table 6-5 RSS values checked for 2 walls and corrections applied by algorithm

	Sensor 1	Sensor 2	Sensor 3	Sensor 4
RSS (dBm)	60.90	83.15	76.07	63.30
Threshold two walls (dBm)	69.73	68.07	70.39	67.69
Beyond two walls	No	yes	yes	no
Corrected Distance (m)	6.10	24	13.87	8.02

Table 6-5 provides the translated distances of the client from each sensor in the last row. The last rows of the two tables when compared tell us that the corrections are identified by the algorithm and applied to arrive at certain readings. This can be seen in appendix A (A.8.2) where algorithm numerical results are shown and the last 'NOTT' gives the status of client with respect to each sensor. Digit '1' means the client is beyond single wall and digit '2' means the client is beyond two walls. The same can now be triangulated to ascertain any overlapping areas. See figure 6-19.

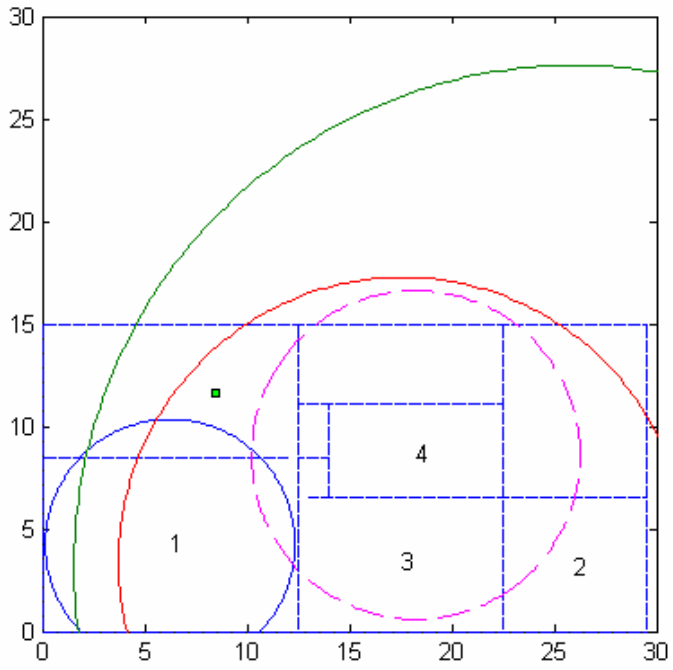

Figure 6-19 Corrected RSS values represented in circles

In step 3, the raw RSS values that are identified to be beyond two walls are now tested against the absolute threshold value calculated for the test area. It is noted that circle 2 represents 22.18m of corrected distance which has been reduced from an exaggerated figure of 139.95m as given in table 6-4. The raw reported strength by sensor 2 was 83.15 dBm. Since it was detected to be beyond two walls, which is evident in figure 6-17 when the client is observed with respect to sensor 2, 10 dB's were subtracted. The resulting 73.15 dBm is now compared to the final absolute threshold of the sensor 2 calculated as 68 dBm (section 4.7). The algorithm finally assigned the value of 68 dBm to sensor 2 in respect of the client as based on the logic described in section 4.7. This 68 dBm is translated to ~24m as shown in the last row of table 6-5. Similarly all values of reported strength of a client that are identified as beyond two walls pass through this test of respective absolute threshold.

Table 6-5, in the last row, gives the corrected RSS values which when translated into circles gives the picture of overlapped and distinct circles as shown in figure 6-19. A solid square dot represents the client position. We can deduce by looking at the figure that circle 1, 2, 3 and 4 are reasonably close to passing through the clients position except for sensor2. To achieve final location estimation, the four sensors are combined in sets of 3s to produce four positions, as explained in section 4.10. Figure 6-20 provides the triangulation result for sensors 1, 2 and 4.

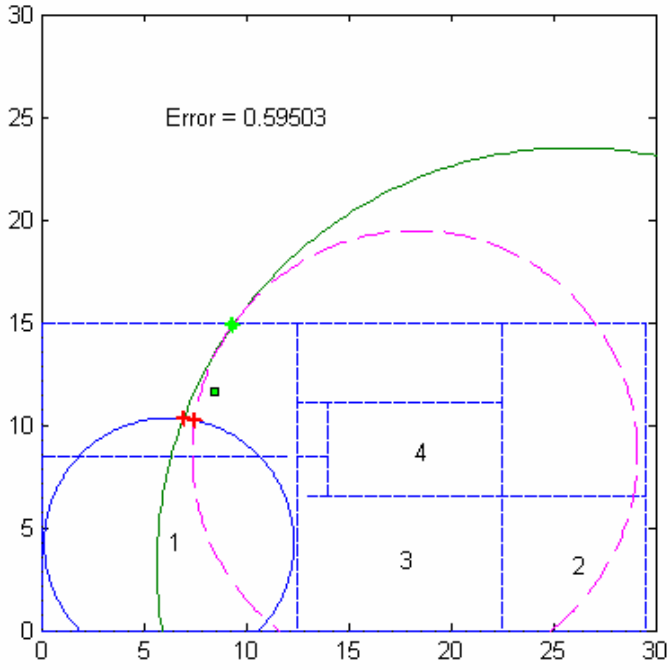

Figure 6-20 Triangulation with client position reported by sensors 1, 2 and 4.

The distance error is 0.59 m, which is less than the 3m designed error. In the original result of figure 6-17 circle 4 is not overlapping with circle 2. This means, in figure 6-20 circle 2 has contracted, while circle 4 has expanded so both meet at a new position with circle 1 remaining unchanged. This can be clearly observed when the two figures (6-19 & 6-20) are compared. This process has brought the estimated position closer to the client. Similarly considering figure 6-21, instead of sensor 1, sensor 3 is introduced with sensor 2 and 4 to obtain a triangulation result from a combination of sensors 2, 3 and 4.

Again comparing this figure to 6-17, sensor 4 is not overlapping with either of the circles 2 or 3. Here in figure 6-19, circle 3 has expanded to meet circle 2 and circle 4. The error reported after triangulation is 3.9m.

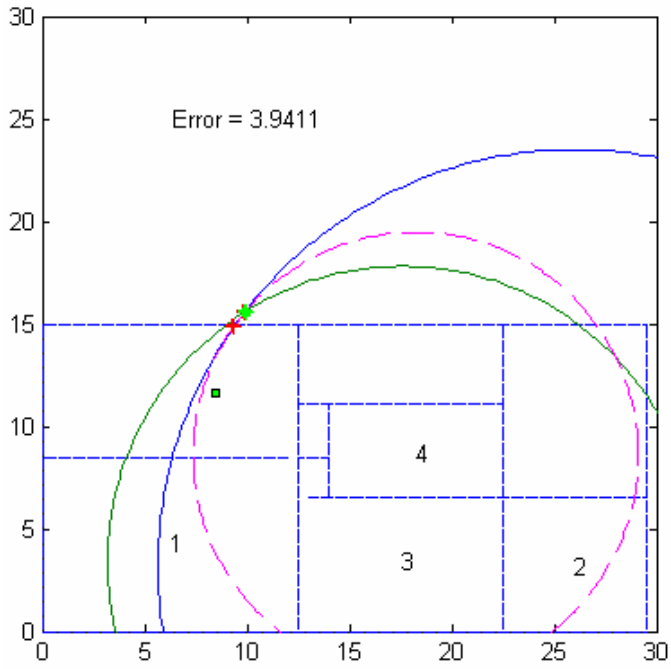

Figure 6-21 Sensors 2,3 and 4 reported position of Client

Similarly combination of sensors 1,2 and 3 reports an error of 1.32m and sensors 1,3,4 reports an error of 1.13m. These results are shown in figures 6-22 and 6-23

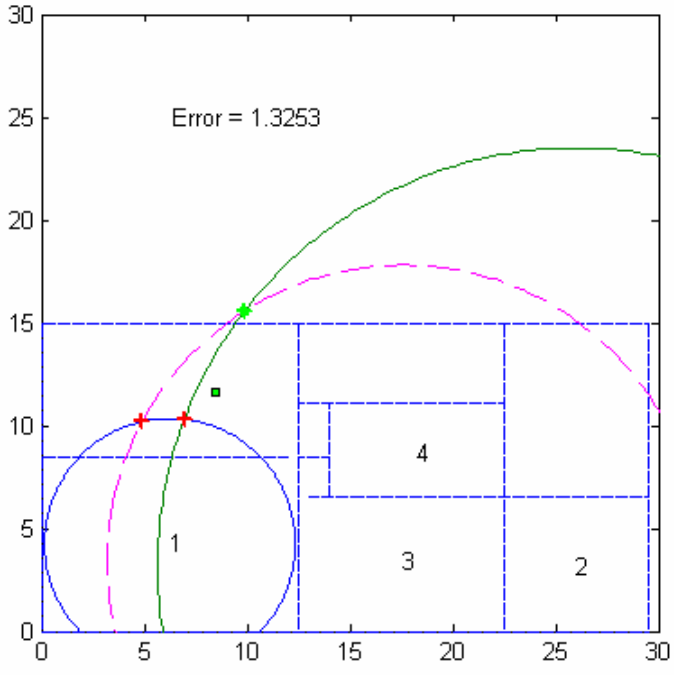

Figure 6-22 Triangulation result by sensors 1,2 and 3.

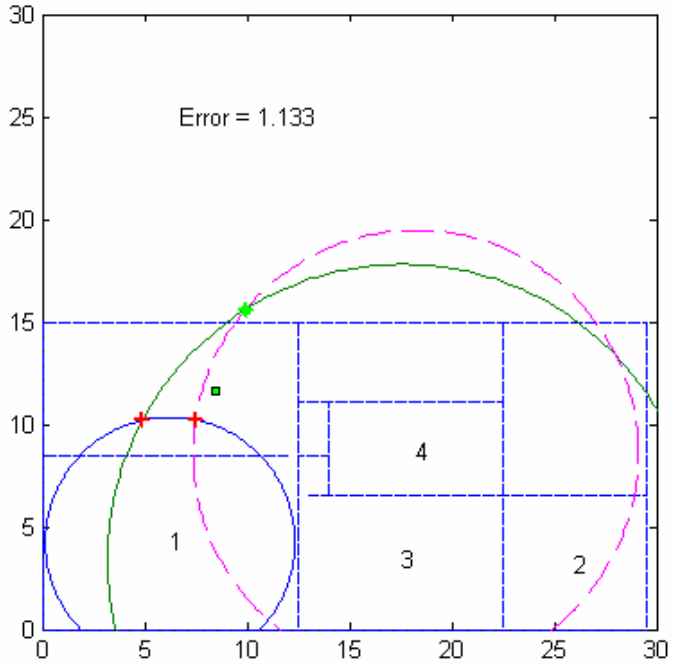

Figure 6-23 Triangulation result for sensors 1,3 and 4

Estimated locations from all four set of sensors in figure 6-20 to 6-23, are averaged (4.10) and the final position is estimated which is given in figure 6-24. Although one set of circles (triangulation), figure 6-19, reported error of almost 3.9m averaging from all 4 estimates gives a much improved error of 1.26m.

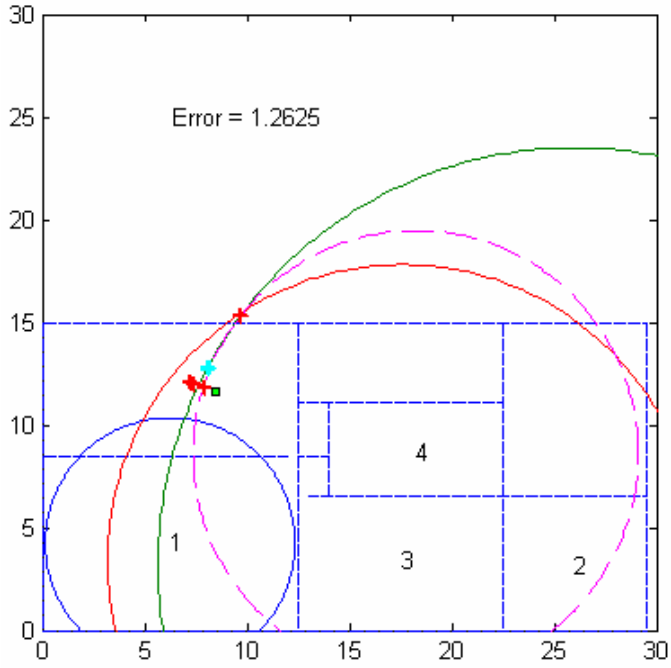

Figure 6-24 Final error based on triangulation results from four set of sensors

We have observed through analysis of the previous figures that the algorithm accurately detects one or two walls between the client and the sensors and applies a correction accordingly. The forced overlapping of circles also reduces the location error.

A client at location 6 in figure 5-14 is discussed in figure 6-25. The outcome, if two of the four sensors report exaggerated values and how this affects the final result, will be examined for one of the worst case location estimates.

6.8.2 Scenario 2 – Example with accurate results

Figures 6-26 to 6-29 show triangulation reported by 4 sensors. The result is an example, which is not accurate when compared to the standard achieved on other occasions. The final location error as reported in figure 6-29 is 4.79m. On the majority of the occasions the results reported are under 3m accuracy when compared to the original client position. The example is included to analyse the progressive improvement in the algorithm.

Figure 6-25 shows four circles, each drawn by the algorithm after applying correction to received signal strength data collected from the four sensors (APs). The original

location of client whose position is being determined is shown in figure 6-25 with a square.

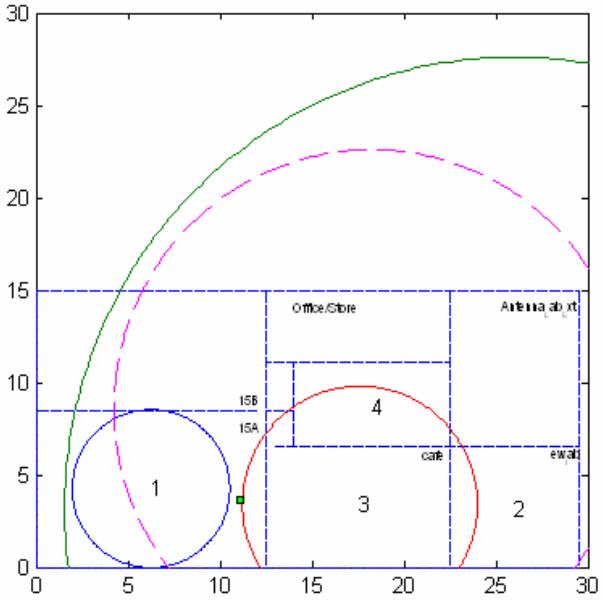

Figure 6-25 Circles generated by algorithm based on received signal strength from each AP (Sensor) having applied correction

The reported signal strength and the correction applied by the algorithm at different stages is given in the table 6-6.

Table 6-6 Translated distances based on raw data before corrections (column 3) and processed data after correction (column 8)

APs (1)	Reported Signal Strength (RSS) dBm (2)	Translated distance (m) (3)	Single wall detected by algorithm (4)	Two walls detected By algorithm (5)	Extra absorption than two walls (6)	Corrected signal strength (dBm) (7)	Translated distance as correct applied (m) (8)
Sensor 1	52.85	4.28	No	No	No	52.85	4.28
Sensor 2	78	77.35	Yes	Yes	Yes	68	24.46
Sensor 3	61.3	11.35	Yes	No	No	56.3	6.39
Sensor 4	73.15	44.25	Yes	Yes	No	63.15	14

The final column of table 6-6 shows the distance of each sensor from the client. There are a few interesting observations from the above data and the figures to follow. The

distance can be calculated using equation 3-13 if loss (signal strength) is known. The same equation is applied by the algorithm to achieve results in column 8 from the RSS values in column 7 of table 6-6. Considering figure 6-26 which shows circle 3 greatly extended when compared to the same circle in figure 6-25. As is explained in section 4.7 that circles reported by the algorithm are made to overlap as is the requirement in figure 6-25, where circle 3 is not overlapping with other circles. Therefore, the algorithm attempts to overlap and in the process incurs undue errors that exceed 5m to 8m for figures 6-26, 6-27 and 6-28. In figure 6-25 circle 3 intersects the position of the client. It is however, greatly stretched in figure 6-26. This occurred since circle 2 and circle 4 are reported away from the client's position. For instance, circle 2 in figure 6-25 is out by 10m and circle 4 is out by 7m approximately.

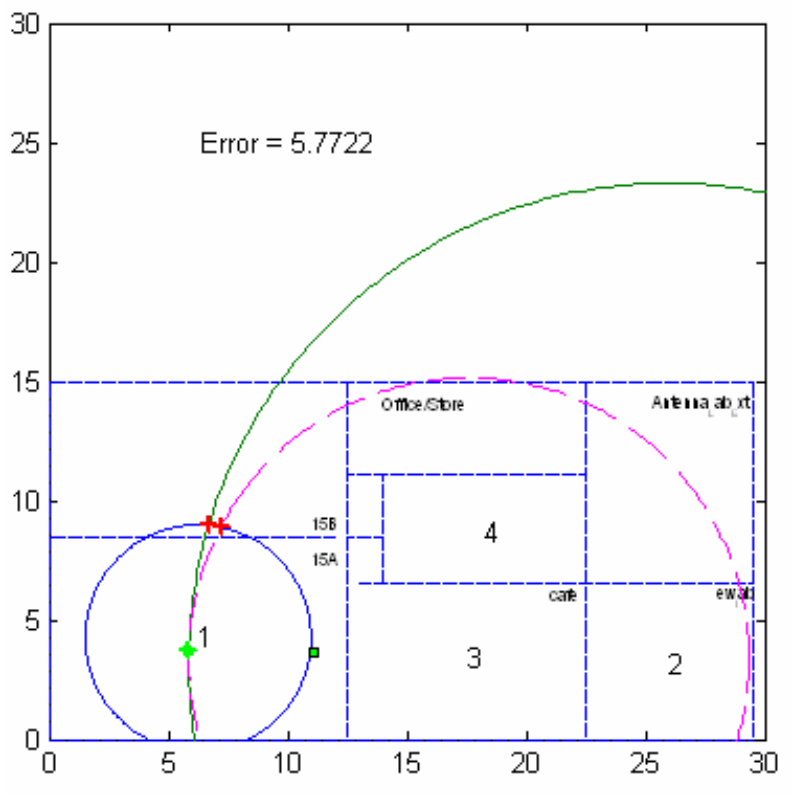

Figure 6-26 Radius of circle 3 has stretched as compared to the same in figure 6-20

With the large errors in distances reported by sensor 2 and 4, the algorithm has still been able to report the final position of the client at 4.79m (figure 6-29) away from the actual

position of the client. The algorithm has worked to report good results despite two of the sensors reporting a large distance error.

The present design will work for more or less all cases as long as the reported signal strength values for a client do not have a large error as has been the case here. Greater errors are likely to occur if any two of the sensors report incorrect signal strengths as has been the case in the result example under discussion where sensor 4 instead of 8m reported the position of the client at approx. 14m. Similarly sensor 2 reported positions at 24.5m whereas the client is actually placed at 15m.

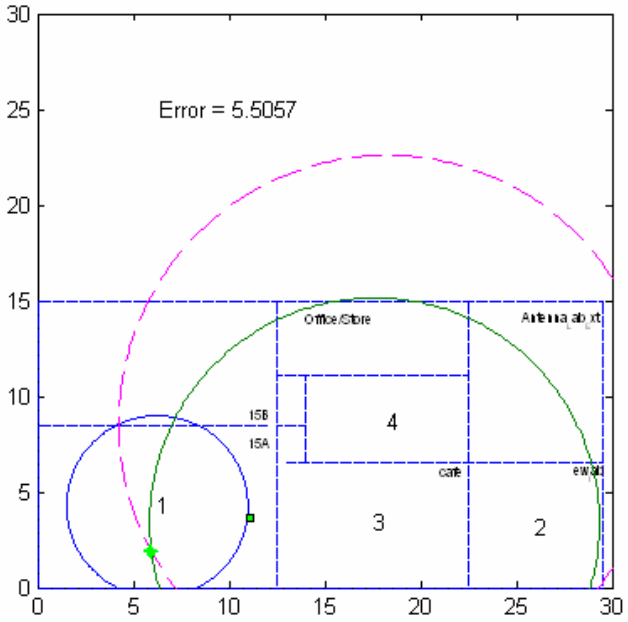

Figure 6-27 **Circle 3 has extended way beyond the client position in effort to intersect circle 4 which caused error to escalate**

By any standard, using a propagation model, this is an acceptable error (see table 2.5). When considered in the context of the number of experiments conducted, only a few results had an error exceeding 4m.

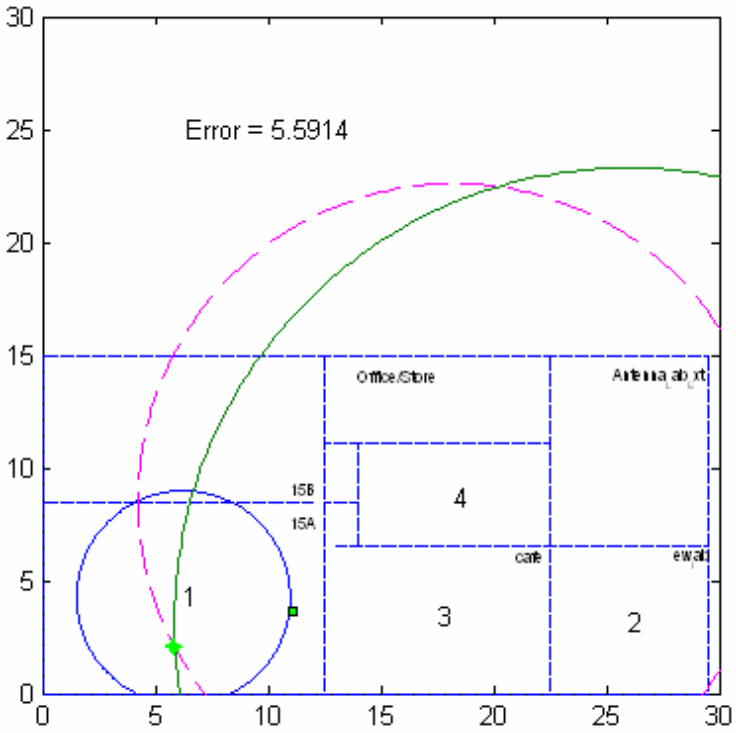

Figure 6-28 Triangulation for sensors 1,2 and 4

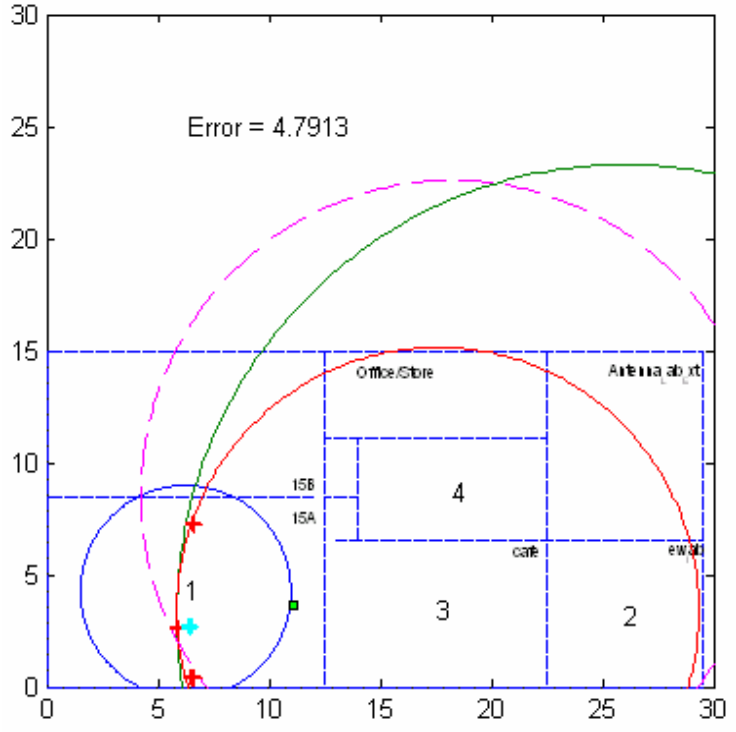

Figure 6-29 Final error as assessed from 4 set of triangulations (data fusion)

6.8.3 Scenario 3 – Improved location estimation using forced overlapping

It is envisaged that there could be many such cases when at least one of the sensors report location data (signal strength) for a client that is an exaggerated value and causes a error. The algorithm is thus improved to detect such situations and apply a correction. The result shown in Figure 6-30 is improved by one and a half metre as compare to figure 6-29.

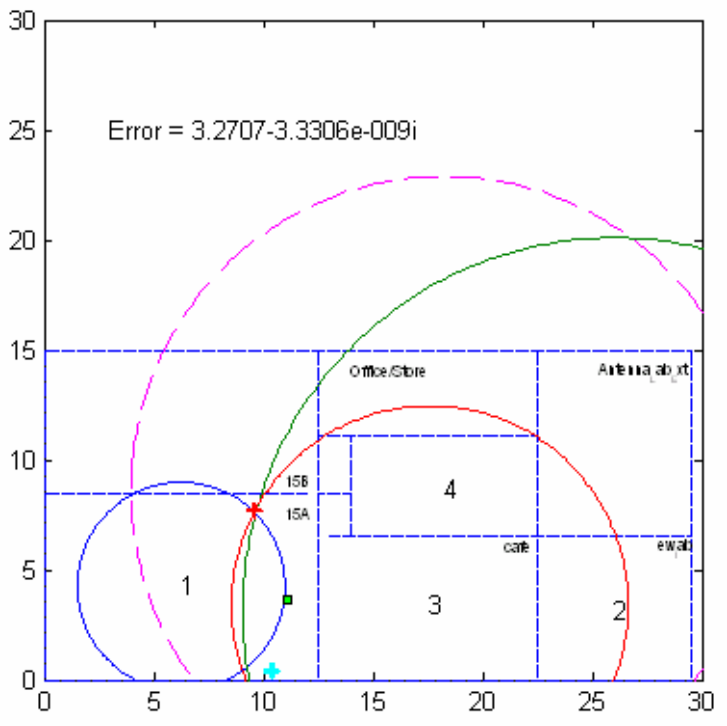

Figure 6-30 Improved results for same data in figure 6-29

Here the algorithm detects the difference between circles which are not overlapping. If the margin is greater than 3m between any two circles then the outer circle which is assumed to be the farthest sensor from the client is contracted to within a 3m difference then both circles are contracted and expanded by an equal distance to overlap.

The first figure of 6-31 shows the triangulation result for location 7 (figure 5-14) as the algorithm applies a correction after detecting walls as explained in section 4.2. The forced overlap further improves the accuracy. The error is reduced from 5.02m to 2.14m. A more detailed result can be viewed in appendix A (A.7).

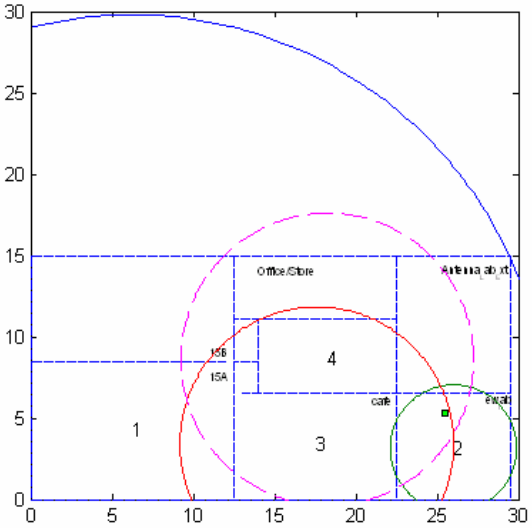

Corrected RSS into distances without overlap

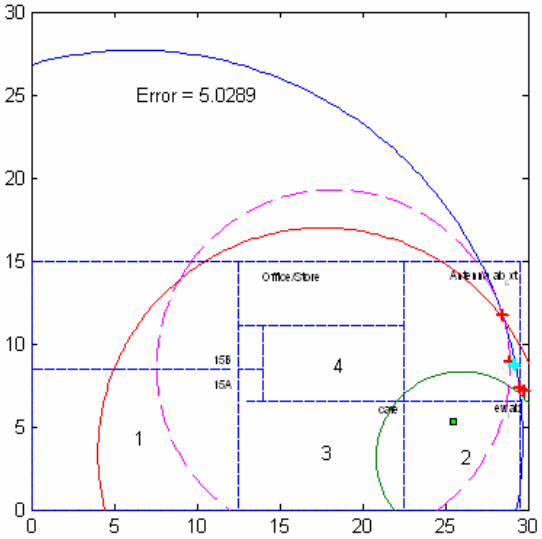

Overlap logic not giving good results

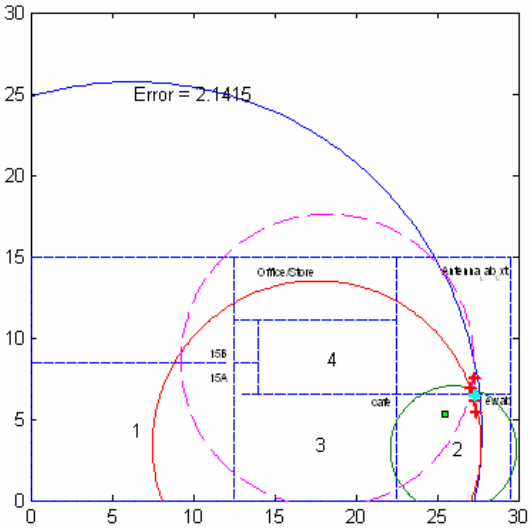

Improved forced overlap logic

Figure 6-31 Forced overlap improved logic shows better results

6.9 Performance evaluation of the geo-location algorithm

Experiments were conducted in multiple locations throughout the test area as shown in figure 5-14. The figure is reproduced here as 6-32 for the ease of comparison with the results summary in figure 6-33. Numerals 1 to 24 show the client locations. Sensor's locations are shown with an asterisk.

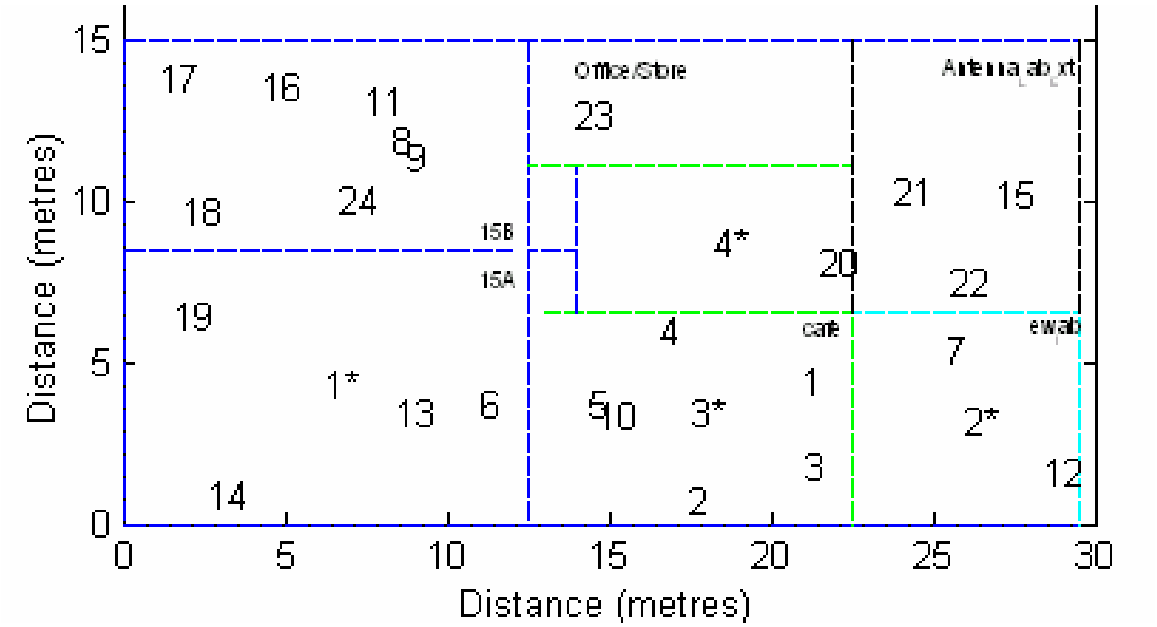

Figure 6-32 Test bed 450 m^2 showing location of clients and sensors

Figure 6-33 provides errors for all positions of clients shown in figure 6-32. The two bars represent the error reported by the algorithm when walls are detected and when walls are not detected. It can be clearly observed that without detecting walls inside a building accurate position reporting is not possible. Results are greatly improved when the algorithm has information on walls between the client and sensors. There is only one instance (position 12) when the client's position reported by the algorithm is better without knowing the walls.

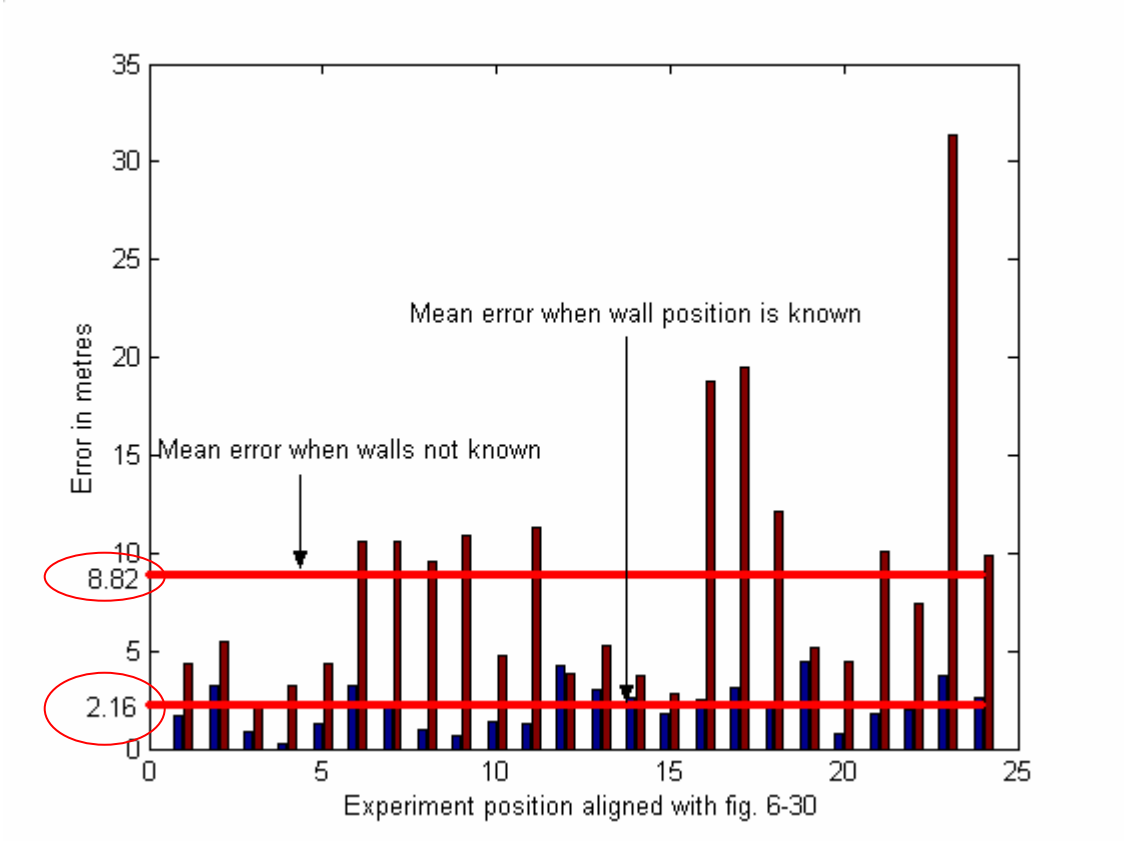

Figure 6-33 Comparison of reported location errors with and without walls

Concentrating on reported positions when walls are detected. As given in figure 6-33, the reported positions are accurate except two readings (position 12 and 19) where the error is greater than 4m range. 75% results have an error below 3m. Average error is 2.16m.

Similarly Figure 6-33 (a) provides errors for all positions of clients shown in figure 6-32. The first bar represents location error for that particular position with frequency diversity applied and the next two graphs represent the location error for the particular positions on channel 6 and 13 respectively. It can be clearly observed that the mean location error has improved to 2.19 m from 4.35 and 4.45 m of mean location error when frequency diversity is not considered.

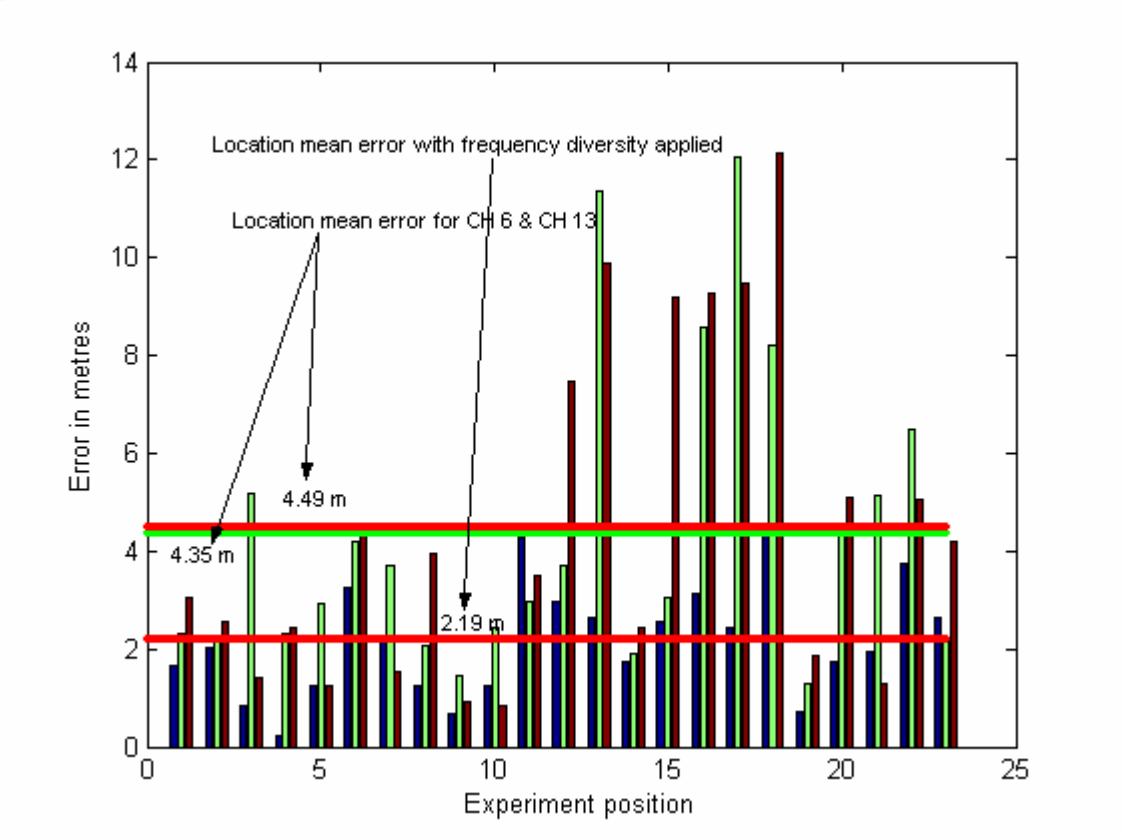

Figure 6-33(a) Comparison of reported mean location error with and without diversity applied

Table 6-7 summarises the results from 24 locations. In table 6-7, more ticks than crosses are observed which means that algorithm is correctly detecting walls for most sensors with respect to the client. However there are a few crosses. For instance row 1 of table 6-7 shows that for figure A.1, sensor 1 and sensor 3 detects 2 and 1 walls for client's position1 in figure 6-32. However looking at the figure the walls reported should have been 1 and 0 for sensor 1 and sensor 3 respectively.

Table 6-7 Correctly detected walls and impact on reported error

Client position as per fig.6-30	Figure as per Append. A	Detected walls b/w client & sensor				Error in reported Position as per fig 6-31	
		S1	S2	S3	S4	Walls detected (m)	Walls not detected (m)
1	A.1	2×	1✓	1×	1✓	1.659	4.32
2	A.2	1✓	1✓	0✓	1✓	3.249	5.49
3	A.3	2×	1✓	0✓	1✓	0.820	2.284
4	A.4	1✓	1✓	0✓	0×	0.241	3.26
5	A.5	1✓	1✓	1×	1✓	1.266	4.35
6	A.6	0✓	2✓	1✓	2✓	3.270	10.58
7	A.7	2✓	0✓	1✓	2✓	2.141	10.58
8	A.8	1✓	2✓	2✓	1✓	0.958	9.60
9	A.9	1✓	2✓	1✓	1✓	0.689	10.94
10	A10	1✓	1✓	0✓	1✓	1.4295	4.76
11	A.11	1✓	2✓	2✓	1✓	1.2505	11.34
12	A.12	2✓	0✓	1✓	2✓	4.2625	3.81
13	A.13	0✓	1×	1✓	1✓	2.9898	5.26
14	A.14	0✓	2✓	1✓	2✓	2.624	3.70
15	A.15	2✓	1✓	1✓	1✓	1.756	2.8
16	A.16	1✓	2✓	2✓	2✓	2.55	18.7
17	A.17	1✓	2✓	2✓	2✓	3.135	19.51
18	A.18	1✓	2✓	1×	2✓	2.436	12.15
19	A.19	0✓	2✓	1✓	2✓	4.403	5.14
20	A.20	1×	1✓	1✓	0✓	0.737	4.47
21	A.21	2✓	1✓	1✓	1✓	1.74	10.06
22	A.22	2✓	1✓	1✓	1✓	1.95	7.46
23	A.23	2✓	2✓	1×	1✓	3.73	31.33
24	A.24	1✓	2✓	1✓	1✓	2.62	9.85

6.9.1 Effect on geolocation accuracy of choosing different values for wall loss

In an indoor environment, different material walls with different attenuation factor are expected to be encountered by RF signal. It is imperative to know the affect of different walls on location accuracy. It will largely depend on the design of a particular algorithm. In order to determine the sensitivity of the designed algorithm discussed in this thesis, three different location positions are experimented with assumed absorption values of walls as 4.5 dB, 6dB and 10 dB. The effect on accuracy is studied which is demonstrated in Figure 6-34 to 6-36.

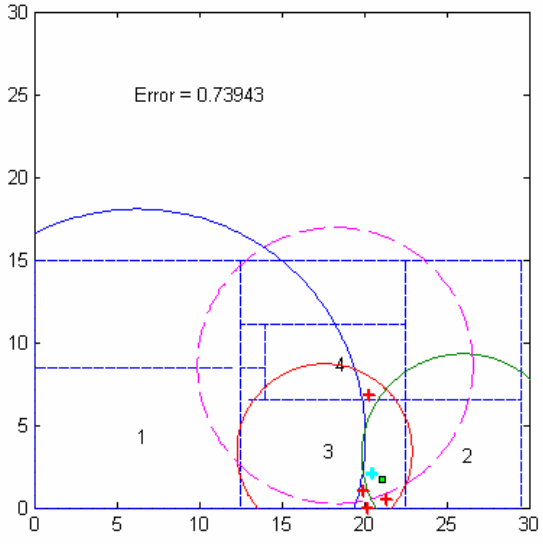

Wall Absorption
4.5 dBm

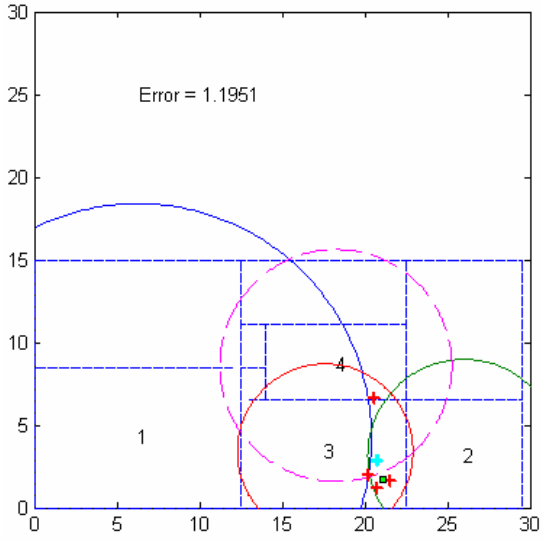

Wall Absorption
6 dBm

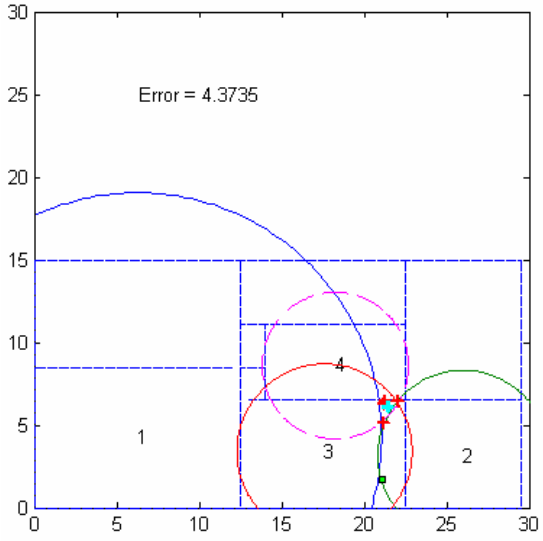

Wall Absorption
10 dBm

Figure 6-34 Location 3 with wall absorption values assumed as 4.5, 6 and 10 dBm

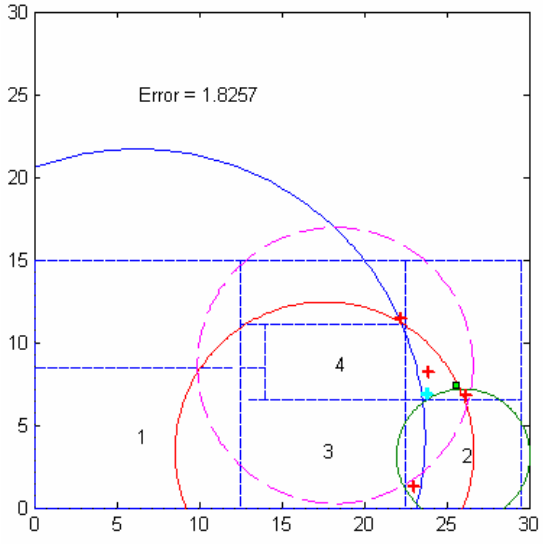

Wall absorption 4.5 dBm

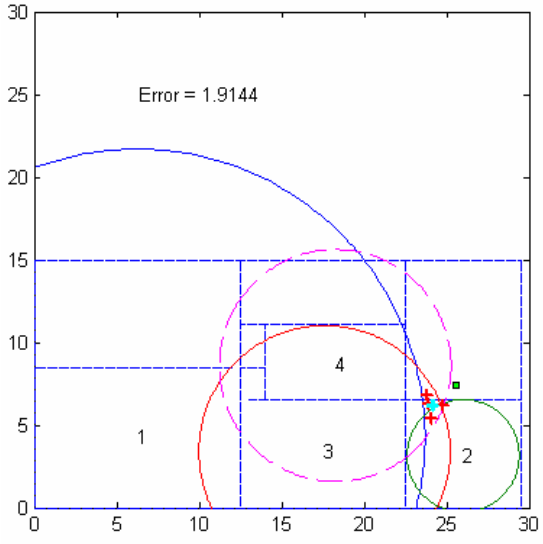

Wall absorption 6 dBm

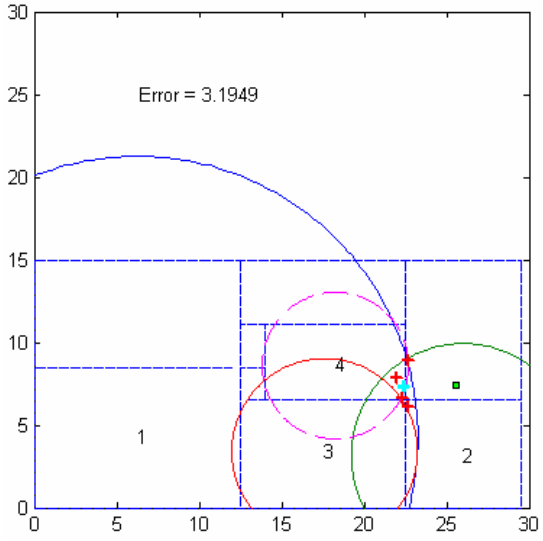

Wall absorption 10 dBm

Figure 6-35 Location 22 with wall absorption values assumed as 4.5, 6 and 10 dBm

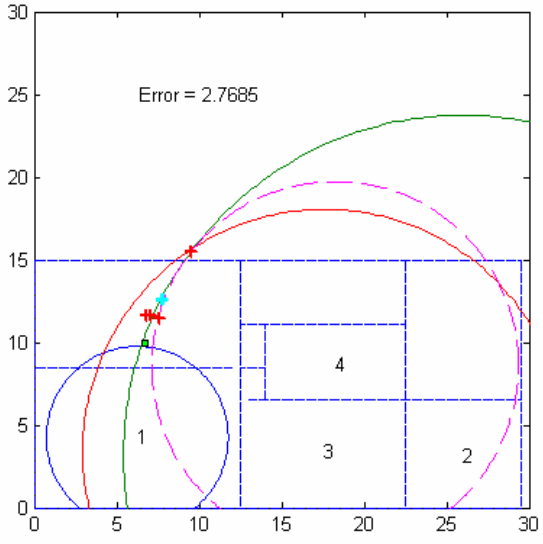

Wall absorption 4.5 dBm

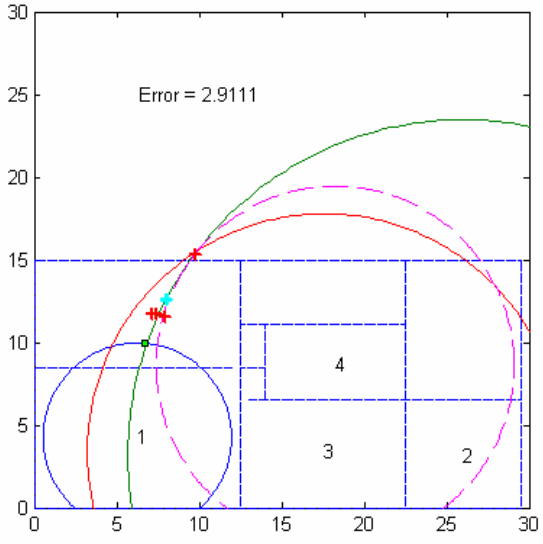

Wall absorption 6.0 dBm

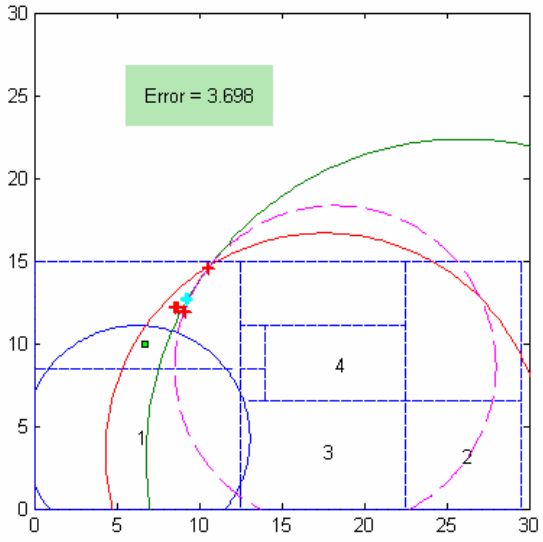

Wall absorption 10 dBm

Figure 6-36 Location 24 with wall absorption values assumed as 4.5, 6 and 10 dBm

The above three figures show that algorithm is robust to changes in wall absorption values. This also proves that the forced overlap logic works fairly well to counter measurement errors and different wall absorption values.

6.9.2 Experiment location results – Discussion

Discussion and reasoning on error results is given below:

- Experiment Location 1: The location of position 1 (figure 6-32) lies in the room with sensor 3. The room has a steel pole as shown in figure 5-4. The location is such that the client is beyond the steel pole with respect to sensor 1 and sensor 3. This could be expected to cause additional losses. It is also very near to the second wall with respect to sensor 1. In addition to these factors the reported signal strengths are expected to vary by 3 to 4 dBm. For this particular example the reported signal strength should have been less than 69.73 dBm (threshold S1) for the algorithm to have correctly assumed that the client is beyond a single wall. The RSS received is 72.4 dBm (A.1.2), an error of 2.5 dBm. The algorithm would be prone to these errors on clients placed at a boundary line near the wall inside or outside. Similarly sensor 3 also reported extra absorption for this position of client due to possibly the same reasons. Experiment locations 3, 4, 5 and 20 also show that the client placed near to a wall has caused the algorithm to determine an inaccurate number of walls. But, as the other three sensors have correctly detected the walls, the data fusion effectively counters any negative effect and manages to keep the error as low as possible.

  Despite the errors in detecting the number of walls in this example, the positional error reported is only 1.69m. After correction of walls the circles (figure A-1) pass close to the client's position. It is obvious that in such scenarios the circle formed after correction will not ideally cut the other 3 circles and will not overlap with one or more other circles as can be observed in the first result of figure A-1 in the appendix. The same is detected by the algorithm

and brought near to the client as shown in the next two results of figure A-1. Forced overlapping has been explained in sections 4.8 and 6.8.

- **Experiment Location 3 (A.3)**: Again the client is placed close to the wall in the room with sensor 3. Sensor 1 has a reported loss equal to 71.69 dBm. The threshold for determining two walls is 69.73. The reason explained for experiment position 1 applies here as well.

- **Experiment Location 13**: Sensor 2 has not determined the number of walls correctly. The RSS reported is 67.61 dBm, which is compared to the threshold of 68.06 dBm. As already explained 3 to 4 dBm variation is to be expected. Here the threshold is missed by 0.46 dB only. The client's RSS is very close to threshold.

- **Experiment Location 18**: Sensor 3 should have detected 2 walls instead of 1 resulting in the circle for sensor 3 after correction (A.18 first figure) falling short of the actual location. It is worth noting that the error is intelligently picked up by algorithm and the forced overlapping feature has brought it close to the actual position.

- **Experiment Location 19**: Walls are correctly detected but the error is on the higher side. Observing figure A.19, it is shown that two sets of triangulation results in the combination of three circles produces good results – an error of 1.6 and 2.7m. However, two set of triangulation results produce larger errors of 5.1 and 8.1m.

  An interesting example which highlights that the placement of client also has an effect with respect to sensors on the reported accuracy (Jonge, 2005). Observing the triangulation result in figure A.19 which produces an 8.1m error is quite perplexing. All three circles are passing very close to the client's actual position and yet the error reported is very high. Sensors 2 and 3 are in line with the client's actual position (the square). This causes the curvature effect of the circle

to induce an error as the intersection point shifts with a slight increase of distance between the two circles (Stansfield, 1947). The same issue causes error in location 17 and location 12. Location 12 is one of the results where the location error is 4.26m when walls are detected and 3.8m when walls are not detected. If we observe the results A.12, and A.12.1, the overlapping is good when walls are detected. But due to the circle curvature error as explained in the above paragraph, the reported error high. It can also be seen that the location is correct in the x axis and is in the same room. Where as in figure A.12.1 (appendix A), the position is reported outside the wall and the averaging resulted in a reported error of 3.8 m, outside the test area.

The following can be deduced from the above discussion:

- The correct detection of walls increase the accuracy and reliability of location estimation.

- Clients placed close to the walls, at times, causes the algorithm to report an incorrect detection of wall. This is, however, random due to the residual variation in RSS values.

- Location of the sensors, if possible, should not be in line to avoid a common line of bearing for the client from two sensors since this causes circle curvature error and causes dilution of precision as described in Location experiment 19 above.

- The forced overlap is working to good effect.

- The algorithm design provides good redundancy. If the RSS is not accurate; it is compensated by some extent by the forced overlap. If one set of three sensors produces an inaccurate result; the effect is minimized by averaging the triangulation results (data fusion) from other sensors.

- The RSS values are demonstrated to be varying in a range of 3 to 5 dB and above 5dB for clients beyond 2 walls. Frequency diversity has given some control over RSS variation but without a sophisticated algorithm getting better positional accuracies is not possible; especially at longer distances when slight change in RSS value causes a lot or error in reported distances.

CHAPTER 7
CONCLUSIONS AND FUTURE WORK

7.1 Summary and findings

The aim of this research was to improve geolocation accuracy inside a building using a Propagation Model approach by considering the indoor propagation environment and correctly determining the presence of walls between a sensor and a client/mobile'.

Wireless access points (APs), which are cost effective and easily available off the shelf can be used to implement a dedicated geolocation setup. It is straightforward to create a small independent geolocation system in parallel to the existing WLAN infrastructure. A dedicated infrastructure provides flexibility in terms of placing APs (sensors) and non interference with main wireless network if frequency channel switching is required. The AP used as sensors are WRT54G ver 2 as mentioned in Chapter 5. These were bought in early part of year 2005. Currently the sensors are not available with same configuration to allow change of firmware feature which was changed for experiments in this thesis. However, an AP with minimum of selected features like recording of RSS values in dBm would be needed for continuation or further work in this thesis.

Experimental results demonstrated that accurate location estimation using a simple propagation model is possible, provided the location of walls is accurately detected. A novel algorithm design is proposed which detects the walls between a client and a sensor using signal strength thresholds. These thresholds are determined by an

algorithm based on the room dimensions. One limitation is that the algorithm assumes that the sensors are placed in the centre of the room.

The effect of the indoor environment was studied in detail and the following was observed:

- A large variation of received signal strength (RSS) values was observed on a single WLAN channel.

- It was shown that frequency diversity applied by averaging over multiple channels reduces the RSS variation to within a small deviation, approximately a 3dB spread.

- Measured RSS values follow free space path loss for LoS locations when frequency diversity is applied. This was also observed by conducting experiments in different rooms and different environment and for different directions.

- In Non-LoS situations walls were shown to be the primary attenuation factor after multipath.

- An average wall absorption figure of 5 dB was determined.

The algorithm, on most occasions, correctly identified the presence of walls. For 24 locations the presence of walls was correctly determined for 87 measurements out of 96. The algorithm resulted in a mean error of 2.16m, compared to approximately 8.82m if walls are not taken into account, thus confirming the necessity to determine the presence of walls for accurate geolocation. The residual errors are caused by a number of factors:

- Clients placed close to the walls, at times, caused the algorithm to report the incorrect detection of a wall. This is however, random due to the residual variation in RSS values.

- It was shown that despite knowing the walls position and controlling the RSS spread, it was still possible that all geolocation circles, at times, did not intersect due to random variation in RSS values. An overlap logic forced the non overlapping circles to overlap. Forced overlapping was most effective when walls were correctly identified.

- It was shown that the effect of one bad result due to one sensor was minimised by the good results of other sensors through forced overlap and averaging.

- It was demonstrated that the algorithm is robust to changes in assumed wall absorption values. It proved that the forced overlap logic used in the design of the algorithm works to good effect.

- The geometry of the relative position of sensors and clients has an impact upon the performance of the system. Although four sensors were used in the experiments reported in this thesis, it was apparent that increasing the number of sensors could provide additional configurations that reduce the impact of some user geometries.

It has been demonstrated in results at appendix 'A' that measurement errors due RSSI sensitivity and wall attenuation can be minimised by using more than 3 sensors. It has been shown that use of 3 sensors in set of 4 combinations produces location estimation for a common client (section 4-10). The results from one of the sensors may not be accurate due measurement errors such as RSS sensitivity or wall attenuation. In this case results from all four set of 3 sensors are averaged, they invariably produces result which is accurate and reliable. Although, it is a possibility that another set of 3 sensors from 4 set of sensors produces result which is better than averaged 4 sensors result but it is not possible to ascertain which set of three sensors from four combination be used. Hence, a little compromise on accuracy but more reliable results are produced by data fusion and forced overlap process (section 4.8). Discussion on experiment location 1 in

section 6.9.2 also explains this effect.The explanation of Contribution 3, later in this Chapter also explains this phenomenon.

The threshold design of algorithm described in this thesis works very well with minimum of information fed in on room / indoor environment. The other option is to know as much information about layout of the room or the test area, which is normally the approach adopted by researchers in previous investigations like product from Network Chemistry. Such products are dependant on calibration with change in environment and are specific to a room/building. The threshold algorithm designed in this thesis is more general in operation and requires only the room's diagonal length. Design is such that knowing a lot of indoor environment (topology) may not help a lot in improving accuracy on present results for the very reason that the sensitivity attached to measuring RSS value will still cause errors and cannot be controlled by knowing topology of a room. During experiments no special attention is given to ensure that room doors are closed or furniture is exactly placed or that how many people are around in the test area environment. This gives generality to the algorithm design. However, the basic design factor assumed in the given threshold such as the centre position of the AP is important and if it is moved from centre location then results from threshold algorithm may not be accurate and some extra information may be required from surroundings. It can however be investigated in future work in continuation to present algorithm.

The performance metric of an indoor geolocation system is defined in terms of positional error accuracy and reliability. Overall mean error calculated for all reported location estimations for this algorithm was 2.16m, which, considering any existing standards for indoor geolocation was excellent. Existing propagation model-based algorithms report a best accuracy of 3.4 m when deploying 4 APs Sharma (2006). The performance of the algorithm proposed in this thesis was again compared to the best of the trainable (finger-printing) based algorithms. The best finger-printing based results are reported by (Kaemarungsi, 2005) for the work carried out by (Xiang, 2004) who claimed an achieved accuracy of 6 feet for 90% of times which is approximately 2m. The next best results are 8.28 ft (2.52m) for 90% of the times. Here it must be noted that

these figures were achieved using finger-printing techniques as explained in Chapter 2 (section 2.3.2), a technique which has considerable disadvantages. The off line phase (collection of RSS signatures) is a tedious and cumbersome process. Moreover it must be repeated every time a change in the environment occurs due to any reason. The results achieved from the algorithm proposed in this thesis are superior and reliable.

One of the considerations that can be argued here is the kind of environment where the experiments are carried out and how accuracies will be affected in different environments. The effect of environment on reported results should be more pronounced in finger printing technique for reporting RSS than using propagation model technique. This is because all indoor environments contain walls, furniture and equipment in differently configured room layouts. If propagation model is working and reporting good accuracy of results in one environment, it should approximately perform fairly well in another environment. A small shift or addition of furniture indoors may not affect propagation model based systems. The design of threshold given in this thesis with minimum of tuning could work with good results in any indoor environment having walls. However, in case of finger printing small changes or additions of furniture position inside building would invalidate the previous data bank of stored signatures which would affect the reported accuracy. So it can be said that for comparison of results using propagation model, the environment is that it is indoors inclusive of walls and furniture. Small changes in position of furniture may not affect the reported positional accuracy margin by much difference.

At present, the majority of research into geolocation applications using RSS is focused on finger-printing techniques rather than Propagation models. As has been demonstrated in this thesis, accurate position estimation with a mean error of 2.16m is possible using a simple propagation model and some limited knowledge of the environment. These results show considerable promise to revive the use of propagation models for indoor geolocation applications.

7.2 Contributions to knowledge

In summary, the research contribution of this work falls into three categories:

- A novel method of using multiple WLAN channels to provide frequency diversity demonstrates that the effect of multipath on received signal strengths may be mitigated.

- A novel geolocation algorithm, which determines the presence of walls between sensors and clients inside a building.

- A Data fusion method which improves the accuracy and reliability of reported location results.

Contribution 1: A novel method of using multiple WLAN channels to provide frequency diversity demonstrates that the effect of multipath on received signal strengths may be mitigated.

At present the use of signal strength methods by deploying triangulation for three or more sensors is considered to be an inaccurate method. This thesis demonstrates that by averaging across WLAN channels, the resulting signal strength value is consistent over time with very little spread as compared to the spread over individual channels. This promises to revive the use of triangulation using the signal strength method for applications such as positioning. This method is much easier to apply and, as demonstrated, the accuracy achieved using this method is comparable to any other existing technique. Moreover the equipment used is inexpensive and available off the shelf at a current cost of no more than 40 GBP.

Contribution 2: A novel geolocation algorithm, which determines the presence of walls between sensors and clients inside a building.

The algorithm takes as input the dimensions of the room which contains the sensor. It accurately determines the location of walls between a sensor and the client using signal strength threshold values. Signal strength readings processed using the method of contribution 1 is translated into distances to triangulate the position of clients. A method of improving estimates by forcing location circles to overlap is also proposed. Many experiments have been conducted to gain confidence on the validity of results.

Contribution 3: A data fusion method which improves the accuracy and reliability of reported location results.

As discussed in Chapter 4 (4.10) and shown in results (appendix A), the final result after averaging from all sets of triangulation results for a common client always remain within the desired accuracy or expected limit. It is possible for one set of triangulation result (3 sensors) to give an error of over 5m but combined with other sets of results that error reduces to less than 3m. On average, the net result is close to the expected value. This method of improving accuracy and reliability is a contribution to knowledge. Many experiments are conducted to gain confidence regarding the validity of the results. A mean accuracy of 2.16m is achieved which is superior to any existing system as per the authors knowledge. Reliability of reporting accurate results fewer than 3m is also high, at 75%.

7.3 Future work

- Since the environment has an effect on the indoor propagation, it would be worth while to carry out further experiments in different environments to see how well the RSS values are gathered in terms of variation when placed at the same distance from different directions. Moreover the measurement errors attached due sensitivity of RSS and wall attenuation in different environments will be different. It would be interesting to investigate how well the generality of designed algorithm behaves in different environment to counter the measurement errors.

- An experiment needs to be conducted, again in a new environment with different or mixed wall materials to confirm that the assumed 5 dB wall absorption factor is reasonable. This may be validated by looking at the correctly reported walls when the algorithm is applied in the new environment.

- The effect on increased reliability and accuracy of algorithm can be studied by increasing the number of sensors (APs) in a selected test area. The averaging from multiple sets of triangulation results in combinations of three from 5 sensors (APs) may improve results.

- Forced overlap is explained in section 4.8 of Chapter 4. Experiments carried out on the logic explained in 4.8 works to good effect as demonstrated in section 6.8.3. Correcting the farthest circle to bring it near to accurate circle is based on an assumption of contracting circle to 3m. Although, this assumption works fine but further investigations can be carried out to change the value of 3m and see the effect on reported accuracy of reported location. Instead of choosing distance this option can be weighed on the basis of received power.

- The scalability issue of the system can be investigated by increasing the number of sensors and with an increase in the size of the test area. Based on received signal strength value, the strongest 4 sensors could be used and others discarded when reporting the RSS values. This is expected to provide a solution for deploying a dedicated system over longer ranges.

- The location reporting system can be extended to 3 dimensions. Floors and multi-stories could be included. Although doing this will entail many new issues to be tackled like a point in centre of room in 3D environment has to be considered. This will then bring in the consideration of antenna patterns viz a viz the height of the client. Another consideration would be the floor losses. With all these factors it is considered that for indoor environment where floors are available an independent two dimensional systems can be deployed on each floor. Looking at the requirements practically, all clients will always be on any

of the floors and need not to be determined from ground floor. However, nonetheless an option exists to investigate into making a 3D indoor geolocation system.

- As observed through experiments, the intersection point or overlap area is not necessarily the exact point of location but is the reported location estimate. More research is required to find methods to minimise the error between reported and actual location.

- An application (end product) can be developed based on research presented in this thesis. It will require automation of data collection, interface between front end and back end. Some issues such as use of software viz a viz processing time will be important considerations.

- The research can be applied for use with the existing WLAN infrastructure, where extended basic service set (EBSS) is used to control the sensors.

REFERENCES

Alavi, B., Pahlavan, K. (2003). Modeling of the distance error for indoor geolocation. *Proceedings of IEEE Conference on Wireless Communications and Networking (WCNC 2003),* **(1)**, pp. 668-672.

Ali, S. and Nobles, P. (2007). A novel indoor location sensing mechanism for IEEE 802.11 b/g Wireless LAN. *Proceedings of IEEE conference, 4th workshop on Positioning, Navigation and Communication (WPNC 07),* pp. 9-15.

Bahl, P. and Padmanabhan, V.N. (2000). RADAR: An inbuilding RF-based user and tracking system. *Proceedings of IEEE Infocom*,(2), pp. 775-784. ISBN: 0-7803-5880-5.

Battiti, R., Brunato, M., and Villani, A. (2002). Statistical learning theory for location fingerprinting in wireless LANS. Technical report [Online]. Available http://rtm.science.unitn.it/~battiti/archive/86.pdf.

Bellusci, G., Yan, J., Janssen, G.J.M. and Tiberius, C.J.M. (2007). An ultra wideband positioning demonstrator using audio signals. *Proceedings of IEEE 4th Workshop on Positioning, Navigation and Communication (WPMC 07)*, Pp. 71-76. ISBN: 1-4244-0870-9.

Borisov, N., Goldberg, I. and Wagner, D. (2001). Intercepting mobile communication: the insecurity of 802.11. *Proceedings of the 7th Annual International on Mobile Computing and Networking*. pp. 180-189.

Bourke, P. (1997). *Intersection of two circles*. [Online]. Available on : http://local.wasp.uwa.edu.au/~pbourke/geometry/2circle/. [Cited 10 June 2007].

Bradwell, J. (2002). Converting signal strength percentage to dBm values.[Online]. WildPackets. Available on: *http:// www . wildpackets . com / elements / whitepapers / Converting_Signal_Strength.pdf.* [Cited 10 September 2005].

Brunato, B. and Kallo, C.K. (2002). *Transparent location fingerprinting for wireless services*. [Online]. Technical report # DIT-02-0071, University of Trento, Italy. Available: http://eprints.biblio.unitn.it/archive/00000227/01/71.pdf. [Cited 23 April 2007].

Caffery, J. and Stuber, G.L. (1998). Subscriber location in CDMA cellular networks. *IEEE Transaction on Vehicular Technology,* **(47)**, pp: 406-416. ISSN: 0018-9545

Carroll, M., and Wysocki. T.A. (2003). Fading characteristics for indoor wireless channels at 5GHz unlicensed bands. *IEEE Joint first Workshop on Mobile Future and Symposium on Trends in Communications.* Pp: 102-105

Cheung, K., Sau, J. and Murch, R.D. (1998). A new empirical model for indoor propagation prediction. *IEEE Transactions on Vehicular Technology, (47), pp: 996-1001.* ISSN: 0018-9545.

Ciurana,M., Cugno,S. and Barcelo-Arroyo,F. (2007). WLAN indoor positioning based on ToA with two reference points. *IEEE proceedings of the 4th workshop on Positioning, Navigation and Communication 2007 (WPNC 07)*, pp. 23-28. ISBN: 1-4222-0870-9.

Coherence Bandwidth- Wikipedia, (2007). *Coherence bandwidth*. [Online]. Available from: http://en.wikipedia.org/wiki/Coherence_bandwidth. [Cited June 2006].

Cheung, K.W., Sau, J.H.M. and Murch, R.D. (1998). A new empirical model for indoor propagation prediction. *Proceedings IEEE Transactions on Vehicular Technology,***(47)**.*pp.*

Chen, Y. and Kobayashi, H. (2002). Signal strength based indoor geolocation. *Proceedings of IEEE International Conference on Communications* pp. 436-439. ISBN: 0-7803-7400-2.

Chiu, CC. and Lin, SW. (1996). Coverage prediction in indoor wireless communication. *IEICE Transaction Communication,* **(E79-B)***,* pp. 1346-1350.

Codepedia, (2007). Geometric dilution of precision (GDOP). [Online]. http:/www.codepedia.com/1/Geometric+Dilution+of+Precision+(DOP). [Accessed July 2007].

Demuth, H.B. and Beale, M. (2004). Neural network toolbox : For use with Matlab. Version 4.04, MathsWorks Inc.

DD-WRT. (2006). *How to install DD-WRT on a Linksys Router*. [Onlne]. Available from : *http://www.testmy.net/t-12222.msg121859#msg121859*. [Cited 10 March 2006].

Devasirvatham, D.M.J., Banerjee, C., Murray, R.R. and Rappaport, D.A. (1991). Four-frequency radio wave propagation measurements of the indoor environment in a large metropolitan commercial building. *IEEE Global telecommunication conference (GLOBECOM'91)*, pp. 1282-1286.

Enge, P. and Mirsa, P. (1999). Special issue on GPS: The global positioning system. *Proceedings IEEE Volume 87**(1)**, pp.* 3-15. ISSN: 0018-9219.

Ganu, S., Krishnakumar, A.S. and Krishman, P. (2004). Infrastructure based location estimation in WLAN networks. *In Proceedings of IEEE WCNC 2004*.

Gast, M.S. (2002). *802.11 Wireless Networks: The definitive Guide*. 1st ed. O'Reilly. ISBN: 0-596-00183-5.

Geier, J. (2002). *Tutorials 802.11 MAC Layer*. [Online]. WiFi planet. Available on : http://www.wi-fiplanet.com /tutorials/article.php/1216351. [Cited 18 May 2006].

Geier, J. (2002). *Assigning 802.11b Access Point Channels*.[Online]. WiFi planet. Available on : http://www.wi-fiplanet.com/tutorials/article.php/972261. [Cited March 2007].

Geier, J. (2003). *Tutorials 802.11 Physical layer.* [Online]. WiFi planet. Available on : http://www.wi-fiplanet.com/tutorials/article.php/2107261. [Cited 01 May 2006].

Getting, I. (1993). Perspective/navigation - The global positioning system. *IEEE Spectrum, **30 (12)***. Pp. 36-47.

Grant, D.B., Rizos, C. and Stolz, A. (1990). Dealing with GPS BIAS: Some theoretical and software considerations, UNISURV S-38, *Report from school of surveying UNSW, Australia.*

Gustafson, D.E., Elwell, J.M. and Soltz, J.A. (2006). Innovative indoor geolocation using RF multipath diversity. *IEEE Position,Llocation and Navigation Symposium,* pp. 904-912. ISBN: 0-7803-9454-2.

Gunther, A. and Hoene, C. (2005). Measuring *round trip times to determine the distance between WLAN Nodes.* [Online]. Proceedings of Networking 2005, Canada. Available on: http://www.tkn.tu-berlin.de / publications / papers / hoene_paper2.pdf. [Cited 17 January 2007].

Guvenc, I., Abdallah, CT., Jordan,R. and Dedeoglu, O. (2003). Enhancements to RSS based indoor tracking systems using Kalman filters. *Proceedings of GSPx and International Signal Processing Conference (ISPS)*, Dallas, TX.

Hashmi, H. (1993). The indoor radio propagation channel. *Proceedings of IEEE, **81(7)**,* pp. 943-968. ISSN: 0018-9219.

Helen, M., Latvala, J., Ikonen, H. And Niittylahati, J. (2001). *Using Calibration in RSSI based location Tracking System.* [Online]. Available on: http://www.cs.tut.fi/sgn/arg/heln/Publications/CSCC2001_Helen.pdf. [Cited June 2007].

Hightower, J. and Borriello, G. (2001). Location system for ubiquitous computing. *IEEE Computer, **34 (8)*** . pp 57-66.

Hightower, J., Brumitt, B. and Borriello, G. (2002). The location stack: A layered model for location in ubiquitous computing. *Proceedings of 4th IEEE Conference on Mobile Computing Systems and Applications*. Pages 22-28. ISBN: 0-7695-1647-5.

Ibraheem, A.I. and Schoebel, J. (2007). Time of Arrival Prediction for WLAN systems using prony algorithm. *IEEE proceedings of the 4th workshop on Positioning, Navigation and Communication 2007 (WPNC 07)*, pp. 29-32. ISBN: 1-4222-0870-9.

IEEE Std 802.11 1997 LAN/MAN Standard committee of the IEEE Computer Society. (1997). *Information technology-Telecommunication and Information Exchange between systems- Local and Metropolitan Area network- Specific requitrements – Part II: Wireless Lan Medium Access Control (MAC) and Physical Layer (PHY) Specifications.*

IEEE Std 802.11b-1999 LAN/MAN Standards committee of the IEEE Computer Society. (1999). *Supplement to IEEE Standard for information technology-Telecommunications and Information exchange between systems- Local and*

Metropolitan area networks- specific requirements- Part II: Wireless LAN Medium Access Control (MAC) and PHY Layer Specifications:

IEEE Std 802.11a – 1999 LAN/MAN Standard committee of the IEEE Computer Society. (1999). *IEEE standard for Information technology- Telecommunication and Information Exchange between systems- Local and Metropolitan Area network- Specific requirements – Part II: Wireless Lan Medium Access Control (MAC) and Physical Layer (PHY) Specifications.*

IEEE Std 802.11g – 2003 LAN/MAN Standard committee of the IEEE Computer Society. (2003). *IEEE standard for Information technology- Telecommunication and Information Exchange between systems- Local and Metropolitan Area network- Specific requirements – Part II: Wireless Lan Medium Access Control (MAC) and Physical Layer (PHY) Specifications.*

ISO (1982). *The reference model of open system interconnection*. ISO international standard IS 7498.

Izquierdo, F., Ciurana, M., Barcelo, F., Paradells, J. and Zola, E. (2006). Performance evaluation of a TOA-based trilateration method to locate terminals in WLAN. *IEEE 1st International Symposium on Wireless Pervasive Computing*. pp. 1-6. ISBN: 0-7803-9410-0.

Jan, R.H. and Lee, Y.R. (2003). An indoor geolocation system for wireless LANs. *Proceedings of IEEE international conference on Parallel Processing Workshops*. Pp. 29-34. ISSN: 1530-2016.

Jonge, D.M. (2005). Benchmarking various untrained localization algorithms. *3rd Twente Student Conference on IT*. Enschede. University of Twente.

Kaemarungsi, K. (2005). *Design of indoor positioning systems based on location finger printing technique*, dissertation for PhD.

Kaemarungsi, K. (2006). Distribution of WLAN received signal strength indication for indoor location determination. *1st international symposium on wireless pervasive computing*. ISBN: 0-78030-9410-0.

Krishnakumar, A. and Krishnan, P. (2005). The theory and practice of signal strength based location estimation. *Proceedings of the IEEE International Conference on Collaborative Computing: Networking, Applications and Work-sharing*. pp. 10. ISBN- 1-4244-0030-9

Krishnamurthy, P. (2002). Position Location in mobile environment. *Proceedings of NSF workshop on Context-aware Mobile Database Management (CAMM).*

Kumar, K.R., Apte, V. and Powar, Y.A. (2006). Improving the accuracy of wireless LAN based location determination systems using Kalman filter and multiple observers. *Proceedings of IEEE conference on Wireless Communication and Networking WCNC* . pp. 463-468. ISSN: 1525-3511.

Ladd, AM., Bekris, KE., Rudys, A., Marceau, G., Kavraki, LE. and Wallach,DS. (2005). Robotics based location sensing using wireless ethernet. *ACM Wireless Networks*, **11(1-2)**, pp.190-204

Li, B., Dempster, A., Rizos, C. And Barnes, J. (2005). *Hybrid Method for Localization using WLAN* . Available on site : http: //www.gmat.unsw.edu.au/ snap/ publications/lib_etal2005c.pdf. [Cited May 2006].

Liu, C., Wu, K. and He, T. (2004). Sensor localization with ring overlapping based on comparison of received signal strength indicator. *Proceedings of IEEE International Conference on Mobile Adhoc and Sensor Systems.* Pp. 516-518.

Lloret, J., Lopez, JJ., Turro, C. and Flores, S. (2004). A fast design model for indoor coverage in 2.4 GHz Wireless LAN. *Ist IEEE International Symposium on Wireless Communication Systems.* Pp. 408-412.

Location-based Services. (2003). Location based services: Finding their place in the market. *In-Stat/MDR, San Jose, CA, Tech. Rep.*

Marias, FG., Papazafeiropoulos, G., Priggouris, S.H. and Merakos, N. (2006). An Innovative Gateway for Indoor Positioning. *EURASIP Journal on Applied Signal Processing, Volume 2006, Article ID 81714.* pp. 1-10. Hindwai Publishing Corporation.

Microsoft developer network (2005). *RSSI Indications*. Available from : http://msdn2.microsoft.com/en-us/library/aa504157.aspx. [Cited on15 May 2005].

Mobile Computing. (2007). *802.11 PHY Layers Chapter 8*. Available from : http://searchmobilecomputing.techtarget.com/searchMobileComputing/downloads/CWAP_ch8.pdf. *[cited 3 June 2007].*

Moen, V., Raddum, H. and Hole, K.J. (2004). Weaknesses in the temporal key hash of WPA. *Mobile Computing and Communications Review*. 8(2). Pages: 76-83.

Murch, R.D., Au, O.C.L., Yau, M.S.F., Tsang, D.H.K., Ko, T.M. and Liu, R.W. (1995). *Wireless communication for hongkong environment*. [Online].Hutchison telephone limited Tech. rep. Available on: http://repository.ust.hk / dspace/bitstream/1783.1/2596/1/wireless1.pdf. [Cited February 2006].

Nerguizian,C., Despins, C. and Affes, S. (2001). *A framework for indoor geolocation using an intelligent system*. [Online]. INRS Telecommunications. 3rd WLAN workshop. Available on : http://www.wlan01.wpi.edu/ proceedings/ wlan44d.pdf. [Cited 03 May 2007]

Network News. (2007). WLAN business growth hits new high. *News on onestopclick online* , [internet]. 12 March. Available from : http://www.onestopclick.com/ news/wlan-growth-hits-new- high_18085698.html. [Cited 10 April 2007].

Ni, L.M, Liu, Y., Lau,Y.C and Patil, A.P (2003). LANDMARC : Indoor location using active RFID. *1st IEEE International Conference on Pervasive Computing and Communications*. pp. 407-415.

Ni, W., Shen, G., Leng, X. and Gui, L. (2006). An indoor location algorithm based on Taylor series expansion and maximum likelihood estimation. *Proceedings of IEEE International Symposium on Personal, Indoor and Mobile Radio Communication,*pp. 1-4. ISBN: 1-4244-0330-8.

Niculescu, D. and Nath, Badri. (2003). Adhoc positioning system (APS) using AoA. *Proceedings of 22nd annual joint conference of IEEE computer and communication societies*, pp. 1734-1743. ISSN: 0743-166X.

Nobles, P. (1999). *Propagation within buildings at 2, 5 17 and 60GHz for wireless broadband data communication*. Ph. D. University of Wales Swansea.

Pahlavan, K., Krishnamurthy, P. and Beneat, J. (1998). Wideband radio propagation modelling for indoor geolocation applications. *IEEE Communications Magazine, **36(4)**,* pp. 60-65.

Pahlavan, K., Li, X., Yianttila, M., Chana, R. and Latva-aho, M. (2000). An overview of wireless indoor geolocation techniques and systems. *Lecture notes in computer science*, **1818**, pp. 1-13. Springer Berlin. ISSN: 0302-9743 (print).

Pahlavan. K., Li,X. and Makela, J.P. (2002). Indoor geolocation science and technology. *IEEE Communications Magazine*, **40(2)**, pp. 112-118 . ISSN: 0163-6804.

Pahlavan, K., Akgul, F.O., Heidri, M, Hatmi, A., Elwell, J.M. and Tingley, RD. (2006). Indoor geolocation in the absence of direct path. *IEEE Wireless Communications Magazine,* **13(6)***,* pp. 50-58. ISSN: 1536-1284.

Pandya, D., Jain, R. and Lupu, E. (2003). Indoor Location Estimation using multiple wireless technologies. *IEEE International Symposium on Personal, Indoor and Mobile Radio Communication,* **3***,* pp.2208-2212.

Parsons, J.D. (2000). *The Mobile Radio Propagation Channel*. 2nd ed. John Willey & Sons. ISBN: 0-471-98857-X.

Patwari, N., O'dea, RJ. And Wang, Y. (2001). Relative location in wireless networks. *Proceedings of IEEE Vehicular Technology Conference VTC 2001*, 2, pp. 1149-1153. ISBN: 0-7803-6728.

Pearn, B. (2004). *Location Awareness in Wireless Networks*. [Online]. *Masters Thesis*. Available on: http://eprints.utas.edu.au/165/01/Thesis.PDF. [Cited 11 Dec 2005].

Perez, DL. (2006). *Indoor location using round trip time for wireless packets between WLAN nodes*.[Online]. Project report. Cork institute of technology, Ireland.Available on: www.aws.cit.ie/Personnel/Papers/Paper294.pdf . [Cited 11 January 2007].

Planet Math, (2007). *Euclidean distance*. [Online]. Planetmath.org. Available on: http://planetmath.org/encyclopedia/EuclideanDistance.html. [Cited 16 February 2007].

Prasithsangaree, P., Krishnamurthy, P., and Chrysanthis, P.K. (2002). On indoor positioning locaction with wireless LANS. *Proceeding IEEE International*

Symposium on Personal , Indoor, and Mobile Radio Communications (PIMRC'02)

Rappaport, T.S. (1989). Indoor radio communications for factories of the future. *IEEE Communication Magazine,* **27(5)**, pp. 15-24. ISSN: 0163-6804.

Rappaport, T.S. and McGillem, CD. (1989). UHF fading in factories. *IEEE Journal selected areas communications, vol 7*. Pages 40-48.

Rappaport, T.S. (1996). *Wireless Communications Principles and Practice*. 2nd ed. New jersey: IEEE press/prentice hall ,Upper Saddle River. ISBN:0-13-042232-0.

Network Chemistry, (2006). RF protect user's guide, version 5. [Online]. Available on www.networkchemistry.com. [Accesed on Feb, 2006].

Roos, T., Myllymaki, P.,Tirri, H., Misikangas, P. and Sievanan, J. (2002). A probabilistic approach to WLAN user location estimation. International Journal of Wireless Information Networks, **9(3)**, pp: 155-164.

Saha, S., Chaudhuri, K., Sanghi, D. and Bhagwat, P. (2003).Location determination of a mobile device using ieee 802.11(b) access point signals. *IEEE Wireless and Networking Conference (WCNC 03).* pp: 1987-1992

Saunders, S.R. (1999).*Antennas and Propagation for Wireless Communication Systems*. Chichester: Wiley and Sons Ltd. ISBN: 0-471-98609-7.

Sayed, A.H., Tarighat, A. and Khajehnouri, N. (2005). Network based wireless location. *IEEE Signal Processing Magazine*, **22(4)**, pp: 24-40. ISSN: 1053-5888.

Seidel, S.Y., Takamizawa, K. and Rappaport, T.S. (1989). Application of second order statistics for an indoor radio channel model. *IEEE 39th Vehicular Technology Conference*, **2**, pp. 888-892.

Seidel, S.Y., and Rappaport, T.S. (1991). 900 MHz path loss measurements and prediction techniques for inbuilding communication system design. *IEEE Proceedings 41st Vehicular Technology Conference*, pp. 613-618.

Seidel, S.Y., and Rappaport, T.S. (1992). 914 MHz path loss prediction models for indoor wireless communication. *IEEE Transaction on Antenna Propagation,**40**,* pp. 207-217.

Small, J., Smailagic, A. and Siewiorek, D.P. (2000). *Determining user location for context aware computing through the use of a wireless LAN infrastructure.* [Online]. Carneige Mellon University. Available online: http://www-2.cs.cmu.edu/»aura/docdir/small00.pdf. [Cited 30 Dec 2006].

Smart Antenna (2000). *Diversity Schemes*. [Online]. Georgia Tech Institute. Available on: http://users.ece.gatech.edu/~mai/tutorial_diversity.htm. [Cited 10 February 2007].

Sharma, N.K. (2006). A weighted centre of mass based trilateration approach for locating wireless devices in indoor environment. *Proceedings of the International Workshop on Mobility Management and Wireless Access*, pp. 112-115. ISBN: 1-59593-488-X.

Siebert, M., Bultmann, D. and Vorobjova, M. (2004). On the reliability of location based networking. *Proceedings of 1st Workshop on Positioning, Navigation and Communication (WPNC'01)*, pp. 107-112.

Stansfield, R.G. (1947). Statistical Theory of DF fixing. *IEE Journal of Electrical Engineers,* **94(III A)**, pp. 762-770.

Stein, J.C. (n.d). *Indoor radio WLAN performance part II: Range performance in a dense office environmemt*. [Online]. White paper, Intersil corporation. Available on: http://reseau.erasme.org/IMG/experience_attenuation.pdf. [Cited 01 July 2007].

Tauber, J.A (2002). *Indoor location systems for pervasive computing*.[Online]. Area exam report, Massachusetts institute of technology. Available on: http://theory.lcs.mit.edu/~josh/papers/location.pdf. [Cited 5 May 2007].

Walker, E., Zepernick, H., and Wysocki, T. (1998). Fading measurements at 2.4 GHz for the indoor radio propagation channel. *Broadband Communications, International Zurich Seminar on Accessing, Transmission, Networking*. pp. 171-176

Walker, J. (2000). *Unsafe at any keysize: an anlysis of WEP encapsulation*. [Online]. Technical Report, (IEEE 802.11-00/362). Available on: http://www.dis.org/wl/pdf/unsafe.pdf. [Cited 13 August 2006].

Wallbaum, M. and Spaniol, O. (2006). Indoor positioning using wireless local area networks. *Proceedings of IEEE John Vincent Atanasoff International Symposium on Modern Computing*, pp. 17-26. ISBN: 0-7695—2643-8.

Wang, Y., Jia, X. and Rizos, C. (2004). *Two new algorithms for indoor wireless positioning system*. [Online]. University of New South Wales (UNSW). Available on: http: // www.gmat.unsw.edu.au/ snap/ publications/ wangy_etal2004a.pdf . [Cited July 2005].

Wang, Y., Jia, X. and Lee, H.K. (2003). An indoors wireless positioning system based on wireless local area network infrastructure. 6th International Symposium on Satelite Navigation Technology including Mobile Positioning and

Location Services. [Online]. http://www. gmat.unsw.edu.au /snap / publications / wangy_etal2003a.pdf. Accessed May 2005.

Wassi, G.I., Charles, D., Grenier, D. and Nerguizian,C. (2005). Indoor location using received signal strength of IEEE 802.11b access point. *Proceedings of IEEE Canadian Conference on Electrical and Computer Engineering*, pp. 1367-1370. ISSN: 0840-7789

Werb, J. and Lanzl, C. (1998). Designing a positioning system for finding things and people indoors. *IEEE Spectrum,* **35(9)**. pp. 71-78. ISSN: 0018-9235.

Wireless Channels (2006). *Multipath Fading , Delay Spread*. [Online]. Wireless Communication reference web site. Available on: http :// www.wireless.per.nl/reference/chaptr03/fading/delayspr.htm. [Cited May 2007].

Wikipedia (2006). *OSI Model*. [Online]. Available on: http://en.wikipedia.org/wiki/ OSI_model. [Cited 13 December 2006].

Wikipedia (2007). *WRT54G*. [Online]. Available on: http://en.wikipedia.org/wiki/ WRT54G. [Cited January 2007].

Wikipedia. (2007). *DD-WRT*. [Online]. Available on : http://en.wikipedia.org/wiki/ DD-WRT. [Cited 10 May 2007].

Wireless Networks. [Online]. *www.iw3iem.it/immagini/wireless/channels. bmp*

Wolfram MathWorld, (2007). *Triangulation point.*[Online]. (Updated 29 June 2007) Available from : http://mathworld.wolfram.com/TriangulationPoint.html. [Cited 11 May 2007].

Xiang, Z., Song, S., Chen, J., Wang, H., Huang,J. and Gao, X. (2004). A Wireless LAN – based Indoor positioning technology. *IBM Journal RES. & DEV, 48(5/6),* . ISSN: 0018-8646. Available on: http://www.research.ibm.com/ journal/rd/485/xiang.html.

Youssef, M. and Agrawala, A. (2003). Small scale compensation for WLAN location determination systems. *IEEE Wireless Communication and Networking conference*, pp. 1974-1978. ISSN: 1525-3511.

Youssef, M., Agrawala, A. and Shankar, A.U. (2003). WLAN location determination via clustering and probability distributions. *IEEE International Conference on Pervasive Computing and Communication*. pp: 23-27.

Zhou, R. (2005). *Architecture and Implementation of Indoor Wireless Positioning System.*[Online]. Masters Thesis, University of Freiburg, Germany. Available on: http://www.ks.uni-freiburg.de/download/diplomarbeit/ WS04/ iwps.pdf. [Cited February 2006].

APPENDIX A

INDOOR LOCATION ALGORITHM EXPERIMENT RESULTS

All results of practical location estimation using location algorithm discussed in Chapter 4 are produced below. They are aligned to the numerals assigned to each result in figure 6-30 for correlating, if required. Each figure has 6 results with last result giving final positional error of determined client's position. All errors are reported in metres.

Layout of Figures for each location experiment: There are six sub figures in figure 1 of each result. The first sub figure for all Location experiments represents results of triangulation when wall corrections are applied to the four sensors. It shows how many circles are overlapping and how close are they passing from the client actual position. After this next four sub figures of figure 1 gives error in reported location when set of three sensors in four different combinations are used for triangulation. A step towards data fusion to achieve final result. These figures show forced overlapping and 4 different results for same client. In the end the sixth sub figure shows final location result after data fusion process of averaging and forced overlapping. All 25 figures , each will have six sub figures as figure 1. Second figure of each location result will show the error reported by algorithm if walls are not accounted for. In third figure, the important numerical values are displayed as calculated by the source program (Matlab) in the process of producing triangulation results.

A.1 Location 1 results

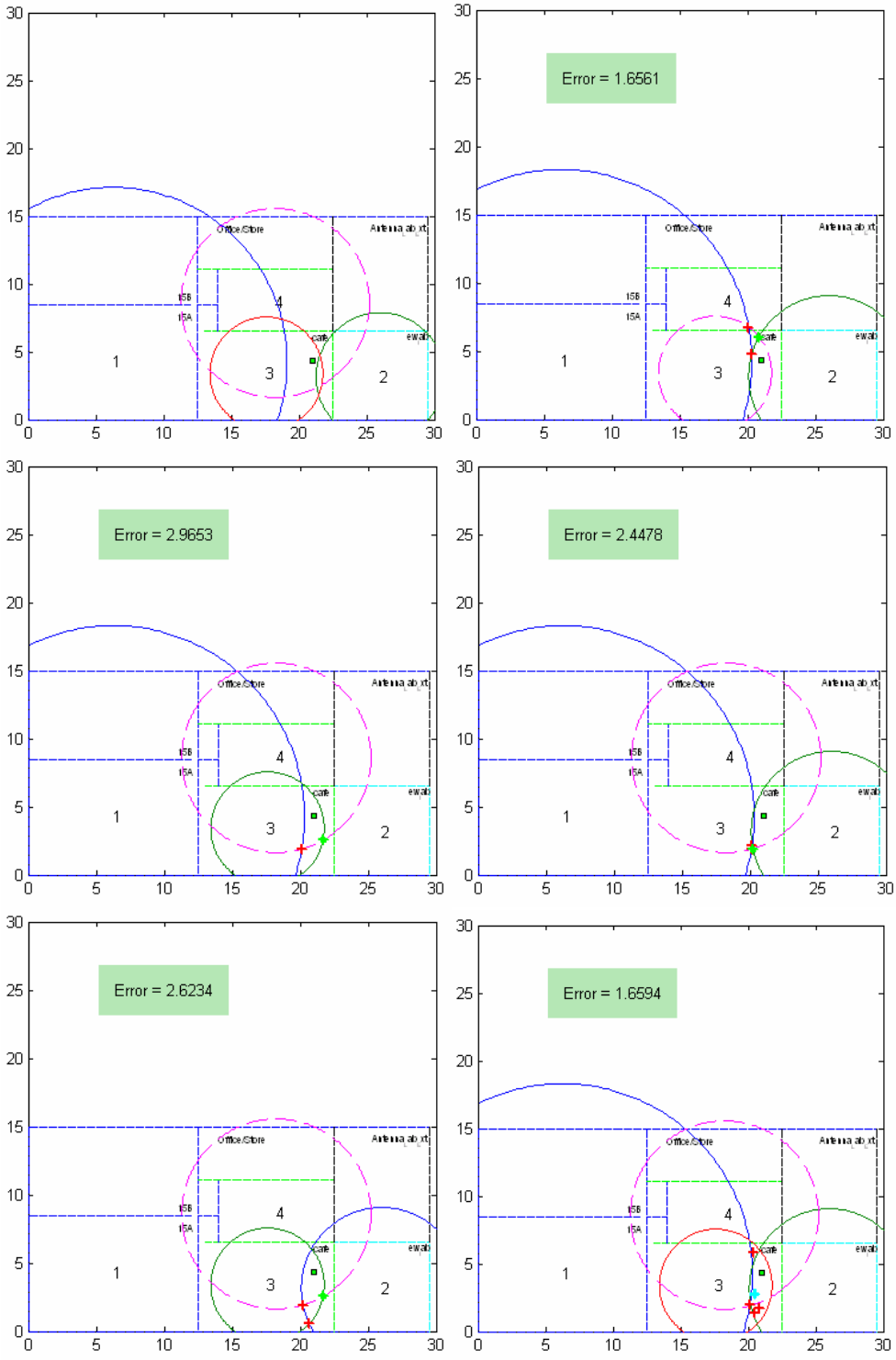

Figure A-1 Estimation Location 1

A.1.1 Location 1 – results when walls not detected

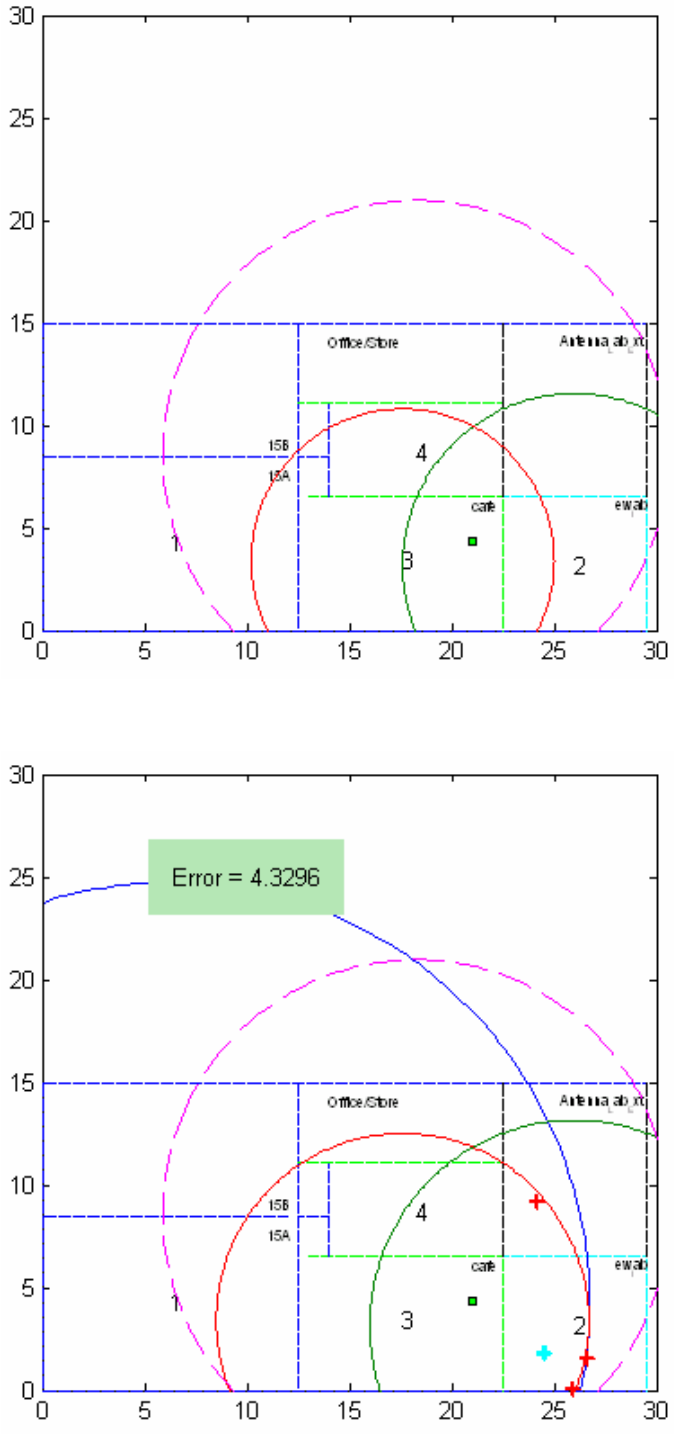

Figure A-1a Estimate location 1 without detection of walls

A.1.2 Numerical result for figure A-1 and A-1a

client_posx = 21

client_posy = 4.3000

loss_sensors = 72.4000 58.7000 57.6100 62.0700

Sig_Strth_Diag_Length = 57.8144 53.7499 55.7399 53.9133

Sig_Strth_Short_Dist = 52.8487 50.3330 50.4677 47.4646

NOTT = 1 1 1 1

wall2_ls_len_sen1 = 16.8029

Two_Wall_TH =

65.8783
69.7377
66.5937
68.0741
63.1274
70.3995
61.0778
67.6975

NOTT = 2 1 1 1

NOTT = 2 1 1 1

A = 40.5500

C = 8.4000

E = 7.4000

D = 12.3700

A2 = 12.8700

C2 = 4.7300

E2 = 4.1700

D2 = 6.9600

A.2 Location 2 results

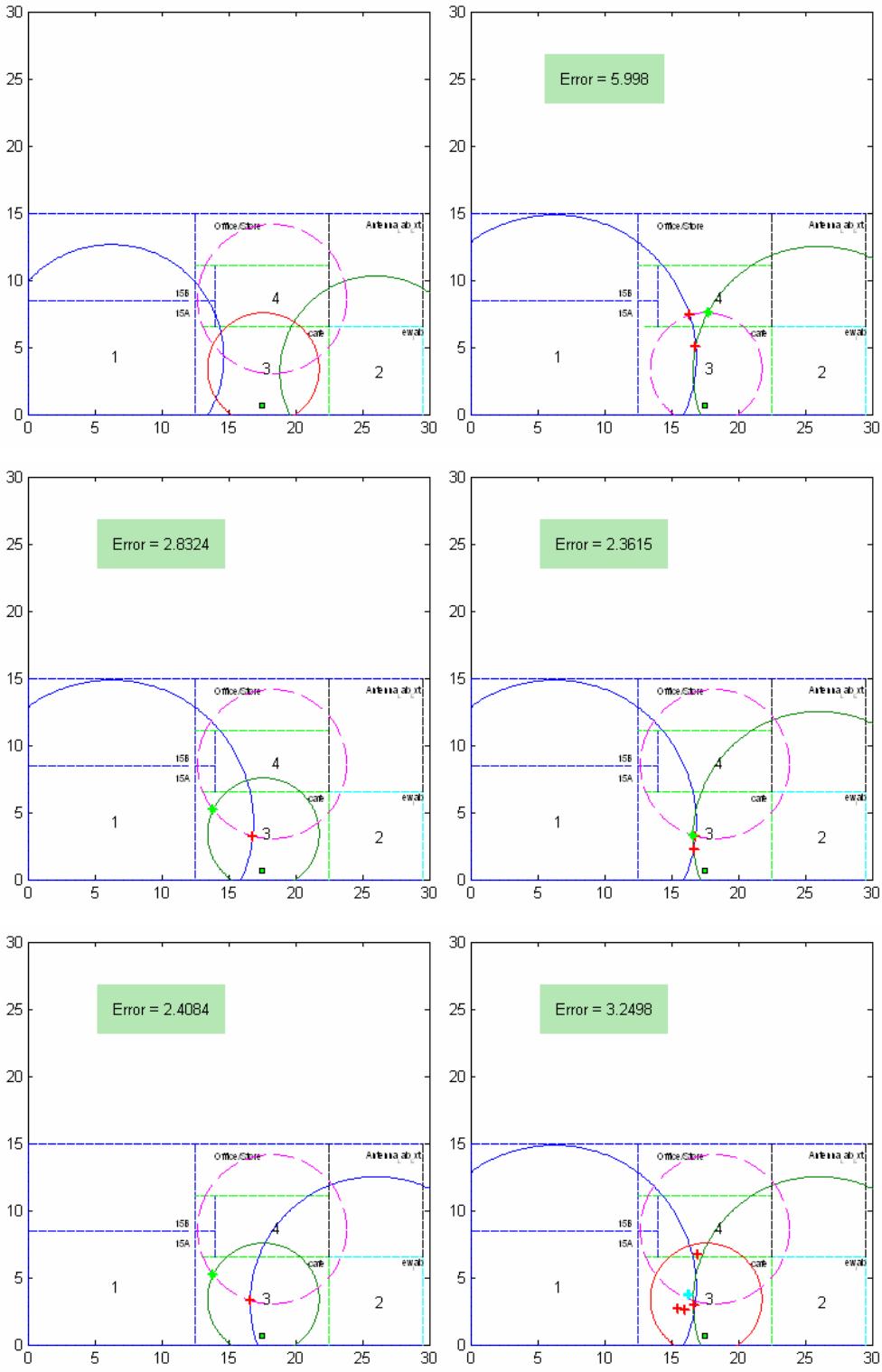

Figure A-2 Estimation Location 2

A.2.1 Location 2 – results if walls not detected

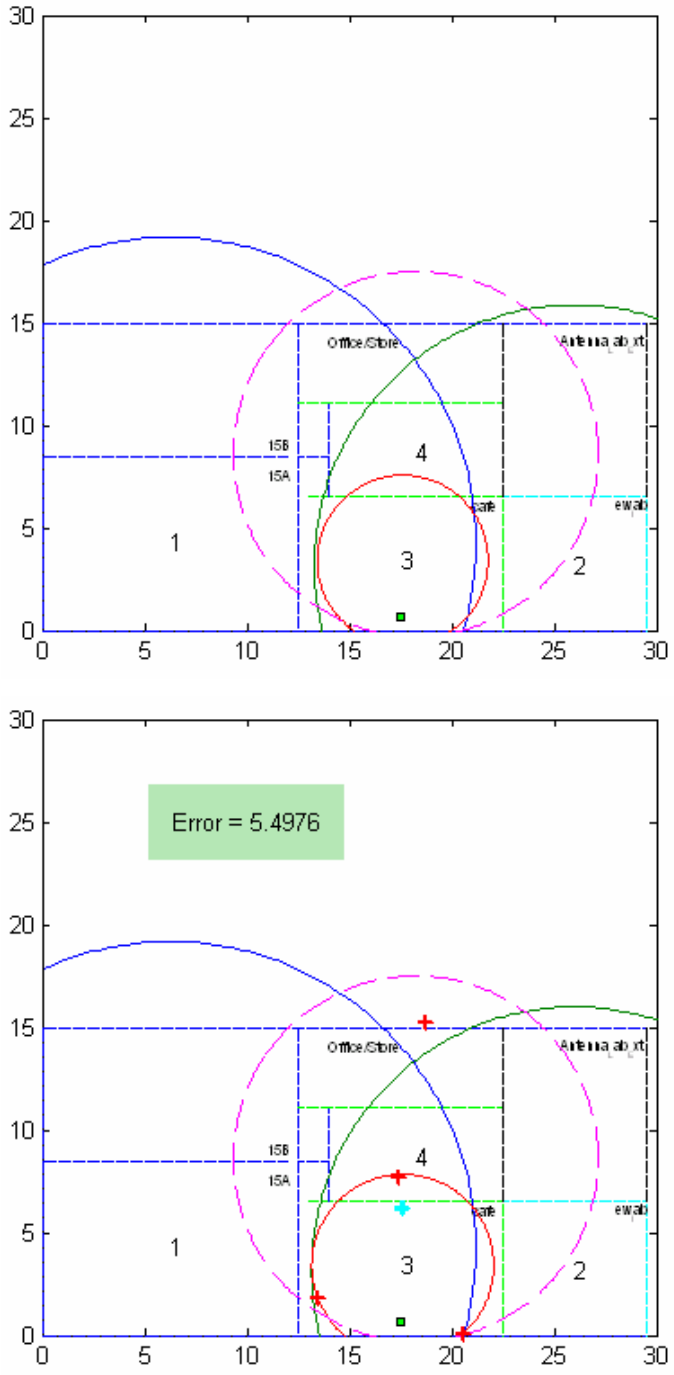

Figure A-2a Estimate location 2 if walls not detected

A.2.2 Numerical result for figure A-2

client_posx = 17.5000

client_posy = 0.7000

loss_sensors = 63.7000 62.3000 52.6000 60.1000

Sig_Strth_Diag_Length = 57.8144 53.7499 55.7399 53.9133

Sig_Strth_Short_Dist = 52.8487 50.3330 50.4677 47.4646

NOTT = 1 1 0 1

Two_Wall_TH =

65.8783

69.7377

66.5937

68.0741

63.1274

70.3995

61.0778

67.6975

NOTT = 1 1 0 1

NOTT = 1 1 0 1

A = 14.9300

C = 12.7200

E = 4.1700

D = 9.8700

A2 = 14.9300

C2 = 7.1600

D2 = 5.5600

A2 = 8.4000

C2 = 7.1600

E2 = 4.1700

D2 = 5.5600

A.3 Location 3 results

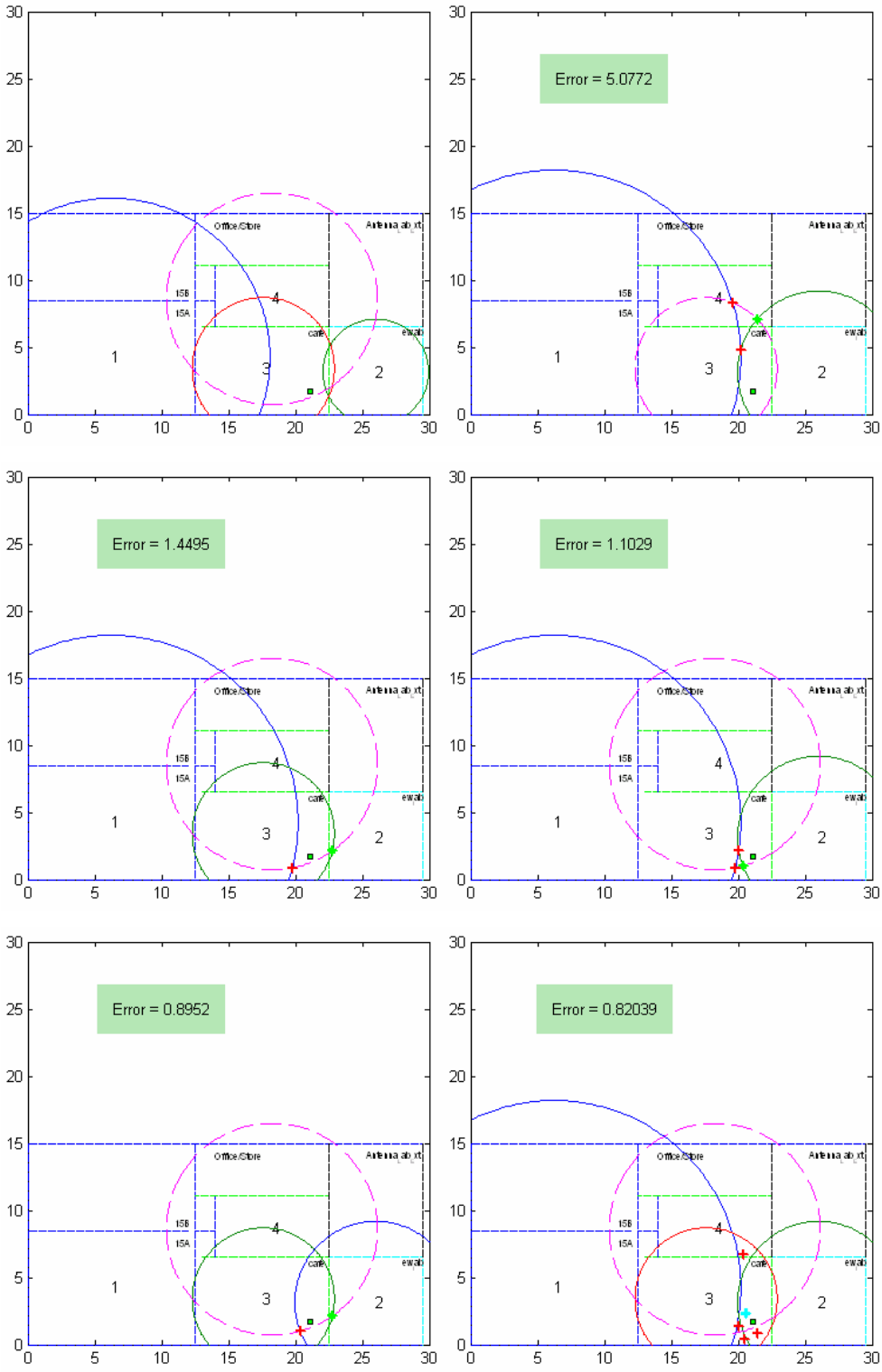

Figure A-3 Estimation Location 3

A.3.1 Location 3 – results with walls not detected

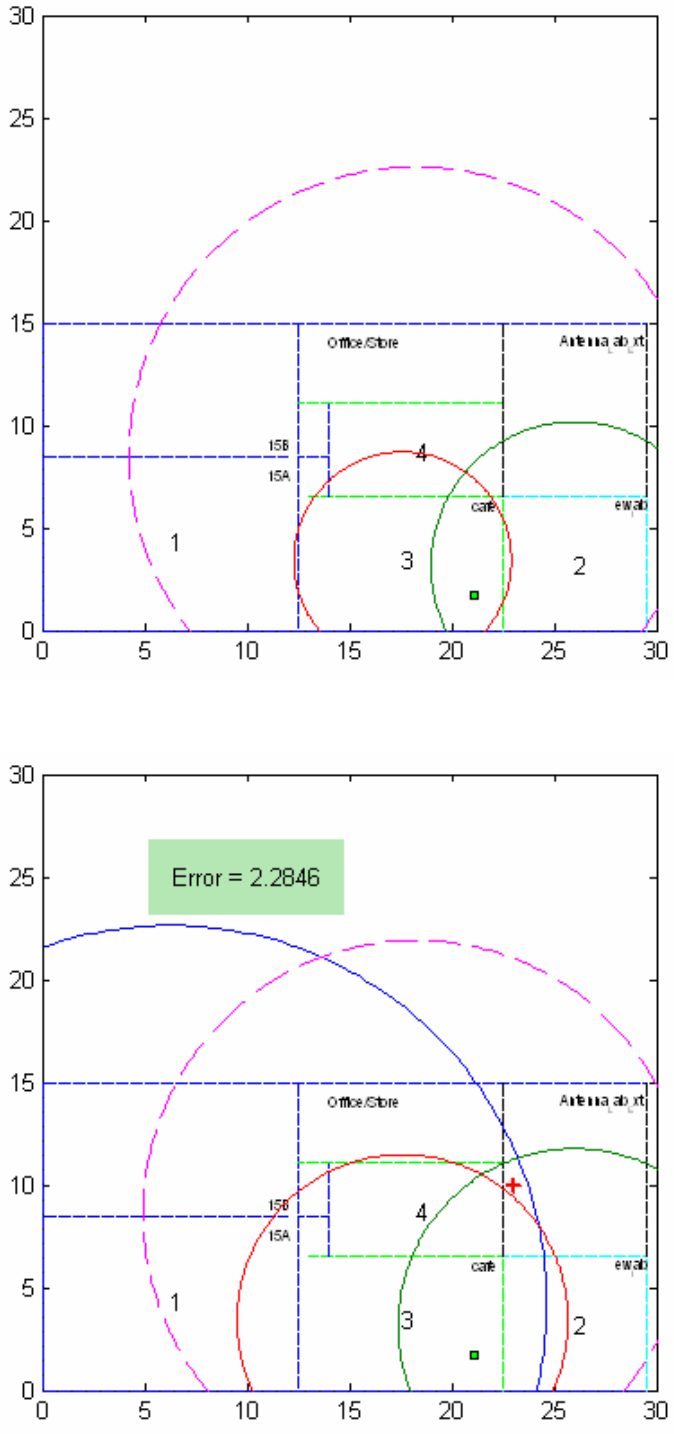

Figure A-3a Estimate Location 3 with walls not detected

A.3.2 Numerical result for figure A-3 and A-3a

client_posx = 21.1000

client_posy = 1.7000

loss_sensors = 71.6900 57.1500 54.6900 63.1500

Sig_Strth_Diag_Length = 57.8144 53.7499 55.7399 53.9133

Sig_Strth_Short_Dist = 52.8487 50.3330 50.4677 47.4646

NOTT = 1 1 0 1

wall2_ls_len_sen1 = 16.8029

Two_Wall_TH =

65.8783

69.7377

66.5937

68.0741

63.1274

70.3995

61.0778

67.6975

NOTT = 2 1 0 1

NOTT = 2 1 0 1

A = 37.4100

C = 7.0200

E = 5.3100

D = 14

A2 = 11.8500

C2 = 3.9500

E2 = 5.3100

D2 = 7.8900

A.4 Location 4 results

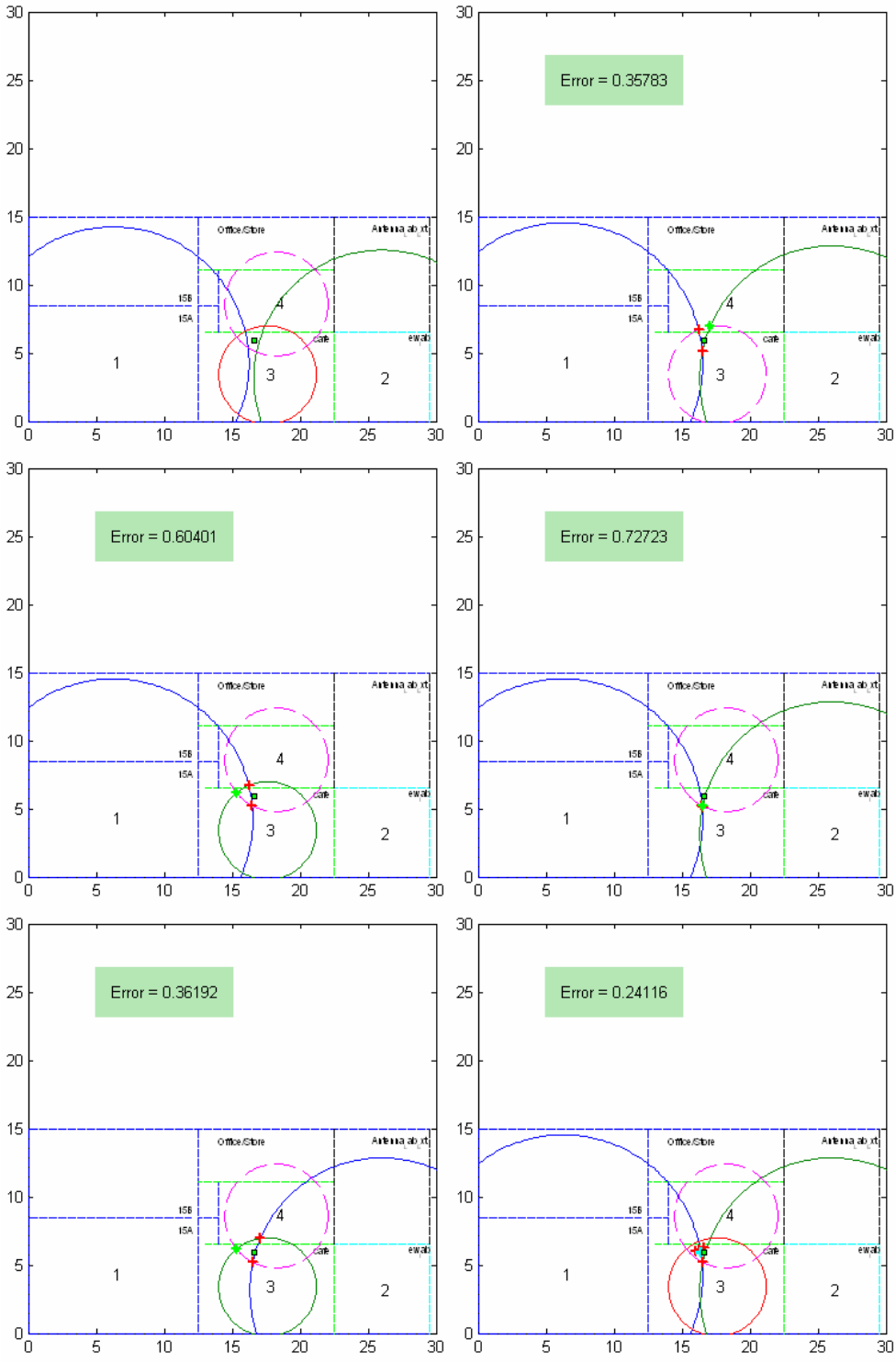

Figure A-4 Estimate Location 4

A.4.1 Location 4 – results when walls not detected

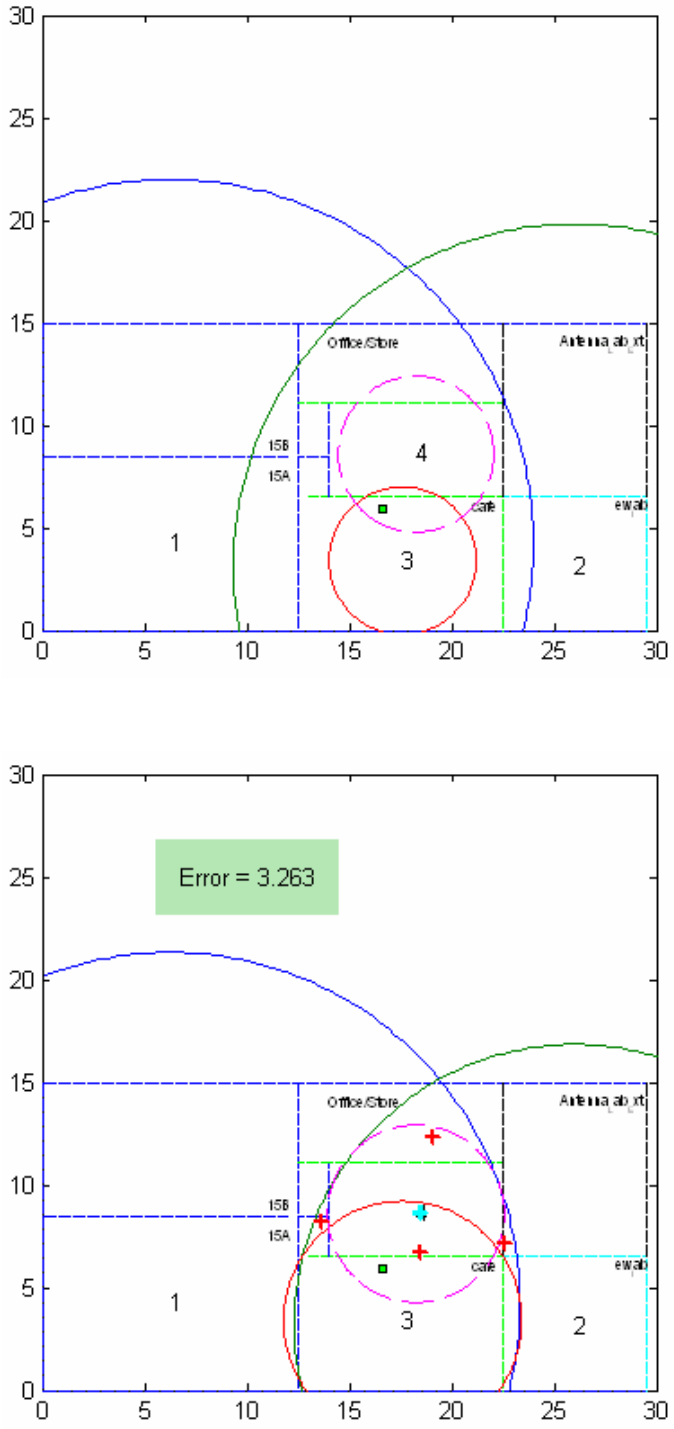

Figure A-4a Estimate location 4 when walls not detected

A.4.2 Numerical results for figure A-4 and A-4a

client_posx = 16.6000

client_posy = 5.9000

loss_sensors = 65.2000 64.6900 51.3000 51.8000

Sig_Strth_Diag_Length = 57.8144 53.7499 55.7399 53.9133

Sig_Strth_Short_Dist = 52.8487 50.3330 50.4677 47.4646

NOTT = 1 1 0 0

Two_Wall_TH =

65.8783

69.7377

66.5937

68.0741

63.1274

70.3995

61.0778

67.6975

NOTT = 1 1 0 0

NOTT = 1 1 0 0

A = 17.7400

C = 16.6700

E = 3.5950

D = 3.8000

A2 = 9.9900

C2 = 9.4000

E2 = 3.5950

D2 = 3.8000

A.5 Location 5 – results

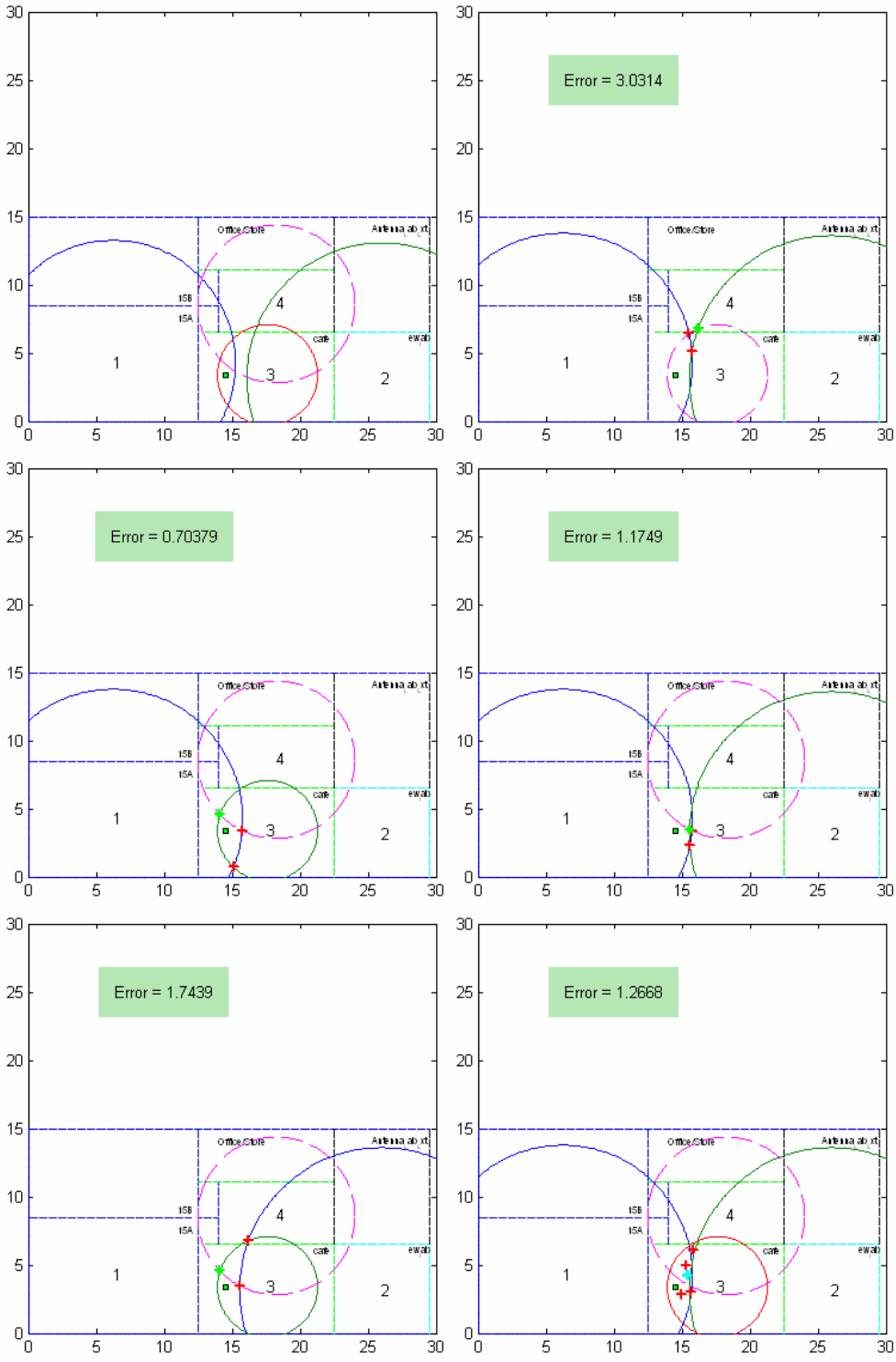

Figure A-5 Estimate Location 5

A.5.1 Location 5 – results when walls not detected

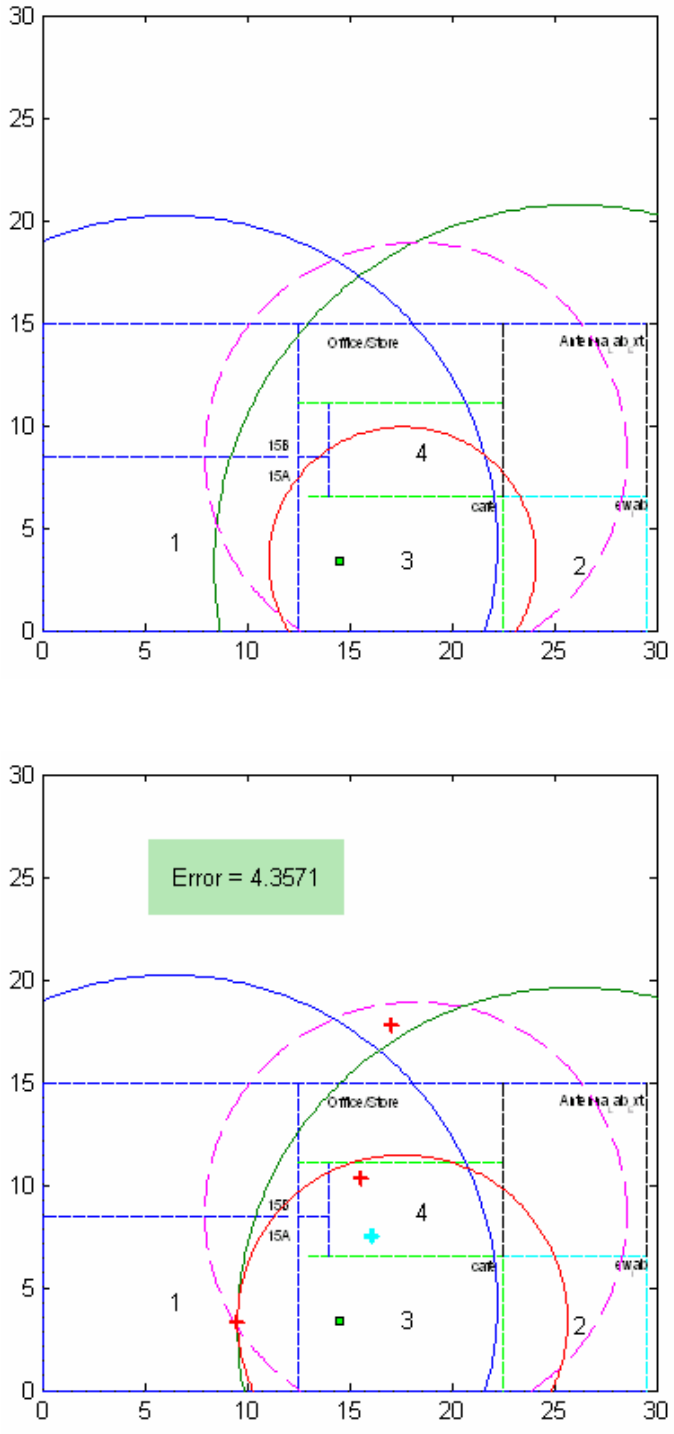

Figure A-5a Estimate location when walls not detected

A.5.2 Numerical results for figure A-5 and A-5a

client_posx = 14.5000

client_posy = 3.4000

loss_sensors = 64.3000 65.1500 56.5000 60.4600

Sig_Strth_Diag_Length = 57.8144 53.7499 55.7399 53.9133

Sig_Strth_Short_Dist = 52.8487 50.3330 50.4677 47.4646

NOTT = 1 1 1 1

Two_Wall_TH =

65.8783

69.7377

66.5937

68.0741

63.1274

70.3995

61.0778

67.6975

NOTT = 1 1 1 1

NOTT = 1 1 1 1

A = 15.9700

C = 17.6000

E = 6.5200

D = 10.3000

A2 = 9

C2 = 9.9200

E2 = 3.6800

D2 = 5.7800

A.6 Location 6 – results

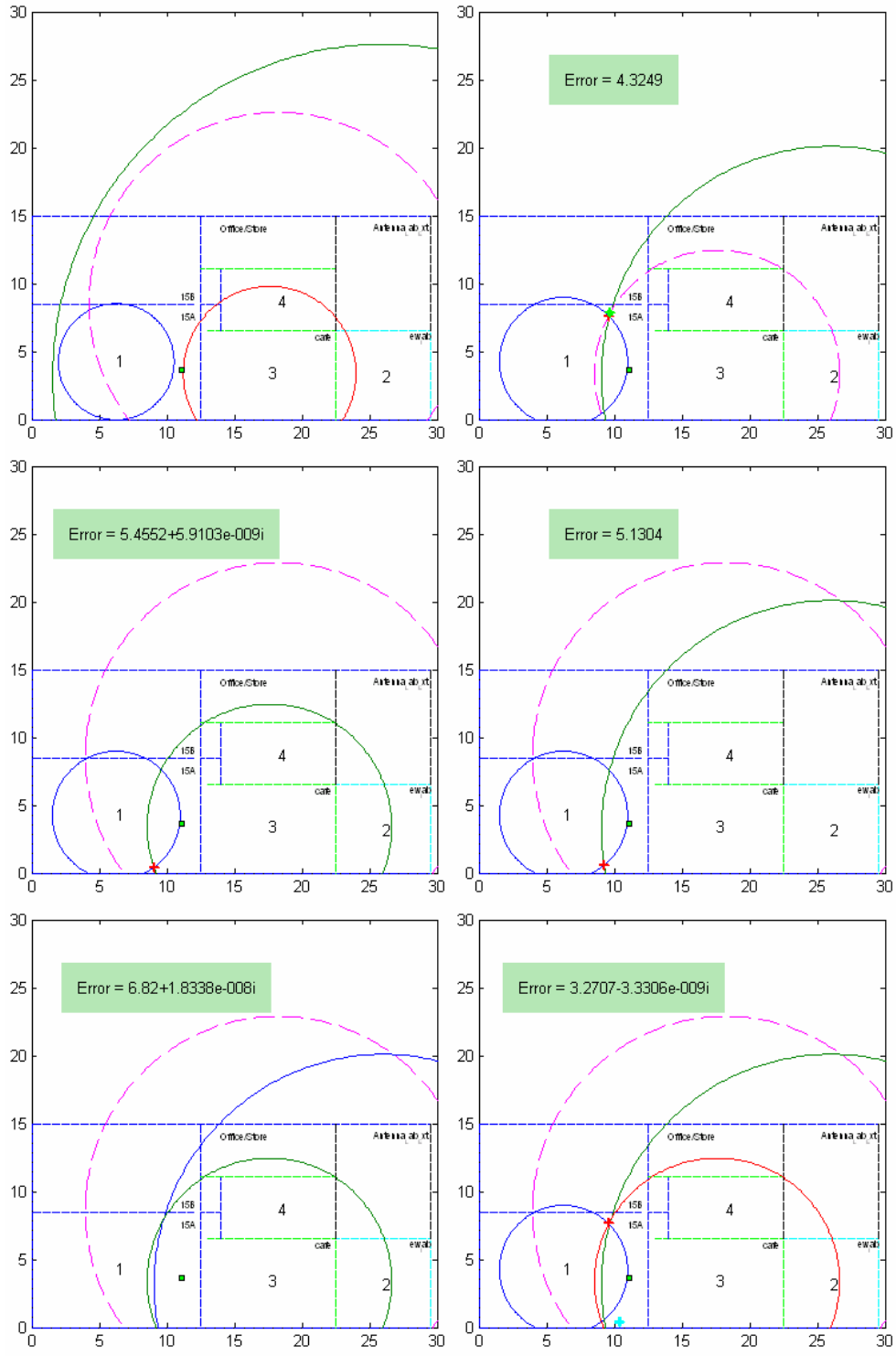

Figure A-6 Estimate Location 6

A.6.1 Location 6 – results when walls are not detected

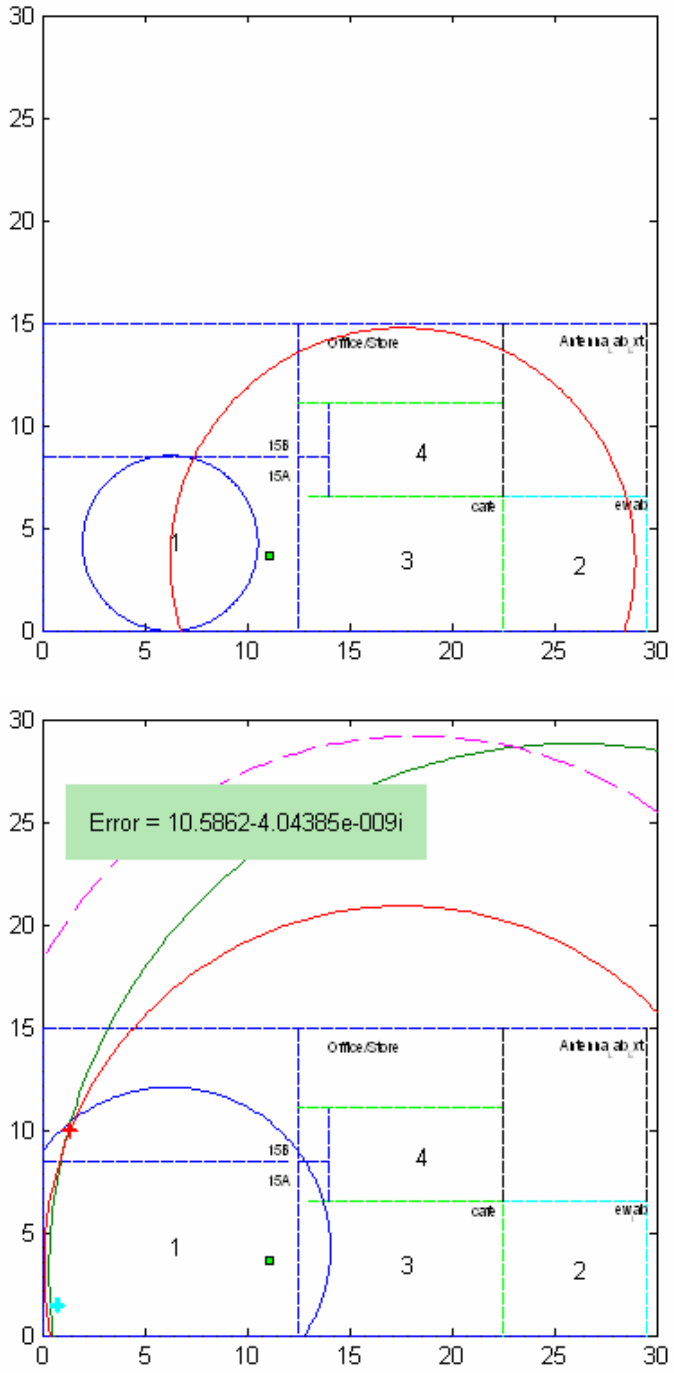

Figure A-6a Estimate location 6 when walls not detected

A.6.2 Numerical result for figure A-6 and A-6a

client_posx = 11.1000

client_posy = 3.6000

loss_sensors = 52.8500 78.0000 61.3000 73.1500

Sig_Strth_Diag_Length = 57.8144 53.7499 55.7399 53.9133

Sig_Strth_Short_Dist = 52.8487 50.3330 50.4677 47.4646

NOTT = 0 1 1 1

Two_Wall_TH =

65.8783

69.7377

66.5937

68.0741

63.1274

70.3995

61.0778

67.6975

NOTT = 0 2 1 2

NOTT = 0 2 1 2

A = 4.2800

C = 77.3500

E = 11.3500

D = 44.2500

A2 = 4.2800

C2 = 24.4600

E2 = 6.3900

D2 = 14

A.7 Location 7 result

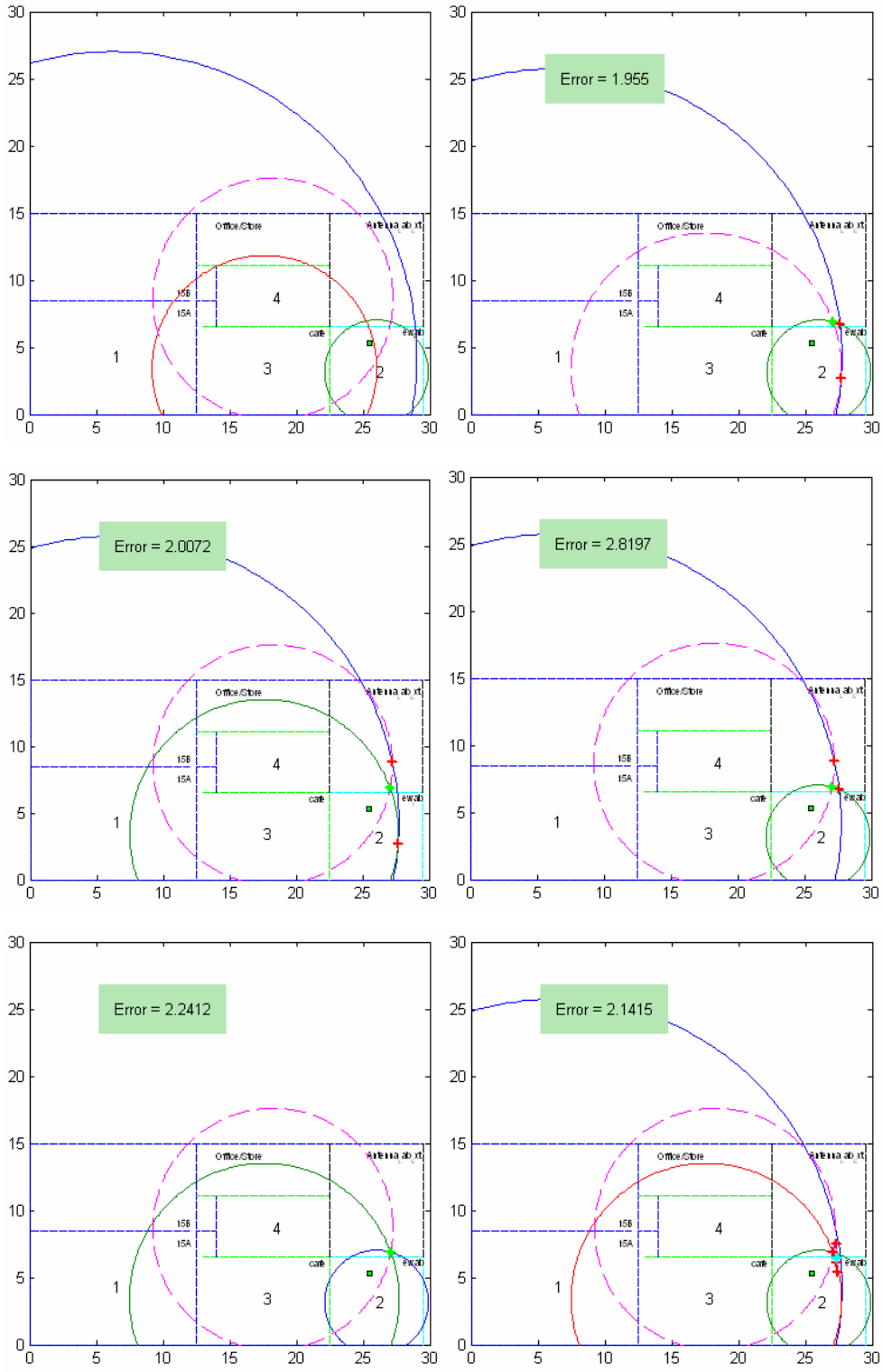

Figure A-7 Estimate Location 7

A.7.1 Location 7 – results if walls are not detected

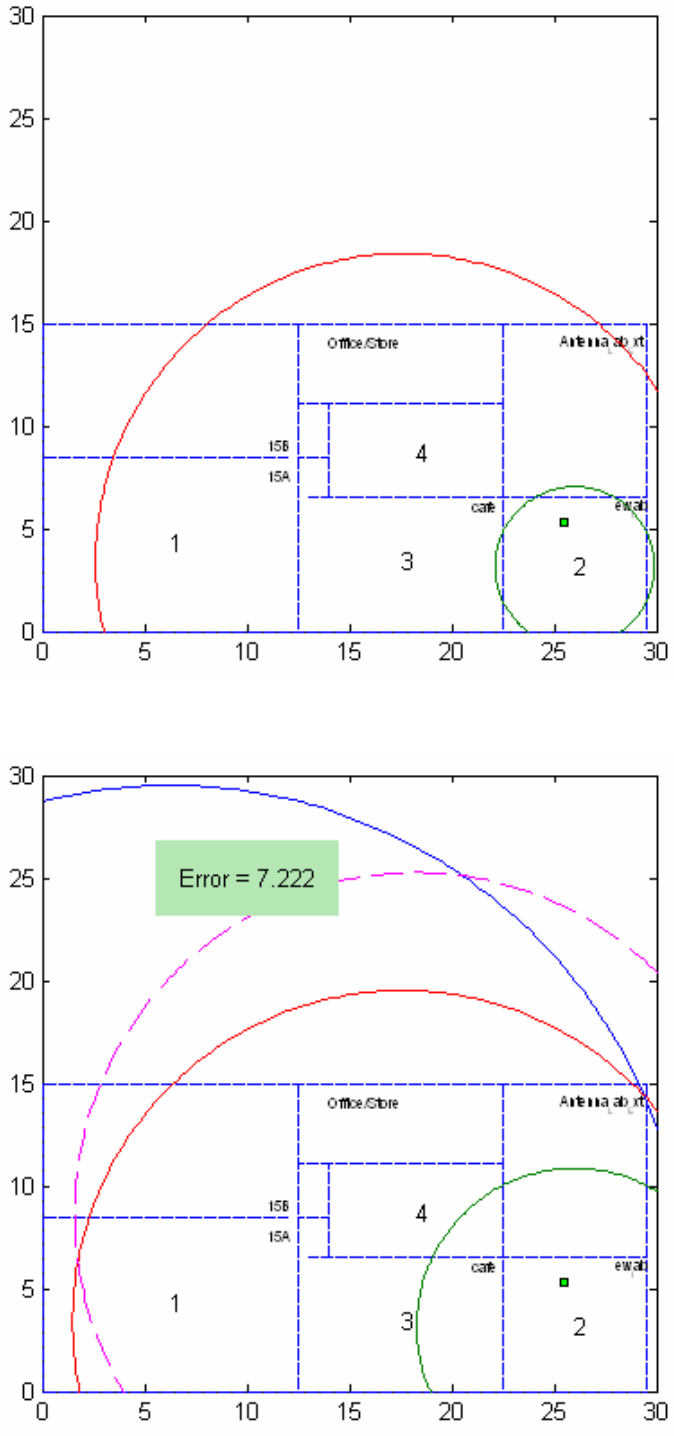

Figure A-7a Estimate location 7 if walls are not detected

A.7.2 Numerical result for figure A-7

client_posx = 25.5000

client_posy = 5.3000

loss_sensors = 80.3800 52.0000 63.7200 69.3000

Sig_Strth_Diag_Length = 57.8144 53.7499 55.7399 53.9133

Sig_Strth_Short_Dist = 52.8487 50.3330 50.4677 47.4646

NOTT = 1 0 1 1

Two_Wall_TH =

65.8783

69.7377

66.5937

68.0741

63.1274

70.3995

61.0778

67.6975

NOTT = 2 0 1 2

NOTT = 2 0 1 2

A = 101.7400

C = 3.8900

E = 15

D = 28.4100

A2 = 22.7700

C2 = 3.8900

E2 = 8.4200

D2 = 9

A.8 Location 8 result

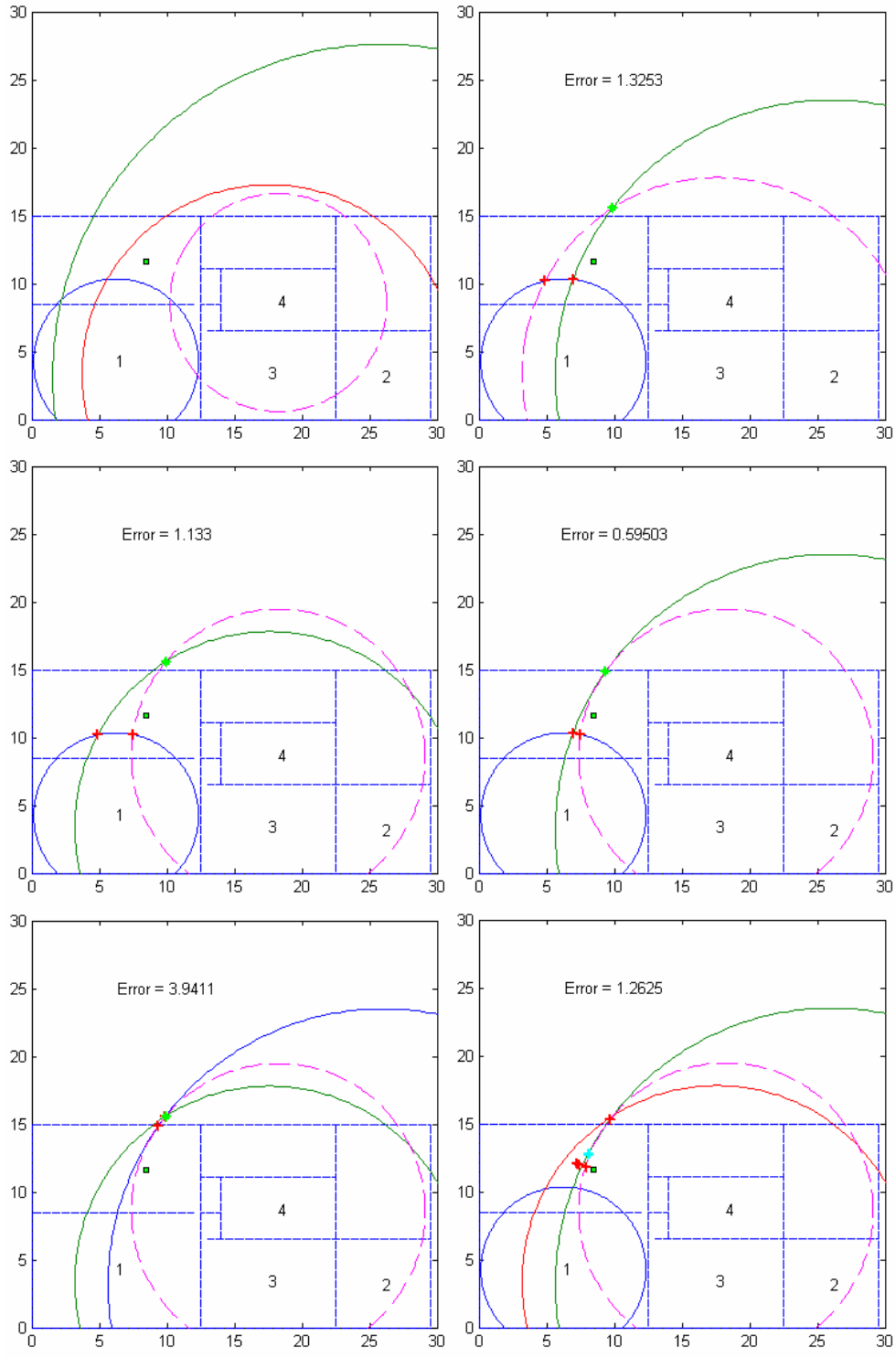

Figure A-8 Estimate Location 8

A.8.1 Location 8 – results if walls are not detected

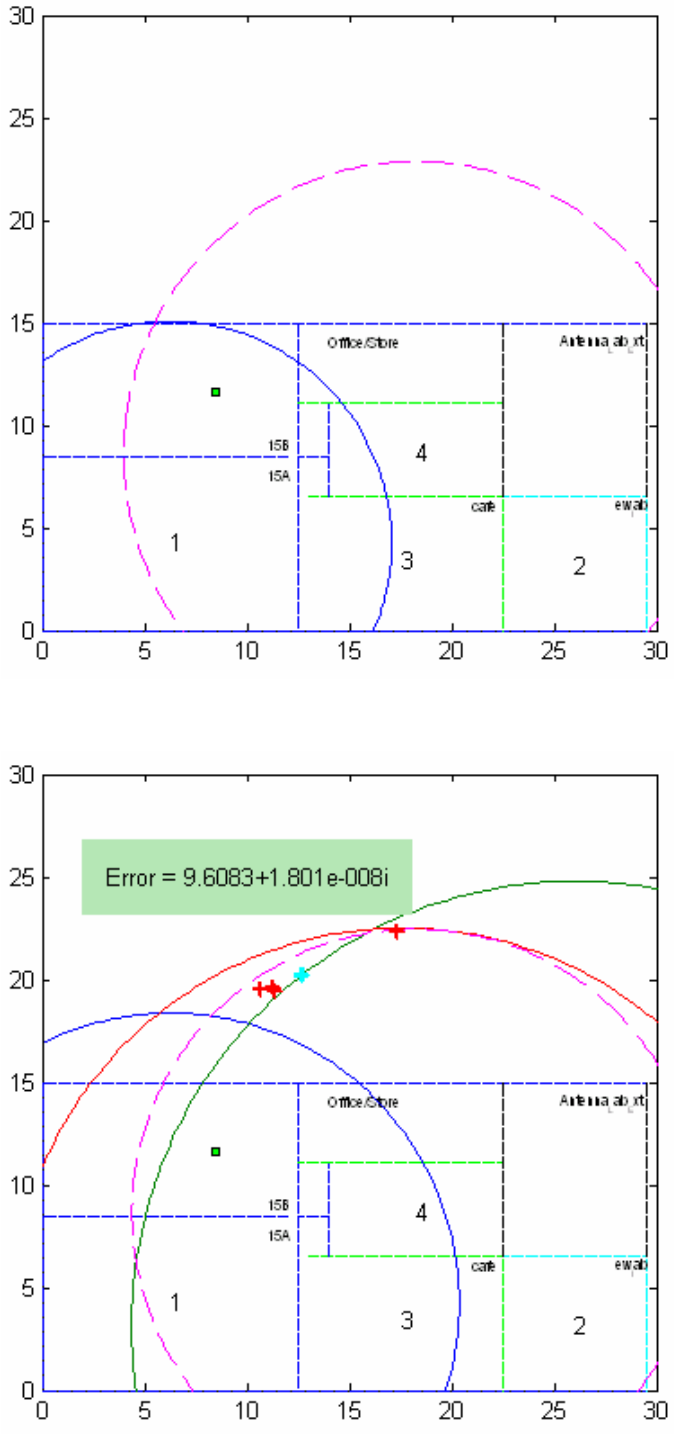

Figure A-8a Estimate location 8 if walls are not detected

A.8.2 Numerical results for figure A-8

client_posx = 8.5000

client_posy = 11.6000

loss_sensors = 60.9000 83.1500 76.0700 63.3000

Sig_Strth_Diag_Length = 57.8144 53.7499 55.7399 53.9133

Sig_Strth_Short_Dist = 52.8487 50.3330 50.4677 47.4646

NOTT = 1 1 1 1

two_Wall_TH =

65.8783
69.7377
66.5937
68.0741
63.1274
70.3995
61.0778
67.6975

NOTT = 1 2 2 1

NOTT = 1 2 2 1

A = 10.8200

C = 139.9500

E = 61.9400

D = 14.2700

A2 = 10.8200

C2 = 24.4600

E2 = 13.8700

D2 = 6.1000

A.9 Location 9 - results

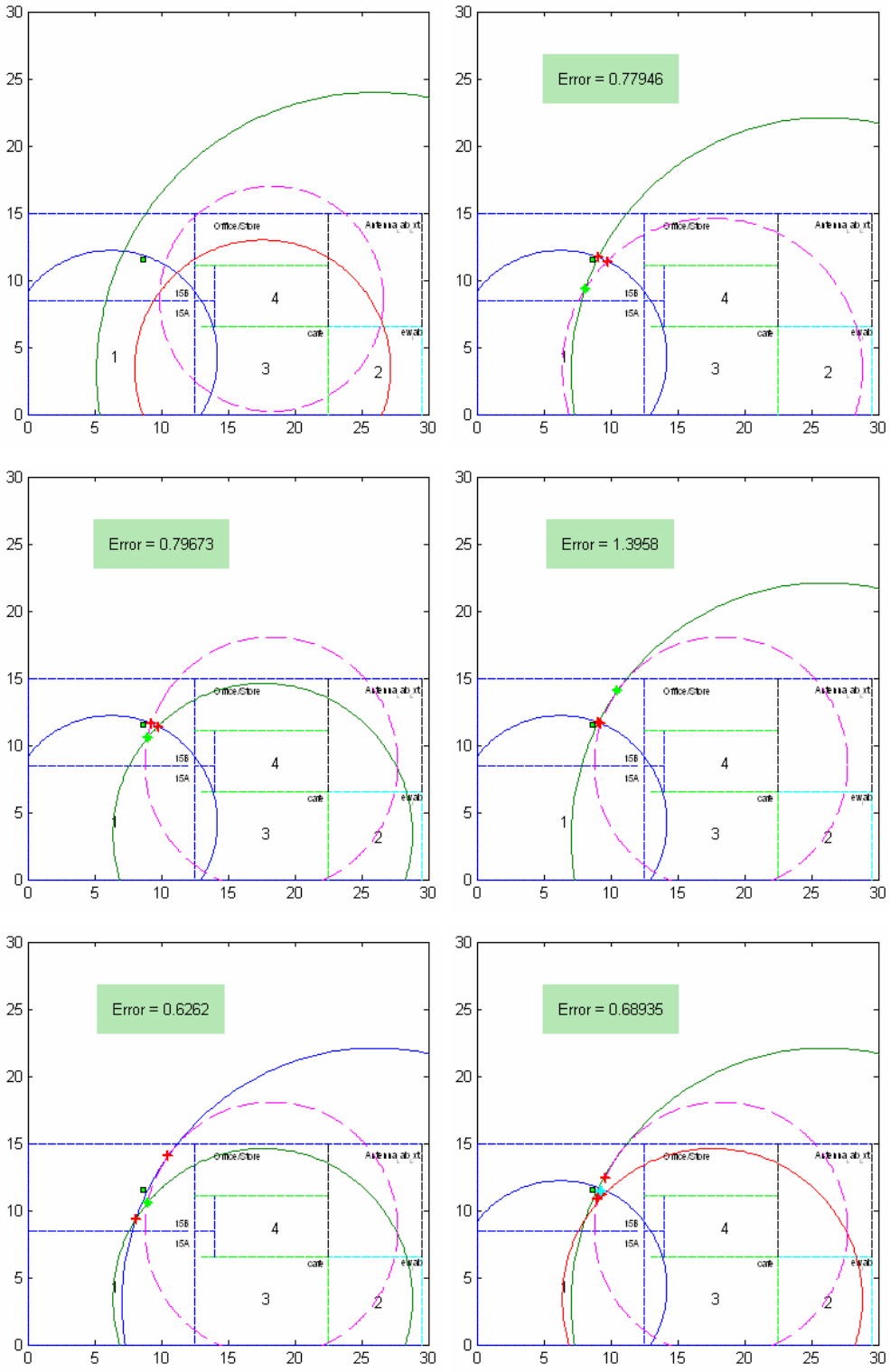

Figure A-9 Estimate Location 9

A.9.1 Location 9 – results if walls are not detected

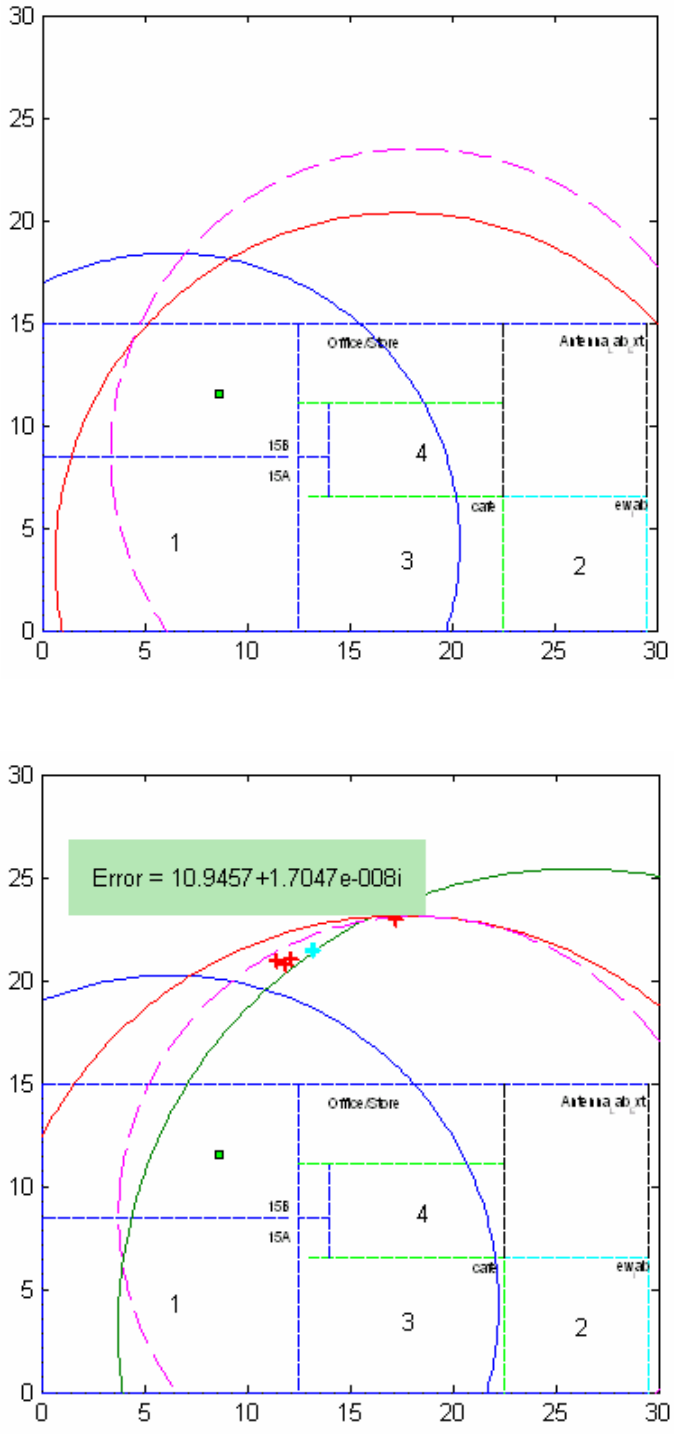

Figure A-9a Estimate location 9 if walls are not detected

A.9.2 Numerical result for figure A-9 and A-9a

client_posx = 8.6000

client_posy = 11.5000

loss_sensors 63.2300 79.6100 64.8400 63.6900

Sig_Strth_Diag_Length = 57.8144 53.7499 55.7399 53.9133

Sig_Strth_Short_Dist = 52.8487 50.3330 50.4677 47.4646

NOTT = 1 1 1 1

Two_Wall_TH =

65.8783

69.7377

66.5937

68.0741

63.1274

70.3995

61.0778

67.6975

NOTT = 1 2 1 1

NOTT = 1 2 1 1

A = 14.1400

C = 93.1100

E = 16.9700

D = 14.9000

A2 = 7.9600

C2 = 20.8400

E2 = 9.5900

D2= 8.3900

A.10 Location 10 - results

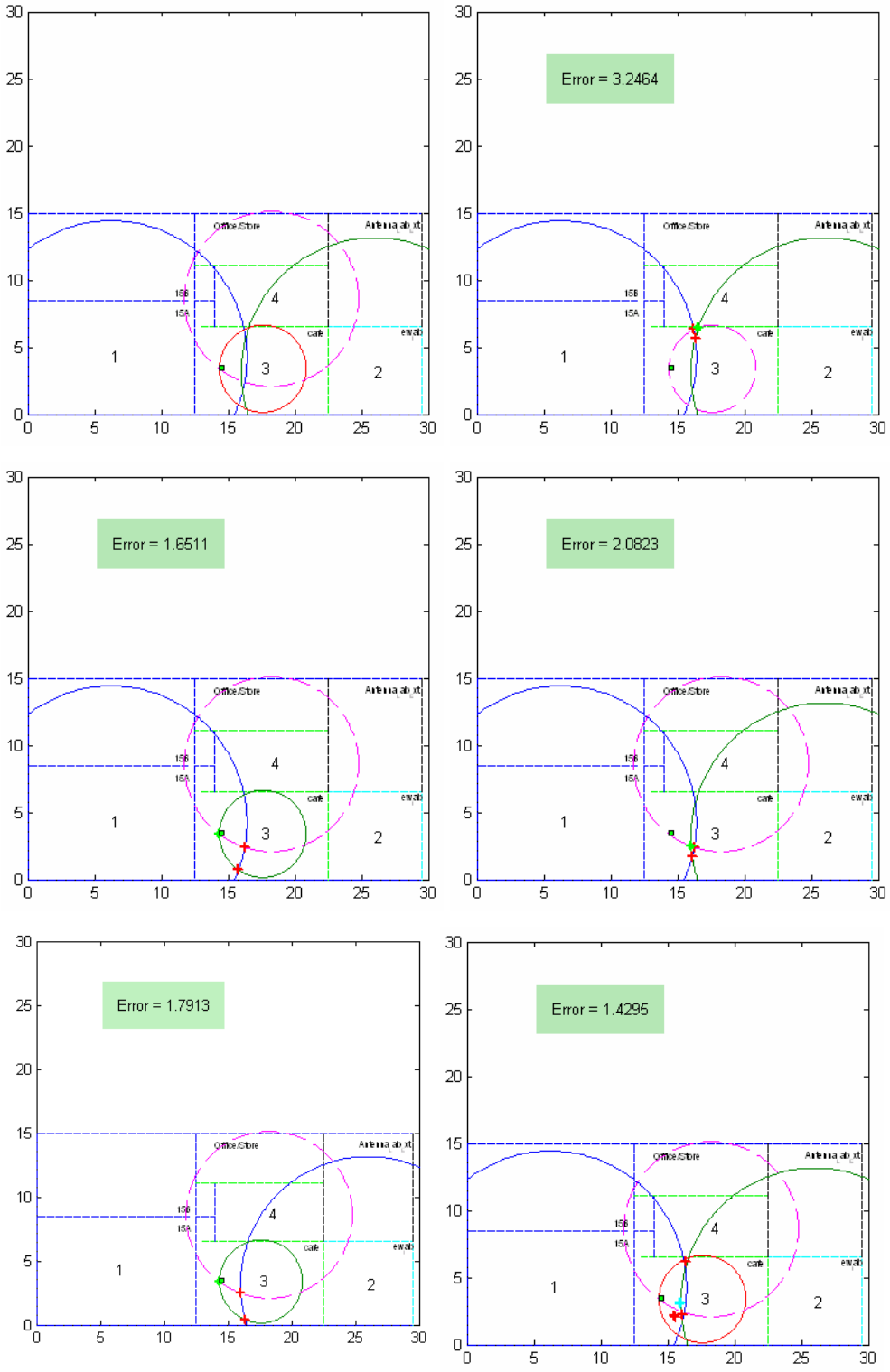

Figure A-10 Estimate Location 10

A.10.1 Location 10 – results if walls not detected

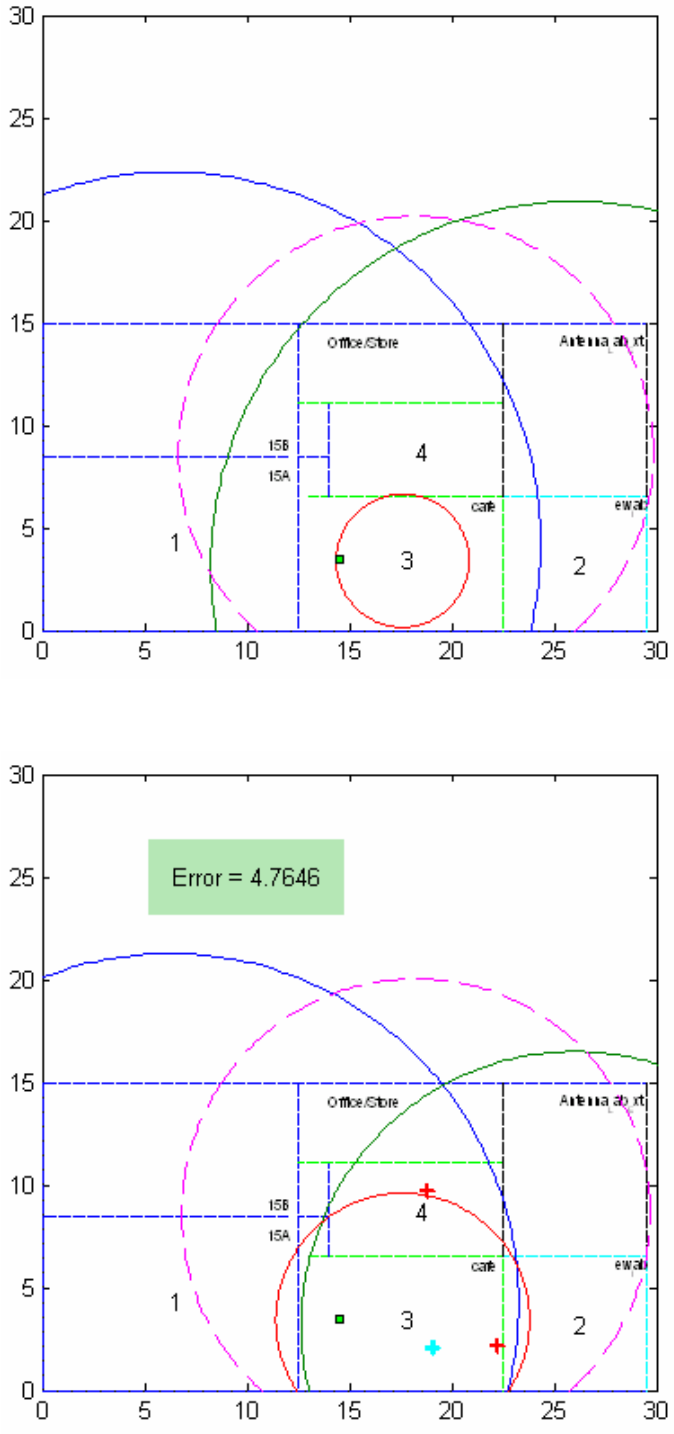

Figure A-10a Estimate Location 10 if walls not detected

A.10.2 Numerical results for figure A-10

client_posx = 14.5000

client_posy = 3.5000

loss_sensors = 65.3800 65.2300 50.4500 61.5000

Sig_Strth_Diag_Length = 57.8144 53.7499 55.7399 53.9133

Sig_Strth_Short_Dist = 52.8487 50.3330 50.4677 47.4646

NOTT = 1 1 0 1

Two_Wall_TH =

65.8783

69.7377

66.5937

68.0741

63.1274

70.3995

61.0778

67.6975

NOTT = 1 1 0 1

NOTT = 1 1 0 1

A = 18.1000

C = 17.7700

E = 3.2450

D = 11.6000

A2 = 10.1700

C2 = 10

E2 = 3.2450

D2 = 6.5200

A.11 Location 11 - results

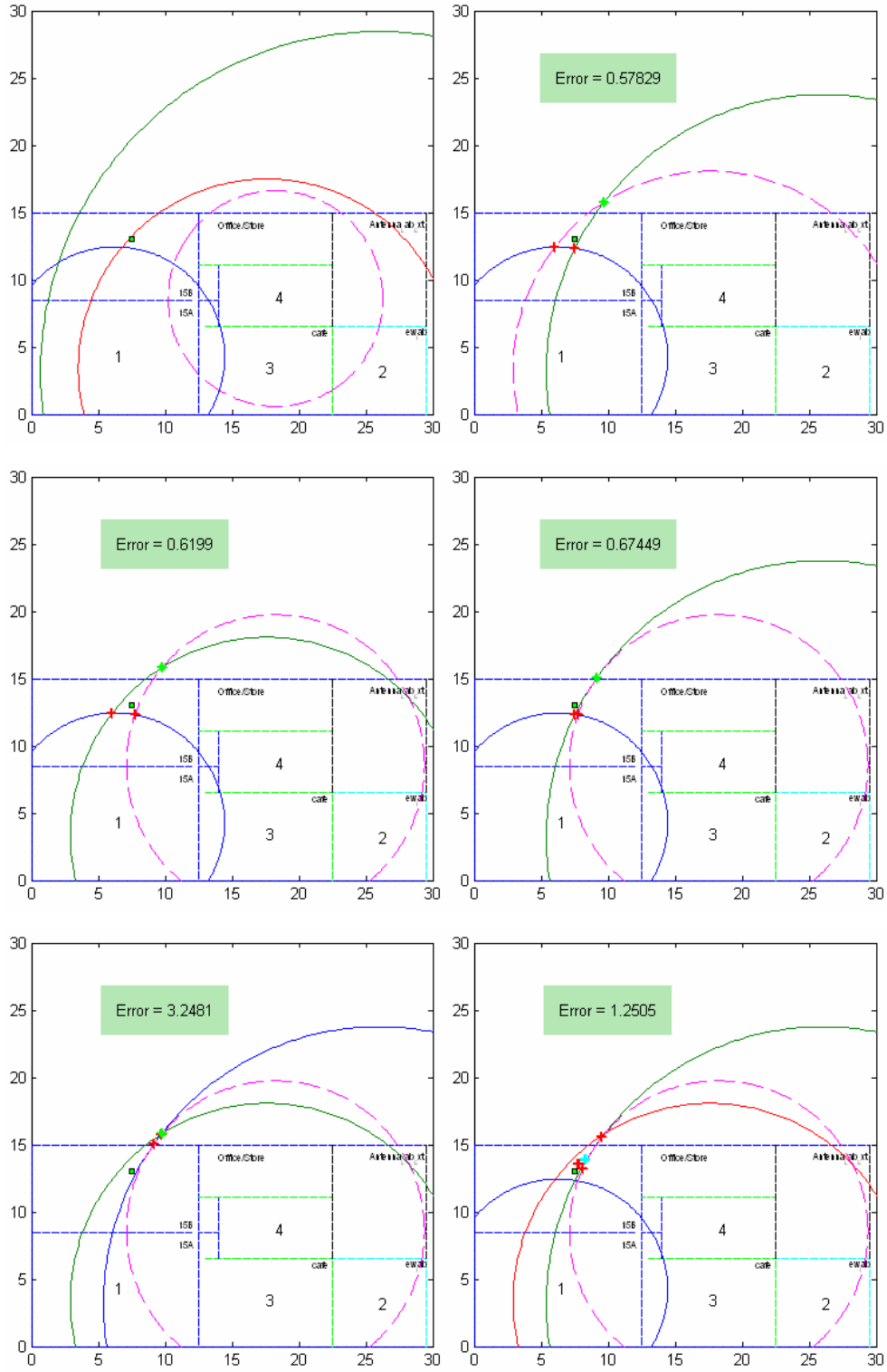

Figure A-11 Estimate Location 11

A.11.1 Location 11 – results if walls are not detected

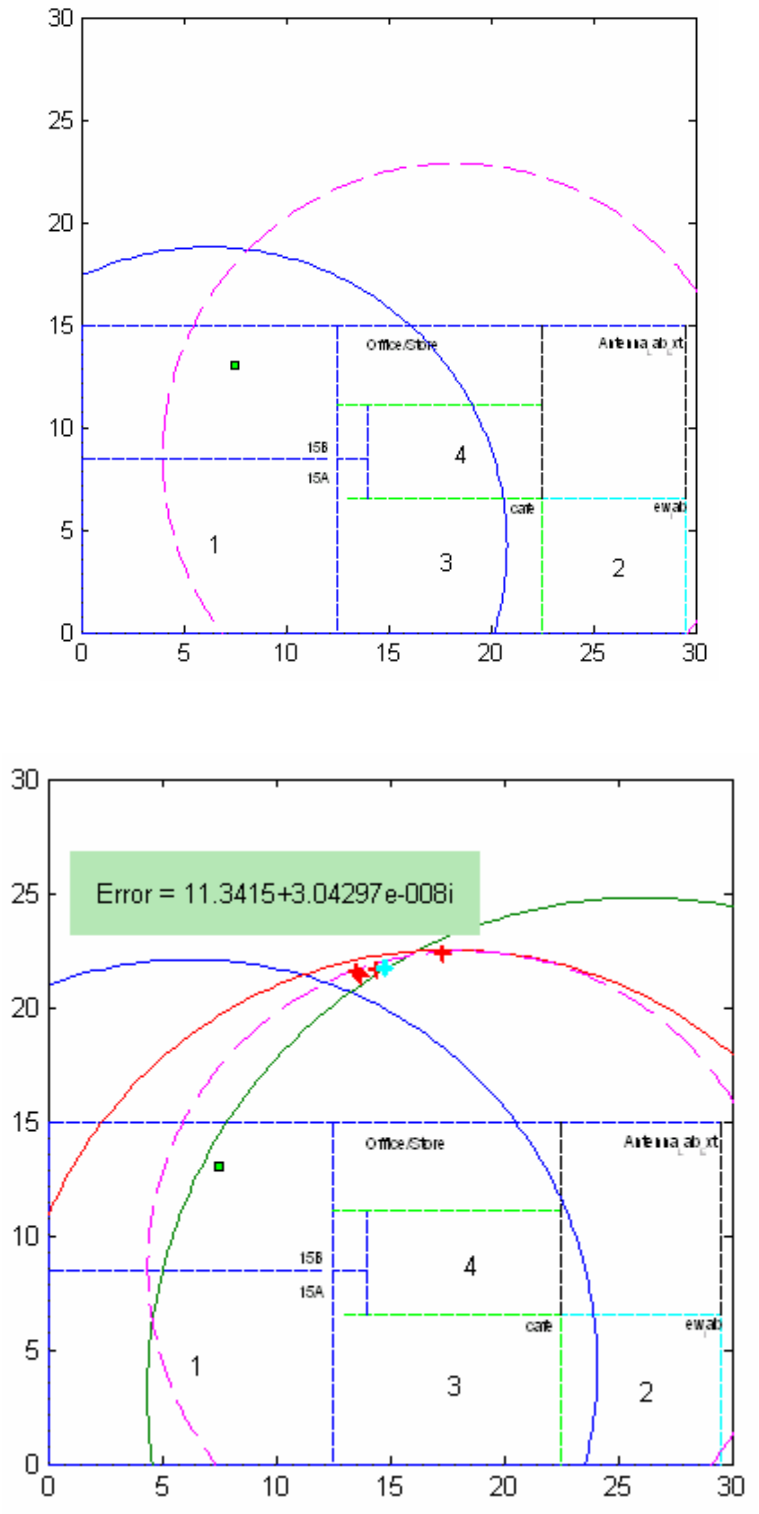

Figure A-11a Estimate Location 11 if walls not detected

A.11.2 Numerical results for figure A-11

client_posx = 7.5000

client_posy = 13

loss_sensors = 63.4600 81.3000 73.2000 63.3000

Sig_Strth_Diag_Length = 57.8144 53.7499 55.7399 53.9133

Sig_Strth_Short_Dist = 52.8487 50.3330 50.4677 47.4646

NOTT = 1 1 1 1

Two_Wall_TH =

65.8783

69.7377

66.5937

68.0741

63.1274

70.3995

61.0778

67.6975

NOTT = 1 2 2 1

NOTT = 1 2 2 1

A = 14.5400

C = 113.1100

E = 44.5100

D = 14.2700

A2 = 8.1900

C2 = 25.3200

E2 = 14.1000

D2 = 8.0200

A.12 Location 12 - results

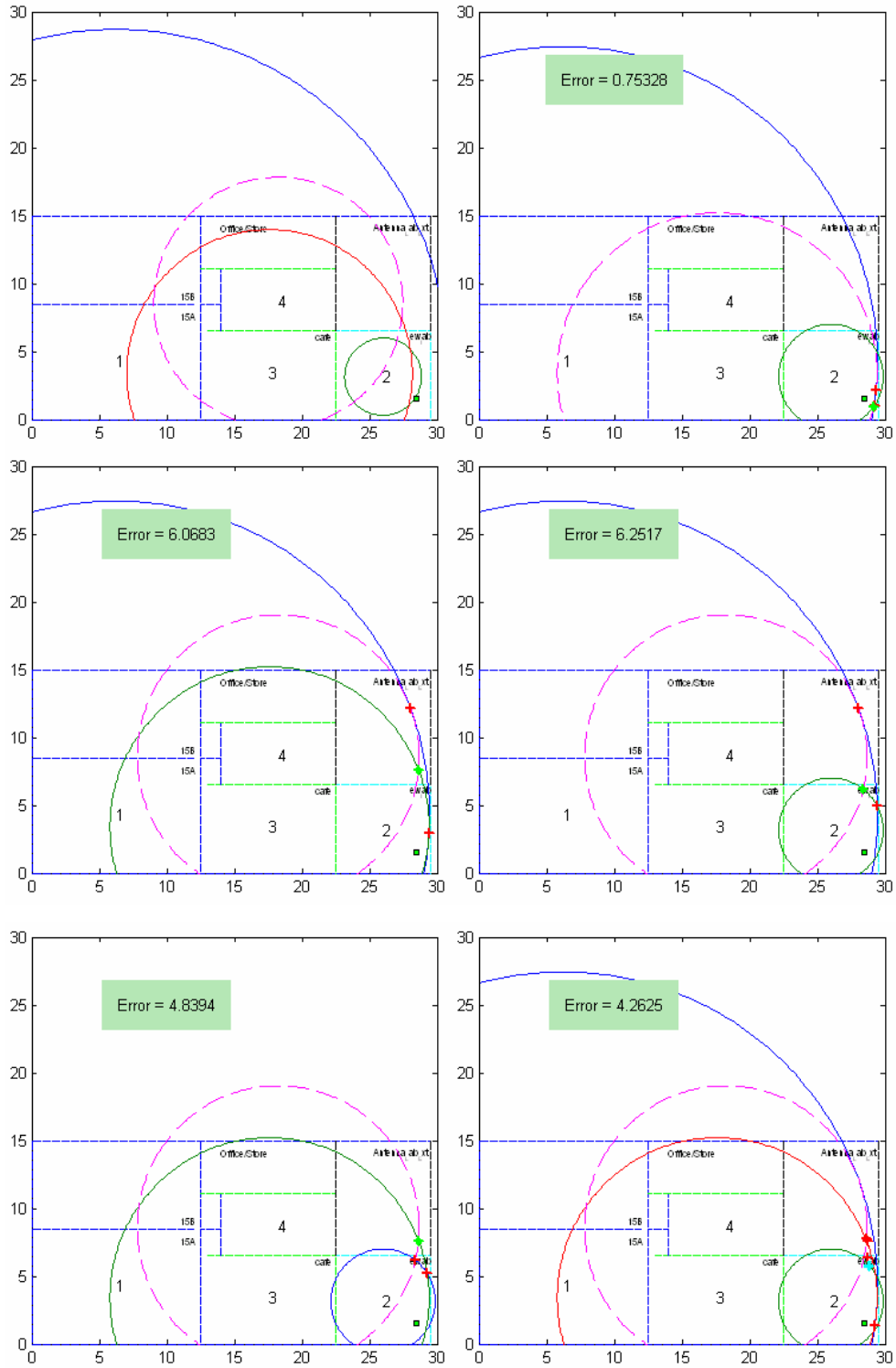

Figure A-12 Estimate location 12

A.12.1 Location 12 – results if walls not detected

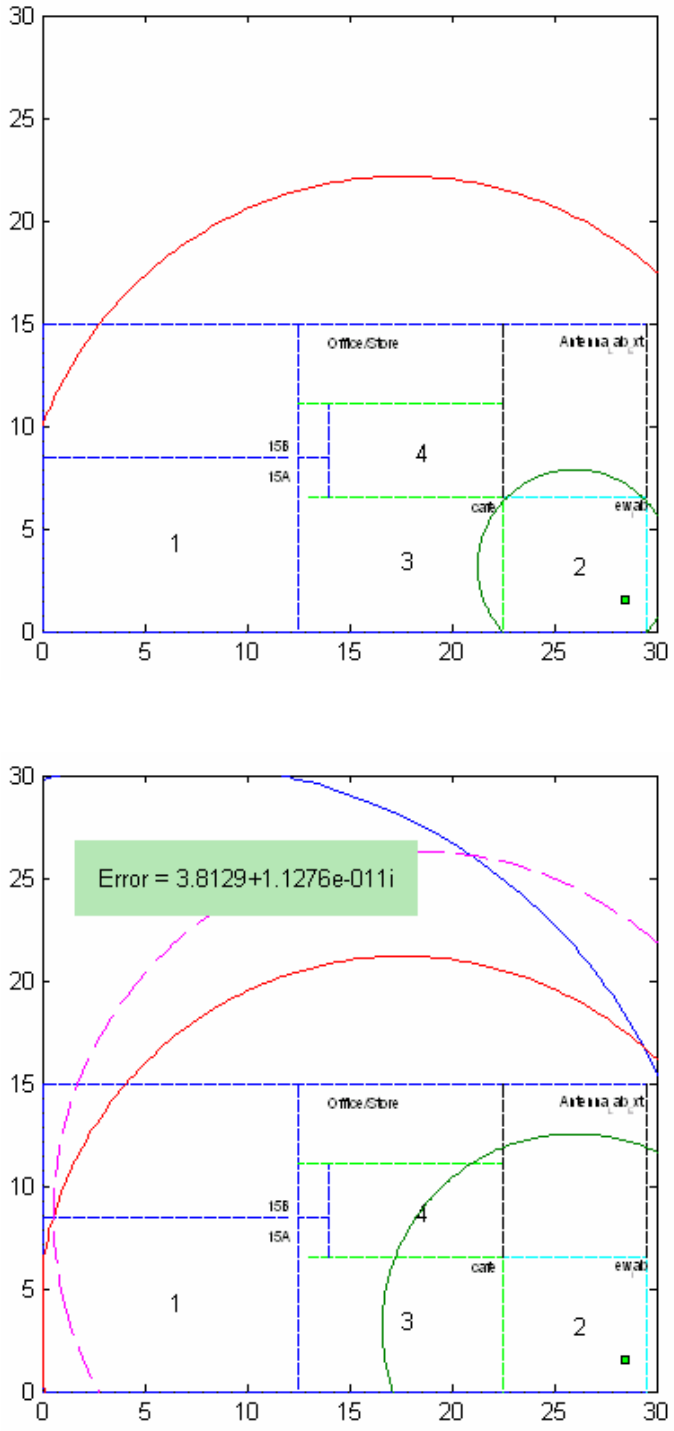

Figure A-12a Estimate location 12 if walls not detected

A.12.2 Numerical results for figure A-12 and A-12a

client_posx = 28.5000

client_posy = 1.5000

loss_sensors = 78.0000 49.3000 65.7000 69.5000

Sig_Strth_Diag_Length = 57.8144 53.7499 55.7399 53.9133

Sig_Strth_Short_Dist = 52.8487 50.3330 50.4677 47.4646

NOTT = 1 0 1 1

Two_Wall_TH =

65.8783

69.7377

66.5937

68.0741

63.1274

70.3995

61.0778

67.6975

NOTT = 2 0 1 2

NOTT = 2 0 1 2

A = 77.3500

C = 2.8450

E = 18.7700

D = 29.0700

A2 = 24.4600

C2 = 2.8450

E2 = 10.5700

D2 = 9.2200

A.13 Location 13 - Results

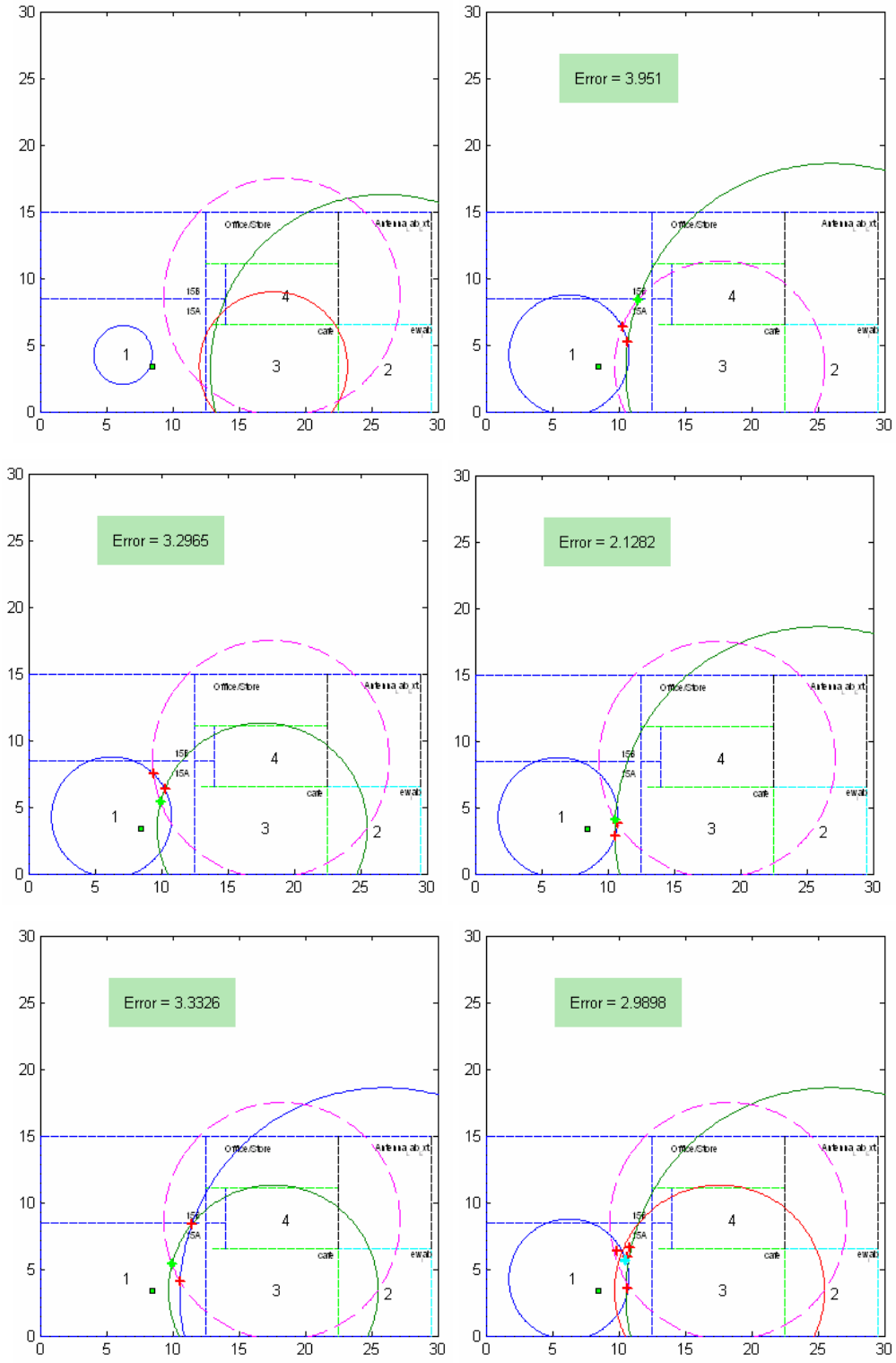

Figure A-13 Estimate location 13

A.13.1 Location 13 – results if walls not detected

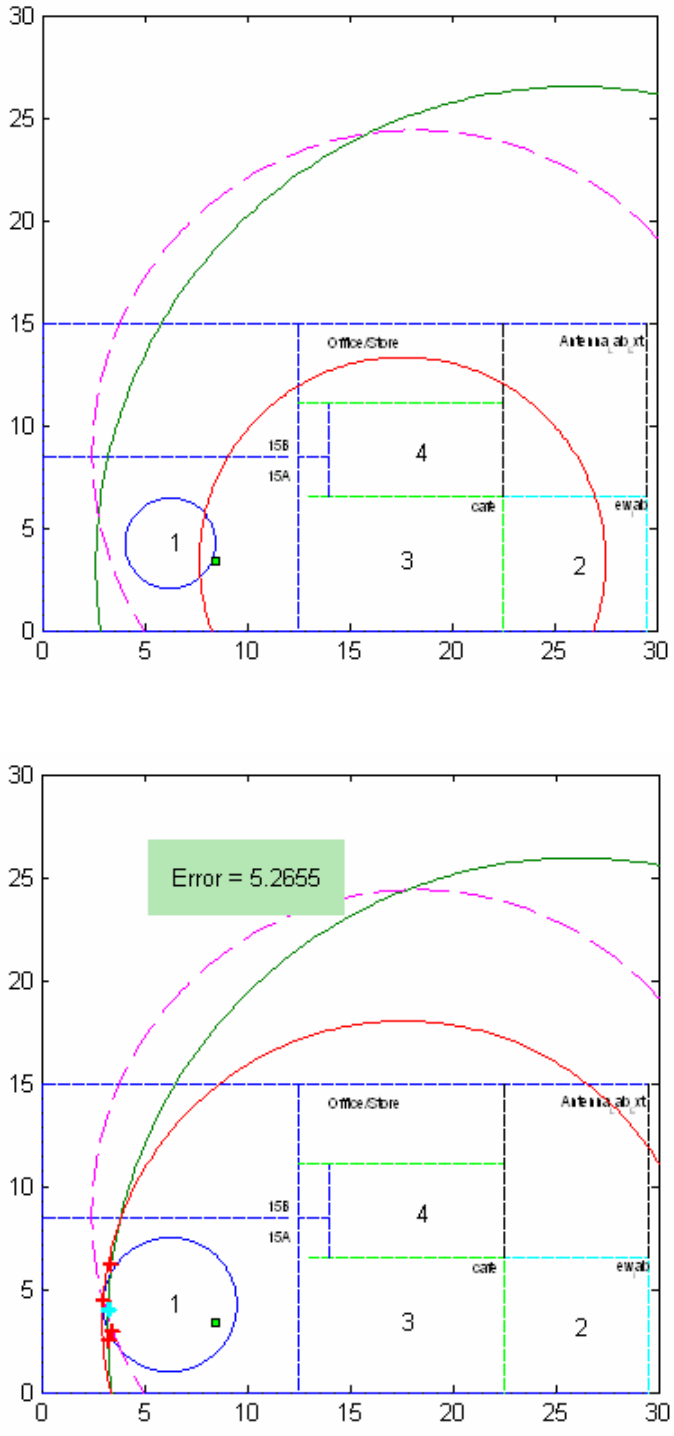

Figure A-13a Estimate location 13 if walls not detected

A.13.2 Numerical results for figure A-13 and A-13a

client_posx = 8.5000

client_posy = 3.4000

loss_sensors = 47.1500 67.6100 60.1500 64.2000

Sig_Strth_Diag_Length = 57.8144 53.7499 55.7399 53.9133

Sig_Strth_Short_Dist = 52.8487 50.3330 50.4677 47.4646

NOTT = 0 1 1 1

Two_Wall_TH =

65.8783

69.7377

66.5937

68.0741

63.1274

70.3995

61.0778

67.6975

NOTT = 0 1 1 1

NOTT = 0 1 1 1

A = 2.2100

C = 23.3800

E = 9.9200

D = 15.8000

A2 = 2.2100

C2 = 13.1500

E2 = 5.5900

D2 = 8.9000

A.14 Location 14 - results

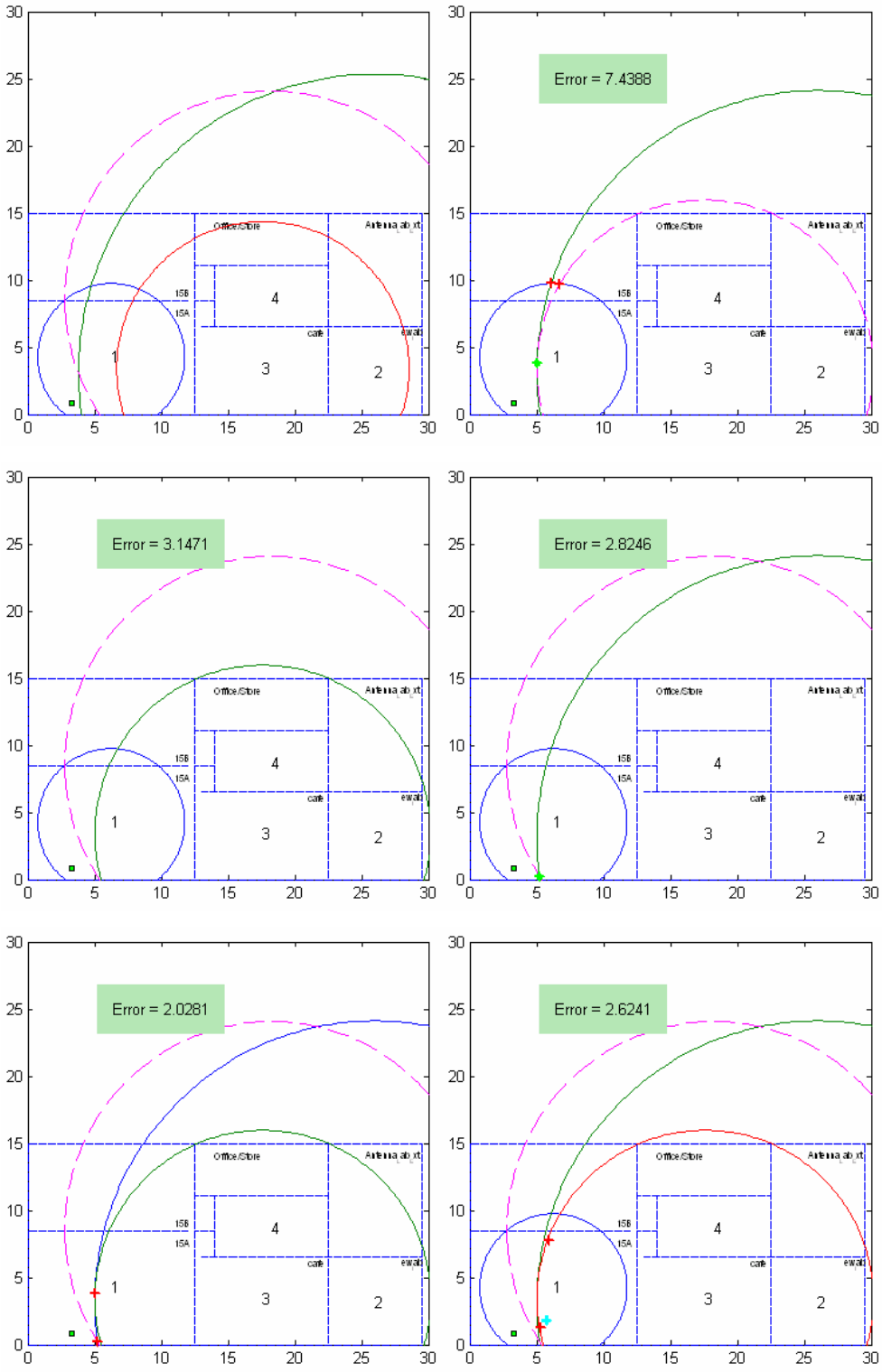

Figure A-14 Estimate Location 14

A.14.1 Location 14 – results if walls not detected

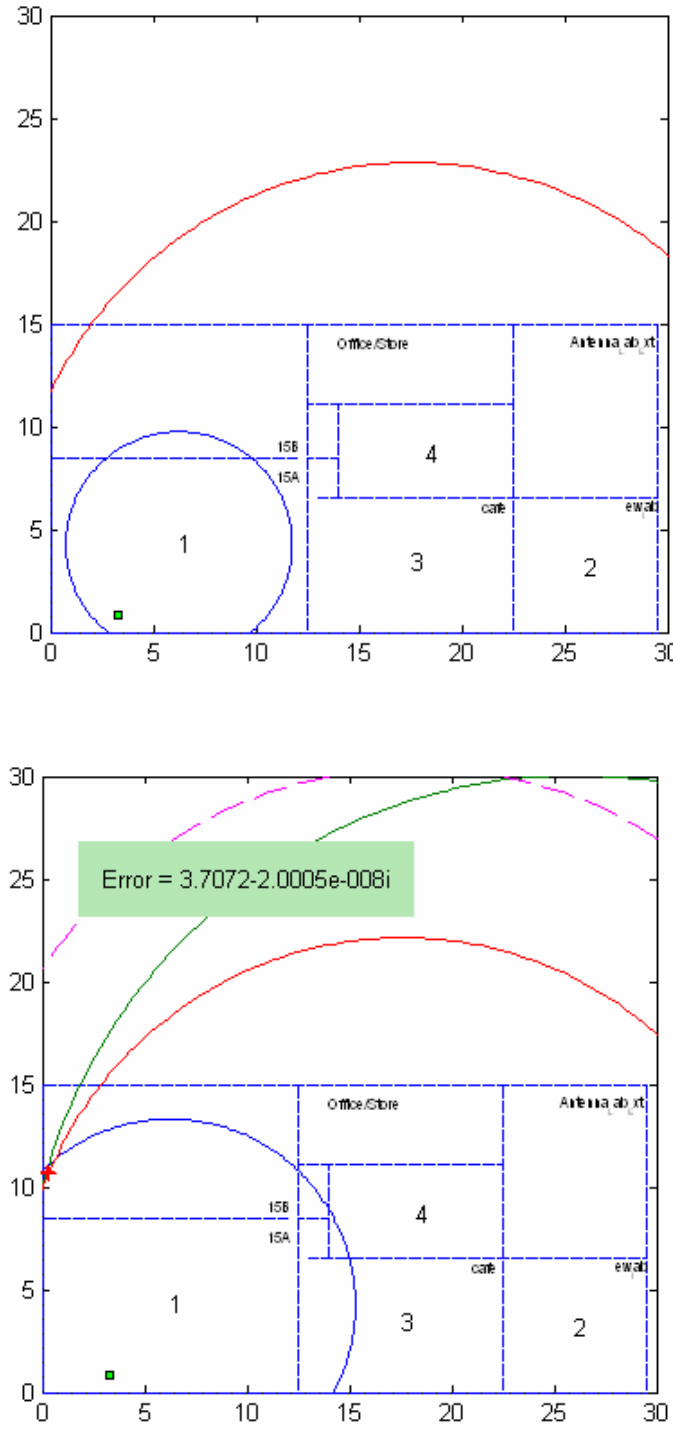

Figure A-14a Estimate location if walls not detected

A.14.2 Numerical result for figure A-14 and A-14a

client_posx = 3.3000

client_posy = 0.8000

loss_sensors = 55.0000 77.1600 66.0000 80.0000

Sig_Strth_Diag_Length = 57.8144 53.7499 55.7399 53.9133

Sig_Strth_Short_Dist = 52.8487 50.3330 50.4677 47.4646

NOTT = 0 1 1 1

Two_Wall_TH =

65.8783

69.7377

66.5937

68.0741

63.1274

70.3995

61.0778

67.6975

NOTT = 0 2 1 2

NOTT = 0 2 1 2

A = 5.5000

C = 70.2200

E = 19.4300

D = 97.3800

A2 = 5.5000

C2 = 22.2000

E2 = 10.9500

D2 = 15.4700

A.15 Location 15 - results

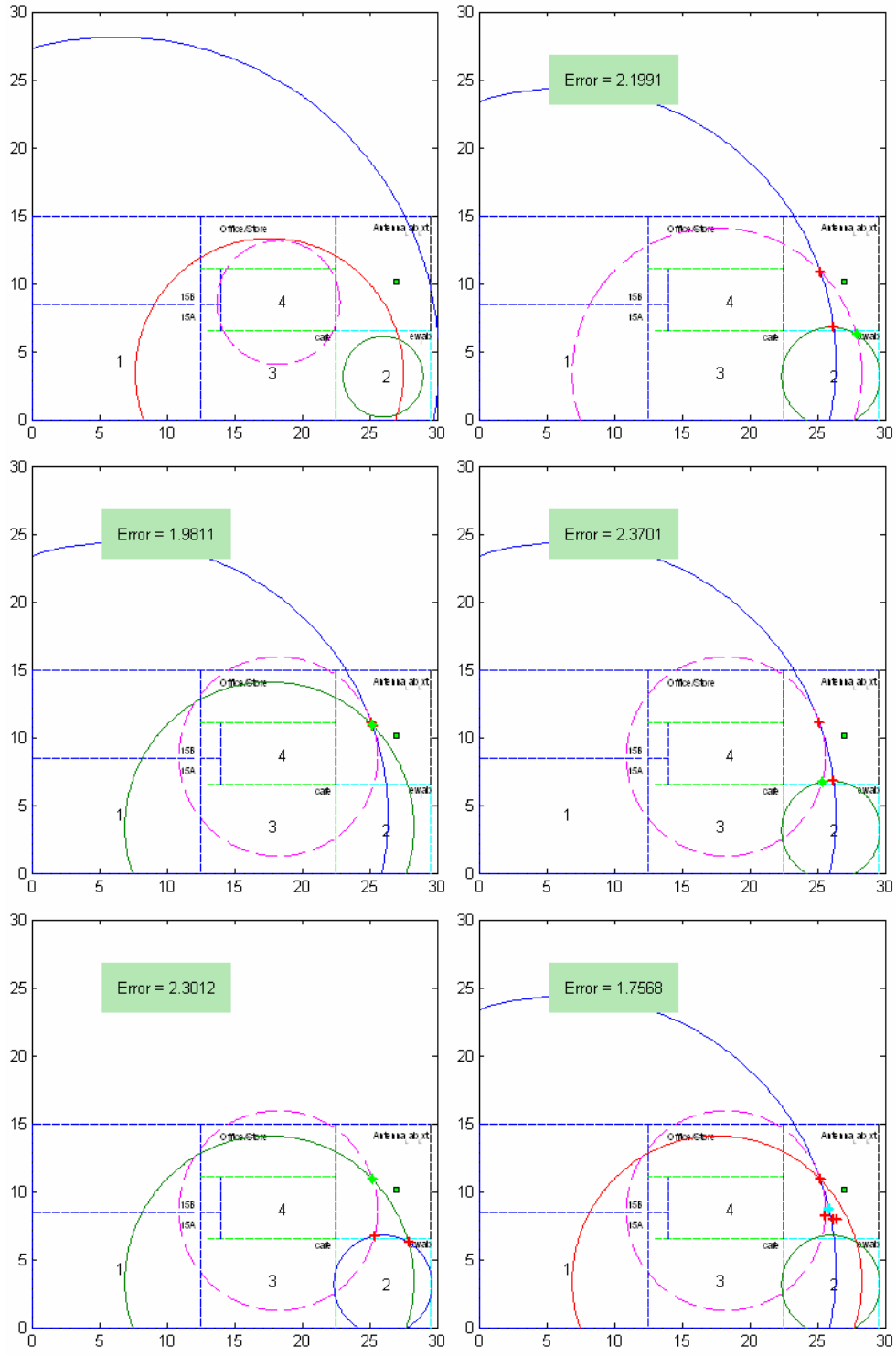

Figure A-15 Estimate Location 15

A.15.1 Location 15 – results if walls not detected

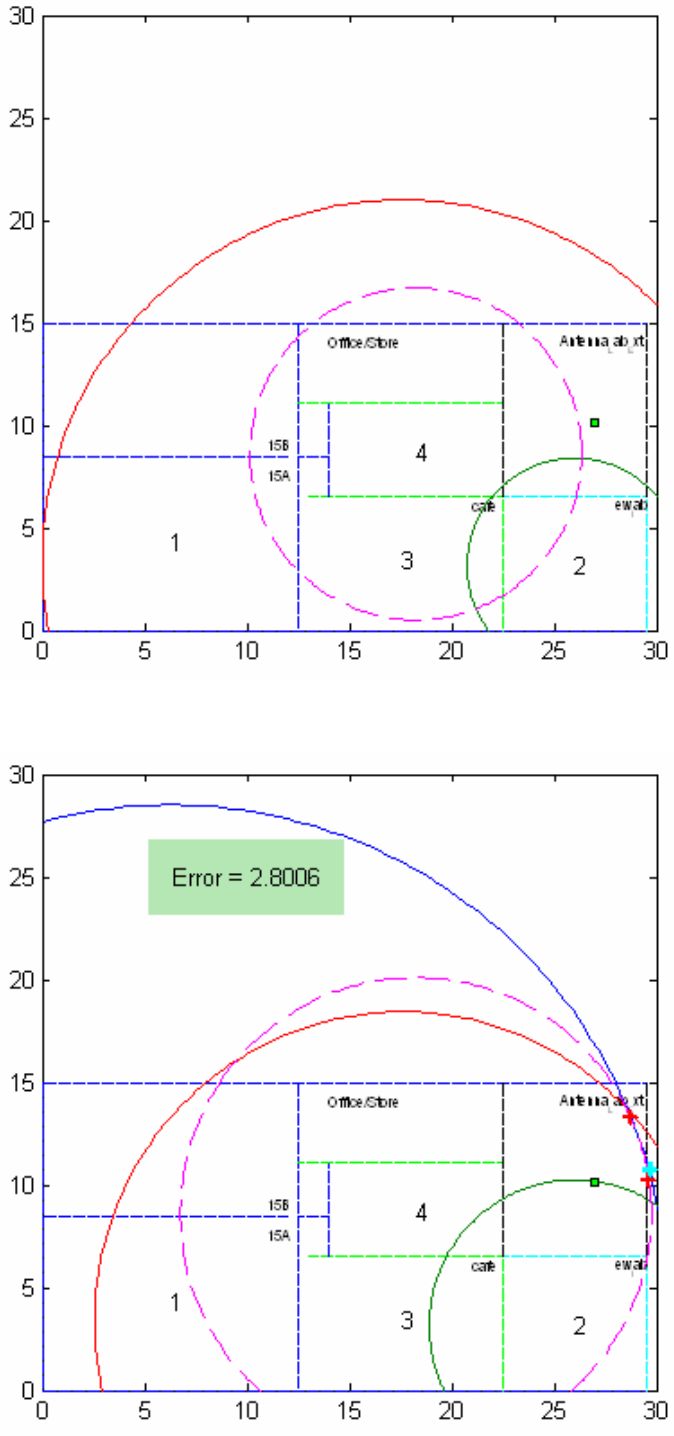

Figure A-15a Estimate location 15 if walls are not detected

A.15.2 Numerical result for figure A-15 and A-15a

client_posx = 27
client_posy = 10.1000
loss_sensors = 80.8000 54.6100 65.1500 58.3800
Sig_Strth_Diag_Length = 57.8144 53.7499 55.7399 53.9133
Sig_Strth_Short_Dist = 52.8487 50.3330 50.4677 47.4646

NOTT = 1 1 1 1

Two_Wall_TH =

65.8783
69.7377
66.5937
68.0741
63.1274
70.3995
61.0778
67.6975

NOTT = 2 1 1 1
NOTT = 2 1 1 1

A = 106.7800
C = 5.2500
E = 17.6000
D = 8.1000
A2 = 23.9000
C2 = 2.9600
E2 = 9.9200
D2 = 4.5600

A.16 Location 16 – results

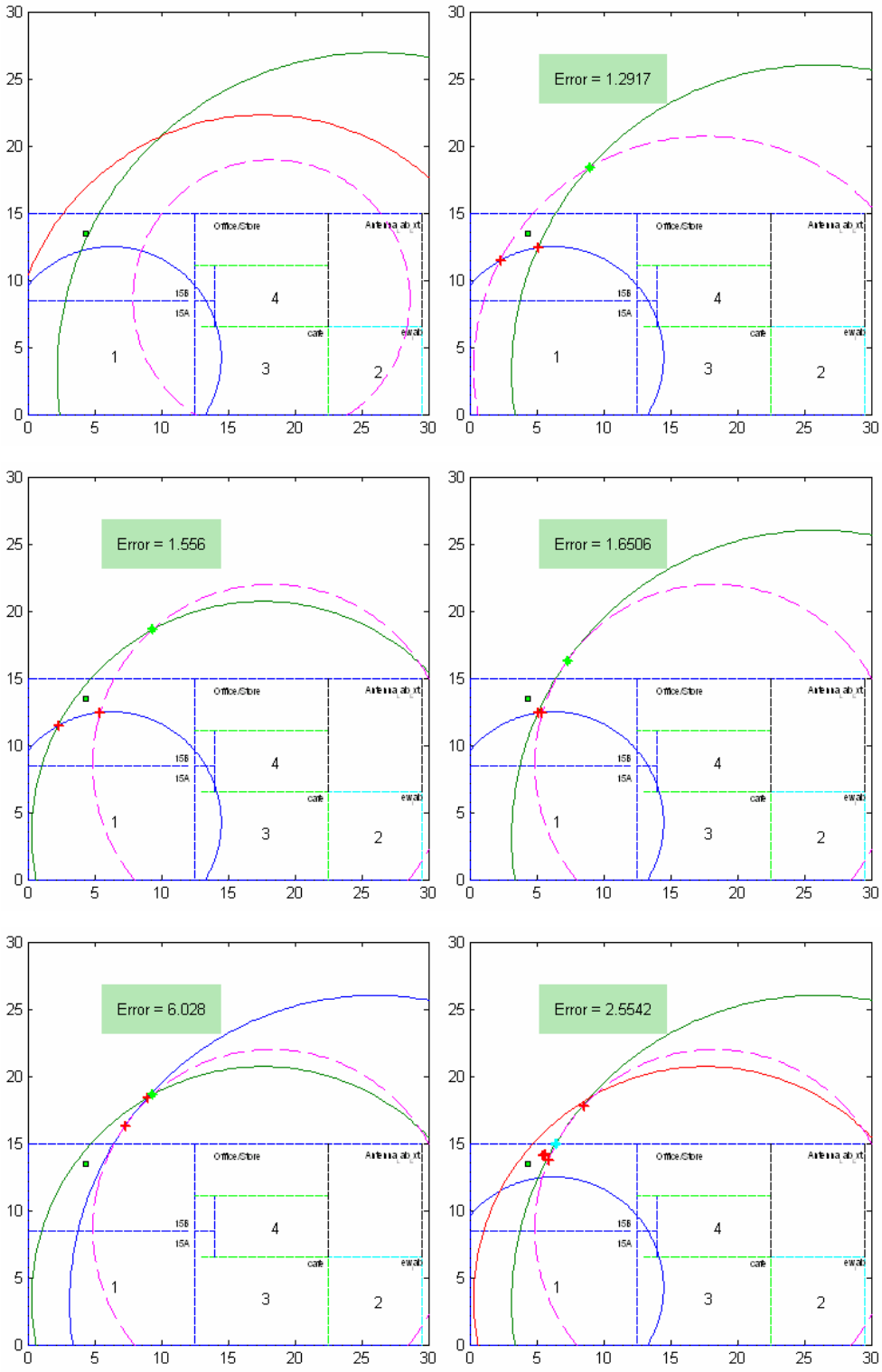

Figure A-16 Estimate location 16

A.16.1 Location 16 – results if walls not detected

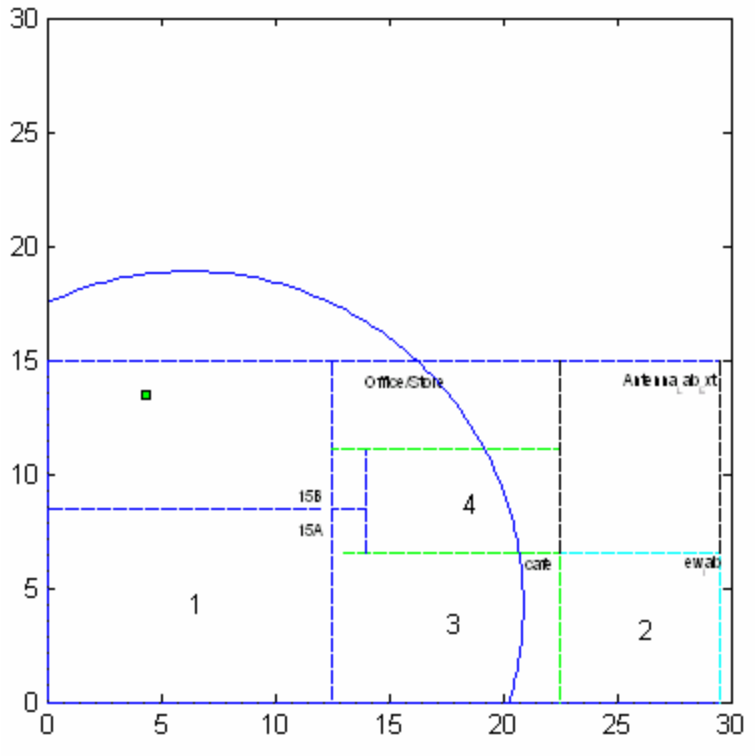

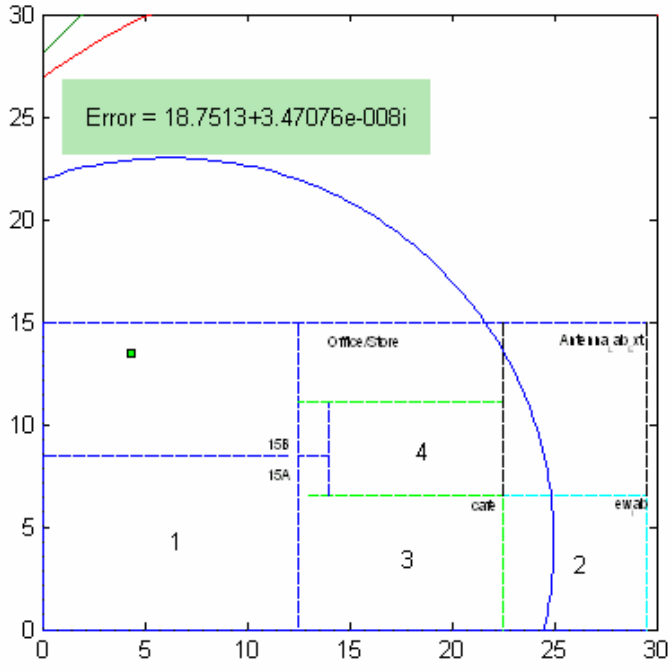

Figure A-16a Estimate location 16 if walls not detected

A.16.2 Numerical results for figure A-16 and A.16a

client_posx = 4.3000

client_posy = 13.5000

loss_sensors = 63.5300 83.7600 78.7600 70.5300

Sig_Strth_Diag_Length = 57.8144 53.7499 55.7399 53.9133

Sig_Strth_Short_Dist = 52.8487 50.3330 50.4677 47.4646

NOTT = 1 1 1 1

Two_Wall_TH =

65.8783

69.7377

66.5937

68.0741

63.1274

70.3995

61.0778

67.6975

NOTT = 1 2 2 2

NOTT = 1 2 2 2

A = 14.6400

C = 150.1400

E = 84.4300

D = 32.7300

A2 = 8.2400

C2 = 23.7900

E2 = 18.9000

D2 = 10.3700

A.17 Location 17 – results

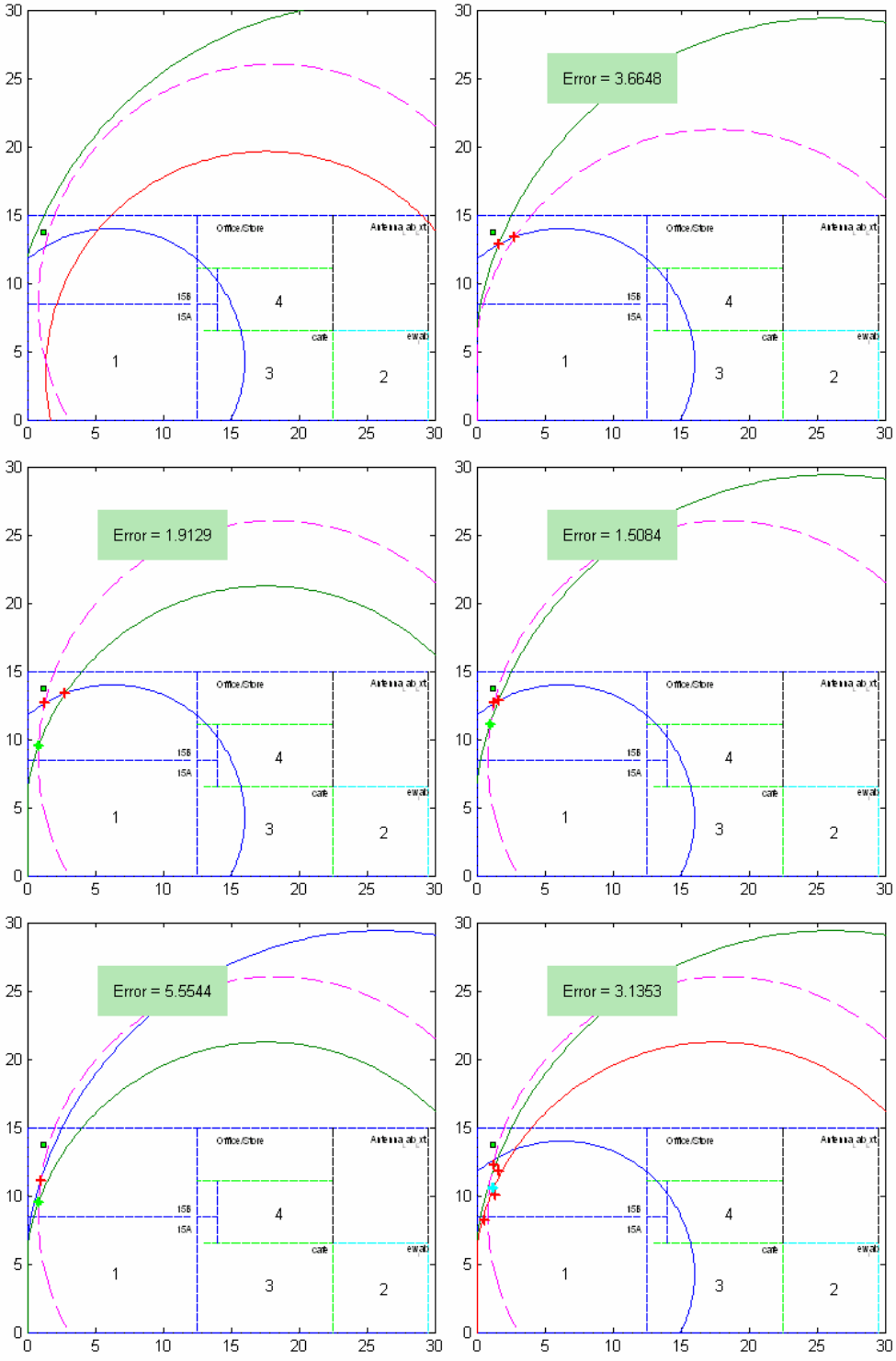

Figure A-17 Location 17

A.17.1 Location 17 – results if walls not detected

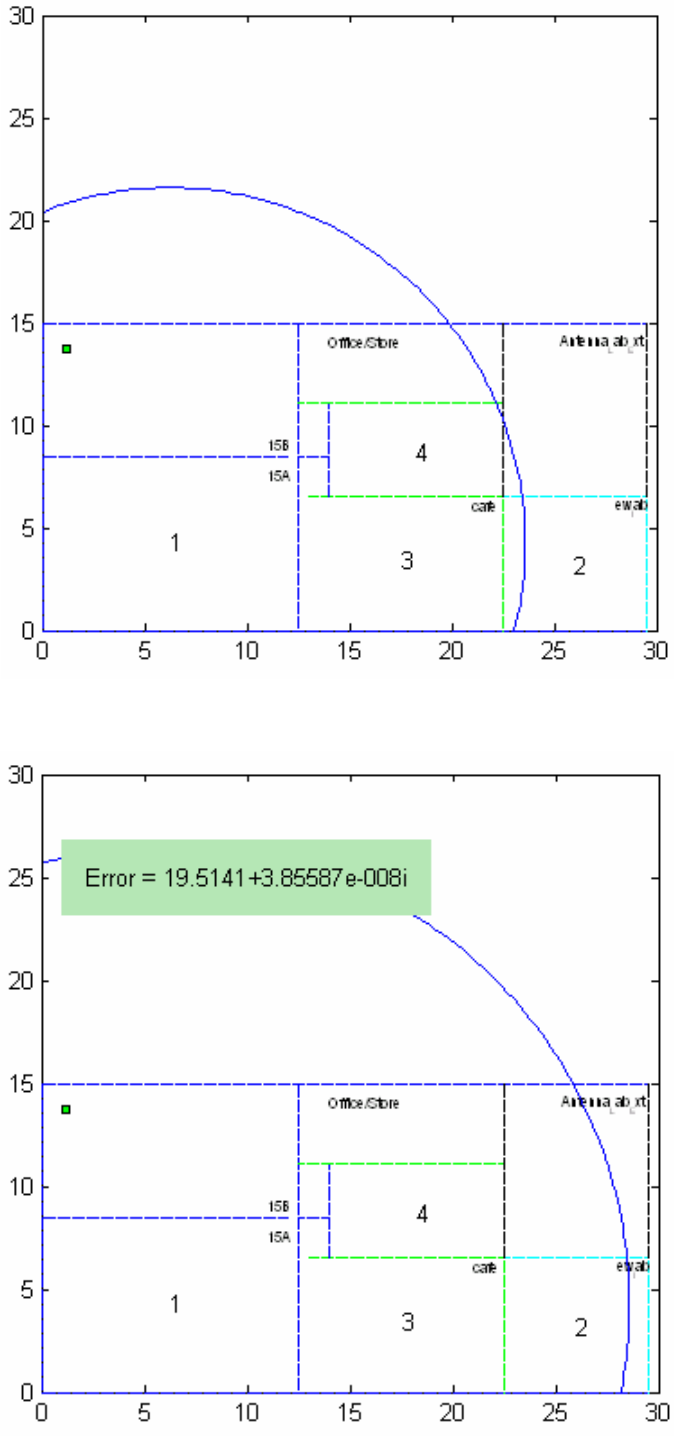

Figure A-17a Location 17 if walls not detected

A.17.2 Numerical resultsfor figure A-17 and A.17a

client_posx = 1.2000

client_posy = 13.7000

loss_sensors = 65.0000 82.0000 80.4600 81.0700

Sig_Strth_Diag_Length = 57.8144 53.7499 55.7399 53.9133

Sig_Strth_Short_Dist = 52.8487 50.3330 50.4677 47.4646

NOTT = 1 1 1 1

Two_Wall_TH =

65.8783
69.7377
66.5937
68.0741
63.1274
70.3995
61.0778
67.6975

NOTT = 1 2 2 2

NOTT = 1 2 2 2

A = 17.3400

C = 122.6000

E = 102.6800

D = 110.1500

A2 = 17.3400

C2 = 27.4400

E2 = 16.2500

D2 = 17.4400

A.18 Location 18 - results

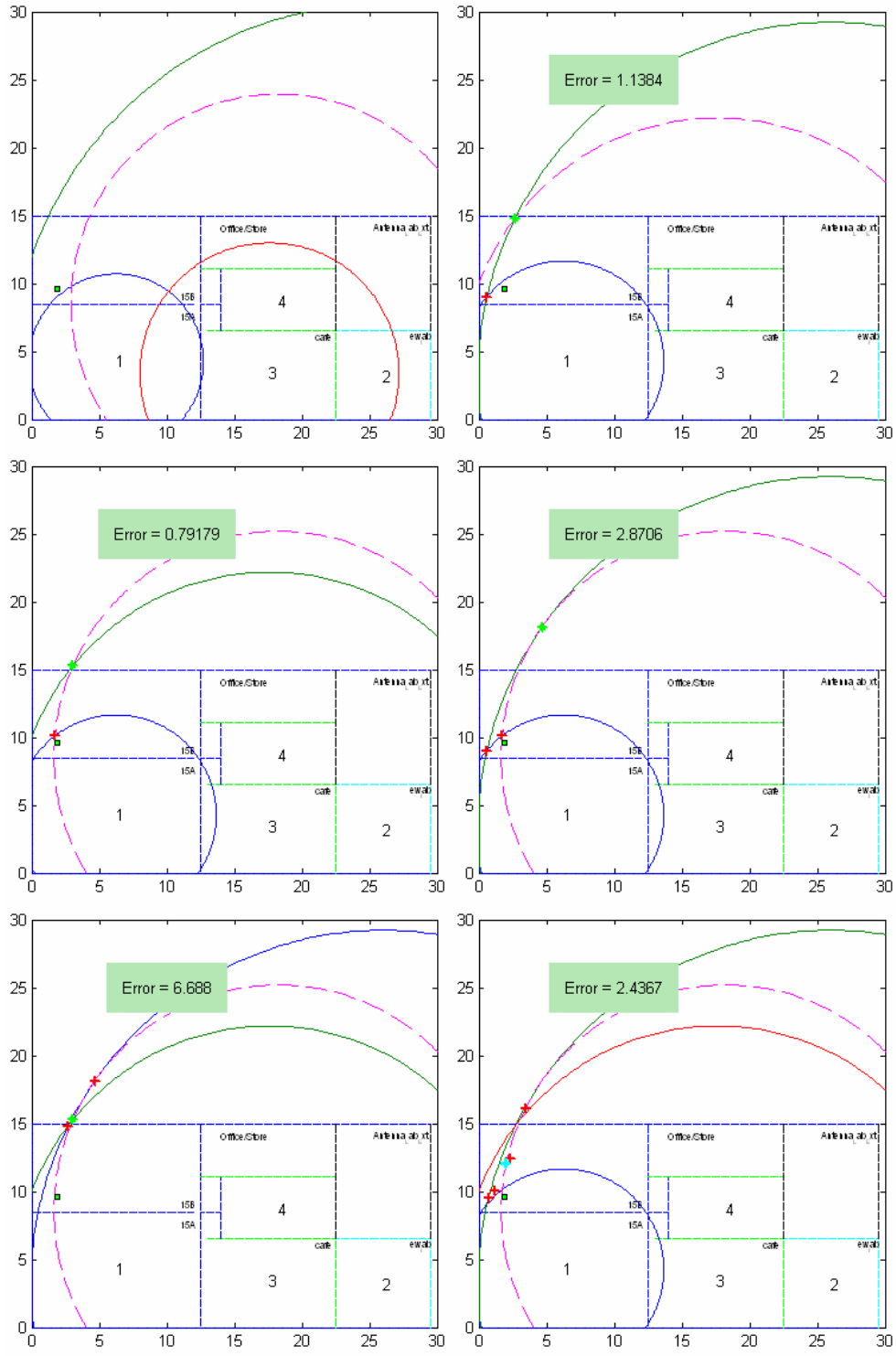

Figure A-18 Location 18

A.18.1 Location 18 results if walls not detected

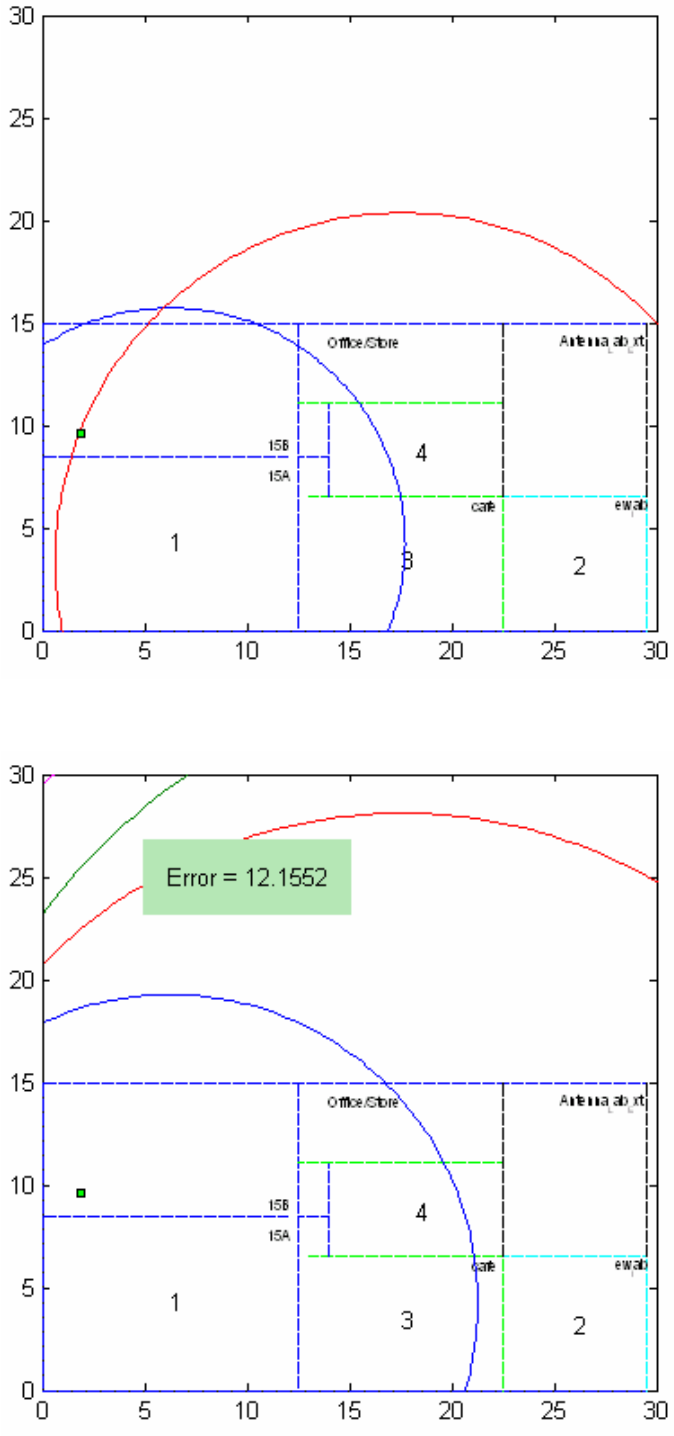

Figure A-18a Estimate location if walls not detected

A.18.2 Numerical results for figure A-18 and A-18a

client_posx = 1.8500

client_posy = 9.6000

loss_sensors = 61.4000 80.2300 64.8400 79.9200

Sig_Strth_Diag_Length = 57.8144 53.7499 55.7399 53.9133

Sig_Strth_Short_Dist = 52.8487 50.3330 50.4677 47.4646

NOTT = 1 1 1 1

Two_Wall_TH =

65.8783

69.7377

66.5937

68.0741

63.1274

70.3995

61.0778

67.6975

NOTT = 1 2 1 2

NOTT = 1 2 1 2

A = 11.4700

C = 100

E = 16.9700

D = 96.4900

A2 = 11.4700

C2 = 22.3800

E2 = 9.5900

D2 = 15.3400

A.19 Location 19 – results

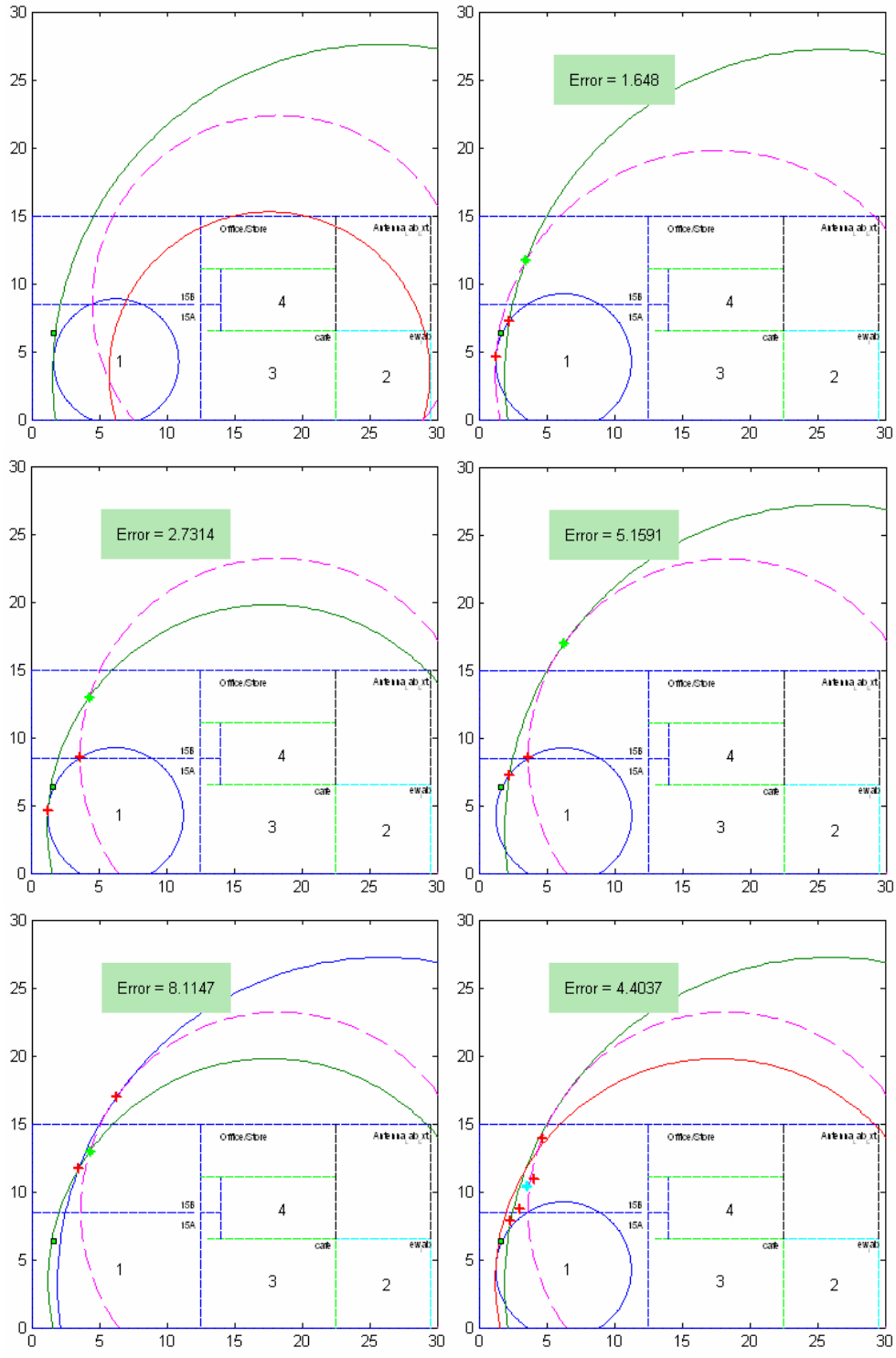

Figure A-19 Estimate Location 19

A.19.1 Location 19 – results if walls not detected

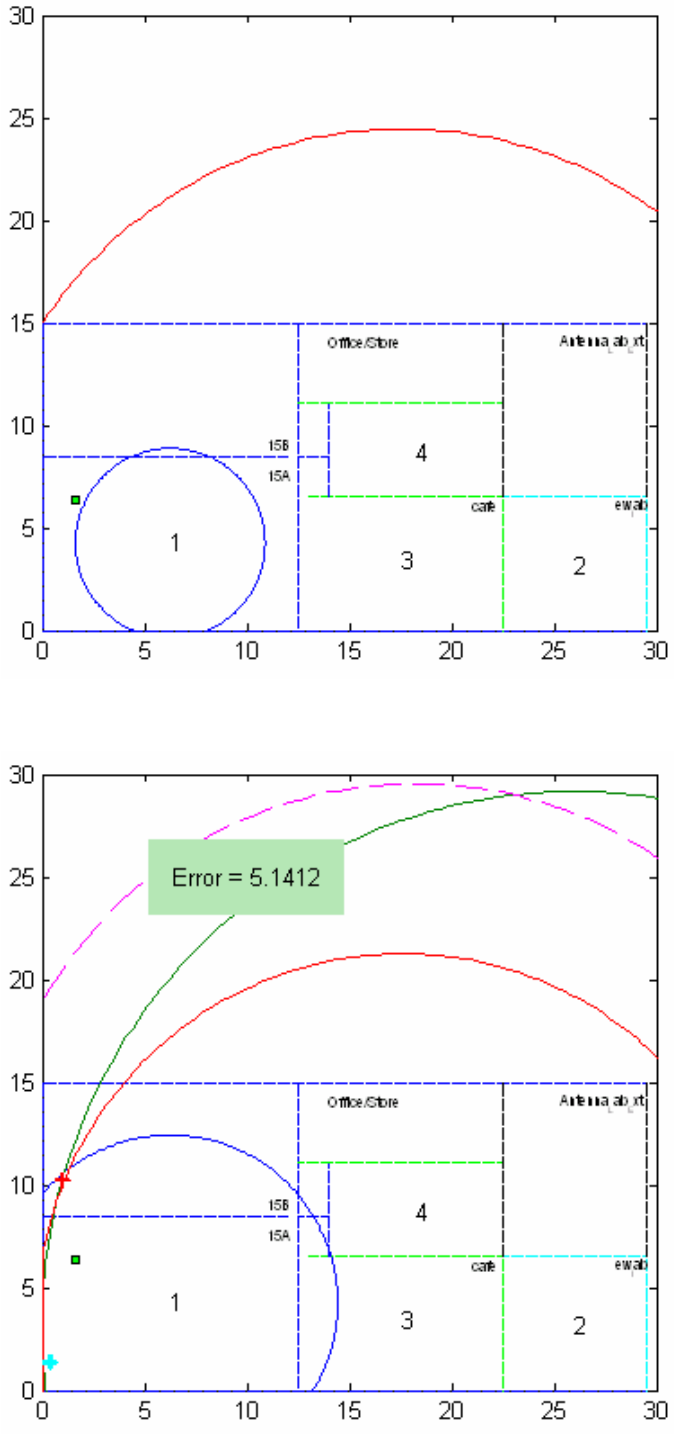

Figure A-19a Estimate location 19 if walls not detected

A.19.2 Numerical results for figure A-19 and A-19a

client_posx = 1.6000

client_posy = 6.4000

loss_sensors = 53.5000 81.0000 66.7000 73.0000

Sig_Strth_Diag_Length = 57.8144 53.7499 55.7399 53.9133

Sig_Strth_Short_Dist = 52.8487 50.3330 50.4677 47.4646

NOTT = 0 1 1 1

Two_Wall_TH =

65.8783

69.7377

66.5937

68.0741

63.1274

70.3995

61.0778

67.6975

NOTT = 0 2 1 2

NOTT = 0 2 1 2

A = 4.6300

C = 109.2600

E = 21.0600

D = 43.5000

A2 = 4.6300

C2 = 24.4600

E2 = 11.8700

D2 = 13.7700

A.20 Location 20 – Results

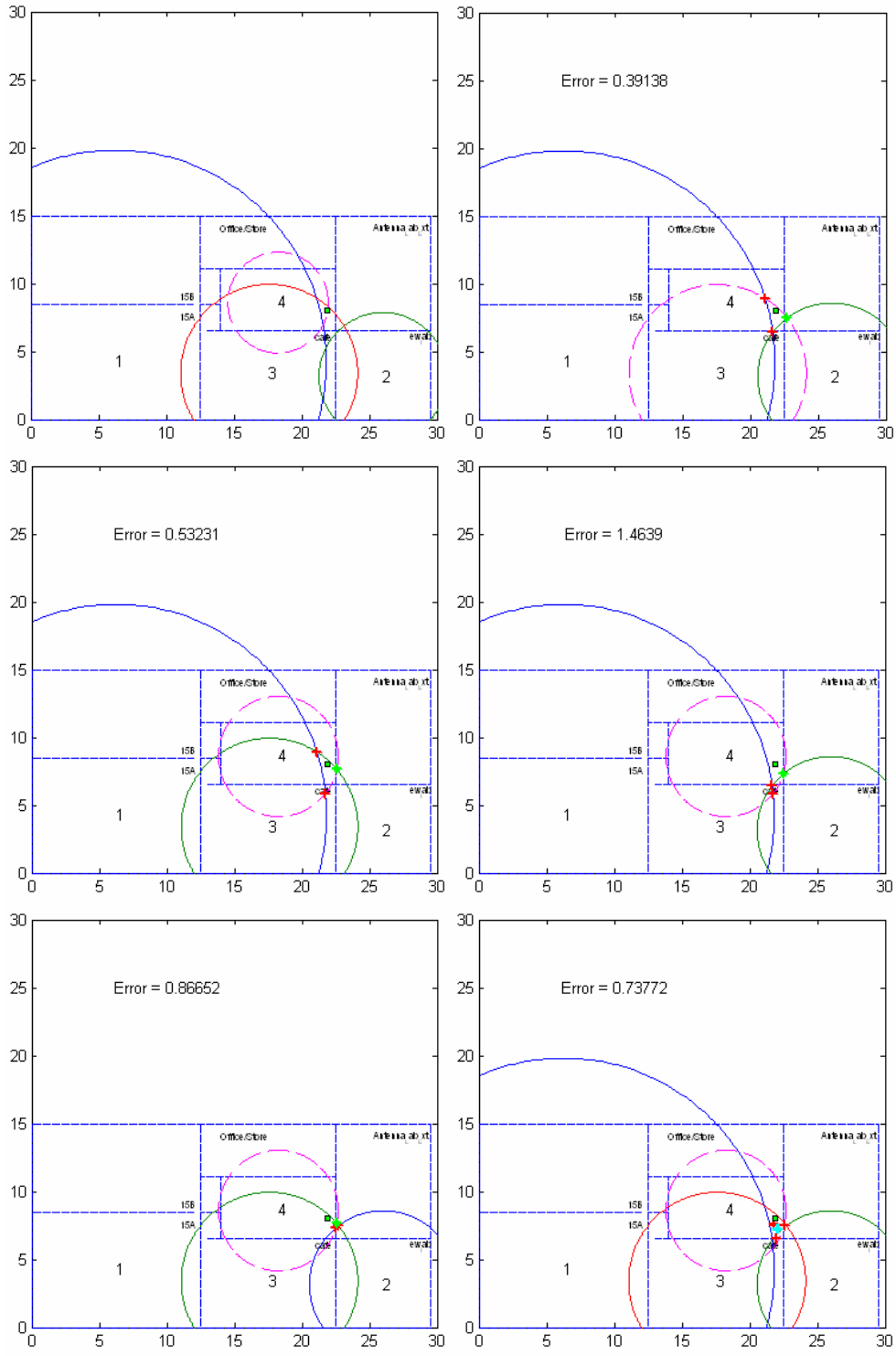

Figure A-20 Location 20

A.20.1 Location 20 – results if walls not detected

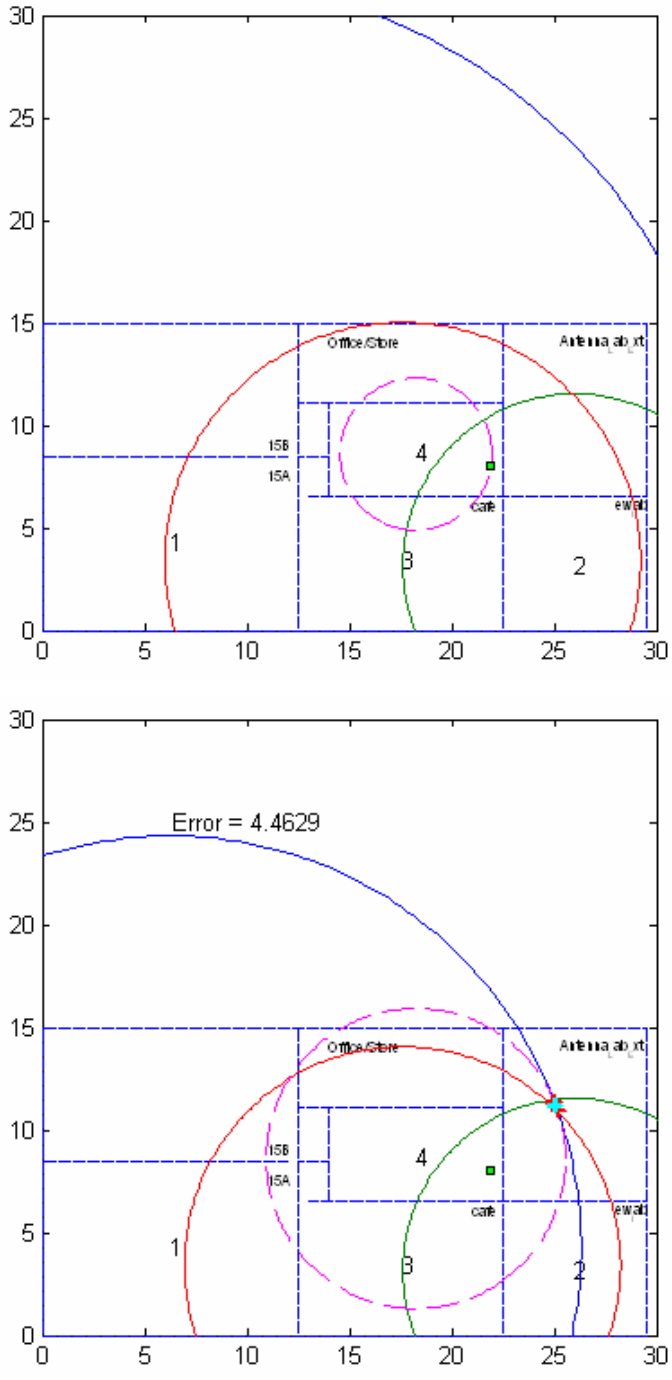

Figure A-20a Location 20 if walls not detected

A.20.2 Numerical results for figure A-20 and A-20a

client_posx = 21.9000
client_posy = 8

loss_sensors = 69.0700 58.6900 61.5300 51.6000
Sig_Strth_Diag_Length = 57.8144 53.7499 55.7399 53.9133
Sig_Strth_Short_Dist = 52.8487 50.3330 50.4677 47.4646

NOTT = 1 1 1 0

Two_Wall_TH =

65.8783
69.7377
66.5937
68.0741
63.1274
70.3995
61.0778
67.6975

NOTT = 1 1 1 0
NOTT = 1 1 1 0
A = 27.6600
C = 8.3900
E = 11.6200
D = 3.7100

A.21 Location 21 – results if walls detected

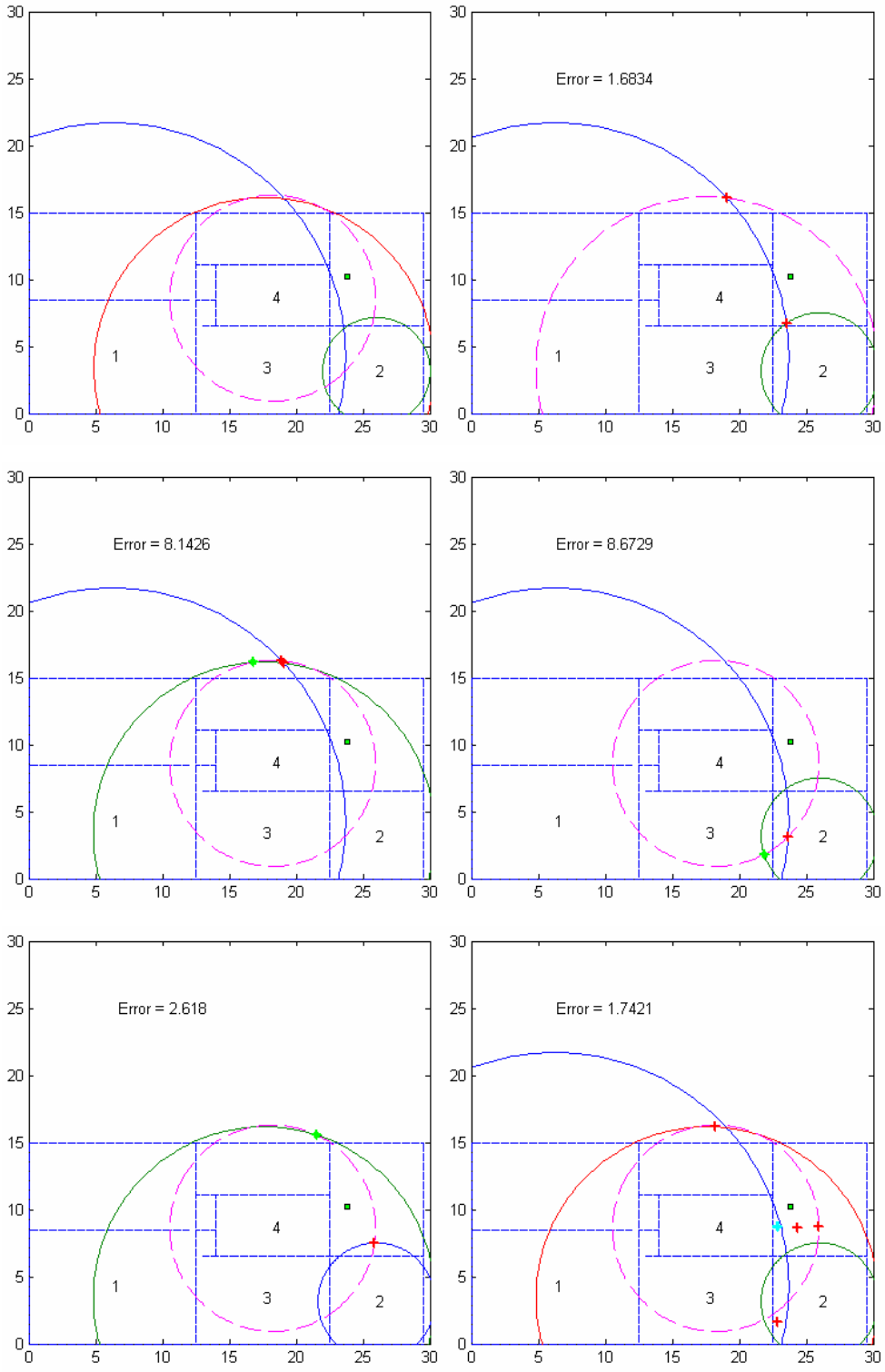

Figure A-21 Location 21

A.21.1 Location 21 – results if walls not detected

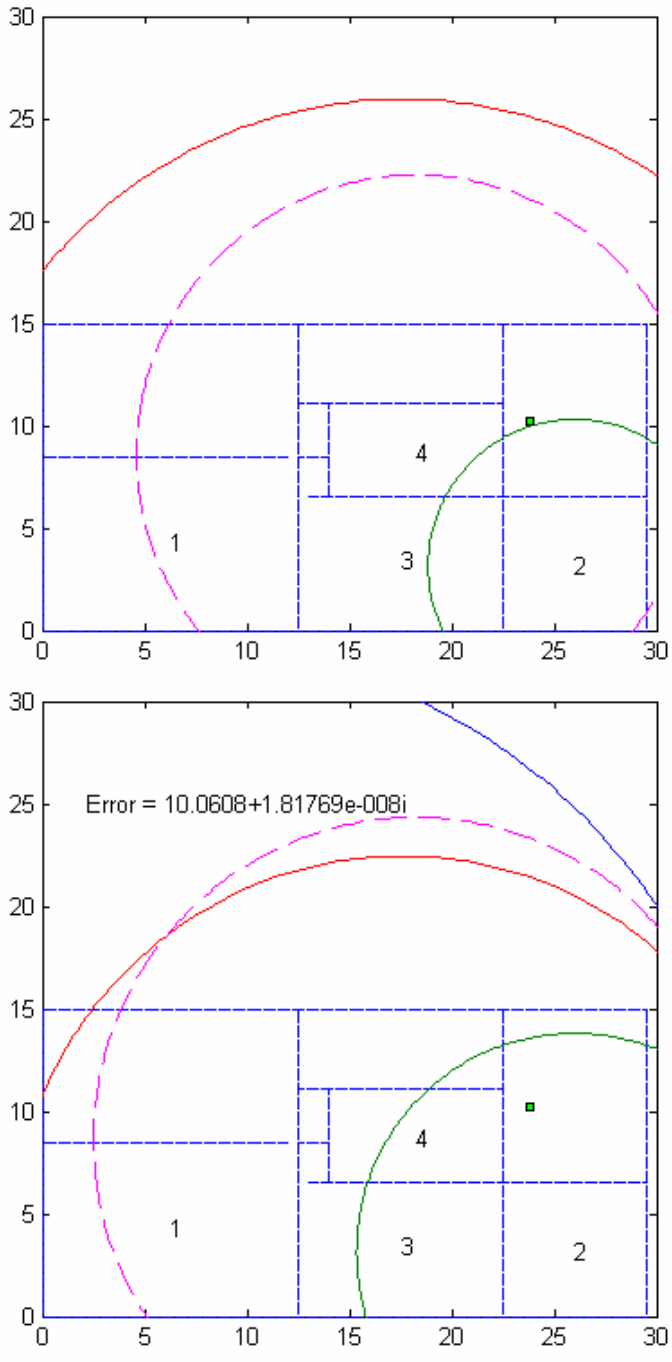

Figure A-21a Location 21 if walls not detected

A.21.2 Numerical results for figure A-21 and A-21a

client_posx = 23.8000

client_posy = 10.2200

Loss_sensors = 81.0700 57.3000 67.3000 62.9200

Sig_Strth_Diag_Length = 57.8144 53.7499 55.7399 53.9133

Sig_Strth_Short_Dist = 52.8487 50.3330 50.4677 47.4646

NOTT = 1 1 1 1

Two_Wall_TH =

65.8783

69.7377

66.5937

68.0741

63.1274

70.3995

61.0778

67.6975

NOTT = 2 1 1 1

NOTT = 2 1 1 1

A = 110.1500

C = 7.1600

E = 22.5600

D = 13.6500

A2 = 110.1500

C2 = 4.0200

E2 = 12.7200

D2 = 7.6900

A.22 Location 22 results

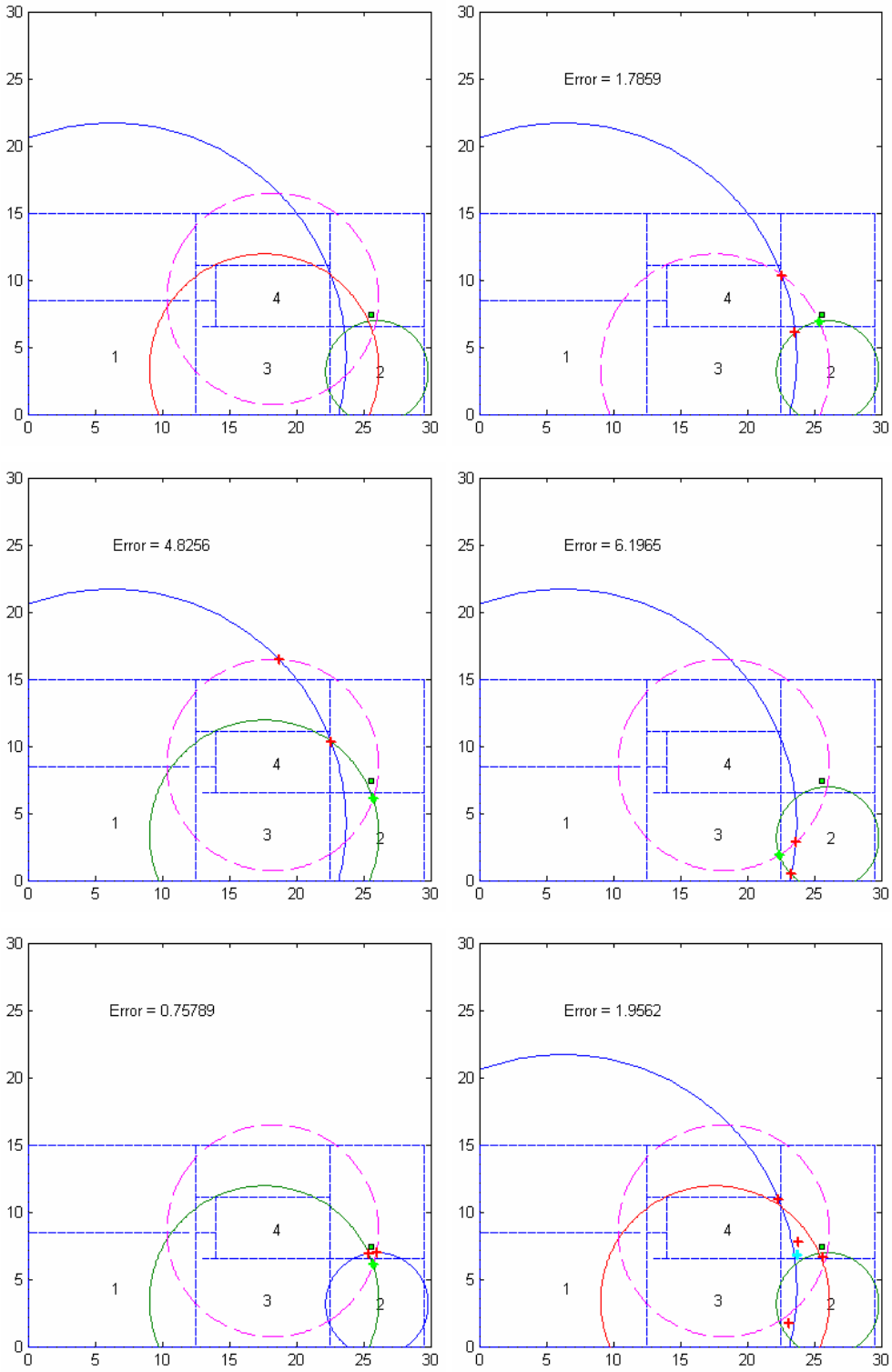

Figure A-22 Estimate location 22

A.22.1 Location 22 – results when walls not detected

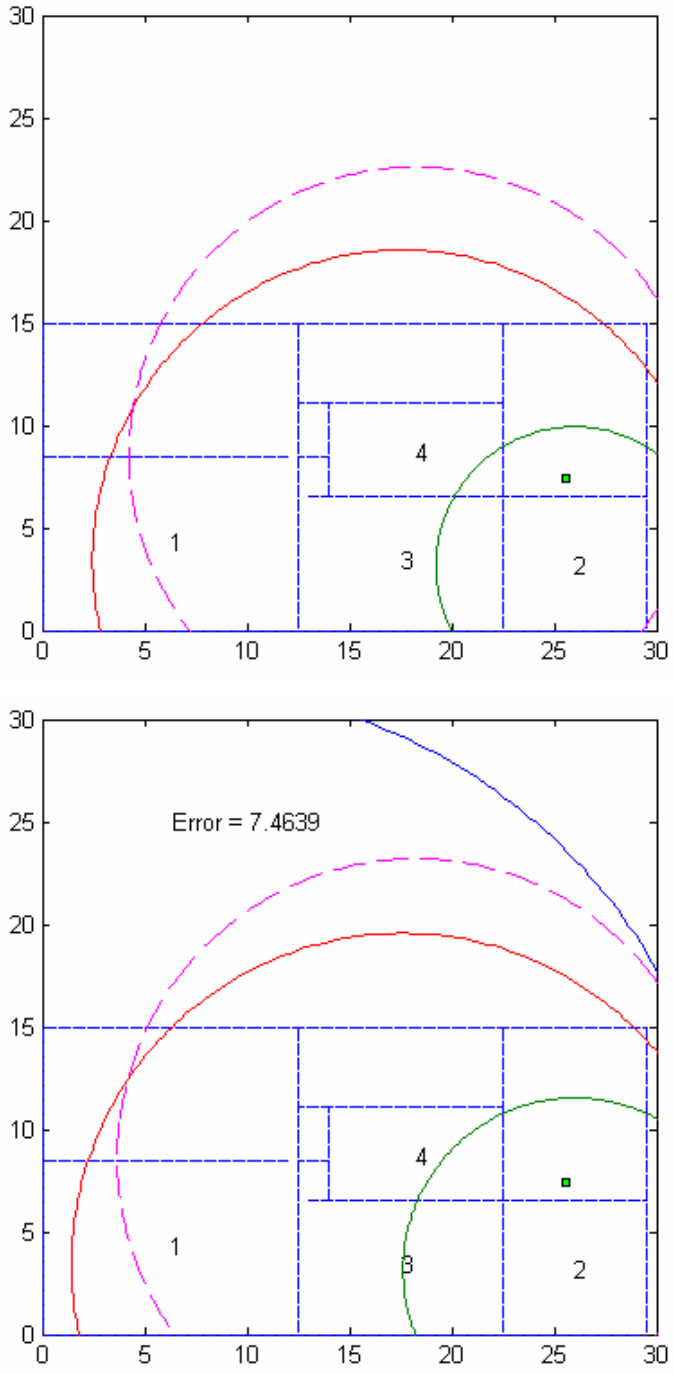

Figure A-22a Estimate location 22 when walls not detected

A.22.2 Numerical results for Figure A-22 and A-22a

client_posx = 25.6000

client_posy = 7.4000

loss_sensors = 81.0700 56.8400 63.8400 63.1500

Sig_Strth_Diag_Length = 57.8144 53.7499 55.7399 53.9133

Sig_Strth_Short_Dist = 52.8487 50.3330 50.4677 47.4646

NOTT = 1 1 1 1

Two_Wall_TH =

65.8783

69.7377

66.5937

68.0741

63.1274

70.3995

61.0778

67.6975

NOTT = 2 1 1 1

NOTT = 2 1 1 1

A = 110.1500

C = 6.7800

E = 15.2000

D = 14

A2 = 110.1500

C2 = 3.8200

E2 = 8.5400

D2 = 7.8900

A.23 Location 23 results

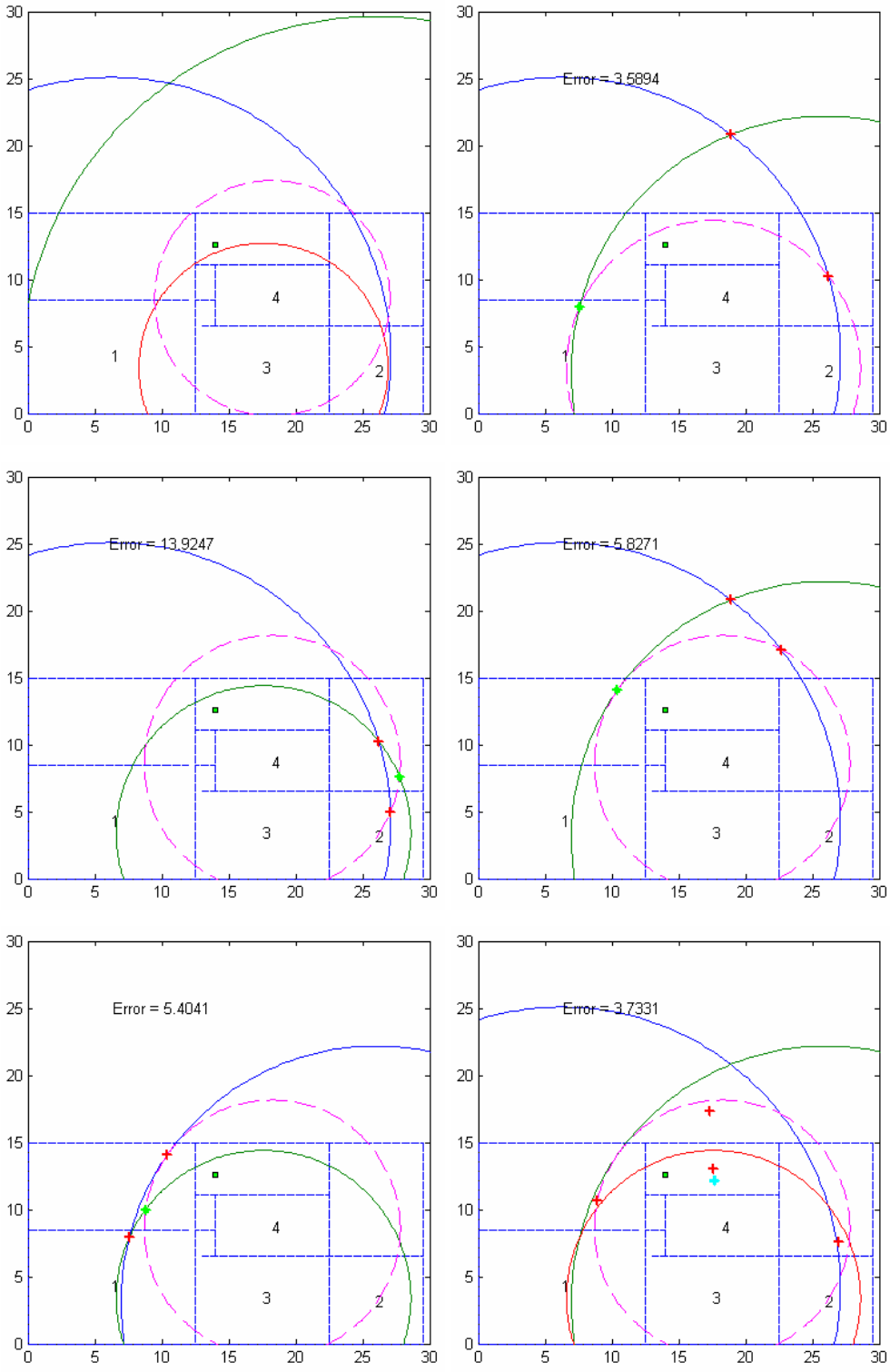

Figure A-23 Estimate location 23

A.23.1 Location 23 – results when walls not detected

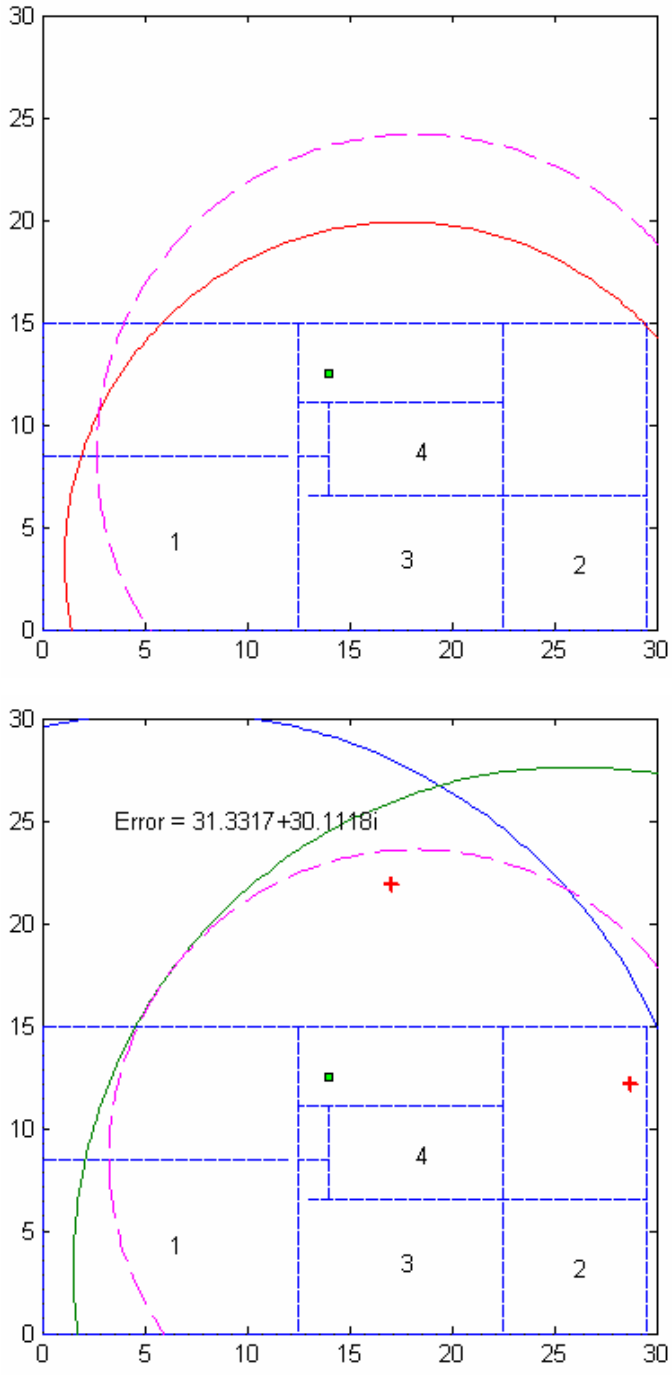

Figure A-23a Estimate location 23 when walls not detected

A.23.2 Numerical results for figures A-23 and A-23a

client_posx = 14

client_posy = 12.5500
loss_sensors = 79.6100 81.6900 64.5800 64.1000
Sig_Strth_Diag_Length = 57.8144 53.7499 55.7399 53.9133

NOTT = 1 1 1 1
Two_Wall_TH =
65.8783
69.7377
66.5937
68.0741
63.1274
70.3995
61.0778
67.6975

NOTT = 2 2 1 1
NOTT = 2 2 1 1

A = 93.1100
C = 118.3000
E = 16.4700
D = 15.6000
A2 = 93.1100
C2 = 26.4800
E2 = 9.3000
D2 = 8.7900

A.24 Location 24 results

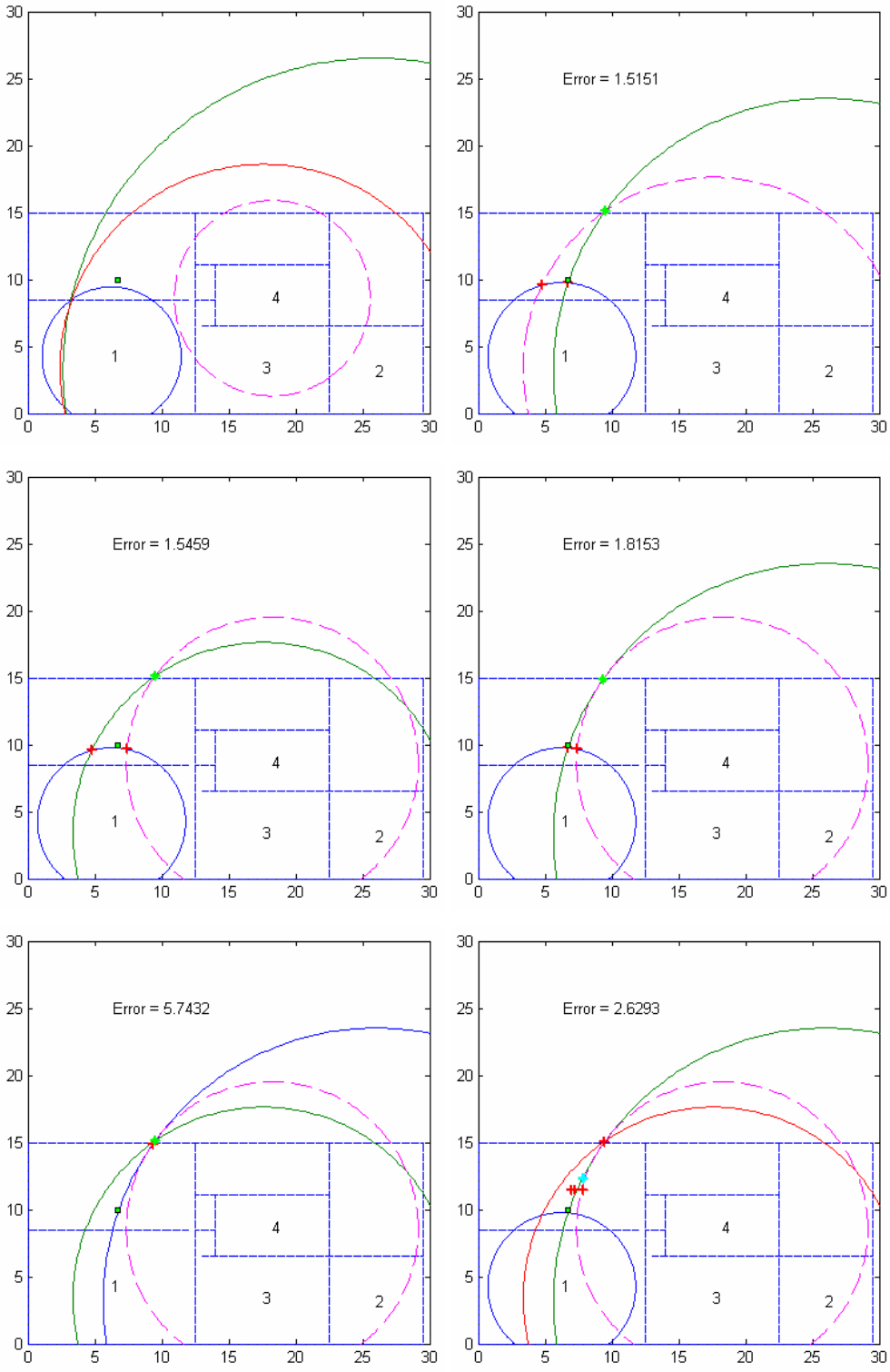

Figure A-24 Estimate location 24

A.24.1 Location 24 – results when walls not detected

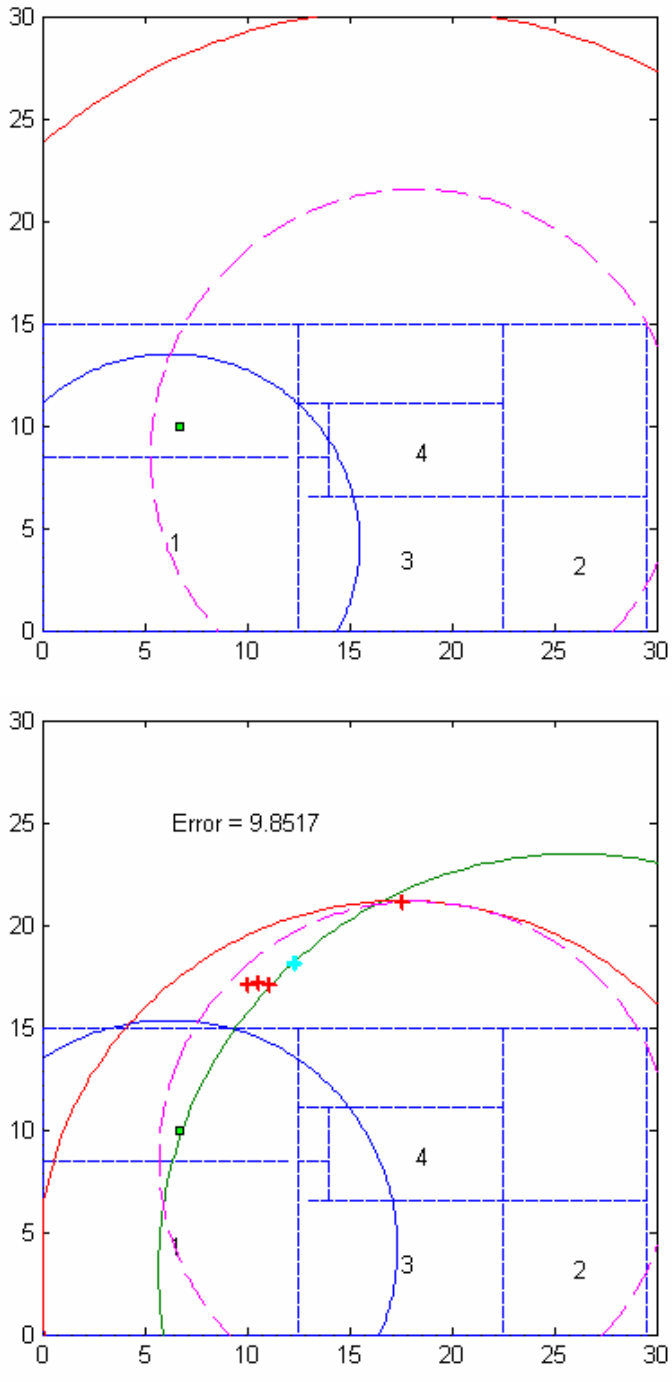

Figure A-24a Estimate location 24 when walls not detected

A.24.2 Numerical results for figures A-24 and A-24a

client_posx = 6.7000

client_posy = 10

loss_sensors = 59.5300 80.6100 68.8400 62.4600

Sig_Strth_Diag_Length = 57.8144 53.7499 55.7399 53.9133

Sig_Strth_Short_Dist = 52.8487 50.3330 50.4677 47.4646

NOTT = 1 1 1 1

Two_Wall_TH =

65.8783

69.7377

66.5937

68.0741

63.1274

70.3995

61.0778

67.6975

NOTT = 1 2 1 1

NOTT = 1 2 1 1

A = 9.2500

C = 104.4700

E = 26.9400

D = 12.9500

A2 = 9.2500

C2 = 23.3800

E2 = 15.2000

D2 = 7.3000

APPENDIX B

PUBLICATIONS